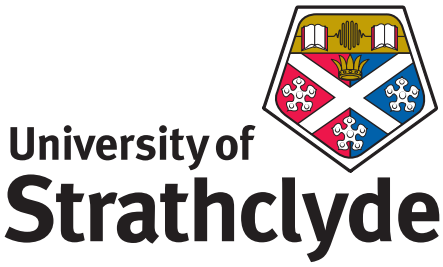

STOCHASTIC MODELLING OF NUTRIENT AND PREDATOR-PREY POPULATIONS

YONGMEI CAI

Department of Mathematics and Statistics

University of Strathclyde

Glasgow, UK

This thesis is submitted to the University of Strathclyde for the degree of Doctor of Philosophy in the Faculty of Science.

Acknowledgements

I would like to extend my most sincere gratitude to my supervisors, Professor Xuerong Mao, Professor Michael Heath and Dr Douglas Speirs for their patient and constant support.

I would like to thank Dr Jiafeng Pan for her encouragement and valuable advice. I also wish to appreciate the support from Dr Yuyuan Li, Dr Hongrui Wang, Dr Wei Liu, Dr Jianqiu Lu and Dr Chang Xu.

I would also like to mention the support from my friends Chengjie, Tadas, Siyang, Ya, Yile, Ran, Hoa, Hazel, Melinda and Soizic.

I thank China Scholarship Council, the MASTS pooling initiative (The Marine Alliance for Science and Technology for Scotland) and the University of Strathclyde for their financial support, the Journal of Applied Mathematical Modelling for accepting my paper.

Finally, a special thank goes to my dearest mom and dad.

Abstract

This thesis first constructs a stochastic differential equation (SDE) model of a fjord nutrient, based on the hydrographic and chemical data collected from the 1991 field campaign implemented in Loch Linnhe. Stochastic modelling approach is able to account for the process noise in the nutrient data. The SDE model is first extended from a deterministic nutrient model by the parameter perturbation scheme. To capture the annual variations in the sea-loch nutrient, the SDE model is refined by considering the complex physical and biological processes that make big effects on the nutrient dynamics. The model is parameterised using the least squares approach. The goodness of fit of the SDE model is assessed by comparing the distribution graphs and by performing statistical tests. The existence of the environmental-type process noise in the nutrient data is illustrated by a residual analysis for the data. Finally a simulation study is carried out to identify the accuracy of the parameter estimation frameworks.

This thesis also studies the stochastic versions of the foraging arena predator-prey system. The impacts of different types of environmental noise on the population dynamics are deduced. First of all, the SDE predator-prey model is formulated by incorporating white noise into the deterministic foraging arena system using the parameter perturbation technique. We then prove that the SDE has a unique global positive solution. We also study the asymptotic moment estimate of the model solution and produce the conditions for the system to be extinct. Furthermore the existence of a stationary distribution is pointed out under certain parametric restrictions. Secondly of all, we take a further step of incorporating telegraph noise and time delay to the stochastic foraging arena system. The stochastically ultimate boundedness, extinction and the pathwise estimation of

the population system are studied. Thirdly, we introduce white noise to more system parameters since all of them can be influenced by the complex variability. Namely, not only the growth rate of prey and the density-dependent mortality rate of predator, but also the quadratic mortality rates of the two species and the capturing rate of predator are perturbed by the stochastic noise. Then we study how the correlations between the Brownian motions affect the long-time properties of the system. The parametric conditions for the system to have a stationary distribution are deduced. Numerical simulations are carried out to substantiate the analytical results.

Contents

Notations

$a.s.$	:	almost surely, or with probability 1.
$A := B$	:	A is defined by B or A is denoted by B.
$\emptyset$	:	the empty set.
$\mathbf{I}_A$	:	the indicator function of a set A, i.e. $\mathbf{I}_A(x) = 1$ if $x \in A$ or otherwise 0.
A^c	:	the complement of A in Ω, i.e. $A^c = \Omega - A$.
$\sigma(\mathcal{C})$	:	the σ-algebra generated by $\mathcal{C}$.
$a \vee b$	:	the maximum of a and b.
$a \wedge b$	:	the minimum of a and b.
$f : A \to B$	:	the mapping f from A to B.
$\mathbb{S}$	:	$=\{1, 2, \cdots, N\}$, the finite state space of a Markov chain.
$\mathbb{R}_+$	:	the set of all nonnegative real numbers, i.e. $\mathbb{R}_+ = [0, \infty)$.
$\mathbb{R}^d$	:	the d-dimensional Euclidean space.
$\mathbb{R}^d_+$	:	$=\{x \in \mathbb{R}^d : x_i > 0, 1 \leqslant i \leqslant d\}$, i.e. the positive cone.
$\mathcal{B}^d$	:	the Borel-σ-algebra on $\mathbb{R}^d$.
$\mathbb{R}^{d\times m}$	:	the space of real $d \times m$-matrices.
$\|x\|$	:	the Euclidean norm of a vector x.
A^T	:	the transpose of a vector or a matrix A.
$\text{trace}(A)$	:	the trace of a square matrix $A = (a_{ij})_{d\times d}$, i.e. $\text{trace}(A) = \sum_{1\leqslant i\leqslant d} a_{ii}$.
$\lambda_{min}(A)$	:	the smallest eigenvalue of a symmetric matrix A.
$\lambda_{max}(A)$	:	the largest eigenvalue of a symmetric matrix A.
$\|A\|$	:	$= \sqrt{\text{trace}(A^T A)}$, i.e. the trace norm of a matrix A.
$\|\|A\|\|$	:	$= \sup\{\|Ax\| : \|x\| = 1\} = \sqrt{\lambda_{max}(A^T A)}$, i.e. the operator norm of a matrix A.
V_x	:	$= (V_{x_1}, \cdots, V_{x_d}) = (\frac{\partial V}{\partial x_1}, \cdots, \frac{\partial V}{\partial x_d})$.
V_{xx}	:	$= (V_{x_i x_j})_{d\times d} = (\frac{\partial^2 V}{\partial x_i \partial x_j})_{d\times d}$.
$C([-\tau, 0]; \mathbb{R}^d)$	:	the space of all continuous $\mathbb{R}^d$-valued functions φ defined on $[-\tau, 0]$ with a norm $\|\|\varphi\|\| = \sup_{-\tau\leqslant\theta\leqslant 0} \|\varphi(\theta)\|$.
$L^p([a, b]; \mathbb{R}^d)$	:	the family of Borel measurable functions $h : [a, b] \to \mathbb{R}^d$ such that $\int_a^b \|h(t)\|^p dt < \infty$.

$\mathcal{L}^p([a,b];\mathbb{R}^d)$	:	the family of $\mathbb{R}^d$-valued $\mathcal{F}_t$-adapted processes $\{f(t)\}_{a\leqslant t\leqslant b}$ such that $\int_a^b \lvert f(t)\rvert^p dt < \infty$ a.s.
$\mathcal{M}^p([a,b];\mathbb{R}^d)$	:	the family of processes $\{f(t)\}_{a\leqslant t\leqslant b}$ in $\mathcal{L}^p([a,b];\mathbb{R}^d)$ such that $\mathbb{E}\int_a^b \lvert f(t)\rvert^p dt < \infty$.
$\mathcal{L}^p(\mathbb{R}_+;\mathbb{R}^d)$	:	the family of processes $\{f(t)\}_{t\geqslant 0}$ such that for every $T>0$, $\{f(t)\}_{0\leqslant t\leqslant T} \in \mathcal{L}^p([0,T];\mathbb{R}^d)$.
$\mathcal{M}^p(\mathbb{R}_+;\mathbb{R}^d)$	:	the family of processes $\{f(t)\}_{t\geqslant 0}$ such that for every $T>0$, $\{f(t)\}_{0\leqslant t\leqslant T} \in \mathcal{M}^p([0,T];\mathbb{R}^d)$.

List of Figures

List of Tables

Chapter 1

Introduction

1.1 Ecological Modelling

Natural systems are complex and diverse. As the saying goes, there are no two identical leaves in the world. To explore the underlying mechanisms and regular rules behind the complex and unpredictable phenomenon, extensive attention has been dedicated to the quantitative modelling of natural systems. Ecological modelling, the mathematical reconstruction and analysis of the ecological dynamics, makes use of the classical mathematical methodologies, biological theories and the techniques from a variety of fields, including computer science and operations research, etc. to understand the complex ecological processes and forecast the ecosystem behaviours [50, 69, 70, 109, 124].

In the late eighteenth century, Malthus [83] first presented basic ideas in population science and explained the associations between the growth and well-being of human population with the development of natural resource. In the nineteenth century, Verhulst's formula [126] of logistic growth was presented to describe the growth behaviours under limited resources. Later on the introduction of the predator-prey interactions by Lotka [79] and Volttera [129] brings a brand new dimension into the study of population ecology. Since then the differential equation approach has become a crucial tool in population ecology. Lindeman [77] pioneered the theory of trophic interrelations, which is influential in modern aquatic community ecology. In 1980s, the development

of object-oriented programming has provided considerable new insights into the ecological modelling [58, 66]. For example, inspired by this technique, Kaiser [66] pointed out the individual based models. Such model introduces more options to synchronously reflect the uncertainties in physiological states of organisms. At the same time the self-organization paradigm [56] was proposed, which has been influential in ecology. Nowadays modelling has become an essential tool to analyse the complexity in the ecological systems. Many researchers have devoted serious efforts to the methodologies and techniques of model construction and use in various branches of ecology (e.g. [114]). In marine ecology, Steele [115] presented a three-dimensional model to analyse the interactions among nutrient, phytoplankton and zooplankton in a two-layered sea. Heath et al. [53] proposed an age-structured population model to examine how different natal fidelity scenarios affect the cod populations in North Sea and West of Scotland. A differential equation model was proposed to identify the impact of fishing on Kenyan coral reefs [96]. In invasion ecology, a deterministic model was formulated to evaluate the spread of feral rape along road verges [41, 124]. Also a two-dimensional model was carried out to assess the invasion of grasslands by pine species [20]. In biogeochemistry, many mathematical models have been dedicated to oxygen and nutrient cycles (e.g. [46]). Mathematical models have also been intensively explored in other fields, including conservation biology [22], epidemiology [97], landscape ecology [51] and genetics ecology [25], etc.

After the construction of a mathematical model, ecologists are concerned with the reliability of the model to represent the real world. In general, the correctness of the model can be identified based on the observed data [39, 124]. Firstly, the available measurements allow modellers to obtain the optimal parameters which minimize the difference between the modelled data and the observed one, rather than empirically determine the parameters based on the expert knowledge. Then the model can be evaluated by testing whether its numerical simulation is consistent with the data. As a result, a desirable model can then be formulated in an iterative procedure by correcting the existing model or constructing an alternative model and examining its numerical correctness [39, 124]. These reflect that the observed data can significantly contribute

to the model evaluation and refinements. On the other hand, ecological data is rarely accurate and inevitably contain error. Recently, Lv [82] revealed the weakness of the conventionally used deterministic models in representing the inherent stochasticity in the data [73, 127]. As elaborated in [13], different types of error in the data need to be handled by different modelling approaches to assure the model reliability. Namely, the model performance benefits from the ecological data, meanwhile the modelling approach employed is limited by the type of error in the data. In the population abundance data, there are two major types of error, observation error and process noise [4, 32]. Observation error, including systematic error and random error, is caused by different methods used to collect data. For example, difficulty in detecting animals due to field conditions or harsh environmental conditions and the imperfect calibration of measurement instruments can lead to the observation error. While process noise can be regarded as variations in the true population abundance due to biotic factors caused by e.g. other organisms sharing its habitat, and abiotic factors such as insolation, weather and geology [4, 32, 50]. The extensively used deterministic models are capable of analysing data driven by observation error but has its limitation in accounting for process noise [82]. Lv et al. [82] emphasised the importance of recognising the process noise in the data as it can help understand the underlying ecological mechanisms. The results from [73] suggest that the process noise is the most important factor in the catch-at-age data for North Sea plaice. As a powerful tool to understand the environmental-type process noise in the data, stochastic modelling has been receiving intensive attention [15, 31, 44, 73, 82, 86].

1.2 Ecological Modelling in a Random World

A deterministic model produces a single outcome under a certain circumstance. It describes the dynamics driven exclusively by internal deterministic mechanisms [69, 109]. However the natural systems are exposed to the external environments with complex variations that cannot essentially be reflected by the deterministic approaches. As a result there is an increasing demand of a modelling approach to interpret such probabilistic nature. This leads to the introduction of stochastic models which assume that the systems are partly

driven by environmental noise [13, 50]. Compared to deterministic models, a stochastic one predicts a set of possible outcome based on their likelihoods or probabilities. Nowadays, stochastic models play an important role in a variety of areas including epidemiology, biology, demography, health care systems, polymer science, physics, telecommunication networks, economics, finance, marketing and social networks [71]. In particular, they can be applied to account for the variations in the biological and medical processes, evaluate the uncertainty in the management decisions, investigate the complexity in psychological and social interactions and develop innovative ideas and methodology to various scientific research [121].

In the past few years, researchers have devoted serious efforts to the development of various stochastic formulations in the ecological applications, including discrete-time Markov chain (DTMC) models, continuous-time Markov chain (CTMC) models and stochastic differential equation (SDE) models. In population ecology, there is an extensive literature concerned with stochastic models. For example, stochastic versions of the classic logistic model

$$\frac{dy}{dt} = ry\Big(1 - \frac{y}{K}\Big)$$

have been intensively studied, including DTMC models [8], CTMC models [109] and SDE models [45]. In addition, Ackleh et al. [2] derived a DTMC model and an SDE model to describe the dynamics of the age-structured juvenile amphibian population coupled with the size-structured adults. Moreover, Markov chain and SDE models have also been widely employed to characterise the dynamical properties of the predator-prey population systems [14, 52, 62–64, 75, 76, 78, 80, 88, 89, 93–95, 119, 134, 135]. In fisheries science, the importance of understanding and accounting for stochasticity has received widespread attention, particularly for stock recruitment. SDE versions of the linear growth models and von Bertalanffy growth model [130] have been formulated to analyse the fish growth and recruitment [81, 104]. Moreover, Gloaguen et al. [43] depicted the fishing vessels trajectories using SDE models. In movement ecology, animal movements patterns have been drawn by SDE models [113]. Moreover, a CTMC model is used to depict animal movement [19]. In chemical ecology, several stochastic approaches have been receiving growing attention [13].

CTMC and DTMC models were used to describe the concentrations of chemical species [13, 85], while SDE models were introduced to mimic the behaviours of the neuronal signal transduction networks [85, 86], the biochemical networks [38] and the transcriptional regulatory networks [26]. In landscape ecology, Markov chain models have been adopted to depict the quantitative and spatial change of landscape features (e.g. [18, 120]) and forecast the future land use tendency [49].

The main differences among these models are the underlying assumptions on the time and state variables. The DTMC models provide discrete time and state variables. The CTMC models give discrete state variables but continuous time. While in an SDE model, both time and state variables are continuous [9]. Most of the stochastic population models are SDE and CTMC models since they are continuous in time [7]. Dennis [30] suggested that an SDE model follows from a diffusion approximation of a CTMC model when the population sizes are large, while Allen and Allen [9] pointed out that the SDE models also work well for small population sizes. Recently, the DTMC models have also been adopted in the population modelling when the species have nonoverlapping generations. The DTMC models are often more biologically realistic. Also compared to the continuous-time systems, the DTMC models are easier formulated and understood [9]. Computational ease is also an important factor to consider. The Markov chain models can lead to a high computational cost, especially for large-scale simulations such as the numerical analysis of the signal transduction networks that exist in cells [85]. While an SDE model is able to dramatically reduce the computational time by simulating its sample path based on e.g. the Euler-Maruyama method and Milstein's approach [57].

1.2.1 SDE Models

Stochastic differential equation (SDE) models are often applied to characterise the dynamics of ecological systems since they take the random external perturbations into account. The SDE models are natural extension of the ordinary differential equation (ODE) models. In an SDE model, the relevant parameters are modelled as stochastic processes or the stochastic processes are added to the driving systems. By including stochasticity into the deterministic models, one can understand the

effects of the environmental noise on the ecological dynamics [85]. In many cases, noise only blurs the system behaviours. However, noise in the nonlinear systems can qualitatively vary the underlying dynamics. Namely, stochastic factors can enhance, diminish or even change the dynamical behaviours [13]. There are various types of stochastic factors [48, 87, 89, 94, 119] and now we focus on white noise and telegraph noise.

1.2.1.1 White Noise

White noise is representative of environmental noise and the effects of such noise on the ecological systems have been extensively explored. White noise can be incorporated to the deterministic models by a routine technique called parameter perturbation [48, 89, 92]. In population ecology, a pioneering work belongs to [92] who discovered that the stochastic versions of the Lotka-Volterra model have more intriguing properties than its deterministic system - even a tiny amount of white noise can suppress an imminent deterministic explosion in many co-habiting species. For example, consider a classic two-dimensional Lotka-Voltera model

$$\begin{aligned} \dot{x}_1(t) &= x_1(t)[b_1 - a_{11}x_1(t) + a_{12}x_2(t)], \\ \dot{x}_2(t) &= x_2(t)[b_2 - a_{22}x_2(t) + a_{21}x_1(t)], \end{aligned} \tag{1.2.1}$$

where $a_{11}, a_{12}, a_{21}, a_{22}, b_1$ and b_2 are positive constants. To avoid explosion of the solution at a finite time, the parameters need to obey $a_{12}a_{21} < a_{11}a_{22}$. Now we illustrate what will happen if the above requirement is not hold. Without loss of generality we may assume $a_{11} = a_{22} = \alpha$, $a_{12} = a_{21} = \beta$, $\alpha^2 < \beta^2$, $b_1 = b_2 = b \geqslant 1$ and $x_1(0) = x_2(0) = x_0 > 0$. We then obtain a simplified equation

$$\dot{x}(t) = x(t)[b + (-\alpha + \beta)x(t)]$$

with the solution

$$x(t) = \frac{b}{-(-\alpha+\beta) + \frac{b+(-\alpha+\beta)x_0}{x_0}e^{-bt}}.$$

Then the expression $\alpha^2 < \beta^2$ causes an explosion of the solution at a finite time $t = \frac{1}{b}(\log(b+(-\alpha+\beta)x_0) - \log((-\alpha+\beta)x_0))$. However, the theory illustrated in [92] indicated that the introduction of white noise can avoid this explosion. This brings a brand new dimension into the study of population modelling. In general, white

noise can stabilise an unstable system, destabilise a stable system or make a stable system become even more stable [10,24,68]. In particular, white noise can suppress or express exponential growth of a system [29]. Moreover, the presence of white noise also can result in a stationary distribution of populations [23, 78, 91, 134]. Furthermore, the effects of white noise on various types of predator-prey models have been extensively analysed [14, 62–64, 78, 80, 88, 93, 95, 134]. In fisheries science, white noise has been found to increase the chance of fish recruitment in simple growth models [104]. In addition, Lv and Pitchford [81] suggested that white noise in the von Bertalanffy growth model can lead to a big positive impact on fish recruitment probability, population mean growth rate and the expected observed growth rate. In conservation ecology, white noise is introduced to a deterministic model to evaluate the growth rates and extinction probabilities of an endangered species [31]. Results show that the existence of white noise is useful for the studies on species preservation. In plant ecology, the randomness of the growth of plant roots in an unpredictable and heterogeneous environment is investigated by an SDE model incorporating white noise. Then the intra- and inter-specific competition between plants with contrasting growth strategies is studied [82, 104]. In chemical ecology, white noise also plays an important role. For example, due to the presence of white noise, a model describing neuronal signal transduction pathways produces stable responses, indicating that the variances of the responses are not increasing with time. Also the model has overcome the problem of producing negative concentrations [85, 86].

1.2.1.2 Telegraph Noise

An SDE model incorporating telegraph noise can characterise the systems where the structures and parameters experience abrupt changes due to abrupt environmental disturbances and changing subsystem interconnections [94], etc. To understand the telegraph noise easily, let us consider the Lotka-Volterra model (1.2.1) incorporating telegraph noise. Telegraph noise can be regarded as a switching between two or more regimes of environments [35, 48]. The switching is memoryless and the waiting time for the next switch has an exponential distribution. The regime switching is then modelled by a finite-state Markov chain [48]. To make it simple, we suppose that there are only two regimes. Namely, the Markov chain

$r(t)$ in the state space $\mathbb{S} = \{1, 2\}$ controls the switching between the environmental regimes. Model (1.2.1) under regime switching can then be described by the following system:

$$\begin{aligned} \dot{x}_1(t) &= x_1(t)[b_1(r(t)) - a_{11}(r(t))x_1(t) + a_{12}(r(t))x_2(t)], \\ \dot{x}_2(t) &= x_2(t)[b_2(r(t)) - a_{22}(r(t))x_2(t) + a_{21}(r(t))x_1(t)], \end{aligned} \tag{1.2.2}$$

where the system parameters $a_{11}(i), a_{12}(i), a_{21}(i), a_{22}(i), b_1(i)$ and $b_2(i)$ are all positive constants for $i \in \mathbb{S}$. This system is operated as follows: when $t = 0$, if $r(0) = 1$, the system obeys equation (1.2.2) with $r(t) = 1$ until time τ_1 when the Markov chain jumps to state 2 from state 1; the system will then obey equation (1.2.2) with $r(t) = 2$ from time τ_1 till time τ_2 when the Markov chain jumps to state 1 from 2. The system will continue to switch as long as the Markov chain jumps. If $r(0) = 2$, the system switches in the similar way. Namely, system (1.2.2) switches from one to another according to the law of Markov chain.

In an ecological system, when random factors make a switching among different deterministic subsystems, the population behaviours become rather complicated to analyse. Hence the introduction of telegraph noise is necessary to deal with this abrupt change in the ecological modelling. Telegraph noise can affect an ecological system significantly. Takeuchi [119] revealed an important influence of telegraph noise on a Lotka-Volterra system: If the two deterministic subsystems have different equilibrium states, the stochastic population system is neither permanent nor dissipative. Slatkin [112] analysed the growths of species experiencing a variable environment in a class of population models under telegraph noise. A stationary distribution of populations has been found in this Markovian environment. In genetic ecology, Paszek [103] presented the ODE models with telegraph noise to analyse the gene regulation with the number of active genes forming a discrete-valued stochastic process in the Chemical Master Equation (CME) regime and the levels of mRNA and protein taking real values. He chose mass action ODEs for the reactions involving mRNA and protein and found that this switching gave a steady-state variance that does not match the underlying CME [61].

Moreover, there is an extensive literature concerned with the combination

of white noise and telegraph noise in an ecological system. In population ecology, Hu et al. [60] showed that the regime switching and white noise make the original system with exponential solution become a new system with solution grow at most polynomial. The influence of both stochastic factors on the multi-dimensional predator-prey models have also been extensively investigated (e.g. [52, 75, 76, 94, 135]). In genetic ecology, Hu et al. [61] proposed an SDE model with Markovian switching for modelling gene regulation. This SDE model has been proved to preserve the biologically relevant measures of mean and variance.

As discussed in section 1.1, stochastic modelling has made an impressive contribution to the analysis of the environmental-type process noise inherent in the ecological data (e.g. [15]). This prospect has attracted a number of researchers engaged in the analysis of ecological data (e.g. [27]). Lewy and Nielsen [73] proposed a stochastic model of age-based fish stock. Parameters were estimated using the likelihood-based Markov Chain Monte Carlo (MCMC) technique. Results suggested that this stochastic model has well explained the process noise in the catch data and stock data. Brillinger et al. [21] built an SDE model that characterises some behaviours of seals by working with the location data for a seal. Parameter inference was performed using the robust linear regression approach. Then the temporal and spatial reasonableness of the model was assessed by inspecting synthetic plots. Gloaguen et al. [44] fitted an SDE model of individuals movement to a data set of fishing vessels trajectories. Parameterization was carried out using four approximate maximum likelihood approaches. Results indicated that the Euler method is not robust to low sampling rates, while the Ozaki local linearization technique is well-performed among the four procedures in the context of movement ecology. Gloaguen et al. [82] formulated an SDE model of individual plant growth of Arabidopsis thaliana. The model was fitted to the experimental data and evaluated within a Bayesian framework. The posterior distribution of the model parameters was sampled by the MCMC algorithm. The success of this model benefited from the stochastic perspective of understanding complex environmental variability in the data. Balzter [15] studied the Markov chain models of vegetation dynamics. Based on several data sets, the reliability of the models was evaluated using the mean square error, Spearman's rank

correlation coefficient and Wilcoxon's signed-rank test.

1.3 Structure of this Thesis

1.3.1 Nutrient Dynamics

Nutrients including carbon (C), nitrogen (N), phosphorus (P) and silicon (Si) are essential for organisms during the cellular processes [116]. In an aquatic environment, the availability and recycling rates of nutrient resources directly regulate the aquatic primary productivity [50, 128]. Moreover, the enrichment of N and P can change the structure and function of an aquatic ecosystem [101]. In coastal ecosystems, nutrients export fluxes affect the water quality and control the nature and magnitude of coastal productivity. Research on the aquatic nutrients has received growing attention. Especially, ecological modelling can be carried out to quantitatively understand the dynamical behaviours of the aquatic nutrients. Lancelot et al. [72] proposed an MIRO model to characterise the seasonal cycles of nutrients including C, N, P and Si in North Sea. The parameters were deduced based on literature reviews and on targeted studies under field and laboratory conditions. Then the validation of the model was examined using the biogeochemical data sets including temperature, nutrients and phytoplankton data collected from three locations in North Sea. Baretta-Bekker et al. [16] adopted an ERSEM model to describe the dynamics of C, P, N and Si in marine enclosures. The model was calibrated with data from mesocosm experiments performed in Knebel Vig, Denmark and then verified with results from experiments conducted in Hylsfjord, Norway. Furthermore, the nutrient dynamics has been widely investigated based on the well-known nutrient-phytoplankton-zooplankton systems [125]. However, to the best of our knowledge, stochastic modelling approach is rarely employed to represent an aquatic nutrient component. Motivated by this, in Chapter 3 we will develop a stochastic differential equation (SDE) model which captures the seasonal changes in the fjord nutrient, based on the hydrographic and chemical data collected from the 1991 field survey carried out in Loch Linnhe. According to section 1.2, such an SDE model can account for the environmental-type process noise in the nutrient data.

1.3.2 Predator-Prey Model and Foraging Arena Scheme

Predator-prey interactions play a crucial role in the relationships between populations. In the past few years, researchers have devoted serious efforts to the studies on the predator-prey systems. In a general predator-prey model (1.3.1), the trophic function λ_2 links the dynamics of prey and predator populations:

$$\frac{dx(t)}{dt} = \lambda_1(x(t))x(t) - \lambda_2(x(t), y(t))y(t) \tag{1.3.1a}$$

$$\frac{dy(t)}{dt} = \gamma\lambda_2(x(t), y(t))y(t) - \lambda_3(y(t))y(t), \tag{1.3.1b}$$

where $x(t)$ and $y(t)$ represent the population densities of prey and predator at time t, $\lambda_1(x(t))$ is the per capita net prey growth in absence of predator, $\lambda_2(x(t), y(t))$ is the density-dependent uptake response of consumers, γ is the trophic efficiency ranging from 0 to 1 and $\lambda_3(y(t))$ is the consumers death rate. Especially, $\lambda_1(x)$ takes the form of $\lambda_1(x) = r$ (exponential growth) or $\lambda_1(x) = r(1 - \frac{x}{K})$ (logical growth) [84], where r is the intrinsic growth rate and K is the carrying capacity. Moreover $\lambda_2(x(t), y(t))$ is called the "functional response" in the prey equations (1.3.1a) and the "numerical response" in the consumers equation (1.3.1b) [6, 54]. The simplest description of the trophic function $\lambda_2(x, y)$ is dependent solely on prey abundance. One is the classic Lotka-Volterra type response in which per capita uptake by the consumers is linearly related to the prey density. Another is Holling type equation [59]. The Holling II function is widely studied in the terrestrial and aquatic food chain models [42]:

$$\lambda_2(x) = u_1 x/(u_2 + x),$$

where u_1 is a maximum uptake rate by the predator and u_2 is a prey half-saturation coefficient. An alternative nonlinear formulation is the Holling III function:

$$\lambda_2(x) = u_1 x^2/(u_2^2 + x^2).$$

In contrast to the prey-dependent uptake response, the trophic function depending on both the prey and consumers abundance suppresses responsiveness by regulating the flux between prey and predator [54]. The simplest form of such uptake regulation is the ratio dependence [6, 11, 12]:

$$\lambda_2(x, y) = \lambda_2(x/y).$$

However, an extreme property happened to the ratio-dependent formulation is that the uptake rate tends to infinity as consumer abundance tends to zero [1]. Hence the concerned model fails to satisfy the continuity condition at origin. To alleviate this property, the Beddington-DeAngelis type was then proposed [17,28]. This type is capable of taking care of a variety of the ecological mechanisms:

$$\lambda_2(x,y) = u_3x/(u_4 + u_5x + y),$$

where u_3/u_4 = predator capture rate and u_5/u_4 = handling time per prey item [67]. Another functional response to avoid the extreme property happened to the ratio dependence model is the foraging arena model pointed out by [3, 131]:

$$\lambda_2(x,y) = sx/(\beta + y),$$

where β is the consumer density at half maximum per capita uptake rate and s/β is the maximum per capita uptake rate by predator. Foraging arenas are common in aquatic systems. They are formed by a series of mechanisms such as the restrictions of the consumer distributions in response to the predation risk due to their own predators and the risk-sensitive foraging behaviour by their prey [3]. Especially, the classic Lotka-Volterra model and the Holling types assume that the individual prey and predator items are distributed in a spatially uniform way. While the foraging arena model considers the spatial and temporal restrictions in predator and prey activities. The foraging arena theory has been widely used in fisheries science to explain and model responses of harvested ecosystems. This is done mainly through the application of Ecosim which is the dynamic modelling part of an ecosystem modelling software suite called *Ecopath with Ecosim (EwE)*. Ecosim is built around foraging arena theory and is capable of fitting historical data on responses of multiple fish populations to harvesting and changes in primary production regimes [3, 131]. The two-dimensional foraging arena predator-prey model can be represented as follows:

$$\begin{aligned} d\bar{x}_1(t) &= \bar{x}_1(t)\Big(a - b\bar{x}_1(t) - \frac{s\bar{x}_2(t)}{\beta + \bar{x}_2(t)}\Big)dt, \\ d\bar{x}_2(t) &= \bar{x}_2(t)\Big(\frac{h\bar{x}_1(t)}{\beta + \bar{x}_2(t)} - c - f\bar{x}_2(t)\Big)dt, \end{aligned} \tag{1.3.2}$$

where $\bar{x}_1(t)$ and $\bar{x}_2(t)$ denote the population densities of prey and predator at time t and a, b, s, β, h, c and f are all positive constants. More precisely, a is

the intrinsic growth rate of prey, c is the density-dependent mortality rate of consumers, $h = \gamma s$, b and f are the quadratic mortality rates of prey and predator respectively. We set $\bar{x}(t) = (\bar{x}_1(t), \bar{x}_2(t))^T$ as the solution to model (1.3.2) with the initial value $\bar{x}_0 = (\bar{x}_1(0), \bar{x}_2(0))^T$. In model (1.3.2), there are two non-negative trivial equilibrium points $\bar{E}_0 = (0, 0)$ and $\bar{E}_1 = (\frac{a}{b}, 0)$. Also an unique interior equilibrium point $\bar{E}^*(\bar{x}_1^*, \bar{x}_2^*)$ with the nullclines

$$(a - b\bar{x}_1^*)(\beta + \bar{x}_2^*) = s\bar{x}_2^*,$$
$$(\beta + \bar{x}_2^*)(c + f\bar{x}_2^*) = h\bar{x}_1^*$$

exists and is globally asymptotically stable provided that $a > \frac{b\beta c}{h}$ [74]. According to section 1.2, population systems are always subject to the complex variations. A natural response is to consider stochastic models. An extensive literature is concerned with the effects of environmental variability on the predator-prey populations [14, 62–64, 75, 76, 78, 80, 88, 93–95, 134]. However, we are not aware of any literature addressing this issue for the foraging arena model. This is the motivation for us to study the stochastic versions of the foraging arena system. In particular, Chapter 4 will study the impact of white noise on the population system. In Chapter 5, we will further incorporate telegraph noise and time delay to the stochastic foraging arena model formulated in Chapter 4 and investigate its long-time properties. Finally in Chapter 6, we will introduce white noise to more parameters of the SDE system established in Chapter 4 and discover how the correlations of the Brownian motions affect the population behaviours.

Chapter 2

Mathematical Background

This chapter aims to introduce some general concepts on the stochastic differential equations (SDEs) and SDEs with Markovian switching. The topic discussed in this chapter includes probability theory, stochastic processes, Brownian motions, stochastic integrals, the Itô formula, stochastic differential equations, Markov processes, generalised Itô's formula, stochastic differential equations with Markovian switching and some useful inequalities. The materials given in this chapter are mainly from [89] and [94].

2.1 Probability Theory

Probability theory deals with mathematical models of trials whose outcomes depend on chance. All the possible outcomes are grouped to form a set Ω, with typical element $\omega \in \Omega$. We only group the observable or interesting events together as a family, $\mathcal{F}$, of subsets of Ω. Such a family, $\mathcal{F}$, has the following properties:

(i) $\emptyset \in \mathcal{F}$, where $\emptyset$ is the empty set;

(ii) $A \in \mathcal{F} \Rightarrow A^C \in \mathcal{F}$, where $A^C = \Omega - A$ is the complement of A in Ω;

(iii) $\{A_i\}_{i \geqslant 1} \subset \mathcal{F} \Rightarrow \bigcup_{i=1}^{\infty} A_i \in \mathcal{F}$.

A family $\mathcal{F}$ satisfying these three properties is known as a σ-algebra. The pair $(\Omega, \mathcal{F})$ is a measurable space, and the elements of $\mathcal{F}$ are called $\mathcal{F}$-measurable sets. If $\mathcal{C}$ is a family of subsets of Ω, there is a smallest σ-algebra $\sigma(\mathcal{C})$ on Ω which

contains $\mathcal{C}$. We say that such $\sigma(\mathcal{C})$ is the σ-algebra generated by $\mathcal{C}$. If $\Omega = R^d$ and $\mathcal{C}$ is the family of all open sets in $\mathbb{R}^d$, then $\mathcal{B}^d = \sigma(\mathcal{C})$ is the Borel σ-algebra and the elements of $\mathcal{B}^d$ are the Borel sets.

A real-valued function $X : \Omega \to \mathbb{R}$ is $\mathcal{F}$-measurable if

$$\{\omega : X(\omega) \leqslant a\} \in \mathcal{F} \qquad \text{for all } a \in \mathbb{R}.$$

The function X is also called a real-valued ($\mathcal{F}$-measurable) random variable. An $\mathbb{R}^d$-valued function $X(\omega) = (X_1(\omega), \cdots, X_d(\omega))^T$ is $\mathcal{F}$-measurable if X_i is $\mathcal{F}$-measurable for all $i = 1, \cdots, d$. Moreover, a $d \times m$-matrix-valued function $X(\omega) = (X_{ij}(\omega))_{d\times m}$ is $\mathcal{F}$-measurable if X_{ij} is $\mathcal{F}$-measurable for all $i = 1, \cdots, d$ and $j = 1, \cdots, m$. The indicator function $\mathbf{I}_A$ of a set $A \subset \Omega$ is

$$\mathbf{I}_A(\omega) = \begin{cases} 1, & \text{for } \omega \in A, \\ 0, & \text{for } \omega \notin A. \end{cases}$$

A probability measure $\mathbb{P}$ on a measurable space $(\Omega, \mathcal{F})$ is a function $\mathbb{P} : \mathcal{F} \to [0, 1]$ satisfying

(i) $\mathbb{P}(\Omega) = 1$;

(ii) for any disjoint sequence $\{A_i\}_{i\geqslant 1} \subset \mathcal{F}$ (i.e. $A_i \cap A_j = \emptyset$ if $i \neq j$)

$$\mathbb{P}\Big(\bigcup_{i=1}^{\infty} A_i\Big) = \sum_{i=1}^{\infty} \mathbb{P}(A_i).$$

The triple $(\Omega, \mathcal{F}, \mathbb{P})$ is called a probability space. If X is a real-valued random variable and is integrable with respect to the probability measure $\mathbb{P}$, the expectation of X with respect to $\mathbb{P}$ is

$$\mathbb{E}X = \int_{\Omega} X(\omega) d\mathbb{P}(\omega)$$

and the variance of X is

$$Var(X) = \mathbb{E}(X - \mathbb{E}X)^2.$$

The pth moment of X is denoted as $\mathbb{E}|X|^p$ ($p > 0$). Given another real-valued random variable Y, the covariance of X and Y is

$$Cov(X, Y) = \mathbb{E}[(X - \mathbb{E}X)(Y - \mathbb{E}Y)].$$

We say X and Y are uncorrelated if $Cov(X,Y) = 0$. For an $\mathbb{R}^d$-valued random variable $X = (X_1, \cdots, X_d)^T$, define $\mathbb{E}X = (\mathbb{E}X_1, \cdots, \mathbb{E}X_d)^T$. For a $d \times m$-matrix-valued random variable $X = (X_{ij})_{d\times m}$, define $\mathbb{E}X = (\mathbb{E}X_{ij})_{d\times m}$. If X and Y are both $\mathbb{R}^d$-valued random variable, the symmetric nonnegative definite $d \times d$ matrix

$$Cov(X,Y) = \mathbb{E}[(X - \mathbb{E}X)(Y - \mathbb{E}Y)^T]$$

is called the covariance matrix.

Let X be an $\mathbb{R}^d$-valued random variable. Then X induces a probability measure μ_X on the Borel measurable space $(\mathbb{R}^d, \mathcal{B}^d)$ defined by

$$\mu_X(B) = \mathbb{P}\{\omega : X(\omega) \in B\} \text{ for } B \in \mathcal{B}^d,$$

and μ_X is called the distribution of X. The expectation of X can be represented as:

$$\mathbb{E}X = \int_{\mathbb{R}^d} x d\mu_X(x).$$

If $g : \mathbb{R}^d \to \mathbb{R}^m$ is Borel measurable, we have the following transformation formula

$$\mathbb{E}g(X) = \int_{\mathbb{R}^d} g(x) d\mu_X(x).$$

Let I be an index set. A family of random variable $\{X_i : i \in I\}$ (whose ranges may differ for different values of the index) is independent if the σ-algebras $\sigma(X_i), i \in I$ generated by them are independent. For example, two random variables $X : \Omega \to \mathbb{R}^d$ and $Y : \Omega \to \mathbb{R}^m$ are independent if and only if

$$\mathbb{P}\{\omega : X(\omega) \in A, Y(\omega) \in B\} = \mathbb{P}\{\omega : X(\omega) \in A\}\mathbb{P}\{\omega : Y(\omega) \in B\}$$

holds for all $A \in \mathcal{B}^d$ and $B \in \mathcal{B}^m$. If X and Y are two independent real-valued integrable random variable, then XY is integrable and

$$\mathbb{E}(XY) = \mathbb{E}X\mathbb{E}Y.$$

If $X, Y \in L^2(\Omega; \mathbb{R})$ are uncorrelated, then

$$Var(X + Y) = Var(X) + Var(Y).$$

If X and Y are independent, they are uncorrelated. If (X, Y) has a normal distribution, then X and Y are independent if and only if they are uncorrelated.

Let $\{A_k\}$ be a sequence of sets in $\mathcal{F}$. Define the upper limit of the sets by

$$\limsup_{k\to\infty} A_k = \{\omega : \omega \in A_k \text{ for infinitely many } k\} = \bigcap_{i=1}^{\infty}\bigcup_{k=i}^{\infty} A_k.$$

Lemma 2.1 (**Borel-Cantelli's lemma**). *(i) If* $\{A_k\} \subset \mathcal{F}$ *and* $\sum_{k=1}^{\infty}\mathbb{P}(A_k) < \infty$, *then*

$$\mathbb{P}\Big(\limsup_{k\to\infty} A_k\Big) = 0.$$

That is, there exists a set $\Omega_0 \in \mathcal{F}$ *with* $\mathbb{P}(\Omega_0) = 1$ *and an integer-valued random variable* k_0 *such that for every* $\omega \in \Omega_0$, *we have* $\omega \notin A_k$ *whenever* $k \geqslant k_0(\omega)$.
(ii) If the sequence $\{A_k\} \subset \mathcal{F}$ *is independent and* $\sum_{k=1}^{\infty}\mathbb{P}(A_k) = \infty$, *then*

$$\mathbb{P}\Big(\limsup_{k\to\infty} A_k\Big) = 1.$$

That is, there exists a set $\Omega_\theta \in \mathcal{F}$ *with* $\mathbb{P}(\Omega_\theta) = 1$ *such that for every* $\omega \in \Omega_\theta$, *there exists a sub-sequence* $\{A_{k_i}\}$ *such that the* ω *belongs to every* A_{k_i}.

Let $A, B \in \mathcal{F}$ and $\mathbb{P}(B) > 0$, the conditional probability of A given the condition B is

$$\mathbb{P}(A|B) = \frac{\mathbb{P}(A \cap B)}{\mathbb{P}(B)}.$$

Now let us introduce a more general concept of conditional expectation. Let $X \in L^1(\Omega;\mathbb{R})$. Let $\mathcal{G} \subset \mathbb{F}$ be a sub-σ-algebra of $\mathcal{F}$ and hence $(\Omega, \mathcal{G})$ forms a measurable space. In general, X is not $\mathcal{G}$-measurable. Now we want to find an integrable $\mathcal{G}$-measurable random variable Y such that

$$\mathbb{E}(\mathbf{I}_G Y) = \mathbb{E}(\mathbf{I}_G X) \quad \text{i.e.} \quad \int_G Y(\omega)d\mathbb{P}(\omega) = \int_G X(\omega)d\mathbb{P}(\omega) \text{ for all } G \in \mathcal{G}.$$

According to the Radon-Nikodym theorem, there exists one such Y, almost surely unique. It is called the conditional expectation of X under the condition $\mathcal{G}$ as

$$Y = \mathbb{E}(X|\mathcal{G}).$$

If $\mathcal{G}$ is the σ-algebra generated by a random variable Y, we have

$$\mathbb{E}(X|\mathcal{G}) = \mathbb{E}(X|Y).$$

2.2 Stochastic Processes

Let $(\Omega, \mathcal{F}, \mathbb{P})$ be a probability space. A filtration is a family $\{\mathcal{F}_t\}_{t\geqslant 0}$ of increasing sub-σ-algebras of $\mathcal{F}$. The filtration is right continuous if $\mathcal{F}_t = \bigcap_{s>t} \mathcal{F}_s$ for all $t \geqslant 0$. Once the probability space is complete, the filtration is said to satisfy the usual conditions if it is right continuous and $\mathcal{F}_0$ contains all $\mathbb{P}$-null sets. Throughout this thesis, unless otherwise specified, we let $(\Omega, \mathcal{F}, \mathbb{P})$ be a complete probability space with a filtration $\{\mathcal{F}_t\}_{t\geqslant 0}$ satisfying the usual conditions. We also define $\mathcal{F}_\infty = \sigma(\bigcup_{t\geqslant 0} \mathcal{F}_t)$, i.e. the σ-algebra generated by $\bigcup_{t\geqslant 0} \mathcal{F}_t$.

A stochastic process is a family $\{X_t\}_{t\in I}$ of $\mathbb{R}^d$-valued random variables with parameter set (or index set) I and state space $\mathbb{R}^d$. The parameter set I could be the halfline $\mathbb{R}_+ = [0, \infty)$, an interval $[a, b]$, the nonnegative integers or even subsets of $\mathbb{R}^d$. For a fixed $t \in I$, we have a random variable

$$\Omega \ni \omega \to X_t(\omega) \in \mathbb{R}^d.$$

While for a fixed $\omega \in \Omega$, we have a function

$$I \ni t \to X_t(\omega) \in \mathbb{R}^d,$$

which is called a sample path of the process. We can also denote the sample path $X_t(\omega)$ by $X(t, \omega)$ and the stochastic process can be regarded as a function of two variables (t, ω) from $I \times \Omega$ to $\mathbb{R}^d$. A stochastic process $\{X_t\}_{t\geqslant 0}$ is often written as $\{X_t\}$, X_t or $X(t)$.

An $\mathbb{R}^d$-valued stochastic process $\{X_t\}_{t\geqslant 0}$ is said to continuous (resp. right continuous, left continuous) if for almost all $\omega \in \Omega$ function $X_t(\omega)$ is continuous (resp. right continuous, left continuous) on $t \geqslant 0$. The stochastic process is integrable if for every $t \geqslant 0$, X_t is an integrable random variable. It is said to be $\{\mathcal{F}_t\}$-adapted if for every t, X_t is $\mathcal{F}_t$-measurable. It is said to be measurable if the stochastic process regarded as a function of two variables (t, ω) from $\mathbb{R}_+ \times \Omega$ to $\mathbb{R}^d$ is $\mathcal{B}(\mathbb{R}_+) \times \mathcal{F}$-measurable, where $\mathcal{B}(\mathbb{R}_+)$ is the family of all Borel sub-sets of $\mathbb{R}_+$.

Now let us introduce a stopping time. A random variable $\tau : \Omega \to [0, \infty]$ (it may take the value ∞) is called an $\{\mathcal{F}_t\}$-stopping time (or simply, stopping

time) if $\{\omega : \tau(\omega) \leqslant t\} \in \mathcal{F}_t$ for any $t \geqslant 0$.

An $\mathbb{R}^d$-valued $\{\mathcal{F}_t\}$-adapted integrable process $\{M_t\}_{t\geqslant 0}$ is a martingale with respect to $\{\mathcal{F}_t\}$ (or simply, martingale) if

$$\mathbb{E}(M_t|\mathcal{F}_s) = M_s \quad \text{a.s. for all } 0 \leqslant s < t < \infty.$$

A stochastic process $X = \{X_t\}_{t\geqslant 0}$ is called square-integrable if $\mathbb{E}|X_t|^2 < \infty$ for every $t \geqslant 0$. If $M = \{M_t\}_{t\geqslant 0}$ is a real-valued square-integrable continuous martingale, then there exists a unique continuous integrable adapted increasing process $\{\langle M, M\rangle_t\}$ such that $\{M_t^2 - \langle M, M\rangle_t\}$ is a continuous martingale vanishing at $t = 0$. The process $\{\langle M, M\rangle_t\}$ is called the quadratic variation of M.

A right continuous adapted process $M = \{M_t\}_{t>0}$ is a local martingale if there exists a nondecreasing sequence $\{\tau_k\}_{k\geqslant 1}$ of stopping times with $\tau_k \uparrow \infty$ a.s. such that every $\{M_{\tau_k \wedge t} - M_0\}_{t\geqslant 0}$ is a martingale. Every martingale is a local martingale, however the converse is not true. If $M = \{M_t\}_{t\geqslant 0}$ and $N = \{N_t\}_{t\geqslant 0}$ are two real-valued continuous local martingales, their joint quadratic variation $\{\langle M, N\rangle\}_{t\geqslant 0}$ is the unique continuous adapted process of finite variation such that $\{M_t N_t - \langle M, N\rangle_t\}_{t\geqslant 0}$ is a continuous local martingale vanishing at $t = 0$. When $M = N, \{\langle M, M\rangle\}_{t\geqslant 0}$ is called the quadratic variation of M.

Theorem 2.2 (**Strong law of large numbers**). *Let $M = \{M_t\}_{t\geqslant 0}$ be a real-valued continuous local martingale vanishing at $t = 0$. Then*

$$\lim_{t\to\infty} \langle M, M\rangle_t = \infty \quad a.s. \quad \Rightarrow \quad \lim_{t\to\infty} \frac{M_t}{\langle M, M\rangle_t} = 0 \quad a.s.$$

and also

$$\limsup_{t\to\infty} \frac{\langle M, M\rangle_t}{t} < \infty \quad a.s. \quad \Rightarrow \quad \lim_{t\to\infty} \frac{M_t}{t} = 0 \quad a.s.$$

2.3 Brownian Motions

In 1828, the Scottish botanist Robert Brown identified the irregular movements of pollen grains known as Brownian motions. A stochastic process $B_t(\omega)$ is adopted to characterise the position of the pollen grain ω at time t.

Definition 2.3. *Let $(\Omega, \mathcal{F}, \mathbb{P})$ be a probability space with a filtration $\{\mathcal{F}_t\}_{t\geqslant 0}$. A (standard) one-dimensional Brownian motion is a real-valued continuous $\{\mathcal{F}_t\}$-adapted process $\{B_t\}_{t\geqslant 0}$ with the following properties:*

(i) $B_0 = 0$ a.s.;

(ii) for $0 \leqslant s < t < \infty$, the increment $B_t - B_s$ is normally distributed with mean zero and variance $t - s$;

(iii) for $0 \leqslant s < t < \infty$, the increment $B_t - B_s$ is independent of $\mathcal{F}_s$.

Some important properties of the Brownian motion are listed below.

(i): $\{-B_t\}$ is a Brownian motion with respect to the same filtration $\{\mathcal{F}_t\}$;

(ii): Let $c > 0$. Define $X_t = \frac{B_{ct}}{\sqrt{c}}$ for $t \geqslant 0$. Then $\{X_t\}$ is a Brownian motion with respect to the filtration $\{\mathcal{F}_{ct}\}$;

(iii): $\{B_t\}$ is a continuous square-integrable martingale and its quadratic variation $\langle B, B\rangle_t = t$ for all $t \geqslant 0$;

(iv): The strong law of large numbers states that

$$\lim_{t\to\infty} \frac{B_t}{t} = 0 \quad \text{a.s.};$$

(v): For almost every $\omega \in \Omega$, the Brownian sample path $B_\cdot(\omega)$ is nowhere differentiable.

Theorem 2.4 (**Law of the Iterated Logarithm**). *For almost every $\omega \in \Omega$, we have*

$$(i)\ \limsup_{t\downarrow 0} \frac{B_t(\omega)}{\sqrt{2t\log\log(1/t)}} = 1 \qquad (ii)\ \liminf_{t\downarrow 0} \frac{B_t(\omega)}{\sqrt{2t\log\log(1/t)}} = -1,$$
$$(iii)\ \limsup_{t\to\infty} \frac{B_t(\omega)}{\sqrt{2t\log\log t}} = 1 \qquad (iv)\ \liminf_{t\to\infty} \frac{B_t(\omega)}{\sqrt{2t\log\log t}} = -1.$$

Definition 2.5. *A d-dimensional process $\{B_t = (B_t^1, \cdots, B_t^d)\}_{t\geqslant 0}$ is called a d-dimensional Brownian motion if every $\{B_t^i\}$ is a one-dimensional Brownian motion and $\{B_t^1\}, \cdots, \{B_t^d\}$ are independent.*

For a d-dimensional Brownian motion, we still have

$$\limsup_{t\to\infty} \frac{|B_t|}{\sqrt{2t\log\log t}} = 1 \quad \text{a.s.}$$

2.4 Stochastic Integrals and the Itô Formula

We shall define the stochastic integral

$$\int_0^t f(s)dB_s$$

with respect to an m-dimensional Brownian motion $\{B_t\}$ for a class of $d \times m$-matrix-valued stochastic processes $\{f(t)\}$. The integral cannot be defined in the ordinary way as the Brownian sample path $B_\cdot(\omega)$ is nowhere differentiable for almost all $\omega \in \Omega$. We first state the concept of simple processes.

Definition 2.6. *A real-valued stochastic process $g = \{g(t)\}_{a \leqslant t \leqslant b}$ is called a simple (or step) process if there exists a partition $a = t_0 < t_1 < \cdots < t_k = b$ of $[a, b]$ and bounded random variables ξ_i, $0 \leqslant i \leqslant k-1$ such that ξ_i is $\mathcal{F}_{t_i}$-measurable and*

$$g(t) = \xi_0 I_{[t_0,t_1]}(t) + \sum_{t=1}^{k-1} \xi_i I_{(t_i,t_{i+1}]}(t). \tag{2.4.1}$$

We denote $\mathcal{M}_0([a, b]; \mathbb{R})$ the family of all such processes.

Definition 2.7. *For a simple process g with the form of (2.4.1) in $\mathcal{M}_0([a, b]; \mathbb{R})$, define*

$$\int_a^b g(t)dB_t = \sum_{i=0}^{k-1} \xi_i (B_{t_{i+1}} - B_{t_i})$$

and call it the stochastic integral of g with respect to the Brownian motion $\{B_t\}$ or the Itô integral.

We then extend the integral definition from simple processes to processes in $\mathcal{M}^2([a, b]; \mathbb{R})$.

Definition 2.8. *Let $f \in \mathcal{M}^2([a, b]; \mathbb{R})$. The Itô integral of f with respect to $\{B_t\}$ is defined by*

$$\int_a^b f(t)dB_t = \lim_{k\to\infty} \int_a^b g_k(t)dB_t \text{ in } L^2(\Omega; \mathbb{R}),$$

where $\{g_k\}$ is a sequence of simple processes such that

$$\lim_{k\to\infty} \mathbb{E} \int_a^b |f(t) - g_k(t)|^2 dt = 0.$$

Let us now introduce some nice properties of the stochastic integral.

Theorem 2.9. *Let $f, g \in \mathcal{M}^2([a,b];\mathbb{R})$ and let α, β be two real numbers. Then*

(i) $\int_a^b f(t)dB_t$ is $\mathcal{F}_b$-measurable;

(ii) $\mathbb{E}\int_a^b f(t)dB_t = 0$;

(iii) $\mathbb{E}|\int_a^b f(t)dB_t|^2 = \mathbb{E}\int_a^b |f(t)|^2 dt$;

(iv) $\int_a^b [\alpha f(t) + \beta g(t)]dB_t = \alpha\int_a^b f(t)dB_t + \beta\int_a^b g(t)dB_t$.

Definition 2.10. *Let $f \in \mathcal{M}^2([0,T];\mathbb{R})$. Define*

$$I(t) = \int_0^t f(s)dB(s) \quad \text{for } 0 \leqslant t \leqslant T,$$

where $I(0) = 0$ by definition. We call $I(t)$ the indefinte Itô integral of f.

Theorem 2.11. *Let $f \in \mathcal{M}^2([0,T];\mathbb{R})$. Then the indefinite integral $I = \{I(t)\}_{0\leqslant t\leqslant T}$ is a square-integrable continuous martingale and its quadratic variation is given by*

$$\langle I, I\rangle_t = \int_0^t |f(s)|^2 ds, \quad 0 \leqslant t \leqslant T.$$

Itô's formula is useful in evaluating the Itô integrals and even plays an essential role in stochastic analysis. Let $B(t) = (B_1(t), \cdots, B_m(t))^T, t \geqslant 0$ be an m-dimensional Brownian motion defined on the complete probability space $(\Omega, \mathcal{F}, \mathbb{P})$ adapted to the filtration $\{\mathcal{F}_t\}_{t\geqslant 0}$.

Definition 2.12. *An n-dimensional Itô process is an $\mathbb{R}^n$-valued continuous adapted process $x(t) = (x_1(t), \cdots, x_n(t))^T$ on $t \geqslant 0$ of the form*

$$x(t) = x(0) + \int_0^t f(s)ds + \int_0^t g(s)dB(s),$$

where $f = (f_1, \cdots, f_n)^T \in \mathcal{L}^1(\mathbb{R}_+;\mathbb{R}^n)$ and $g = (g_{ij})_{n\times m} \in \mathcal{L}^2(\mathbb{R}_+;\mathbb{R}^{n\times m})$. We shall say that $x(t)$ has a stochastic differential $dx(t)$ on $t \geqslant 0$ given by

$$dx(t) = f(t)dt + g(t)dB(t).$$

Let $C^{2,1}(\mathbb{R}^n \times \mathbb{R}_+;\mathbb{R})$ denote the family of all real-valued functions $V(x,t)$ defined on $\mathbb{R}^n \times \mathbb{R}_+$ such that they are continuously twice differentiable in x and once in t. If $V \in C^{2,1}(\mathbb{R}^n \times \mathbb{R}_+;\mathbb{R})$, we set

$$V_t = \frac{\partial V}{\partial t}, \quad V_x = \Big(\frac{\partial V}{\partial x_1}, \cdots, \frac{\partial V}{\partial x_n}\Big),$$

$$V_{xx} = \Big(\frac{\partial^2 V}{\partial x_i \partial x_j}\Big)_{n\times n} = \begin{bmatrix} \frac{\partial^2 V}{\partial x_1 \partial x_1} & \cdots & \frac{\partial^2 V}{\partial x_1 \partial x_n} \\ \vdots & & \vdots \\ \frac{\partial^2 V}{\partial x_n \partial x_1} & \cdots & \frac{\partial^2 V}{\partial x_n \partial x_n}. \end{bmatrix}$$

Theorem 2.13 (**Itô's formula**). *Let $x(t)$ be an n-dimensional Itô process on $t \geqslant$ with the stochastic differential*

$$dx(t) = f(t)dt + g(t)dB(t),$$

where $f \in \mathcal{L}^1(\mathbb{R}_+; \mathbb{R}^n)$ and $g \in \mathcal{L}^2(\mathbb{R}_+; \mathbb{R}^{n\times m})$. Let $V \in C^{2,1}(\mathbb{R}^n \times \mathbb{R}_+; \mathbb{R})$. Then $V(x(t), t)$ is a real-valued Itô process with its stochastic differential given by

$$\begin{aligned} dV(x(t),t) = &\Big[V_t(x(t),t) + V_x(x(t),t)f(t) + \frac{1}{2}trace(g^T(t)V_{xx}(x(t),t)g(t))\Big]dt \\ &+ V_x(x(t),t)g(t)dB(t) \ \ a.s. \end{aligned}$$

Let us now state a multiplication table:

$$\begin{aligned} dtdt = 0, \qquad & dB_i dt = 0, \\ dB_i dB_i = dt, \qquad & dB_i dB_j = 0 \quad \text{if } i \neq j. \end{aligned}$$

For exmaple,

$$dx_i(t)dx_j(t) = \sum_{k=1}^{m} g_{ik}(t)g_{jk}(t)dt.$$

2.5 Stochastic Differential Equations

Let $(\Omega, \mathcal{F}, \mathbb{P})$ be a complete probability space with a filtration $\{\mathcal{F}_t\}_{t\geqslant 0}$ satisfying the usual conditions. Let $B(t) = (B_1(t), \cdots, B_m(t))^T, t \geqslant 0$ be an m-dimensional Brownian motion defined on the probability space. Let $0 \leqslant t_0 < T < \infty$. Let x_0 be an $\mathcal{F}_{t_0}$-measurable $\mathbb{R}^d$-valued random variable such that $\mathbb{E}|x_0|^2 < \infty$. Let $f : \mathbb{R}^d \times [t_0, T] \to \mathbb{R}^d$ and $g : \mathbb{R}^d \times [t_0, T] \to \mathbb{R}^{d\times m}$ be both Borel measurable. Consider the d-dimensional stochastic differential equation of Itô type

$$dx(t) = f(x(t), t)dt + g(x(t), t)dB(t) \quad \text{on } t_0 \leqslant t \leqslant T \tag{2.5.1}$$

with initial value $x(t_0) = x_0$. By the definition of stochastic differential, this equation is equivalent to the following stochastic integral equation:

$$x(t) = x_0 + \int_{t_0}^{t} f(x(s), s)ds + \int_{t_0}^{t} g(x(s), s)dB(s) \quad \text{on } t_0 \leqslant t \leqslant .T \tag{2.5.2}$$

Definition 2.14. *An $\mathbb{R}^d$-valued stochastic process $\{x(t)\}_{t_0 \leqslant t \leqslant T}$ is called a solution of equation* (2.5.1) *if it have the following properties*

(i): $\{x(t)\}$ is continuous and $\mathcal{F}_t$-adapted;

(ii): $\{f(x(t),t)\} \in \mathcal{L}^1([t_0,T];\mathbb{R}^d)$ and $\{g(x(t),t)\} \in \mathcal{L}^2([t_0,T];\mathbb{R}^{d\times m})$;

(iii): equation (2.5.2) *holds for all $t \in [t_0,T]$ with probability 1.*

A solution $\{x(t)\}$is said to be unique if any other solution $\{\bar{x}(t)\}$ is indistinguishable from $\{x(t)\}$, that is

$$\mathbb{P}\{x(t) = \bar{x}(t) \text{ for all } t_0 \leqslant t \leqslant T\} = 1.$$

The following theorem provides the conditions that guarantee the existence and uniqueness of the solution to (2.5.1).

Theorem 2.15. *Assume that there exist two positive constants $\bar{K}$ and K such that*
(i) (Lipschitz condition) for all $x, y \in \mathbb{R}^d$ and $t \in [t_0,T]$

$$|f(x,t) - f(y,t)|^2 \vee |g(x,t) - g(y,t)|^2 \leqslant \bar{K}|x-y|^2; \tag{2.5.3}$$

(ii) (Linear growth condition) for all $(x,t) \in \mathbb{R}^d \times [t_0,T]$

$$|f(x,t)|^2 \vee |g(x,t)|^2 \leqslant K(1+|x|^2). \tag{2.5.4}$$

Then there exists a unique solution $x(t)$ to equation (2.5.1) *and the solution belongs to $\mathcal{M}^2([t_0,T];\mathbb{R}^d)$.*

Theorem 2.16. *Assume that the linear growth condition* (2.5.4) *holds, but the Lipschitz condition* (2.5.3) *is replaced by the following local Lipschitz condition: for every integer $n \geqslant 1$, there exists a positive constant K_n such that for all $t \in [t_0,T]$ and all $x, y \in \mathbb{R}^d$ with $|x| \vee |y| \leqslant n$,*

$$|f(x,t) - f(y,t)|^2 \vee |g(x,t) - g(y,t)|^2 \leqslant K_n|x-y|^2. \tag{2.5.5}$$

Then there exists a unique solution $x(t)$ to equation (2.5.1) *in $\mathcal{M}^2([t_0,T];\mathbb{R}^d)$.*

Theorem 2.17. *Assume that the local Lipschitz condition* (2.5.5) *holds, but the linear growth condition* (2.5.4) *is replaced by the monotone condition: There exists a positive constant K such that for all $(x,t) \in \mathbb{R}^d \times [t_0, T]$*

$$x^T f(x,t) + \frac{1}{2}|g(x,t)|^2 \leqslant K(1+|x|^2).$$

There exists a unique solution $x(t)$ to equation (2.5.1) *in $\mathcal{M}^2([t_0,T];\mathbb{R}^d)$.*

In general, non-linear stochastic differential equations do not have explicit solutions, however, it is possible to provide explicit solutions to linear equations. First consider the linear stochastic differential equation

$$dx(t) = F(t)x(t)dt + \sum_{k=1}^{m} G_k(t)x(t)dB_k(t) \tag{2.5.6}$$

on $[t_0,T]$, where $F(t) = (F_{ij}(t))_{d\times d}$ and $G_k(t) = (G^k_{ij}(t))_{d\times d}$ are Borel-measurable and bounded. For every $j = 1, \cdots, d$, let e_j be the unit column-vector in the x_j-direction, i.e.

$$e_j = (\underbrace{0, \cdots, 0, 1}_{\text{j}}, 0, \cdots, 0)^T.$$

Let $\Phi_j(t) = (\Phi_{1j}(t), \cdots, \Phi_{dj}(t))^T$ be the solution of equation (2.5.6) with initial value $x(t_0) = e_j$. Define the $d \times d$ matrix

$$\Phi(t) = (\Phi_1(t), \cdots, \Phi_d(t)) = (\Phi_{ij}(t))_{d\times d}.$$

We call $\Phi(t)$ the fundamental matrix of equation (2.5.6).

Theorem 2.18. *Given the initial value $x(t_0) = x_0$, the unique solution of equation* (2.5.6) *is*

$$x(t) = \Phi(t)x_0.$$

Lemma 2.19. *Let $a(\cdot), b_k(\cdot)$ be real-valued borel measurable bounded functions on $[t_0,T]$. Then*

$$y(t) = y_0 \exp\Big[\int_{t_0}^{t}\Big(a(s) - \frac{1}{2}\sum_{k=1}^{m} b_k^2(s)\Big)ds + \sum_{k=1}^{m}\int_{t_0}^{t} b_k(s)dB_k(s)\Big]$$

is the unique solution to the scalar linear stochastic differential equation

$$dy(t) = a(t)y(t)dt + \sum_{k=1}^{m} b_k(t)y(t)dB_k(t)$$

on $[t_0,T]$ with initial value $y(t_0) = y_0$.

Now consider a general d-dimensional linear stochastic differential equation

$$dx(t) = (F(t)x(t) + f(t))dt + \sum_{k=1}^{m}(G_k(t)x(t) + g_k(t))dB_k(t) \tag{2.5.7}$$

on $[t_0, T]$ with initial value $x(t_0) = x_0$. Equation (2.5.6) is called the corresponding homogeneous equation of system (2.5.7). The unique solution of (2.5.7) can then be deduced by the following variation-of-constants formula.

Theorem 2.20. *The unique solution of equation* (2.5.7) *can be expresses as*

$$\begin{aligned} x(t) = \Phi(t)\Big(x_0 + \int_{t_0}^{t} \Phi^{-1}(s)\Big[f(s) - \sum_{k=1}^{m} G_k(s)g_k(s)\Big]ds \\ + \sum_{k=1}^{m}\int_{t_0}^{t} \Phi^{-1}(s)g_k(s)dB_k(s)\Big), \end{aligned}$$

where $\Phi(t)$ *is the fundamental matrix of the corresponding homogeneous equation* (2.5.6).

2.6 Markov Processes

This section concerns some basic concepts about a Markov process. An n-dimensional $\mathcal{F}_t$-adapted process $X = \{X_t\}_{t\geqslant 0}$ is called a Markov process if the following Markov property is satisfied: for all $0 \leqslant s \leqslant t < \infty$ and $A \in \mathcal{B}(\mathbb{R}^n)$,

$$\mathbb{P}(X(t) \in A|\mathcal{F}_s) = \mathbb{P}(X(t) \in A|X(s)).$$

An equivalent statement is: for any bounded Borel measurable function $\varphi : \mathbb{R}^n \to \mathbb{R}$ and $0 \leqslant s \leqslant t < \infty$,

$$\mathbb{E}(\varphi(X(t))|\mathcal{F}_s) = \mathbb{E}(\varphi(X(t))|X(s)).$$

The transition probability or function of the Markov process is a function $P(s, x; t, A)$ defined on $0 \leqslant s \leqslant t < \infty$, $x \in \mathbb{R}^n$ and $A \in \mathcal{B}(\mathbb{R}^n)$, with the following properties:

(i) For every $0 \leqslant s \leqslant t < \infty$ and $A \in \mathcal{B}(\mathbb{R}^n)$,

$$\mathbb{P}(s, X(s); t, A) = \mathbb{P}(X(t) \in A|X(s));$$

(ii) $\mathbb{P}(s,x;t,\cdot)$ is a probability measure on $\mathcal{B}(\mathbb{R}^n)$ for every $0 \leqslant s \leqslant t < \infty$ and $x \in \mathbb{R}^n$;

(iii) $\mathbb{P}(s,\cdot;t,A)$ is Borel measurable for every $0 \leqslant s \leqslant t < \infty$ and $A \in \mathcal{B}(\mathbb{R}^n)$;

(iv) The Kolmogorov-Chapman equation

$$\mathbb{P}(s,x;t,A) = \int_{\mathbb{R}^n} \mathbb{P}(u,y;t,A)\mathbb{P}(s,x;u,dy)$$

holds for any $0 \leqslant s \leqslant u \leqslant t < \infty, x \in \mathbb{R}^n$ and $A \in \mathcal{B}(\mathbb{R}^n)$.

A Markov process $X = \{X(t)\}_{t\geqslant 0}$ is said to be homogeneous if its transition probability $\mathbb{P}(s,x;t,A)$ is stationary, that is,

$$\mathbb{P}(s+u,x;t+u,A) = \mathbb{P}(s,x;t,A)$$

for all $0 \leqslant s \leqslant t < \infty, x \in \mathbb{R}^n, u \geqslant 0$ and $A \in \mathcal{B}(\mathbb{R}^n)$.

A stochastic process $X = \{X(t)\}_{t\geqslant 0}$ defined on a probability space $(\Omega, \mathcal{F}, \mathbb{P})$ with values in a countable set Ξ (to be called the state space of the process), is called a continuous-time Markov chain if for any finite set $0 \leqslant t_1 < t_2 < \cdots < t_n < t_{n+1}$ of "times", and corresponding set $i_1, i_2, \cdots, i_{n-1}, i, j$ of states in Ξ such that $\mathbb{P}\{X(t_n) = i, X(t_{n-1}) = i_{n-1}, \cdots, X(t_1) = i_1\} > 0$, we have

$$\begin{aligned}\mathbb{P}\{X(t_{n+1}) = j | X(t_n) = i, X(t_{n-1}) = i_{n-1}, \cdots, X(t_1) = i_1\} \\ = \mathbb{P}\{X(t_{n+1}) = j | X(t_n) = i\}.\end{aligned}$$

If for all s,t such that $0 \leqslant s \leqslant t < \infty$ and all $i,j \in \Xi$ the conditional probability $\mathbb{P}\{X(t) = j | X(s) = i\}$ depends only on $t-s$, we say that the process $X = \{X(t)\}_{t\geqslant 0}$ is homogeneous. In this case, $\mathbb{P}\{X(t) = j | X(s) = i\} = \mathbb{P}\{X(t-s) = j | X(0) = i\}$, and the function

$$\mathbb{P}_{ij}(t) = \mathbb{P}\{X(t) = j | X(s) = i\}, i, j \in \Xi, t \geqslant 0,$$

is known as the transition function or transition probability of the process. The function $P_{ij}(t)$ is standard if $\lim_{t\to 0} \mathbb{P}_{ii}(t) = 1$ for all $i \in \Xi$.

Theorem 2.21. *Let $\mathbb{P}_{ij}$ be a standard transition function, then $\gamma_i := \lim_{t\to 0} \frac{1-\mathbb{P}_{ii}}{t}$ exists (but may be ∞) for all $i \in \Xi$.*

A state $i \in \Xi$ is said to be stable if $\gamma_i < \infty$.

Theorem 2.22. *Let P_{ij} be a standard transition function, and let j be a stable state. Then $\gamma_{ij} = P'_{ij}(0)$ exists and is finite for all $i \in \Xi$.*

Let $\gamma_{ij} = -\gamma_i$ and $\Gamma = (\gamma_{ij})_{i,j\in\Xi}$. Γ is called the generator of the Markov chain. If the state space is finite which we can take to be $\mathbb{S} = \{1, 2, \cdots, N\}$, then the process is called a continuous-time finite Markov chain. Throughout this thesis, we assume that all Markov chains are finite and all states are stable. For such a Markov chain, almost every sample path is right continuous step function.

Theorem 2.23. *Let $P(t) = (P_{ij}(t))_{N\times N}$ be the transition probability matrix and $\Gamma = (\gamma_{ij})_{N\times N}$ be the generator of a finite Markov chain. Then*

$$P(t) = e^{t\Gamma}.$$

It is useful to emphasise that a continuous-time Markov chain $X(t)$ with generator $\Gamma = \{\gamma_{ij}\}_{N\times N}$ can be represented as a stochastic integral with respect to a Poisson random measure. Indeed, let Δ_{ij} be consecutive, left closed, right open intervals of the real line each having length γ_{ij} such that

$$\begin{aligned}
\Delta_{12} &= [0, \gamma_{12}),\\
\Delta_{13} &= [\gamma_{12}, \gamma_{12} + \gamma_{13}),\\
&\vdots\\
\Delta_{1N} &= \Big[\sum_{j=2}^{N-1} \gamma_{1j}, \sum_{j=2}^{N} \gamma_{1j}\Big),\\
\Delta_{21} &= \Big[\sum_{j=2}^{N} \gamma_{1j}, \sum_{j=2}^{N} \gamma_{1j} + \gamma_{21}\Big),\\
\Delta_{23} &= \Big[\sum_{j=2}^{N} \gamma_{1j} + \gamma_{21}, \sum_{j=2}^{N} \gamma_{1j} + \gamma_{21} + \gamma_{23}\Big),\\
&\vdots\\
\Delta_{2N} &= \Big[\sum_{j=2}^{N} \gamma_{1j} + \sum_{j=1,j\neq 2}^{N} \gamma_{2j}, \sum_{j=2}^{N} \gamma_{1j} + \sum_{j=1,j\neq 2}^{N} \gamma_{2j}\Big)
\end{aligned}$$

and so on. Define a function $h : \mathbb{S} \times \mathbb{R} \to \mathbb{R}$ *by*

$$h(i,y) = \begin{cases} j-i, & \text{if } y \in \Delta_{ij} \\ 0, & \text{otherwise.} \end{cases} \tag{2.6.1}$$

Then

$$dX(t) = \int_{\mathbb{R}} h(X(t-), y)\nu(dt, dy),$$

with initial condition $X(0) = i_0$*, where* $\nu(dt, dy)$ *is a Poisson random measure with intensity* $dt \times \mu(dy)$*, in which* μ *is the Lebesgue measure on* $\mathbb{R}$*.*

2.7 Generalised Itô's Formula

Let $(\Omega, \mathcal{F}, \{\mathcal{F}_t\}_{t\geqslant 0}, \mathbb{P})$ be a complete probability space with a filtration $\{\mathcal{F}_t\}_{t\geqslant 0}$ satisfying the usual conditions (i.e. it is increasing and right continuous while $\mathcal{F}_0$ contains all $\mathbb{P}$-null sets). Let $B(t) = (B_t^1, \cdots, B_t^m)^T$ be an m-dimensional Brownian motion defined on the probability space. Let $r(t), t \geqslant 0$ be a right-continuous Markov chain on the probability space taking values in a finite state space $\mathbb{S} = \{1, 2, \cdot, N\}$ with generator $\Gamma = (\gamma_{ij})_{N\times N}$ given by

$$\mathbb{P}\{r(t+\delta) = j | r(t) = i\} = \begin{cases} \gamma_{ij}\delta + o(\delta), & \text{if } i \neq j \\ 1 + \gamma_{ii}\delta + o(\delta), & \text{if } i = j, \end{cases}$$

where $\delta > 0$. Here $\gamma_{ij} \geqslant 0$ is transition rate from i to j if $i \neq j$ while

$$\gamma_{ii} = -\sum_{j\neq i} \gamma_{ij}.$$

We assume that the Markov chain $r(\cdot)$ is independent of the Brownian motion $B(\cdot)$.

Let $x(t)$ be an n-dimensional Itô process on $t \geqslant 0$ with the stochastic differential

$$dx(t) = f(t)dt + g(t)dB(t),$$

where $f \in \mathcal{L}^1(\mathbb{R}_+, \mathbb{R}^n)$ and $g \in \mathcal{L}^2(\mathbb{R}_+, \mathbb{R}^{n\times m})$. Let $C^{2,1}(\mathbb{R}^n \times \mathbb{R}_+ \times \mathbb{S}; \mathbb{R})$ be the family of all real-valued functions $V(x,t,i)$ on $\mathbb{R}^n \times \mathbb{R}_+ \times \mathbb{S}$ which are continuously

twice differentiable in x and once in t. If $V \in C^{2,1}(\mathbb{R}^n \times \mathbb{R}_+ \times \mathbb{S}; \mathbb{R})$, define an operator LV from $\mathbb{R}^n \times \mathbb{R}_+ \times \mathbb{S}$ to $\mathbb{R}$ by

$$LV(x,t,i) = V_t(x,t,i) + V_x(x,t,i)f(t) + \frac{1}{2}\text{trace}[g^T(t)V_{xx}(x,t,i)g(t)] + \sum_{j=1}^{N} \gamma_{ij}V(x,t,j),$$

where

$$V_t(x,t,i) = \frac{\partial V(x,t,i)}{\partial t}, \quad V_x(x,t,i) = \Big(\frac{\partial V(x,t,i)}{\partial x_1}, \cdots, \frac{\partial V(x,t,i)}{\partial x_n}\Big)$$

and

$$V_{xx}(x,t,i) = \Big(\frac{\partial^2 V(x,t,i)}{\partial x_i \partial x_j}\Big)_{n\times n}.$$

Let us now state the generalised Itô formula.

Theorem 2.24. *If $V \in C^{2,1}(\mathbb{R}^n \times \mathbb{R}_+ \times \mathbb{S}; \mathbb{R})$, then for any $t \geqslant 0$*

$$\begin{aligned} V(x(t),t,r(t)) = V(x(0),0,r(0)) &+ \int_0^t LV(x(s),s,r(s))ds \\ &+ \int_0^t V_x(x(s),s,r(s))g(x(s),s,r(s))dB(s) \\ &+ \int_0^t \int_{\mathbb{R}} (V(x(s),s,i_0 + h(r(s),l)) - V(x(s),s,r(s)))\mu(ds,dl), \end{aligned}$$

where the function h is defined by (2.6.1) *and $\mu(ds,dl) = \nu(ds,dl) - \mu(dl)ds$ is a martingale measure, while ν and μ have been determined at the end of Section 2.6.*

2.8 Stochastic Differential Equations with Markovian Switching

We assume that the Markov chain $r(\cdot)$ is $\mathcal{F}_t$-adapted but independent of the Brownian motion $B(\cdot)$. A stochastic differential equation with Markovian switching is in the form

$$dx(t) = f(x(t),t,r(t))dt + g(x(t),t,r(t))dB(t), \quad t_0 \leqslant t \leqslant T \tag{2.8.1}$$

with initial data $x(t_0) = x_0 \in L^2_{\mathcal{F}_{t_0}}(\Omega; \mathbb{R}^n)$ and $r(t_0) = r_0$, where r_0 is an $\mathbb{S}$-valued $\mathcal{F}_{t_0}$-measurable random variable and

$$f : \mathbb{R}^n \times \mathbb{R}_+ \times \mathbb{S} \to \mathbb{R}^n \text{ and } g : \mathbb{R}^n \times \mathbb{R}_+ \times \mathbb{S} \to \mathbb{R}^{n\times m}.$$

Definition 2.25. *An $\mathbb{R}^n$-valued stochastic process $\{x(t)\}_{t_0\leqslant t\leqslant T}$ is a solution of equation* (2.8.1) *if the following properties hold:*

(i): $\{x(t)\}_{t_0\leqslant t\leqslant T}$ is continuous and $\mathcal{F}_t$-adapted;

(ii): $\{f(x(t),t,r(t))\}_{t_0\leqslant t\leqslant T}\in\mathcal{L}^1([t_0,T];\mathbb{R}^n)$ while $\{g(x(t)),t,r(t)\}_{t_0\leqslant t\leqslant T}\in\mathcal{L}^2([t_0,T];\mathbb{R}^{n\times m})$;

(iii): for any $t\in[t_0,T]$, equation

$$x(t)=x(t_0)+\int_{t_0}^t f(x(s),s,r(s))ds+\int_{t_0}^t g(x(s),s,r(s))dB(s)$$

holds with probability 1.

Theorem 2.26. *Assume that there exist two positive constants $\bar{K}$ and K such that the following two properties hold:*

(Lipschitz condition) for all $x,y\in\mathbb{R}^n, t\in[t_0,T]$ and $i\in\mathbb{S}$

$$|f(x,t,i)-f(y,t,i)|^2\vee|g(x,t,i)-g(y,t,i)|^2\leqslant\bar{K}|x-y|^2 \tag{2.8.2}$$

(Linear growth condition) for all $(x,t,i)\in\mathbb{R}^n\times[t_0,T]\times\mathbb{S}$

$$|f(x,t,i)|^2\vee|g(x,t,i)|^2\leqslant K(1+|x|^2). \tag{2.8.3}$$

Then there exists a unique solution $x(t)\in\mathcal{M}^2([t_0,T];\mathbb{R}^n)$ to equation (2.8.1).

Theorem 2.27. *Assume that (local Lipschitz condition) for every integer $k\geqslant 1$, there exists a positive constant h_k such that for all $t\in[t_0,T], i\in\mathbb{S}$ and those $x,y\in\mathbb{R}^n$ with $|x|\vee|y|\leqslant k$,*

$$|f(x,t,i)-f(y,t,i)|^2\vee|g(x,t,i)-g(y,t,i)|^2\leqslant\bar{h}_k|x-y|^2, \tag{2.8.4}$$

Then there exists a unique maximal local solution to equation (2.8.1).

Theorem 2.28. *Assume that the local Lipschitz condition* (2.8.4) *and the linear growth condition* (2.8.3) *are satisfied. Then the conclusions of Theorem 2.26 still hold.*

Theorem 2.29. *Assume that the local Lipschitz condition* (2.8.4) *holds, but the linear growth condition* (2.8.3) *is replaced with the following monotone condition: There exists a positive constant K such that for all $(x,t,i)\in\mathbb{R}\times[t_0,T]\times\mathbb{S}$*

$$x^Tf(x,t,i)+\frac{1}{2}|g(x,t,i)|^2\leqslant K(1+|x|^2).$$

There there exists a unique solution $x(t)$ to equation (2.8.1) *in $\mathcal{M}^2([t_0,T];\mathbb{R})$.*

2.9 Useful Inequalities

In this section we state some frequently used inequalities which we adopt in this thesis. We start from the simplest one:

$$2ab \leqslant a^2 + b^2, \quad \forall a, b \in \mathbb{R}.$$

It then follows that

$$2ab \leqslant \epsilon a^2 + \frac{1}{\epsilon} b^2, \quad \forall a, b \in \mathbb{R} \text{ and } \forall \epsilon > 0.$$

Young's inequality states that

$$|a|^{\beta}|b|^{(1-\beta)} \leqslant \beta|a| + (1-\beta)|b|, \forall a, b \in \mathbb{R} \text{ and } \forall \beta \in [0, 1].$$

Another important one is **Hölder's inequality**:

$$|\mathbb{E}(X^T Y)| \leqslant (\mathbb{E}|X|^p)^{1/p} (\mathbb{E}|Y|^q)^{1/q}$$

if $p > 1, 1/p + 1/q = 1, X \in L^p$ and $Y \in L^q$. An application of Hölder's inequality implies

$$(\mathbb{E}|X|^r)^{1/r} \leqslant (\mathbb{E}|X|^p)^{1/p}$$

if $0 < r < p < \infty$ and $X \in L^p$. **Chebyshev's inequality** is given as

$$\mathbb{P}\{\omega : |X(\omega)| \geqslant c\} \leqslant c^{-p} \mathbb{E}|X|^p$$

if $c > 0, p > 0, X \in L^p$.

Theorem 2.30 (**Gronwall's inequality**). *Let $T > 0$ and $c \geqslant 0$. Let $u(\cdot)$ be a Borel measurable bounded non-negative function on $[0, T]$, and let $v(\cdot)$ be a non-negative integrable function on $[0, T]$. If*

$$u(t) \leqslant c + \int_0^t v(s)u(s)ds \quad \textit{for all } 0 \leqslant t \leqslant T,$$

then

$$u(t) \leqslant c \exp\Big(\int_0^t v(s)ds \Big) \quad \textit{for all } 0 \leqslant t \leqslant T.$$

The following theorem is known as the Burkholder-Davis-Gundy inequality.

Theorem 2.31. *Let $g \in \mathcal{L}^2(\mathbb{R}_+;\mathbb{R}^{n\times m})$. For $t \geqslant 0$, define*

$$x(t) = \int_0^t g(s)dB(s) \quad \textit{and} \quad A(t) = \int_0^t |g(s)|^2 ds.$$

Then for every $p > 0$, there exist universal positive constants c_p and C_p, which are only dependent on p, such that

$$c_p \mathbb{E}|A(t)|^{p/2} \leqslant \mathbb{E}(\sup_{0\leqslant s\leqslant t} |x(s)|^p) \leqslant C_p \mathbb{E}|A(t)|^{p/2}$$

for all $t \geqslant 0$. In particular, one may take

$$\begin{aligned} c_p = (p/2)^p, \qquad & C_p = (32/p)^{p/2} && \textit{if } 0 < p < 2; \\ c_p = 1, \qquad & C_p = 4 && \textit{if } p = 2; \\ c_p = (2p)^{-p/2}, \qquad & C_p = [p^{p+1}/2(p-1)^{p-1}]^{p/2} && \textit{if } p > 2. \end{aligned}$$

Theorem 2.32 (**The exponential martingale inequality**)**.** *Let $g = (g_1, \cdots, g_m) \in \mathcal{L}^2(\mathbb{R}_+;\mathbb{R}^{1\times m})$, and let T, α, β be any positive numbers. Then*

$$\mathbb{P}\Big\{ \sup_{0\leqslant t\leqslant T} \Big[\int_0^t g(s)dB(s) - \frac{\alpha}{2}\int_0^t |g(s)|^2 ds \Big] > \beta \Big\} \leqslant e^{-\alpha\beta}.$$

Chapter 3

Stochastic Modelling of Sea-Loch Nutrient

3.1 Introduction

The enrichment of nutrients in an aquatic ecosystem can affect the water quality, regulate the aquatic primary productivity and even change the structure and function of the environment [50, 101, 128]. The importance of understanding the dynamical behaviours of the aquatic nutrients has been increasingly recognised. In particular, mathematical modelling is a powerful tool to describe the changes in the aquatic nutrient resources. In 1991, a comprehensive field campaign was carried out by Marine Scotland Science in Loch Linnhe, where a large amount of hydrographic and chemical data were collected. The high-resolution measurements allow us to model the fjord nitrate, which is often most limiting to the phytoplankton growth [40]. Stochastic modelling approach is employed in this chapter to interpret the environmental-type process noise in the nitrate data [15, 31, 31, 44, 73, 82, 82, 86]. More precisely, this chapter aims to formulate an SDE model which captures the seasonal trends of the surface nitrate in Loch Linnhe. Meanwhile, the reliability of our model can be evaluated based on the observed data [39].

The structure of this chapter is as follows: Section 3.2 and 3.3 briefly introduce the physical and biological environment of Loch Linnhe respectively. In

section 3.4, we formulate a stochastic differential equation (SDE) model of the fjord nitrate and then study the model fit for the one-month data. In section 3.5, our model is refined to capture the annual variability in the fjord nitrate. This requires the consideration of the complex physical and biological processes which make big effects on the dynamics of the sea-loch nitrate. Meanwhile we construct a separate SDE model which depicts the variations in the sea-loch salinity. By combining the salinity model with the existing nitrate one, we obtain a coupled SDE system. Section 3.6 illustrates the existence of the process noise in the nitrate and salinity data, based on the residual analysis for the data. In section 3.7, we design a simulation study to examine the accuracy of our parameter estimation techniques. We finally draw a conclusion in section 3.8.

3.2 Physical Environment of Loch Linnhe

Sea lochs, also known as fjords, are narrow arms of the open sea which extend many miles inland from mountainous coasts. There are many fjords on the coasts of Greenland, Iceland, New Zealand, Norway and Scotland, etc. [50, 118]. Loch Linnhe is a sea loch on the west coast of Scotland from Firth of Lorn to Fort William in a SW-NE direction and is about 50 kilometres long. The fundamental physical features of the fjord ecosystem are the basis for the biology, ecology and productivity of the region. The interactions between the bathymetry, meteorological forcing, freshwater inflows and tides complicate the circulation patterns and eventually form an estuarine circulation. These lead to a complex hydrographic environment of Loch Linnhe. This section gives a brief introduction on the physical characteristics of Loch Linnhe.

3.2.1 Winds

The prevailing wind directions in Loch Linnhe are from the southwest and from the east. Due to the fact that side lochs are oriented in different directions, wind forcing is variable in space. Wind in fjords often affects the distributions of temperature and salinity. In dynamically wide systems, the strong winds can cause up-and downwelling events. In Loch Linnhe, up-and downwelling areas can interact and the system is influenced by different wind forcing, meanwhile the local bathymetry

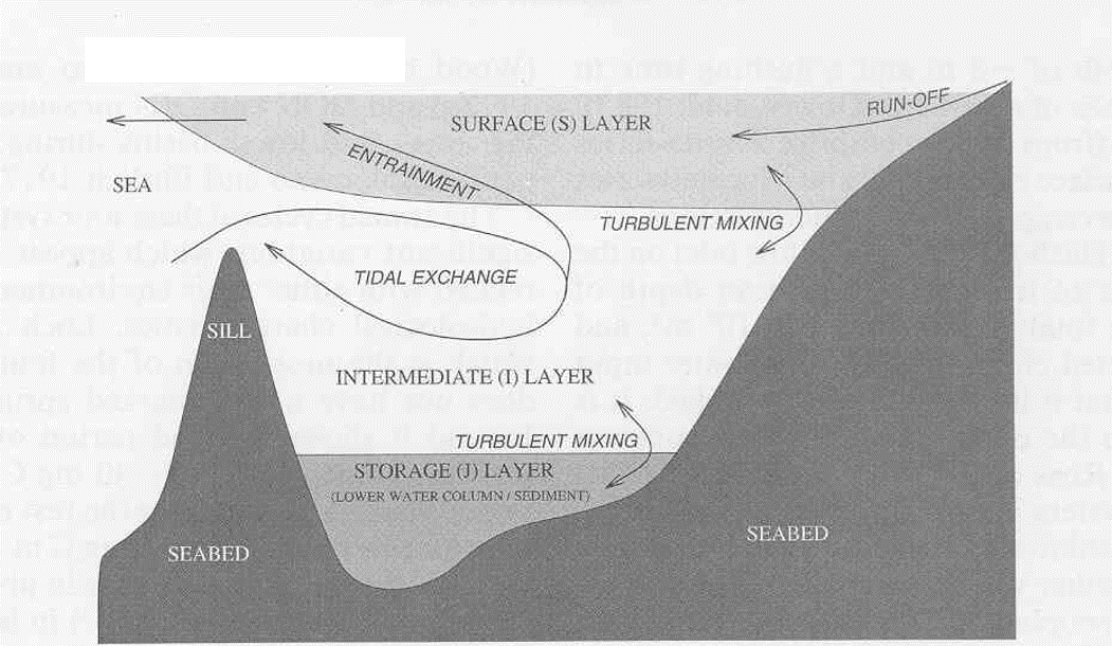

Figure 3.1: A schematic representation of fjord hydrodynamics (picture from [50]).

makes the circulation more complex. Outer Loch Linnhe is dynamically wide. In wind-free conditions, the shallow water flowing downwards hugs the western coastline [106]. However the presence of wind forcing results in different surface patterns [122]. Especially, prevailing winds from the southwest push surface layer across the loch to the eastern coast, and winds from southeast push shallow water up to the Corran Narrows.

3.2.2 Tides

In a fjord ecosystem, tidal flows around the sill are often turbulent and at high velocity, causing a strong mixing between open sea and deep water (figure 3.1). Moreover the deep water is coupled to the surface layer by tidal upwelling and turbulent diffusion [50]. In Loch Linnhe, tides are dominated by the semi-diurnal M2 tide with amplitudes of 1.30 m at the northern end of the loch and 1.26 m at the southern end. Tidal flows through the Corran Narrows can reach 2.5 ms^{-1} at spring tides, causing strong mixing around the sill [99]. The dynamics at the sills can lead to deep-water renewal. Rabe and Hindson [106] pointed out that tides have a bigger effect on the currents below the wind-influenced surface layer.

3.2.3 Freshwater

Fjords always occur in mountainous regions with high rainfall [50]. In Loch Linnhe, the mean annual rainfall is between 2200 and 2800 mmy^{-1} and in the high-lying areas it can exceed 2800 mmy^{-1} (UK Met Office). Close to sea level, the average rainfall from 1981 to 2010 was 1681 mmy^{-1} at Dunstaffnage and 1809 mmy^{-1} at Tulloch Bridge near Fort William (UK Met Office). According to [37], the observed mean freshwater inflow to Loch Linnhe system is $7553 \times 10^6 m^3 y^{-1}$. In particular, 47% comes from the catchment area of inner Loch Linnhe and Loch Eil, and 40% originates from the catchment of Loch Etive. Freshwater inflows by the largest rivers Lochy and Nevis are monitored by the Centre for Ecology and Hydrography (CEH, National River Flow Archive).

3.2.4 Estuarine Circulation

In Loch Linnhe, the interactions between the bathymetry, winds, tides, freshwater inflows and Earth's rotation form an estuarine circulation, which conforms the classical theory of estuarine circulation [117]. This makes the hydrographic environment in Loch Linnhe complex and varied spatially and temporally. The shallow water with salinities sometimes below 20 flows out of the loch while a deeper layer with salinities between 30 and 33 flows into the system. The exchange across sills due to tidal streams lead to deep-water renewal.

3.3 Biological Environment of Loch Linnhe

A group of physical factors due to fjords' rather subtle hydrodynamics deeply affect the biological components of a sea-loch ecosystem. The basic interactions of these biological components can be illustrated by an aquatic food web (Figure 3.2), where the inorganic nutrient links all the trophic levels. Firstly, a phytoplankton group, often dominated by a single phytoplankton species, takes up dissolved inorganic nutrient, and is grazed by zooplankton which is also frequently dominated by a single species. Then zooplankton is consumed by carnivores (jellyfish). Faecal pellets and dead individuals from these living plants and animals enter the detritus. The nutrient they contain is remineralised to inorganic nutrient by

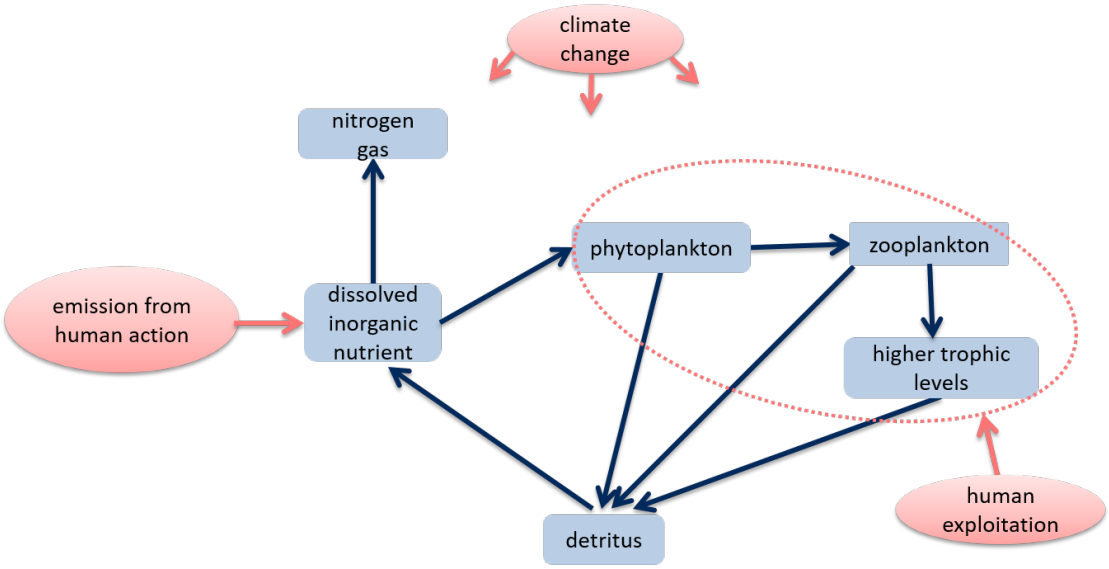

Figure 3.2: A schematic representation of an aquatic food web.

bacterial action in the sediment. Through denitrification the dissolve nutrient is converted to nitrogen gas [50]. Human activities result in strong alterations in the structure and function of the ecosystems [123]. Figure 3.2 suggests the two main ways in which human influence a food web. Firstly human-related activities such as industrial effluents, agricultural runoff and municipal sewage can cause eutrophication [72]. Secondly, over-fishing may disrupt the food chain and finally destroy the balance of the ecology. Moreover, an aquatic system is affected by climate change. In particular, the variations in the water temperature can alter the fundamental ecological processes and the geographic distribution of the species [65].

In Loch Linnhe, ecological research is carried out to understand biodiversity, biogeochemistry and plankton and benthic ecology through observations and ecosystem modelling. In particular, Marine Scotland Science has implemented a comprehensive field program in 1991. This campaign has provided a variety of hydrographic and chemical measurements, including the hydro-chemistry, phytoplankton taxonomy, zooplankton net (30 um) and OPC profiles, carbon, nitrate and ammonia uptake, zooplankton excretion and gut fluorescence, micro-heterotroph production, bacterial production, and sediment nitrate and ammonia

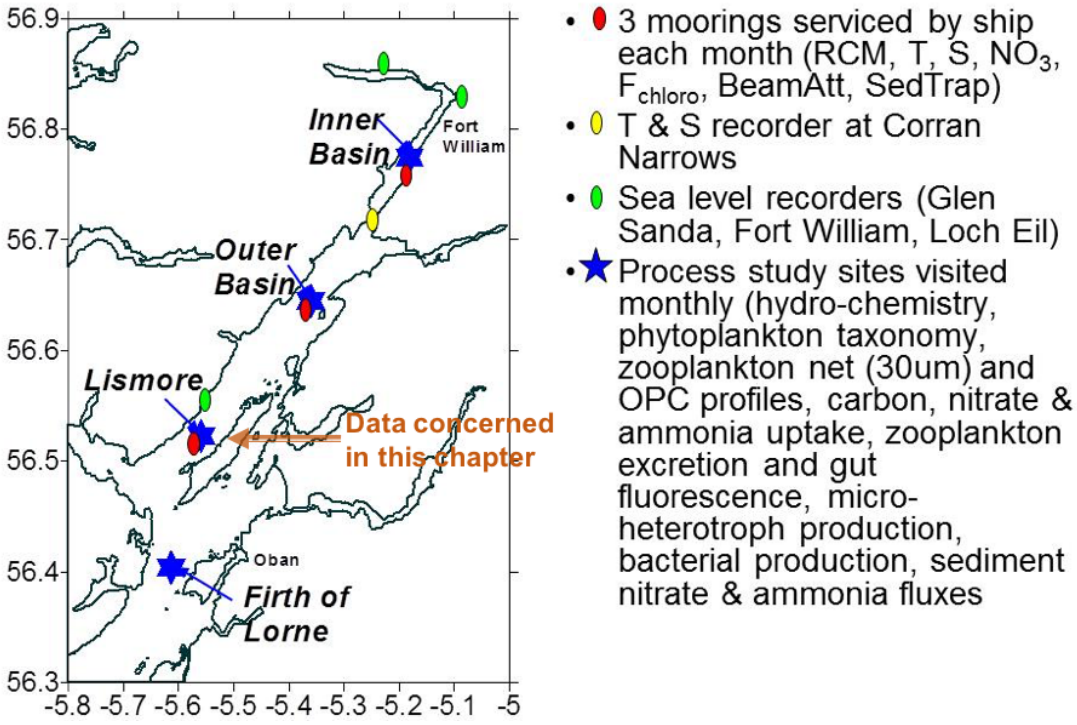

Figure 3.3: Locations of the moorings and process-study sites during the 1991 study in Loch Linnhe (picture from [105]). Data covered in this chapter were collected from the outer basin during the monthly process studies.

fluxes. More details about this program are described below.

3.3.1 The 1991 Field Campaign

During 1991, the vessel "Lough Foyle" conducted sampling through 12 surveys at about 30-day intervals in Loch Linnhe. The main sampling areas were the Firth of Lorn and the inner and outer basins of Loch Linnhe. A series of methods were used to implement intensive surveys in the loch and an area of the open sea outside the loch in the Firth of Lorn. Firstly, the ARIES system [36] was towed in a vertically undulating track along the axis of the loch and out to the sea. Next the instruments were towed on a track at a depth of 4 m and the track travelled back and forth across the loch in a horizontal plane. Finally a Methot-Isaacs-Kidd Trawl (MIKT) was deployed at ten sites along the axis of the loch to sample the fish larvae and macroplankton on each cruise. Apart from these mobile surveys, four

fixed sampling stations were set up on each of the 12 cruises to carry out process studies (Figure 3.3). The stations included two in the outer basin, one in the Firth of Lorn and one in the inner basin of Loch Linnhe. In these three locations, the instrumented moorings were maintained during the study period from January 1991 to February 1992, and the instruments were serviced at monthly intervals (Figure 3.3). More information about this field campaign can be found in [105].

Data from the 1991 Surveys

The 1991 field program provided us with a variety of hydrographic and chemical data. All the data are held by Marine Scotland Science. Figure 3.4 and 3.5 show some time series of the high-resolution data collected from the outer basin (Figure 3.3) during the monthly process studies. These observations are used to examine our model reliability.

Surface Nitrate Data The moored nitrate instruments were replaced regularly, causing different amplitudes of instrument error in the nitrate data (see Figure 3.4(a)). This can lead to difficulties in data fitting. Hence we modify the nitrate data by scaling the instrument error using the formula:

$$x_m(t) = \frac{\sigma_i}{\sigma_c(t)}(x_o(t) - \bar{x}_o(t)) + \bar{x}_o(t),$$

where $x_o(t)$ represents the nitrate observation from a certain instrument at time t, $x_m(t)$ is the corresponding modified nitrate at time t, σ_i is the ideal value for the standard deviation determined by the data from June to September, $\sigma_c(t)$ denotes the standard deviation of the nitrate observation from a certain instrument, $\bar{x}_o(t)$ is the average value of the nitrate data from a certain instrument. The modified surface nitrate data are shown in Figure 3.4(a).

Sea Level Data The moored sea-level instruments were replaced regularly. This may result in an offset provided that a new instrument was not replaced at exactly the same position as the old one. As a result, the sea-level data is modified by taking out the possible offsets (Figure 3.4(b)).

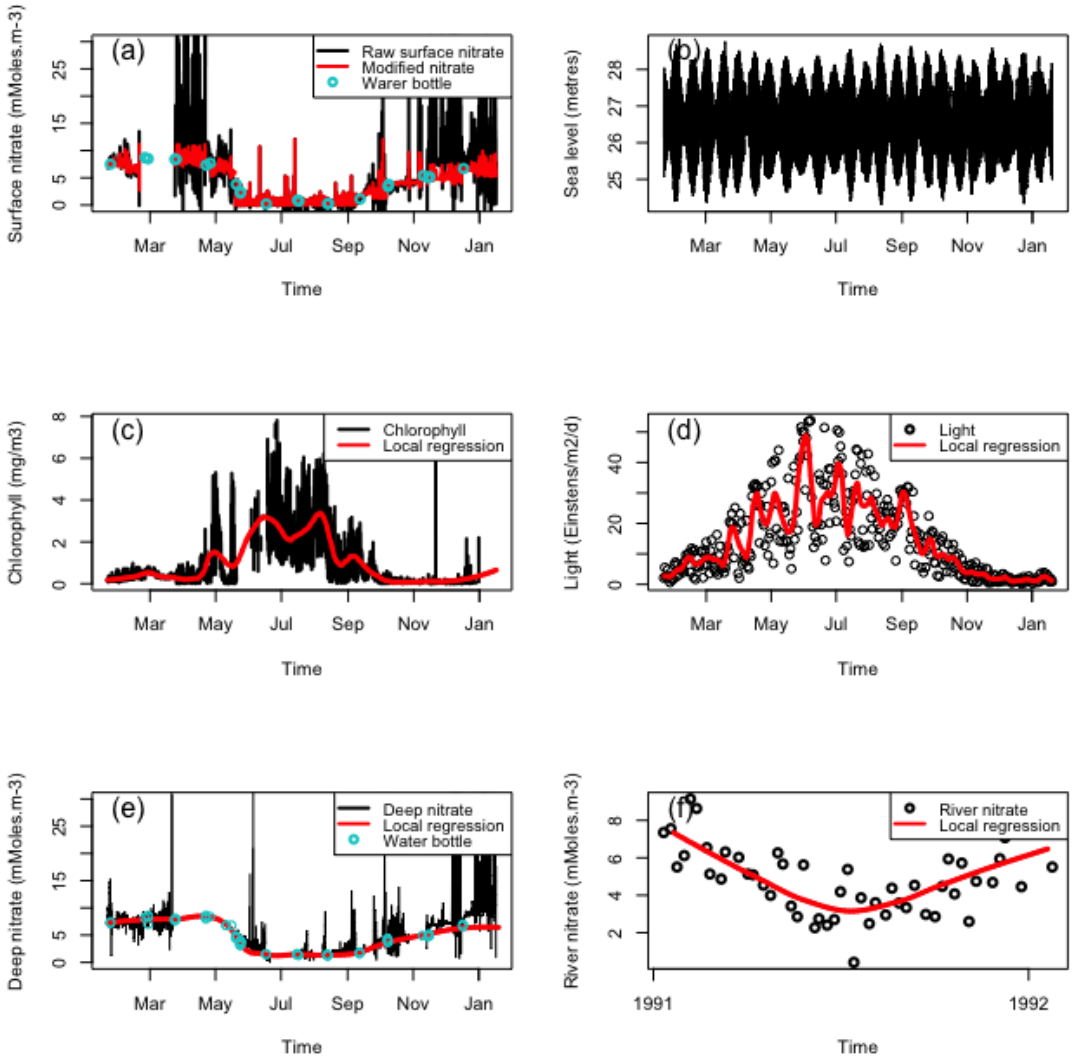

Figure 3.4: (a) Time series of the hourly surface nitrate concentrations ($mMoles \cdot m^{-3}$) from the moored nitrate analysers (black lines), its modified version (red lines) and water bottle data (green points). (b) Modified sea level data ($metres$) from moored sensor. (c) Hourly chlorophyll data (mg/m^3) and its local regression. (d) Integrated light intensity $Einstens/m^2/d$ and its local regression. (e) Hourly deep nitrate data ($mMoles \cdot m^{-3}$), its local regression and the water bottle data. (f) River nitrate ($mMoles \cdot m^{-3}$) and its local regression.

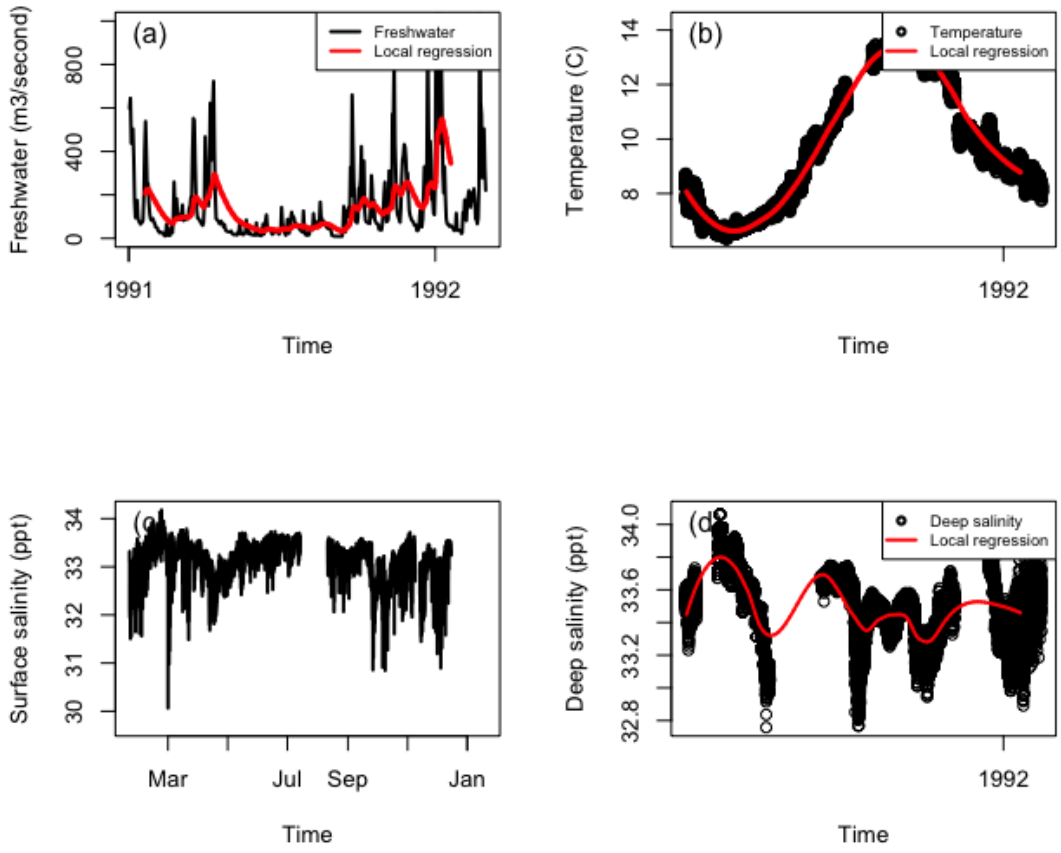

Figure 3.5: (a) Daily averaged flow rates of freshwater (m^3/sec) from rivers and rainfall and its local regression. (b) Temperature records (^oC) and its local regression. (c) Hourly surface salinity data (ppt). (d) Hourly deep salinity data (ppt) and its local regression.

Other Data We also have chlorophyll data, light intensity records, deep nitrate, river nitrate, freshwater inflow rates, temperature data and shallow and deep salinity data from the surveys. Due to the different measurement time of the data and the missing values contained in the data, we smooth the observed data by calculating the corresponding estimated hourly values. The hourly values for most data sets are approximated using the local regression (LOESS) approach. While the exponentially weighted moving average (EWMA) technique is employed for the freshwater input rates as the current inflow rate also depends on the previous run-off.

3.4 Model Fit for the One-month Data

The measurements collected from the 1991 field campaign allow us to model the complex variations in the surface nitrate in Loch Linnhe. An SDE model is then formulated by incorporating white noise into a deterministic nutrient model, based on the parameter perturbation scheme. Then we study the model fit for the one-month period data (21 April to 19 May 1991).

3.4.1 Model Set-up

Recently, Heath et al. [54] proposed a simplest mathematical model of a nutrient resource x in a food web:

$$dx(t) = (I - \mu x(t))dt, \tag{3.4.1}$$

where I is the external input rate of the nutrient and μ is the nutrient uptake rate by primary producers. Due to the probabilistic nature, the nutrient consumption rate μ may be influenced by some environmental factors such as temperature fluctuations. Parameter perturbation is a routine way to introduce the environmental noise to the deterministic dynamic systems [14, 47, 92, 93, 95]. Suppose that μ is stochastically perturbed with

$$\mu \to \mu + \tilde{\sigma}(x(t))\dot{B}(t),$$

where $\dot{B}(t)$ is a white noise and $\tilde{\sigma}(x(t)) > 0$ represents the noise intensity, this perturbed system can be described by the Itô equation:

$$dx(t) = (I - \mu x(t))dt + \bar{\sigma}(x(t))dB(t),$$

where $\bar{\sigma}(x) = -x\tilde{\sigma}(x)$. If we let

$$\bar{\sigma}(x) = \sigma \quad \text{or} \quad \bar{\sigma}(x) = \sigma x \quad \text{or} \quad \bar{\sigma}(x) = \sigma\sqrt{x},$$

where σ is a constant to be determined, we then respectively obtain the mean-reverting Ornstein-Uhlenbeck (OU) process [89, 111]:

$$dx(t) = (I - \mu x(t))dt + \sigma dB(t), \tag{3.4.2}$$

the mean-reverting process [89, 132]:

$$dx(t) = (I - \mu x(t))dt + \sigma x(t)dB(t) \tag{3.4.3}$$

and the mean-reverting square-root process [89]:

$$dx(t) = (I - \mu x(t))dt + \sigma\sqrt{|x(t)|}dB(t). \tag{3.4.4}$$

A general form for these models is the mean-reverting theta process [89]:

$$dx(t) = (I - \mu x(t))dt + \sigma|x(t)|^{\theta}dB(t). \tag{3.4.5}$$

By letting $\theta = 0, 1$ and $\frac{1}{2}$, model (3.4.2)–(3.4.4) are then deduced respectively. In the next section, the parameters of model (3.4.2)-3.4.4 are approximated using the least squares method.

3.4.2 Parameter Estimation

This section focuses on the parameter estimation for model (3.4.2)–(3.4.4). We use the general model (3.4.5) to introduce the estimation procedure. Firstly, the Euler-Maruyama (EM) scheme [57, 89] is used to approximate the path of the process (3.4.5) such that the discretised form of (3.4.5) can be rearranged as a regression model. Then the regression theory can be applied to estimate the model parameters [47, 102, 107].

Given a stepsize $\Delta > 0$ and setting $t_k = k\Delta$ for $k = 0, 1, 2, ...$ and $X_0 = x(0)$, the EM scheme produces the approximations $X_k \approx x(t_k)$ of the form

$$X_k = X_{k-1} + (I - \mu X_{k-1})\Delta + \sigma |X_{k-1}|^\theta \Delta B_k \tag{3.4.6}$$

for $k = 1, 2, ...$, where $\Delta B_k = B(t_k) - B(t_{k-1})$, provided that the stepsize Δ is small enough. Given $\{X_k : 0 \leq k \leq n\}$ for the time interval $[0, T]$, where $T = n\Delta$ for any positive integer n, one may rearrange equation (3.4.6) to get

$$\frac{X_k - X_{k-1}}{|X_{k-1}|^\theta} = \frac{I\Delta}{|X_{k-1}|^\theta} - \frac{\mu X_{k-1}\Delta}{|X_{k-1}|^\theta} + \sigma\sqrt{\Delta} Z_k, \tag{3.4.7}$$

where $Z_k \sim \mathbb{N}(0, 1)$ for $1 \leq k \leq n$. Let

$$y_k = \frac{X_k - X_{k-1}}{|X_{k-1}|^\theta}, \qquad u_k = \frac{1}{|X_{k-1}|^\theta}, \qquad v_k = \frac{X_{k-1}}{|X_{k-1}|^\theta}$$

and

$$\alpha = I\Delta, \qquad \beta = -\mu\Delta, \qquad \gamma = \sigma\sqrt{\Delta}, \tag{3.4.8}$$

equation (3.4.7) is rewritten as

$$y_k = \alpha u_k + \beta v_k + \gamma Z_k, \quad 1 \leq k \leq n, \tag{3.4.9}$$

where each γZ_k is a normally distributed random variable with mean 0 and variance γ^2. Then the observations $\{y_k, \mu_k, v_k\}_{k=0}^n$ are calculated. According to the multiple linear regression in the general matrix form introduced by Rawlings [107]

$$Y = M\rho + \epsilon, \tag{3.4.10}$$

where

$$Y = \begin{pmatrix} y_1 \\ y_2 \\ \vdots \\ y_n \end{pmatrix}, \qquad M = \begin{pmatrix} 1 & m_{11} & m_{12} & ... & m_{1p} \\ 1 & m_{21} & m_{22} & ... & m_{2p} \\ \vdots & \vdots & \vdots & \ddots & \vdots \\ 1 & m_{n1} & m_{n2} & \cdots & m_{np} \end{pmatrix},$$

$$\rho = \begin{pmatrix} \rho_0 \\ \rho_1 \\ \vdots \\ \rho_p \end{pmatrix}, \qquad \epsilon = \begin{pmatrix} \epsilon_1 \\ \epsilon_2 \\ \vdots \\ \epsilon_n \end{pmatrix},$$

with p a non-negative integer and $\epsilon_k \sim N(0, \eta^2)$ for $1 \leq k \leq n$ and $\eta > 0$, we may regard equation (3.4.9) as a multiple linear regression model which can be written in the matrix form of (3.4.10) by setting

$$M = \begin{pmatrix} u_1 & v_1 \\ u_2 & v_2 \\ \vdots & \vdots \\ u_n & v_n \end{pmatrix}, \qquad \rho = \begin{pmatrix} \alpha \\ \beta \end{pmatrix}, \qquad \epsilon = \begin{pmatrix} \gamma Z_1 \\ \gamma Z_2 \\ \vdots \\ \gamma Z_n, \end{pmatrix}$$

where $\eta = \gamma$ and remaining Y the same as in the general form. Then from the regression theory, we may derive the estimators for θ and γ based on the least squares method. From equation (3.4.10), we obtain that

$$\hat{\rho} = \begin{pmatrix} \hat{\alpha} \\ \hat{\beta} \end{pmatrix} = (M^T M)^{-1}(M^T Y) = \begin{pmatrix} S_{uu} & S_{uv} \\ S_{uv} & S_{vv} \end{pmatrix}^{-1} \cdot \begin{pmatrix} S_{uy} \\ S_{vy} \end{pmatrix}$$

and

$$\hat{\gamma} = \sqrt{\frac{\sum_{k=1}^{n} \left(y_k - \hat{\alpha} u_k - \hat{\beta} v_k\right)^2}{n-2}},$$

where

$$S_{uu} = \sum_{k=1}^{n} u_k^2, \quad S_{vv} = \sum_{k=1}^{n} v_k^2, \quad S_{uv} = \sum_{k=1}^{n} u_k v_k, \quad S_{yu} = \sum_{k=1}^{n} y_k u_k, \quad S_{yv} = \sum_{k=1}^{n} y_k v_k.$$

By (3.4.8), we further obtain the estimators for σ, I and μ as

$$\hat{I} = \frac{\hat{\alpha}}{\Delta}, \qquad \hat{\mu} = \frac{\hat{\beta}}{-\Delta}, \qquad \hat{\sigma} = \frac{\hat{\gamma}}{\sqrt{\Delta}}.$$

Let us consider a one-year period (T=1). As the nitrate data are available hourly, the stepsize Δ is set to be $1/(365 \times 24) = 0.0001170412$ (the time unit is one year), where (365×24) denotes the total hours in one year. Consequently, by applying the estimation technique elaborated above, the estimators $\hat{I}$, $\hat{\mu}$ and $\hat{\sigma}$ of model (3.4.2)–(3.4.4) are obtained accordingly. Results are shown in Table 3.1.

Parameter estimator	$\hat{I}$	$\hat{\mu}$	$\hat{\sigma}$
Model (3.4.2)	8980.72	1326.06	115.00
Model (3.4.3)	13619.71	2031.72	51.93
Model (3.4.4)	12966.39	1910.77	62.25

Table 3.1: Parameter estimation for model (3.4.2)–(3.4.4).

3.4.3 Model Selection

So far we have obtained three candidate models (3.4.2)–(3.4.4) for the fjord nitrate. The correctness of each model is assessed by comparing the probability distribution of the simulation data of each candidate model with that of the nitrate data. This is done by comparing the corresponding statistics and the distribution graphs. Furthermore, we perform a statistical test, the Kolmogorov-Smirnov (K-S) test [108], to investigate any differences in the distributions between the model simulations and the nitrate data. Namely, the hypothesis

> H_0: The simulation data of model (3.4.2) (or (3.4.3), (3.4.4)) follow the same distribution as the modified nitrate data does;
>
> H_1: The simulation data of model (3.4.2) (or (3.4.3), (3.4.4)) does not follow the same distribution as the modified nitrate data does

is considered. If the distribution of the model simulation is consistent with that of the nitrate data, this model is able to fit the nitrate data in distribution. After the model-selection procedure, the goodness of fit of the model is then evaluated by a normality test.

Firstly, from Table 3.2, both the mean values and standard deviations of the simulation data of model (3.4.2) and (3.4.4) are close to the corresponding statistics of the nitrate data. In the contrast, the standard deviation of the simulation data of model (3.4.3) is far from that of the nitrate observations. Secondly, from Figure 3.6(a)-(c), the distribution graph for model (3.4.2) is the closest to that for the nitrate data. Moreover, the p-value of 0.07 in the K-S test suggests that model (3.4.2) has captured the variations in the sea-loch nitrate in distribution.

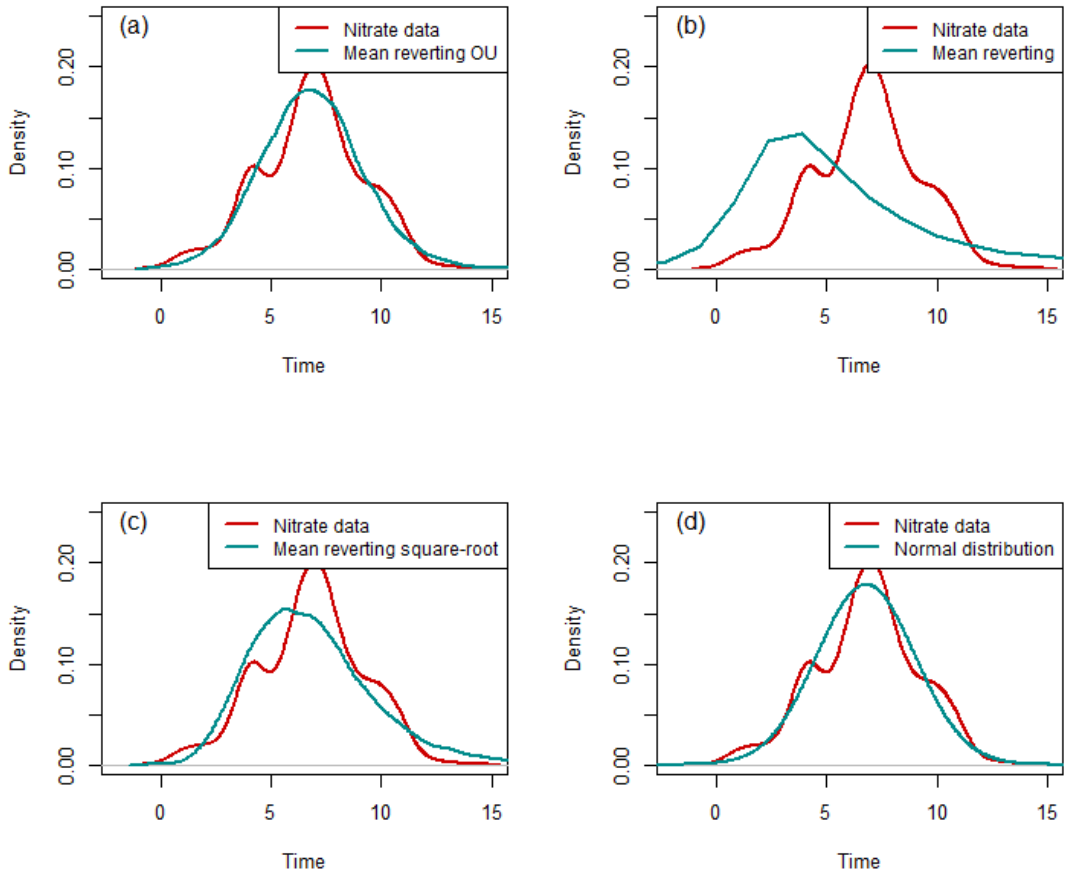

Figure 3.6: (a)-(c) Probability distribution comparisons between the nitrate records and the simulated solutions of the SDE model (3.4.2)–(3.4.4). (d) The distribution of the nitrate observations compared with the standard normal distribution. The SDE model (3.4.2)–(3.4.4) are simulated by the Euler-Maruyama scheme with stepsize $1/(365 \times 24)$ and the initial value 6.81 (the average value of the one-month nitrate data).

	Mean	Standard deviation	P-value
Modified nitrate data	6.81	2.32	–
Simulation data of model (3.4.2)	6.86	2.27	0.07
Simulation data of model (3.4.3)	6.99	15.85	< 0.0001
Simulation data of model (3.4.4)	6.84	2.80	< 0.0001
Normality test for model (3.4.2)	–	–	0.017

Table 3.2: Basic statistics of the modified nitrate data and the simulated solutions to model (3.4.2)–(3.4.4). The p-values are produced in the K-S test examining any differences in the distributions between the model simulations and the nitrate data or examining whether the nitrate data follow $\mathbb{N}(\frac{\hat{I}}{\hat{\mu}}, \frac{\hat{\sigma}^2}{2\hat{\mu}})$. The SDE models are simulated by Euler-Maruyama method with stepsize $1/(365 \times 24)$ and the initial value 6.81 (the average value of the one-month nitrate data).

To verify the above results, we evaluate the goodness of fit of model (3.4.2) by a normality test. According to the variation-of-constants formula (Theorem 2.20), the solution to model (3.4.2) is

$$x(t) = e^{-\mu t}x_0 + \frac{I}{\mu}(1 - e^{-\mu t}) + \sigma \int_0^t e^{-\mu(t-s)}dB(s). \tag{3.4.11}$$

We therefore obtain that the mean

$$\mathbb{E}x(t) = e^{-\mu t}\mathbb{E}x_0 + \frac{I}{\mu}(1 - e^{-\mu t}) + \sigma \int_0^t e^{-\mu(t-s)}dB(s) \to \frac{I}{\mu} \quad \text{as } t \to \infty$$

and the variance

$$Var(x(t)) = e^{-2\mu t}Var(x_0) + \frac{\sigma^2}{2\mu}(1 - e^{-2\mu t}) \to \frac{\sigma^2}{2\mu} \quad \text{as } t \to \infty.$$

It then follows from (3.4.11) that the solution $x(t)$ to model (3.4.2) approaches the normal distribution

$$\mathbb{N}\Big(\frac{I}{\mu}, \frac{\sigma^2}{2\mu}\Big)$$

asymptotically as $t \to \infty$ for arbitrary initial value $x(0)$ [89, p.103]. As a result, to investigate whether model (3.4.11) is able to fit the nitrate data, we carry out a normality test:

H_0: The nitrate data follow $\mathbb{N}(\frac{\hat{I}}{\hat{\mu}}, \frac{\hat{\sigma}^2}{2\hat{\mu}})$;

H_1: The nitrate data does not follow $\mathbb{N}(\frac{\hat{I}}{\hat{\mu}}, \frac{\hat{\sigma}^2}{2\hat{\mu}})$.

From Table 3.2, the normality test produces a p-value of 0.017, which is consistent with the previous results in the K-S test. Therefore we conclude that model (3.4.2) outperforms the other two models to fit the one-month nitrate data. In other words, the diffusion coefficient of our SDE model has been identified by the nitrate data. In the next section we would like to improve our model fit by exploring the effects of tides on the nitrate dynamics.

3.4.4 Model Fit Improvement

Recall that model (3.4.2) assumes a constant external input rate of nutrient resource. From section 3.2.2, however, the turbulent tidal flows may cause a dynamical change in the nitrate input rate. Assuming that the nitrate input rate is linearly related to sea-level, model (3.4.2) is corrected to

$$dx(t) = (oh(t) - \mu x(t))dt + \sigma dB(t), \tag{3.4.12}$$

where o is a constant to be determined and $h(t)$ refers to the sea levels with units of metres. Model (3.4.12) is then parameterised with the observed data.

Parameter Estimation

Let us consider a one-year duration. As the nitrate data are measured hourly, the stepsize is $\Delta = 1/(365 \times 24) = 0.0001170412$ (the time unit is one year), where (365×24) denotes the total hours in one year. Consequently, by applying the estimation approach proposed above, the estimators $\hat{o}$, $\hat{\mu}$ and $\hat{\sigma}$ of the SDE model (3.4.12) are deduced (Table 3.3).

Parameter estimator	$\hat{o}$	$\hat{\mu}$	$\hat{\sigma}$
Model (3.4.12)	323.88	1276.02	115.34

Table 3.3: Parameter estimation for model (3.4.12).

Model Fit Analysis

The goodness of fit of model (3.4.12) is analysed in two ways. On the one hand, the probability distribution of the simulation data of model (3.4.12) is compared with that of the nitrate data. This is done by comparing the corresponding statistics and by performing a statistical test, K-S test [108]. Namely, the hypothesis

> H_0: The simulation data of model (3.4.12) follow the same distribution as the modified nitrate data does;
>
> H_1: The simulation data of model (3.4.12) does not follow the same distribution as the modified nitrate data does

is considered. On the other hand, we provide a theorem which shows that the goodness of fit can be analysed by a normality test.

From Table 3.4, both the mean value and standard deviation of model

	Mean	Standard deviation	P-value
Modified nitrate data	6.81	2.32	–
Simulation data of model (3.4.12)	6.75	2.31	0.075
Normality test for model (3.4.12)	–	–	0.032

Table 3.4: Basic statistics of the modified nitrate data and the simulated solution to model (3.4.12). The p-values are produced in the K-S test examining any differences in the distributions between the model simulation and the nitrate data or examining whether the normalised nitrate data follow $\mathbb{N}\big(0, \frac{\hat{\sigma}^2}{2\hat{\mu}}\big)$. The SDE model (3.4.12) is simulated by the Euler-Maruyama approach with stepsize $1/(365 \times 24)$ and the initial value 6.81 (the average value of the one-month nitrate data).

(3.4.12) are close to the corresponding statistics of the nitrate data. Furthermore, the K-S test produces a p-value of 0.075, indicating that model (3.4.12) is able to fit the changes in the fjord nitrate.

Now we would like to assess the model fit by a normality test. By the variation-of-constants formula (Theorem 2.20), the solution to model (3.4.12) is

$$x(t) = e^{-\mu t}x(0) + oe^{-\mu t}\int_0^t e^{\mu s}h(s)ds + \sigma\int_0^t e^{\mu(s-t)}dB(s). \tag{3.4.13}$$

Assuming that the surface nitrate and sea levels both have a period of N, we define the following three functions:

$$\begin{aligned} H : [0, N] \to \mathbb{R} \quad &: \quad H(t) = \int_0^t e^{\mu s} h(s) ds; \\ m : [0, N] \to \mathbb{R} \quad &: \quad m(t) = o e^{-\mu t} \left(H(t) + \frac{H(N)}{e^{\mu N} - 1} \right); \\ \delta : \mathbb{R}_+ \to [0, N] \quad &: \quad \delta(t) = t - \left[\frac{t}{N} \right] N, \quad t \geq 0, \\ & \qquad \text{where } \left[\frac{t}{N} \right] \text{ is the integer part of } \frac{t}{N}. \end{aligned}$$

Theorem 3.1. *With the notations above, as $t \to \infty$*

$$x(t) - m(\delta(t)) \sim \mathbb{N}\Big(0, \frac{\sigma^2}{2\mu}\Big), \tag{3.4.14}$$

where $m(\delta(t))$ is the asymptotic periodic mean.

Proof. It follows from (3.4.13) that the distribution of solution $x(t)$ approaches the normal distribution with mean

$$\mathbb{E}x(t) = e^{-\mu t} \mathbb{E}x(0) + o e^{-\mu t} \int_0^t e^{\mu s} h(s) ds,$$

and variance

$$\begin{aligned} Var(x(t)) &= e^{-2\mu t} Var(x(0)) + e^{-2\mu t} \sigma^2 \int_0^t e^{2\mu s} ds \\ &= e^{-2\mu t} Var(x(0)) + \frac{\sigma^2}{2\mu} (1 - e^{-2\mu t}). \end{aligned}$$

Namely,

$$x(t) \sim \mathbb{N}\Big(e^{-\mu t} \mathbb{E}x(0) + o e^{-\mu t} \int_0^t e^{\mu s} h(s) ds, e^{-2\mu t} Var(x(0)) + \frac{\sigma^2}{2\mu} (1 - e^{-2\mu t}) \Big)$$

For $t \in [fN, (f+1)N], f = 0, 1, 2, \cdots,$

$$o e^{-\mu t} \int_0^t e^{\mu s} h(s) ds = o\Big(e^{-\mu t} \int_{fN}^t e^{\mu s} h(s) ds + e^{-\mu t} \int_0^{fN} e^{\mu s} h(s) ds \Big)$$

$$= o\Big(e^{-\mu t} e^{\mu f N} \int_{fN}^t e^{\mu (s - fN)} h(s - fN) ds + e^{-\mu t} \sum_{i=0}^{f-1} \int_{iN}^{(i+1)N} e^{\mu s} h(s) ds \Big)$$

$$= o\Big(e^{\mu(fN-t)}\int_0^{t-fN} e^{\mu s}h(s)ds + e^{-\mu t}\sum_{i=0}^{f-1} e^{\mu iN}\int_{iN}^{(i+1)N} e^{\mu(s-iN)}h(s-iN)ds\Big)$$
$$= o\Big(e^{-\mu\delta(t)}\int_0^{\delta(t)} e^{\mu s}h(s)ds + (e^{-\mu t}-e^{-\mu\delta(t)})\frac{\int_0^N e^{\mu s}h(s)ds}{1-e^{\mu N}}\Big).$$

We then obtain that

$$\begin{aligned}
&\lim_{t\to\infty}\Big(\mathbb{E}x(t) - m(\delta(t))\Big)\\
&= \lim_{t\to\infty}\Big(oe^{-\mu t}\int_0^t e^{\mu s}h(s)ds - m(\delta(t))\Big)\\
&= \lim_{t\to\infty}\Big(oe^{-\mu\delta(t)}\int_0^{\delta(t)} e^{\mu s}h(s)ds + o(e^{-\mu t}-e^{-\mu\delta(t)})\frac{\int_0^N e^{\mu s}h(s)ds}{1-e^{\mu N}} - m(\delta(t))\Big)\\
&= \lim_{t\to\infty}\Big(oe^{-\mu\delta(t)}\Big(\int_0^{\delta(t)} e^{\mu s}h(s)ds - \frac{\int_0^N e^{\mu s}h(s)ds}{1-e^{\mu N}}\Big) - m(\delta(t))\Big)\\
&= \lim_{t\to\infty}\Big(oe^{-\mu\delta(t)}\Big(H(\delta(t)) - \frac{N(N)}{1-e^{\mu N}}\Big) - m(\delta(t))\Big)\\
&= \lim_{t\to\infty}(m_1(\delta(t)) - m_1(\delta(t))) = 0.
\end{aligned}$$

and

$$\lim_{t\to\infty} Var(x(t)) = \frac{\sigma^2}{2\mu}.$$

Therefore $x(t) - m(\delta(t)) \sim \mathbb{N}\big(0, \frac{\sigma^2}{2\mu}\big)$ for arbitrary $x(0)$ as $t \to \infty$ [89]. □

Theorem 3.1 shows that the normalisation of the solution to model (3.4.12) approaches $\mathbb{N}(0, \frac{\sigma^2}{2\mu})$ asymptotically as $t \to \infty$. Let x_k for $k = 0, 1, 2, \cdots$ denote the observed nitrate data at time t_k. Then to examine whether model (3.4.12) can fit the nitrate data, we can then test whether the normalised nitrate data $x_k - m(\delta(t_k))$ for $k = 0, 1, 2, \cdots$ also follows $\mathbb{N}(0, \frac{\sigma^2}{2\mu})$. That is, the hypothesis

H_0: The normalised nitrate data follow $\mathbb{N}(0, \frac{\hat{\sigma}^2}{2\hat{\mu}})$;

H_1: The normalised nitrate data does not follow $\mathbb{N}(0, \frac{\hat{\sigma}^2}{2\hat{\mu}})$

is considered. Figure 3.7(c) shows that the distribution graph of the normalised nitrate data is close to the normal distribution in figure. From Table 3.4, the normality test provides a p-value of 0.032, showing that the model fit has been improved by including the sea-level dynamics.

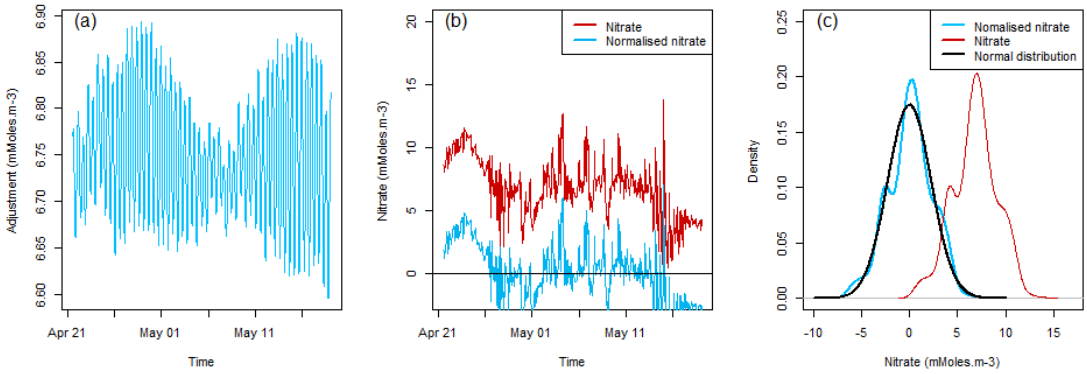

Figure 3.7: (a) The asymptotic periodic mean m for model (3.4.12). (b) The modified nitrate data and the normalised nitrate data. (c) Probability distributions of the one-month nitrate data and the normalised nitrate data, comparing to the normal distribution $\mathbb{N}(0, \frac{\hat{\sigma}^2}{2\hat{\mu}})$.

3.5 Model Fit for the One-year Data

The goodness of fit of model (3.4.12) for the one-month period data has been analysed in the previous section. Figure 3.4(a) suggests that the one-year data contain much more seasonal variability. As a result, our model need to be refined by considering more complicated physical and biological processes in the Loch Linnhe ecosystem. The SDE model is formulated in an iterative procedure by correcting the existing model and evaluating its goodness of fit based on the observed data. Due to the page limit, this section only presents the final model. All the interim models can be found in Appendix A.

3.5.1 Model Refinements

To match our model to the one-year data, we need to study more physical and biological factors that can contribute to the dynamics of shallow nitrate in Loch Linnhe. First of all, model (3.4.12) assumes a constant uptake rate of nitrate by phytoplankton. In fact, the uptake rate is often dependent on the phytoplankton abundance. Secondly, section 3.2 indicates that the turbulent tidal stream can result in a mixing between surface and deep water. Consequently the net tidal

exchange rate of nitrate in the surface layer can be represented as:

$$oh(t)(x_d(t) - x(t)),$$

where $x_d(t)$ represents the deep nitrate concentrations ($mMoles \cdot m^{-3}$). Thirdly, section 3.2.3 suggests that the high rate of freshwater run-off from rainfall and rivers is an additional essential source of surface nitrate. Meanwhile, there is a stream of water flowing out to the ocean. Furthermore, water temperature can cause the changes in the surface nitrate by affecting the strength of *nitrification* and *denitrification*. Nitrate can be produced from ammonia production by *nitrification*. Then *denitrification* is performed by bacterial species to convert nitrate to nitrogen gas. The intensity of the complex bacterial action is dependent on the water temperature. Consequently, we use temperature fluctuations to measure the net impact of *nitrification* and *denitrification* on the nitrate dynamics. By including the above processes, the nitrate model can be refined as:

$$\begin{aligned} dx(t) = [&oh(t)(x_d(t) - x(t)) - \mu_1 p(t)x(t) + (\mu_2 x_r(t) - \mu_3 x(t))w(t) \\ &+ \mu_4 D(t)]dt + \sigma dB(t), \end{aligned} \tag{3.5.1}$$

where $p(t)$ refers to the chlorophyll abundance (mg/m^3) which is an index of phytoplankton, $x_r(t)$ denotes the nitrate concentrations ($mMoles \cdot m^{-3}$) in the rivers Lochy and Nevis flowing into Loch Linnhe at Fort William, $w(t)$ is the freshwater flow rates (m^3/sec) into Loch Linnhe from river and rainfall, $D(t)$ represents the water temperature (^oC), and o, μ_1, μ_2, μ_3 and μ_4 are constants to be estimated. The parameter estimation for model (3.5.1) is conducted in the following part.

Parameter Estimation

Let us consider a one-year duration. As the surface nitrate data are measured hourly, the stepsize is $\Delta = 1/(365 \times 24) = 0.0001170412$ (the time unit is one year), where (365×24) denotes the total hours in one year. The parameter estimation is given in Table 3.5. Unfortunately, we found that the values of $\hat{\mu}_2$ and $\hat{\mu}_3$ are unexplained in the context of biology. In the next part we will combine the nitrate model (3.5.1) with a separate model of surface salinity in Loch Linnhe. The interactions between the coupled system might help us obtain a group of biologically interpretable parameters.

Parameter estimator	$\hat{o}$	$\hat{\mu}_1$	$\hat{\mu}_2$	$\hat{\mu}_3$	$\hat{\mu}_4$	$\hat{\sigma}$
Model (3.5.1)	82.41	405.02	-1.04	-1.80	-73.74	50.14

Table 3.5: Parameter estimation for model (3.5.1).

3.5.2 Stochastic Modelling for Shallow Salinity

Salt is a passive tracer in a sea-loch environment. This section explores the dynamical variations in the shallow salinity in Loch Linnhe. Firstly, shallow water is mostly coupled to deep by tidal upwelling and turbulence. Hence the net tidal exchange rate of salinity in the surface layer can be represented as

$$o_s h(t)(s_d(t) - s(t)),$$

where $s_d(t)$ denotes the deep salinity at time t and o_s is a constant to be defined. Secondly, the surface water is flushed by a high rate of freshwater run-off from river and rainfall. Meanwhile, a stream of water flows out to the open sea. As a result, the shallow salinity is diluted by the freshwater with a rate

$$\mu_s w(t),$$

where the constant μ_s is assumed to equal μ_3 in (3.5.1) . Consequently the salinity model is formulated as

$$ds(t) = [o_s h(t)(s_d(t) - s(t)) - \mu_3 w(t)s(t)]dt + \sigma_s dB(t), \tag{3.5.2}$$

where σ_s is a constant to be estimated. By combining the nitrate model (3.5.1) with the salinity model (3.5.2), we obtain a coupled equation:

$$dx(t) = [oh(t)(x_d(t)-x(t))-\mu_1 p(t)x(t)+(\mu_2 x_r(t)-\mu_3 x(t))w(t)+\mu_4 D(t)]dt+\sigma dB(t), \tag{3.5.3a}$$

$$ds(t) = [o_s h(t)(s_d(t) - s(t)) - \mu_3 w(t)s(t)]dt + \sigma_s dB(t). \tag{3.5.3b}$$

In the following part, this coupled equation is parameterised with the observed data.

3.5.3 Parameter Estimation

Let us consider a one-year duration. As the surface nitrate data and salinity data are measured hourly, the stepsize is $\Delta = 1/(365 \times 24) = 0.0001170412$ (the

time unit is one year), where (365×24) denotes the total hours in one year. From Table 3.6, the parameters are consistent with their biological meanings. The results benefit from the interactions between the coupled system (3.5.3)

Parameter estimator	$\hat{o}$	$\hat{o}_s$	$\hat{\mu}_1$	$\hat{\mu}_2$	$\hat{\mu}_3$	$\hat{\mu}_4$	$\hat{\sigma}$	$\hat{\sigma}_s$
Model (3.5.3)	33.02	75.57	305.59	1.05	0.07	-97.99	10.64	50.14

Table 3.6: Parameter estimation for model (3.5.3).

3.5.4 Goodness of Fit

	P-value
Normality test for model (3.5.3a)	< 0.01
Normality test for model (3.5.3b)	< 0.01

Table 3.7: The p-values are produced in the K-S test examining whether the normalised nitrate or salinity data follow $\mathbb{N}(0, 1)$.

In this section, the goodness of fit of model (3.5.3) is assessed. We will introduce a theorem which suggests that the model fit can be evaluated by examining whether the normalised nitrate and salinity data are standard normally distributed. This is done by comparing the distribution graphs and by carrying out a normality test (K-S test).

Assuming that the surface nitrate, sea levels, chlorophyll data, deep nitrate, freshwater input rate, river nitrate, temperature, surface and deep salinity all have a period of N, we define the following functions.

$$
\begin{aligned}
T &: \mathbb{R}_+ \to \mathbb{R}_+ : \qquad T(t) = \exp\Big(\int_0^t (oh(s) + \mu_1 p(s) + \mu_3 w(s))ds\Big);\\
T_1 &: \mathbb{R}_+ \to \mathbb{R}_+ : \qquad T_1(t) = ox_d(t)h(t) + \mu_2 x_r(t)w(t) + \mu_4 D(t);\\
H_1 &: [0, N] \to \mathbb{R} : \qquad H_1(t) = \int_0^t T_1(s)T(s)ds;\\
H_2 &: [0, N] \to \mathbb{R} : \qquad H_2(t) = \int_0^t T^2(s)ds;
\end{aligned}
$$

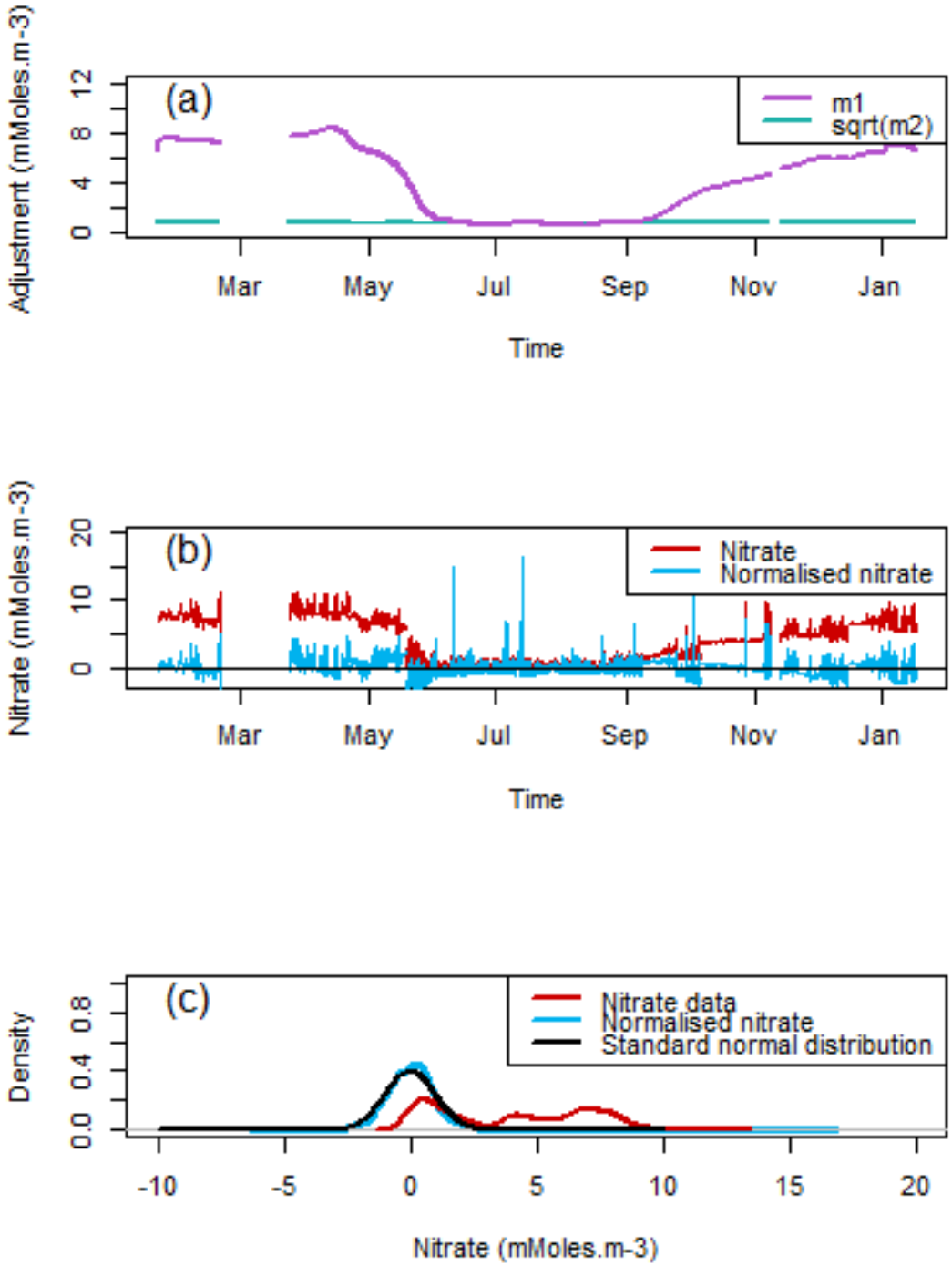

Figure 3.8: (a) The asymptotic periodic mean m_1 and standard deviation $\sqrt{m_2}$ for model (3.5.3a). (b) The modified nitrate data and the normalised nitrate. (c) Probability distributions of the modified nitrate data and the normalised nitrate data, comparing to the standard normal distribution $\mathbb{N}(0, 1)$.

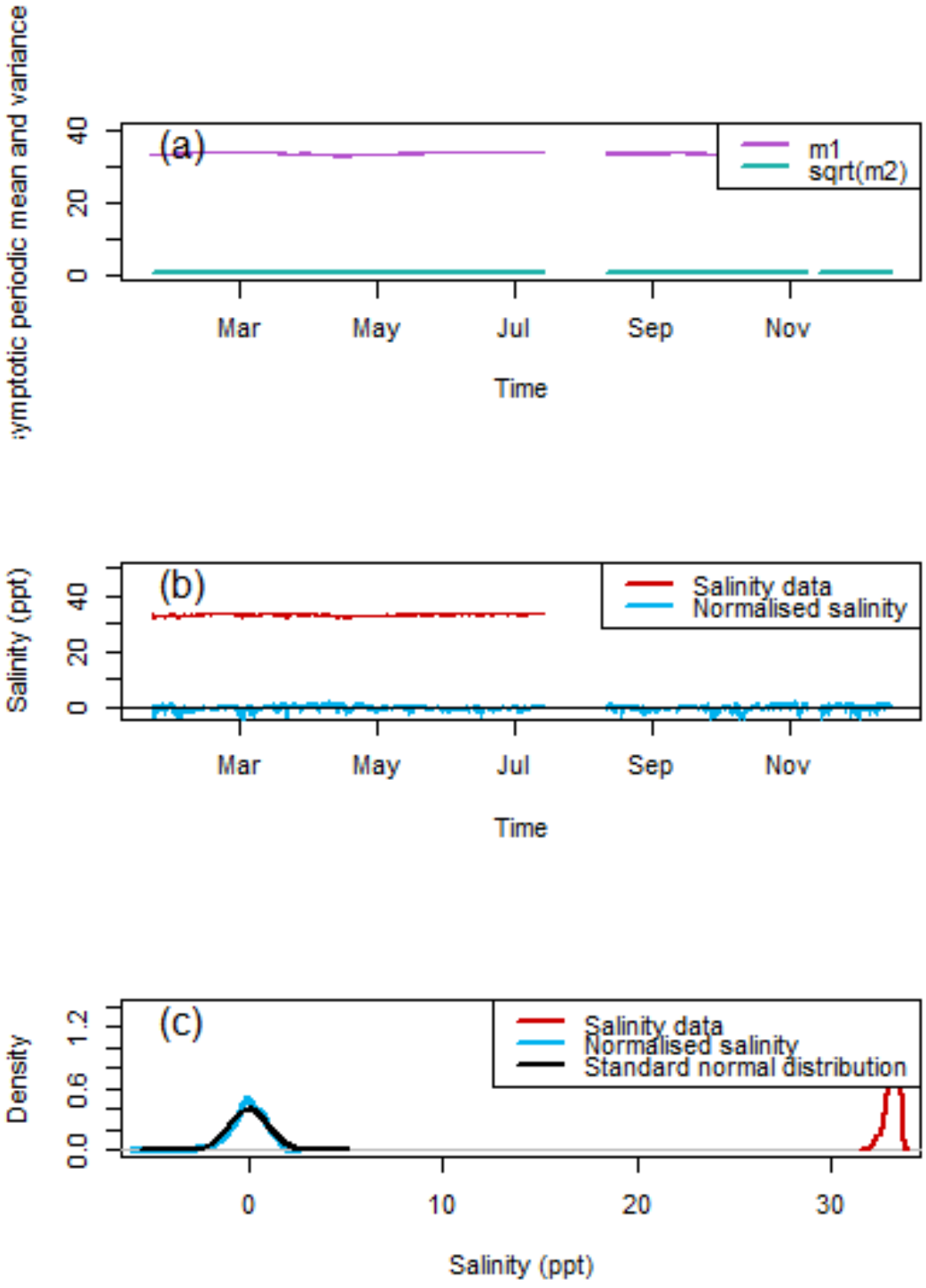

Figure 3.9: (a) The asymptotic periodic mean m_{s1} and standard deviation $\sqrt{m_2}$ for model (3.5.3b). (b) The hourly salinity data and the normalised salinity data. (c) Probability distributions of the salinity data and the normalised salinity, comparing to the standard normal distribution $\mathbb{N}(0, 1)$.

$$
\begin{aligned}
m_1 : [0,N] \to \mathbb{R} : \qquad & m_1(t) = \frac{1}{T(t)}\Big(H_1(t) + \frac{H_1(N)}{T(N)-1}\Big);\\
m_2 : [0,N] \to \mathbb{R} : \qquad & m_2(t) = \frac{\sigma^2}{T^2(t)}\Big(H_2(t) + \frac{H_2(N)}{T^2(N)-1}\Big);\\
T_s \ : \ \mathbb{R}_+ \to \mathbb{R}_+ : \qquad & T_s(t) = \exp\Big(\int_0^t (o_s h(s) + \mu_s w(s))\Big);\\
H_{s1} : [0,N] \to \mathbb{R} : \qquad & H_{s1}(t) = \int_0^t o_s s_d(s) h(s) T_s(s) ds;\\
H_{s2} : [0,N] \to \mathbb{R} : \qquad & H_{s2}(t) = \int_0^t T_s^2(s) ds;\\
m_{s1} : [0,N] \to \mathbb{R} : \qquad & m_{s1}(t) = \frac{1}{T_s(t)}\Big(H_{s1}(t) + \frac{H_{s1}(N)}{T_s(N)-1}\Big);\\
m_{s2} : [0,N] \to \mathbb{R} : \qquad & m_{s2}(t) = \frac{\sigma_s^2}{T_s^2(t)}\Big(H_{s2}(t) + \frac{H_{s2}(N)}{T_s^2(N)-1}\Big);\\
\delta : \mathbb{R}_+ \to [0,N] : \qquad & \delta(t) = t - \big[\frac{t}{N}\big]N, \quad t \geq 0,\\
& \text{where } \big[\frac{t}{N}\big] \text{ is the integer part of } \frac{t}{N}.
\end{aligned}
$$

Theorem 3.2. *With the notations above, as $t \to \infty$ the solution to model* (3.5.3) *obeys*

$$\frac{x(t) - m_1(\delta(t))}{\sqrt{m_2(\delta(t))}} \sim \mathbb{N}(0,1) \tag{3.5.4}$$

and

$$\frac{s(t) - m_{s1}(\delta(t))}{\sqrt{m_{s2}(\delta(t))}} \sim \mathbb{N}(0,1), \tag{3.5.5}$$

where m_1 and m_2 are the asymptotic periodic mean and variance for the modified surface nitrate data and m_{s1} and m_{s2} are the asymptotic periodic mean and variance for the salinity data respectively.

Proof. With the notations above, the solution to model (3.5.3a) is

$$x(t) = \frac{1}{T(t)}\Big(x(0) + H_1(t) + \sigma \int_0^t T(s) dB(s)\Big);$$

For any initial value $x(0)$, the solution $x(t)$ obeys normal distribution with mean

$$\mathbb{E}x(t) = \frac{1}{T(t)}\mathbb{E}x(0) + \frac{H_1(t)}{T(t)} = \frac{x(0)}{T(t)} + \frac{H_1(t)}{T(t)}$$

and variance

$$Var(x(t)) = \frac{1}{T^2(t)} Var(x(0)) + \frac{\sigma^2}{T^2(t)} \int_0^t T^2(s) ds$$

.For $t \in [fN, (f+1)N]$ with $f = 0, 1, 2, \cdots$, we obtain

$$\frac{H_1(t)}{T(t)} = \frac{1}{T(t)} \int_0^t T_1(s) T(s) ds = \frac{1}{T(t)} \int_0^{fN} T_1(s) T(s) ds + \frac{1}{T(t)} \int_t^{fN} T_1(s) T(s) ds,$$

where

$$\begin{aligned}
&\frac{1}{T(t)} \int_0^{fN} T(s) T_1(s) ds = \frac{1}{T(t)} \cdot \sum_{i=0}^{f-1} \int_{iN}^{(i+1)N} T(s) T_1(s) ds \\
&= \frac{1}{T(t)} \sum_{i=0}^{f-1} \int_{iN}^{(i+1)N} T(s) T_1(s - iN) ds = \frac{1}{T(t)} \sum_{i=0}^{f-1} \int_0^N T(s + iN) T_1(s) ds \\
&= \frac{1}{T(t)} \sum_{i=0}^{f-1} T(iN) \int_0^N T(s) T_1(s) ds = \frac{1}{T(t)} \frac{1 - T(fN)}{1 - T(N)} \int_0^N T(s) T_1(s) ds \\
&= \frac{1}{1 - T(N)} \Big(\frac{1}{T(t)} - \frac{T(fN)}{T(t)} \Big) \int_0^N T(s) T_1(s) ds \\
&= \frac{1}{1 - T(N)} \Big(\frac{1}{T(t)} - \frac{1}{T(t - fN)} \Big) \int_0^N T(s) T_1(s) ds \\
&= \frac{1}{1 - T(N)} \Big(\frac{1}{T(t)} - \frac{1}{T(\delta(t))} \Big) \int_0^N T(s) T_1(s) ds,
\end{aligned}$$

and

$$\begin{aligned}
&\frac{1}{T(t)} \int_{fN}^t T(s) T_1(s - fN) ds = \frac{1}{T(t)} \int_{fN}^t T(s) T_1(s - fN) ds \\
&= \frac{1}{T(t)} \int_0^{t - fN} T(s + fN) T_1(s) ds = \frac{T(fN)}{T(t)} \int_0^{t - fN} T(s) T_1(s) ds \\
&= \frac{1}{T(t - fN)} \int_0^{t - fN} T(s) T_1(s) ds = \frac{1}{T(\delta(t))} \int_0^{\delta(t)} T(s) T_1(s) ds.
\end{aligned}$$

Therefore

$$\begin{aligned}
&\frac{H_1(t)}{T(t)} = \frac{1}{T(t)} \int_0^t T(s) T_1(s) ds \\
&= \frac{1}{1 - T(N)} \Big(\frac{1}{T(t)} - \frac{1}{T(\delta(t))} \Big) \int_0^N T(s) T_1(s) ds + \frac{1}{T(\delta(t))} \int_0^{\delta(t)} T(s) T_1(s) ds.
\end{aligned}$$

We thus obtain that

$$\lim_{t \to \infty} (\mathbb{E}x(t) - m_1(\delta(t)))$$

$$= \lim_{t\to\infty} \Big(\frac{x(0)}{T(t)} + \frac{H_1(t)}{T(t)} - m_1(\delta(t))\Big)$$
$$= \lim_{t\to\infty} \Big(\frac{1}{T(t)} \int_0^t T(s)T_1(s)ds - m_1(\delta(t))\Big)$$
$$= \lim_{t\to\infty} \Big(\frac{1}{1-T(N)}\Big(\frac{1}{T(t)} - \frac{1}{T(\delta(t))}\Big) \int_0^N T(s)T_1(s)ds + \frac{1}{T(\delta(t))} \int_0^{\delta(t)} T(s)T_1(s)ds$$
$$- m_1(\delta(t))\Big)$$
$$= \lim_{t\to\infty} \Big(\frac{1}{1-T(N)}\Big(- \frac{1}{T(\delta(t))}\Big) \int_0^N T(s)T_1(s)ds + \frac{1}{T(\delta(t))} \int_0^{\delta(t)} T(s)T_1(s)ds$$
$$- m_1(\delta(t))\Big)$$
$$= \lim_{t\to\infty} \Big(- \frac{1}{T(\delta(t))(1-T(N))} \int_0^N T(s)T_1(s)ds + \frac{1}{T(\delta(t))} \int_0^{\delta(t)} T(s)T_1(s)ds$$
$$- m_1(\delta(t))\Big)$$
$$= \lim_{t\to\infty} \Big(\frac{1}{T(\delta(t))}\Big(H_1(\delta(t)) - \frac{H_1(N)}{1-T(N)}\Big) - m_1(\delta(t))\Big)$$
$$= \lim_{t\to\infty} (m_1(\delta(t)) - m_1(\delta(t))) = 0.$$

Similarly, we can deduce that

$$\lim_{t\to\infty} \frac{Var(x(t))}{m_2(\delta(t))} = \lim_{t\to\infty} \frac{\sigma^2}{m_2(\delta(t))T^2(t)} \int_0^t T^2(s)ds$$
$$= \lim_{t\to\infty} \Big(\frac{\sigma^2}{T^2(\delta(t))} \int_0^{\delta(t)} T^2(s)ds + \frac{\sigma^2}{1-T^2(N)}\Big(\frac{1}{T^2(t)} - \frac{1}{T^2(\delta(t))}\Big) \cdot$$
$$\int_0^N T^2(s)ds\Big) \Big/ m_2(\delta(t))$$
$$= \lim_{t\to\infty} \Big(\frac{\sigma^2}{T^2(\delta(t))} \int_0^{\delta(t)} T^2(s)ds + \frac{\sigma^2}{1-T^2(N)}\Big(- \frac{1}{T^2(\delta(t))}\Big) \int_0^N T^2(s)ds\Big) \Big/ m_2(\delta(t))$$
$$= \lim_{t\to\infty} \frac{\sigma^2}{T^2(\delta(t))}\Big(\int_0^{\delta(t)} T^2(s)ds - \frac{1}{1-T^2(N)} \int_0^N T^2(s)ds\Big) \Big/ m_2(\delta(t))$$
$$= \lim_{t\to\infty} \frac{\sigma^2}{T^2(\delta(t))}\Big(H_2(\delta(t)) - \frac{H_2(N)}{1-T^2(N)}\Big) \Big/ m_2(\delta(t)) = \lim_{t\to\infty} \frac{m_2(\delta(t))}{m_2(\delta(t))} = 1.$$

Consequently (3.5.4) follows immediately. Assertion (3.5.5) can be proved in the same way and hence omitted. □

Theorem 3.2 shows that the normalisation of the solution to model (3.5.3) follows the standard normal distribution $\mathbb{N}(0,1)$ asymptotically. Let x_k and s_k

for $k = 0, 1, 2, \cdots$ denote the observed nitrate data and salinity data at time t_k respectively. Then to examine whether model (3.5.3) is able to fit the nitrate and salinity data respectively, we could then test whether the normalised nitrate data

$$\frac{x_k - m_1(\delta(t_k))}{\sqrt{m_2(\delta(t_k))}} \text{ for } k = 0, 1, 2, \cdots \tag{3.5.6}$$

and the normalised salinity data

$$\frac{s_k - m_{s1}[\delta(t_k)]}{\sqrt{m_{s2}[\delta(t_k)]}} \text{ for } k = 0, 1, 2, \cdots \tag{3.5.7}$$

also follow $\mathbb{N}(0, 1)$. Figure 3.8 suggests that the distributions of the normalised nitrate and salinity data are graphically close to the standard normal distribution. Furthermore, the normality tests are performed for system (3.5.3). Namely, the two hypotheses

H_0: Normalised nitrate data follow $\mathbb{N}(0, 1)$;

H_1: Normalised nitrate data does not follow $\mathbb{N}(0, 1)$

and

H_0: Normalised salinity data follow $\mathbb{N}(0, 1)$;

H_1: Normalised salinity data does not follow $\mathbb{N}(0, 1)$

are examined respectively. From Table 3.7, the p-values are too small to suggest good model fit.

3.6 Error Inherent in the Data

As revealed in [13], different types of error in the data should be handled by different modelling approaches to assure the model reliability. This chapter employs stochastic modelling to account for the environmental-type process noise in the data. In this section, we conduct a residual analysis for the data to illustrate the presence of such error type. We first assume that the data are driven by observation error. This type of error can be interpreted by the corresponding ordinary differential equation (ODE) system:

$$dx(t) = [oh(t)(x_d(t) - x(t)) - \mu_1 p(t)x(t) + (\mu_2 x_r(t) - \mu_3 x(t))w(t) + \mu_4 D(t)]dt, \tag{3.6.1a}$$

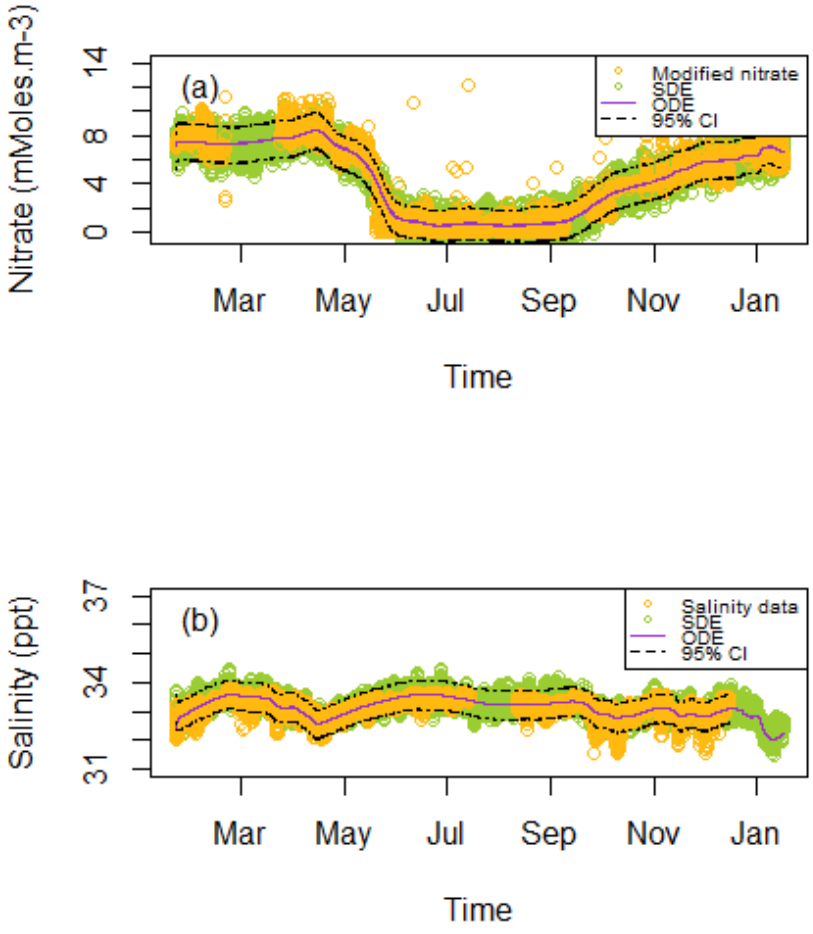

Figure 3.10: Time series of the modified nitrate data and the salinity data, simulations for the ODE model (3.6.1) and the SDE model (3.5.3) and the 95% confidence intervals of the solution to SDE model (3.5.3).

Initial Values for the Parameters	o	o_s	μ_1	μ_2	μ_3
(50,200,300,1,0.5,-100,32.5,6.8)	497.08	8.31	1339.83	5.51	0.02
(80,150,100,0.5,5,-200,32.5,7)	497.18	8.33	1339.51	5.51	0.02
(40,100,200,4,10,-150,32.5,7.5)	493.37	8.23	1346.50	5.48	0.02
(100,300,50,0.1,2,-250,32.5,7.5)	496.86	8.34	1340.91	5.51	0.02
(120,150,350,1.5,5,-250,32.5,7.5)	494.86	8.27	1347.33	5.50	0.02

Initial Values for the Parameters	μ_4	$x(0)$	$s(0)$	Convergence
(50,200,300,1,0.5,-100,32.5,6.8)	-687.05	7.14	32.45	Yes
(80,150,100,0.5,5,-200,32.5,7)	-687.30	7.14	32.45	Yes
(40,100,200,4,10,-150,32.5,7.5)	-679.74	7.14	32.45	Yes
(100,300,50,0.1,2,-250,32.5,7.5)	-686.53	7.14	32.45	Yes
(120,150,350,1.5,5,-250,32.5,7.5)	-682.29	7.14	32.45	Yes

Table 3.8: Parameter estimation for the ODE model (3.6.1) based on the five groups of initial values for the parameters.

$$ds(t) = [o_s h(t)(s_d(t) - s(t)) - \mu_3 w(t) s(t)]dt. \tag{3.6.1b}$$

Then the residuals of the data are approximated by taking away the simulation data of the ODE model (3.6.1) from the observed data. Provided that the residuals are normally distributed, we conclude that the data are driven by observation error. If the residual patterns contain obvious seasonal trends, process noise might exist in the data.

The ODE model (3.6.1) is parameterised based on the least squares approach. More precisely, the parameters are approximated by minimising the residual sum of square value using the R function `optim`. This R function can obtain a general-purpose minimisation based on the Nelder–Mead algorithm [98]. The initial values for the parameters to be estimated are required in the R function. From the biological meanings of the model parameters, o, o_s, μ_1, μ_2 and μ_3 are supposed to be positive and μ_4 could be any real number. Based on these prior information, five sets of randomly chosen initial values are used in estimation (Table 3.8). This estimation scheme produces a convergent result which is not sensitive to the given initial values. With the corresponding estimated parameters,

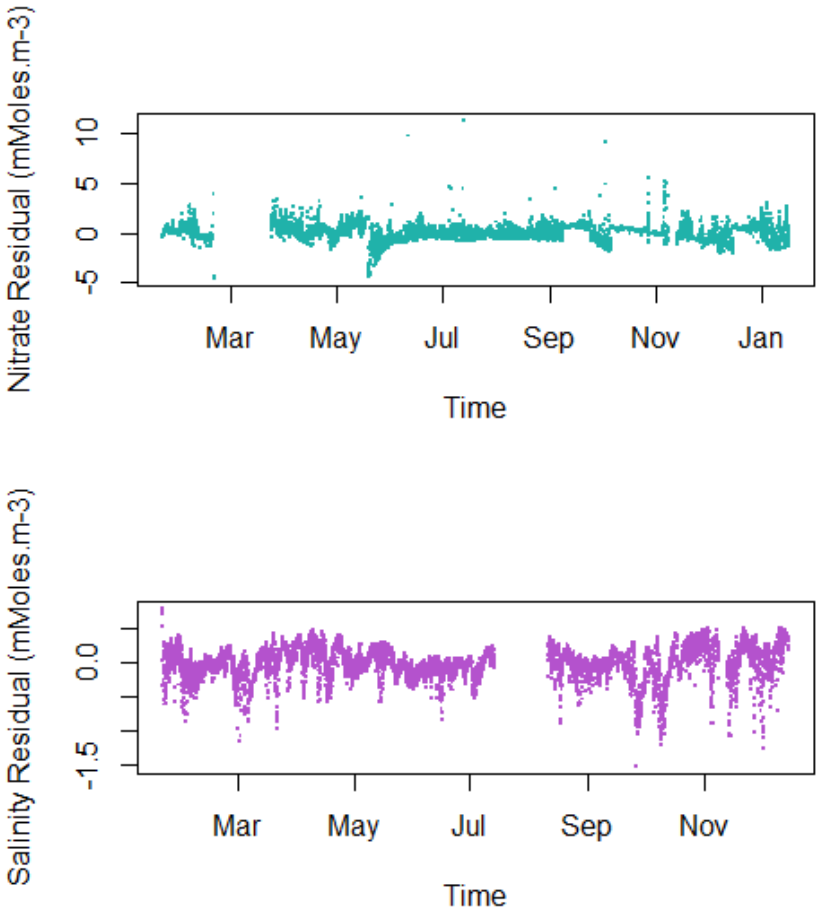

Figure 3.11: Residual patterns for the fjord nitrate and salinity data.

the ODE model (3.6.1) is then simulated using the Euler-Maruyama method with stepsize $1/(365 \times 24)$ and initial value determined by the parameter estimation. Figure 3.10 shows that the ODE simulations pass through the average values of the nitrate and salinity observations throughout the year, suggesting good model fit. From Figure 3.11, the seasonal trends in the residual patterns indicate the possible existence of the process noise in the data. Such error type has been analysed by our SDE model.

		o	o_s	μ_1	μ_2	μ_3
True Parameter		90	40	200	1	0.1
SDE Model		87.62	42.45	203.25	0.86	0.11
ODE	(10,100,300,10,1,-200,32.5,7.5)	431.43	134.44	255.06	2.34	1.07
	(50,50,250,3,0.5,-300,32.5,7.5)	430.31	134.04	254.29	2.34	1.07
	(80,200,100,5, 2,-250,32.5,7.5)	432.89	134.75	255.51	2.34	1.07
	(100,150,90,0.5,10,-50,32.5,7.5)	431.34	134.34	254.82	2.34	1.07

		μ_4	$x(0)$	$s(0)$	σ	σ_s
True Parameter		-100	–	–	60	20
SDE Model		-93.80	–	–	60.33	19.78
ODE	(10,100,300,10,1,-200,32.5,7.5)	-160.20	4.99	32.04	–	–
	(50,50,250,3,0.5,-300,32.5,7.5)	-159.75	4.99	32.01	–	–
	(80,200,100,5, 2,-250,32.5,7.5)	-160.61	4.99	32.06	–	–
	(100,150,90,0.5,10,-50,32.5,7.5)	-160.10	4.99	32.05	–	–

Table 3.9: Parameter estimation for the simulation data driven by process noise.

3.7 Simulation Study

This section aims to illustrate the accuracy of the parameter estimation techniques for the SDE and ODE models introduced in section 3.4.2 and 3.6 respectively. Recall that both modelling approaches are parameterised based on the least squares method. More precisely, in the SDE parameter estimation procedure, the discretised form of the SDE generated from the Euler-Maruyama scheme is rearranged as a regression model. Hence the estimators are deduced based on the regression theory. In a deterministic model, the parameters are approximated by minimising the residual sum of square value based on the well-known Nelder-Mead algorithm. In this section, a simulation study is carried out by producing two data sets driven by process noise and observation error respectively. This is achieved by deriving the simulation data of the SDE model (3.5.3) and the ODE model (3.6.1) with a group of biologically meaningful parameters using the Euler-Maruyama scheme. A group of independent noise collected from the normal distribution are additionally added to the ODE simulation data. As a result, we obtain two sets of data driven by process noise and observation error respectively. Then the

		o	o_s	μ_1	μ_2	μ_3
True Parameter		90	40	200	1	0.1
SDE Model		300.1	266.45	595.01	3.59	0.67
ODE	(50,50,250,3,0.5,-300,32.5,7.5)	70.32	37.71	154.11	0.78	0.09
	(80,200,100,5,2,-250,32.5,7.5)	70.39	37.55	154.29	0.78	0.09
	(100,150,90,0.5, 10,-50,32.5,7.5)	70.24	37.35	153.99	0.78	0.09
	(200,50,150,10,1,-75,32.5,7.5)	70.41	37.76	154.33	0.78	0.09

		μ_4	$x(0)$	$s(0)$	σ	σ_s
True Parameter		-100	–	–	–	–
SDE Model		-343.80	–	–	47.04	5.12
ODE	(50,50,250,3,0.5,-300,32.5,7.5)	-77.82	7.09	32.41	–	–
	(80,200,100,5,2,-250,32.5,7.5)	-77.90	7.09	32.40	–	–
	(100,150,90,0.5, 10,-50,32.5,7.5)	-77.72	7.09	32.41	–	–
	(200,50,150,10,1,-75,32.5,7.5)	-77.93	7.09	32.41	–	–

Table 3.10: Parameter estimation for the simulation data driven by observation error.

stochastic and deterministic estimation frameworks are used to approximate the parameters for the two data sets. The accuracy of the estimation techniques is then evaluated by comparing the estimated values with the underlying true parameters.

Table 3.9 and Table 3.10 show the parameter estimation for the data driven by process noise and observation error respectively. It suggests that the SDE estimation procedure can approximate the underlying parameters for the data driven by process noise, while the ODE estimation approach is capable of capturing the true parameters for the data with observation error. In Table 3.10, one may recognize that the ODE estimation is not perfectly close to the true parameters. One possible reason is that the ODE estimation procedure involves the Euler-Maruyama simulations which cause computational error. In addition, the SDE and ODE estimation frameworks always produce very different groups of parameters for a specific set of data. This reflects the importance of adopting appropriate modelling approaches for the ecological data.

3.8 Conclusions and Discussion

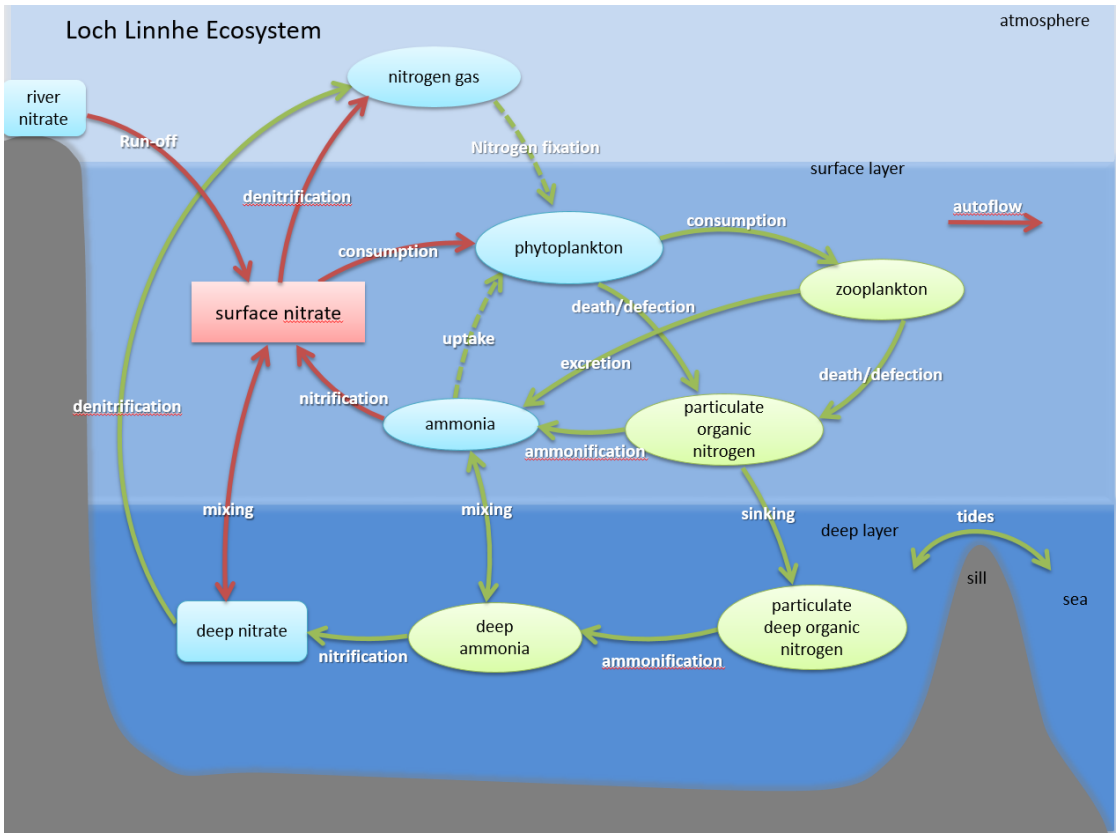

Figure 3.12: Loch Linnhe ecosystem. Nutrient transformations and the material transport associated with water movements are shown by solid arrows. Transformations by dashed arrow does not occur in Loch Linnhe but happens in the tropical water.

In this chapter, we have constructed an SDE model which captures the dynamical behaviours of the sea-loch nitrate, based on the hydrographic and chemical data collected from the 1991 field program implemented in Loch Linnhe. Stochastic modelling was employed to account for the process noise in the nitrate data. The SDE model of nitrate was developed by incorporating the white noise into the deterministic model of nutrient (3.4.1). In section 3.4, we considered the model fit of the one-month data. The diffusion coefficient of the SDE model measuring the noise intensity was identified based on the observed data. The goodness of fit has been assessed by comparing the distribution of the nitrate

data with that of the model simulation and by testing whether the nitrate data follow $\mathbb{N}(\frac{\hat{I}}{\hat{\mu}}, \frac{\hat{\sigma}^2}{2\hat{\mu}})$. The results from the K-S tests have indicated good model fit. In section 3.5, the model fit of the one-year nitrate data was explored. To capture the annual changes in the sea-loch nitrate, our model has been refined by incorporating more physical and biological factors that can contribute to the nitrate dynamics in Loch Linnhe. In addition, we also set up a separate SDE model which describes the dynamics of the shallow salinity in Loch Linnhe. By combining the salinity model with the existing nitrate model, we then obtained a coupled equation (3.5.3). The goodness of fit of the coupled system has been assessed by examining whether the normalised nitrate and salinity data follow the standard normal distribution. In the normality test, the p-value was too small to suggest good model fit. From a statistical point of view, the convincing results of the statistical tests are always based on a large amount of long-duration data, while the one-year period data is obviously not enough. On the other hand, the distribution graph of the normalised data for model (3.5.3) has become much closer to the standard normal distribution, compared to the graph for any interim model shown in Appendix A. This revealed that the SDE model (3.5.3) has recognised more annual seasonality in the fjord nitrate and salinity. Due to the low p-value, we cannot say that the SDE model (3.5.3) has successfully been able to characterise the dynamics of the shallow nitrate and salinity. However, we would conclude that currently model (3.5.3) has been the best one for describing the nitrate and salinity dynamics in Loch Linnhe.

Figure 3.12 shows a schematic representation of the Loch Linnhe ecosystem. Firstly, the shallow nitrate is consumed by a phytoplankton group, which is then grazed by zooplankton. Faecal pellets and dead individuals from these functional groups contain organic nitrogen, which is converted to ammonia by *ammonification*. Then *nitrification* is performed by bacterial species to produce nitrate from the ammonia production. Meanwhile, nitrate is converted to nitrogen gas by *denitrification*. Tidal streams can lead to an intense mixing between the shallow and deep water. The surface layer is additionally flushed by the freshwater run-off from river and rainfall. Meanwhile a stream of water flows out to the ocean. These biological and physical processes build up a full story of the sea-

loch nitrate, which has been mathematically represented by the SDE model (3.5.3).

In section 3.6, we conducted a residual analysis for the nitrate and salinity data in order to illustrate the existence of the process noise in the observed data. We first supposed that the nitrate and salinity data were solely driven by the observation noise, which can be explained by the corresponding ODE model (3.6.1). The parameter estimation for the ODE model was performed using the least squares method. Figure 3.10 showed good fit of the ODE model, with the simulations passing through the average values of the observed data over the whole year. As a result, the residuals patterns were deduced by taking away the simulated solutions to the ODE model (3.6.1) from the observed data. From Figure 3.11, the residuals for the data were not normally distributed, reflecting either that the process noise was contained in the data, or that the correct models of nitrate and salinity have not been found. In the former case, the process noise has been interpreted by the SDE model (3.5.3). Although the possible presence of the process noise has been illustrated, we have not been able to detect the dominant error type in the data. On the other hand, section 3.7 designed a simulation study to verify the accuracy of the parameter estimation approaches for the ODE and SDE models. The results also confirmed the ability of the SDE model (3.5.3) to account for the process noise and the corresponding ODE model (3.6.1) to explain the observation error. In particular, the ODE and SDE estimation frameworks have provided us with very different parameters for a specific set of data, indicating the importance of detecting the dominant error in the data. In other words, we need to develop a statistical technique to separate the observation error and the process noise in the data. Bayesian state-space modelling has been increasing used to address this issue [4, 32], however, the strong assumptions behind it are not applicable to our data. This becomes our important future work.

We have analysed the ability of the ODE model (3.6.1) and the SDE model (3.5.3) to deal with different types of error inherent in the data. Now we would like to point out another difference between the two modelling approaches. The simulation for the ODE model is fixed with a specific group of parameters and

initial values. On the other hand, the simulation for the SDE model is different each time due to the presence of the environmental variability. From Theorem 3.2, this uncertainty can be characterised by the 95% confidence intervals of the solutions to the SDE model (3.5.3):

$$m_1(\delta(t_k)) - 1.96\sqrt{m_2(\delta(t_k))} \leqslant x(t_k) \leqslant m_1(\delta(t_k)) + 1.96\sqrt{m_2(\delta(t_k))}$$

and

$$m_{s1}(\delta(t_k)) - 1.96\sqrt{m_{s2}(\delta(t_k))} \leqslant s(t_k) \leqslant m_{s1}(\delta(t_k)) + 1.96\sqrt{m_{s2}(\delta(t_k))}$$

for $k = 0, 1, 2, \cdots$. The confidence intervals were shown in Figure 3.10. Apparently most nitrate and salinity measurements have been bounded by the corresponding intervals, suggesting good model fit.

Chapter 4

Stochastic Predator-Prey Population System with Foraging Arena Scheme

4.1 Introduction

The predator-prey interactions play a crucial role in the food-web dynamics. Especially, the foraging arena type predator-prey system (1.3.2) considers the spatial and temporal restrictions in the predator and prey activities. Some general properties of such system can be found in section 1.3.2. In this chapter, we will investigate how the environmental noise affect the system behaviours.

This chapter is organised as follows: In section 4.2, the foraging arena population system is formulated as a stochastic differential equation (SDE). In section 4.3, we verify the existence of a positive global solution to this SDE model. Next in section 4.4, we explore the asymptotic moment estimation of the system. Moreover the parametric condition for the system to be extinct is developed in section 4.5. In section 4.6, the stationary distribution of this SDE system is examined. In section 4.7, we perform some computer simulations to illustrate our results. We then give a conclusion in section 4.8. Most of the work in this chapter has been published in [23].

4.2 SDE Foraging Arena Predator-prey System

In the remaining chapters, unless stated otherwise, we let $(\Omega, \{\mathcal{F}_t\}_{t\geqslant 0}, \mathbb{P})$ be a complete probability space with a filtration $\{\mathcal{F}_t\}$ satisfying the usual conditions (i.e.it is right continuous and increasing while $\mathcal{F}_0$ contains all $\mathbb{P}$-null sets). Let $B(t) = (B_1(t), B_2(t))^T$ be a two-dimensional Brownian motion defined on this probability space. Now recall the foraging arena predator-prey system defined in (1.3.2) in section 1.3.2. Due to the random nature of the population system, some environmental factors such as temperature fluctuations and the changes in the composition of the nutrient resource may vary the intrinsic prey growth rate and the consumer death rate in model (1.3.2). Suppose that a and c are stochastically perturbed with

$$a \to a + \sigma_1 \dot{B}_1(t) \quad \text{and} \quad c \to c + \sigma_2 \dot{B}_2(t),$$

where $B_1(t)$ and $B_2(t)$ are two independent Brownian motions and the two positive constants σ_1 and σ_2 represent the intensities of the white noise. As a result, this perturbed system is given by

$$dx_1(t) = x_1(t)\Big(a - bx_1(t) - \frac{sx_2(t)}{\beta + x_2(t)}\Big)dt + \sigma_1 x_1(t) dB_1(t) \tag{4.2.1a}$$

$$dx_2(t) = x_2(t)\Big(\frac{hx_1(t)}{\beta + x_2(t)} - c - fx_2(t)\Big)dt - \sigma_2 x_2(t) dB_2(t), \tag{4.2.1b}$$

where $x_1(t)$ and $x_2(t)$ represent the population densities of prey and predator in model (4.2.1) at time t. We set $x(t) = (x_1(t), x_2(t))^T$ as the solution of model (4.2.1) with the initial value $x_0 = (x_1(0), x_2(0))^T$.

4.3 Global Positive Solution

To investigate the dynamical behaviours of model (4.2.1), the existence of a unique global positive solution is verified first. The coefficients of the SDE model (4.2.1) are locally Lipschitz continuous, however, they do not satisfy linear growth condition (Theorem 2.15). Hence the existing general existence-and-uniqueness theorem on SDEs is not applicable to model (4.2.1) and there exists a unique maximal local solution to model (4.2.1). That is, the solution may exit from $\mathbb{R}^2_+$ space at a finite time [92, 94]. In this section, we shall show that the solution of model (4.2.1) is positive and global as in [47, 92].

Theorem 4.1. *For any given initial value $x_0 \in \mathbb{R}^2_+$, there is a unique solution $x(t)$ to equation (4.2.1) on $t \geqslant 0$ and the solution will remain in $\mathbb{R}^2_+$ with probability 1, namely $x(t) \in \mathbb{R}^2_+$ for all $t \geqslant 0$ almost surely.*

Proof. Since the coefficients of the equation (4.2.1) are locally Lipschitz continuous, for any given initial value $x_0 \in \mathbb{R}^2_+$, there is a unique maximal local solution $x(t)$ on $t \in [0, \tau_e)$, where τ_e is the explosion time (exit time) from $\mathbb{R}^2_+$. To show that this solution is global, we need to verify $\tau_e = \infty$ a.s. Let $k_0 > 0$ be sufficiently large for $x_1(0)$ and $x_2(0)$ lying within the interval $\left[\frac{1}{k_0}, k_0\right]$. For each integer $k \geqslant k_0$, define the stopping time

$$\tau_k = \inf\{t \in [0, \tau_e) : x_i(t) \notin \left(\frac{1}{k}, k\right) \text{ for some } i = 1, 2\}.$$

Obviously, τ_k is increasing as $k \to \infty$. Set $\tau_\infty := \lim_{t\to\infty} \tau_k$ and whence $\tau_\infty \leqslant \tau_e$ a.s. Hence to complete the proof, we need to show that

$$\tau_\infty = \infty \quad \text{a.s.} \tag{4.3.1}$$

If (4.3.1) is not true, there are three constants $T > 0, k_1 \geqslant k_0$ and $\epsilon \in (0, 1)$ such that

$$\mathbb{P}(\Omega_k) \geqslant \epsilon \text{ for all } k \geqslant k_1, \text{ where } \Omega_k = \{\tau_k \leqslant T\}.$$

Define a C^2-function $V : \mathbb{R}^2_+ \to \mathbb{R}_+$ by $V(x) = x_1 - \log x_1 + x_2 - \log x_2$. From the Itô formula (Theorem 2.13),

$$dV(x(t)) = LV(x(t))dt + (\sigma_1 x_1(t) - \sigma_1)dB_1(t) - (\sigma_2 x_2(t) - \sigma_2)dB_2(t),$$

where

$$\begin{aligned} LV(x) &= -a + \frac{sx_2}{\beta + x_2} + c + \frac{\sigma_1^2}{2} + \frac{\sigma_2^2}{2} + (a+b)x_1 + \frac{hx_1x_2}{\beta + x_2} + (f-c)x_2 - \frac{sx_1x_2}{\beta + x_2} \\ &\quad - \frac{hx_1}{\beta + x_2} - bx_1^2 - fx_2^2 \\ &\leqslant -a + s + c + \frac{\sigma_1^2}{2} + \frac{\sigma_2^2}{2} + (a + b + h)x_1 + (f - c)x_2 - bx_1^2 - fx_2^2, \end{aligned}$$

which is bounded, say by Q, in $\mathbb{R}^2_+$. Consequently,

$$\mathbb{E}V(x(\tau_k \wedge T)) \leqslant V(x_0) + Q\mathbb{E}(\tau_k \wedge T) \leqslant V(x_0) + QT. \tag{4.3.2}$$

Moreover for all $\omega \in \Omega_k$, $x_1(\tau_k, \omega)$ or $x_2(\tau_k, \omega)$ equals either k or $\frac{1}{k}$. Hence

$$V(x(\tau_k)) \geqslant (k - \log k) \wedge \Big(\sqrt{\frac{1}{k}} + \log k\Big).$$

This with (4.3.2) infers

$$V(x_0) + QT \geqslant \mathbb{E}(I_{\Omega_k} V(x(\tau_k))) \geqslant \epsilon\Big((k - \log k) \wedge \Big(\sqrt{\frac{1}{k}} + \log k\Big)\Big).$$

This leads to a contradiction as we let $k \to \infty$,

$$\infty > V(x_0) + QT = \infty.$$

So we have $\tau_\infty = \infty$ a.s. □

4.4 Asymptotic Moment Estimate

After analysing the global positive solution of model (4.2.1), we now explore the long-time dynamical behaviours of the prey and predator populations.

Theorem 4.2. *For any $\theta > 0$, there exists a positive constant $K(\theta)$ such that for any initial value $x_0 \in \mathbb{R}^2_+$,*

$$\limsup_{t\to\infty} \mathbb{E}|x(t)|^\theta \leqslant K(\theta).$$

Proof. Applying the Itô formula to $e^{\eta t}(x_1^\theta(t) + x_2^\theta(t)$ for any $\eta > 0$ and $\theta > 0$,

$$\begin{aligned} e^{\eta t}(x_1^\theta(t) + x_2^\theta(t)) = x_1^\theta(0) + x_2^\theta(0) + \int_0^t e^{\eta s} f(x(s))ds + \theta\sigma_1 \int_0^t e^{\eta s} x_1^\theta(s) dB_1(s) \\ - \theta\sigma_2 \int_0^t e^{\eta s} x_2^\theta(s) dB_2(s), \end{aligned} \tag{4.4.1}$$

where

$$\begin{aligned} f(x) = \Big(a\theta + \frac{1}{2}\theta(\theta-1)\sigma_1^2 + \eta\Big)x_1^\theta + \Big(-c\theta + \frac{1}{2}\theta(\theta-1)\sigma_2^2 + \eta\Big)x_2^\theta - \frac{s\theta x_1^\theta x_2}{\beta + x_2} \\ + \frac{h\theta x_1 x_2^\theta}{\beta + x_2} - b\theta x_1^{\theta+1} - f\theta x_2^{\theta+1}. \end{aligned}$$

For $\theta \geqslant 1$, the Young inequality yields

$$\frac{x_1 x_2^\theta}{\beta + x_2} \leqslant x_1 x_2^{\theta-1} \leqslant \frac{x_1^\theta}{\theta} + \frac{\theta - 1}{\theta} x_2^\theta.$$

Hence

$$f(x) \leqslant \left(a\theta + \frac{1}{2}\theta(\theta-1)\sigma_1^2 + h + \eta\right)x_1^\theta + \left((\theta-1)h - c\theta + \frac{1}{2}\theta(\theta-1)\sigma_2^2 + \eta\right)x_2^\theta - b\theta x_1^{\theta+1} - f\theta x_2^{\theta+1},$$

which is bounded, say by $K^*(\theta)$. Moreover, it follows from (4.4.1) that

$$\mathbb{E}\Big[e^{\eta(t\wedge\tau_k)}\Big(x_1^\theta(t\wedge\tau_k) + x_2^\theta(t\wedge\tau_k)\Big)\Big] \leqslant x_1^\theta(0) + x_2^\theta(0) + K^*(\theta)\int_0^{t\wedge\tau_k} e^{\eta s}ds.$$

Letting $k \to \infty$ and then $t \to \infty$ yields

$$\limsup_{t\to\infty} \mathbb{E}\big[x_1^\theta(t) + x_2^\theta(t)\big] \leqslant \lim_{t\to\infty} \frac{1}{e^{\eta t}}\left(x_1^\theta(0) + x_2^\theta(0) + \frac{K^*(\theta)(e^{\eta t}-1)}{\eta}\right) = \frac{K^*(\theta)}{\eta}.$$

On the other hand, we have

$$|x|^2 \leqslant 2\max(x_1^2, x_2^2), \text{ so } |x|^\theta \leqslant 2^{\theta/2}\max\left(x_1^\theta, x_2^\theta\right) \leqslant 2^{\theta/2}(x_1^\theta + x_2^\theta).$$

As a result,

$$\limsup_{t\to\infty} \mathbb{E}|x(t)|^\theta \leqslant 2^{\theta/2}\limsup_{t\to\infty} \mathbb{E}[x_1^\theta(t) + x_2^\theta(t)] \leqslant \frac{2^{\theta/2}K^*(\theta)}{\eta} = K(\theta). \tag{4.4.2}$$

For $0 < \theta < 1$, Hölder's inequality yields

$$\mathbb{E}|x(t)|^\theta \leqslant \big(\mathbb{E}|x(t)|\big)^\theta.$$

Hence from (4.4.2)

$$\limsup_{t\to\infty} \mathbb{E}|x(t)|^\theta \leqslant \limsup_{t\to\infty} \big(\mathbb{E}|x(t)|\big)^\theta \leqslant K(\theta).$$

□

4.5 Extinction

In this section, we investigate the conditions for the system to be extinct.

Lemma 4.3. *A one-dimensional Brownian motion $\{W_t\}_{t\geqslant 0}$ has the property that for almost every $\omega \in \Omega$,*

$$\lim_{t\to\infty} \frac{\min_{0\leqslant u\leqslant t} W(u,\omega)}{t} = \lim_{t\to\infty} \frac{\max_{0\leqslant u\leqslant t} W(u,\omega)}{t} = 0. \tag{4.5.1}$$

Proof. According to Theorem 2.4, for any $n > 0$, there exists a positive random variable ρ_n such that for almost every $\omega \in \Omega$,

$$-(1+n)\sqrt{2t\log\log t} \leqslant W(t,\omega) \leqslant (1+n)\sqrt{2t\log\log t} \quad \text{for all } t \geqslant \rho_n(\omega).$$

It then follows that for almost every $\omega \in \Omega$,

$$\max_{0\leqslant u\leqslant t} W(u,\omega) \leqslant \max_{0\leqslant u\leqslant \rho_n(\omega)} W(u,\omega) + (1+n)\sqrt{2t\log\log t}.$$

This implies

$$0 \leqslant \lim_{t\to\infty} \frac{\max_{0\leqslant u\leqslant t} W(u)}{t} \leqslant 0 \quad \text{a.s.}$$

Hence we obtain

$$\lim_{t\to\infty} \frac{\max_{0\leqslant u\leqslant t} W(u)}{t} = 0 \quad \text{a.s.}$$

Similarly, we also have

$$\lim_{t\to\infty} \frac{\min_{0\leqslant u\leqslant t} W(u)}{t} = 0 \quad \text{a.s.}$$

□

Theorem 4.4. *For any initial value $x_0 \in \mathbb{R}^2_+$,*
(a) if

$$2a < \sigma_1^2, \tag{4.5.2}$$

both $x_1(t)$ and $x_2(t)$ tend to zero exponentially as $t \to \infty$ with probability 1;
(b) if

$$\sigma_1^2 < 2a < \phi, \tag{4.5.3}$$

where

$$\phi = \sigma_1^2 + \frac{2b\beta c}{h} + \frac{b\beta\sigma_2^2}{h}, \tag{4.5.4}$$

$x_1(t)$ obeys

$$\lim_{t\to\infty} \frac{1}{t}\int_0^t x_1(u)du = \frac{2a-\sigma_1^2}{2b} \quad \text{a.s.}$$

and $x_2(t)$ tends to zero exponentially as $t \to \infty$ with probability 1.

Proof. (a) Applying the Itô formula on $\log x_1(t)$, we have

$$\begin{aligned} d\log x_1(t) &= \left(a - bx_1(t) - \frac{\sigma_1^2}{2} - \frac{sx_2(t)}{\beta + x_2(t)}\right)dt + \sigma_1 dB_1(t) \\ &\leqslant \left(a - \frac{\sigma_1^2}{2}\right)dt + \sigma_1 dB_1(t). \end{aligned} \tag{4.5.5}$$

Integrating from 0 to t and dividing by t, we get

$$\frac{1}{t}\log x_1(t) \leqslant \frac{1}{t}\log x_1(0) + a - \frac{\sigma_1^2}{2} + \frac{\sigma_1 B_1(t)}{t}.$$

Letting $t \to \infty$ and by the strong law of large numbers for martingales (Theorem 2.2),

$$\lim_{t\to\infty} \frac{\sigma_1 B_1(t)}{t} = 0 \quad \text{a.s.}$$

and thus from condition (4.5.2)

$$\limsup_{t\to\infty} \frac{1}{t}\log x_1(t) \leqslant a - \frac{\sigma_1^2}{2} < 0 \quad \text{a.s.}$$

as required. Hence $x_1(t)$ tends to zero exponentially as $t \to \infty$ and

$$\lim_{t\to\infty} \frac{1}{t}\int_0^t x_1(u)du = 0 \quad \text{a.s.} \tag{4.5.6}$$

Meanwhile

$$d\log x_2(t) = \Big(\frac{hx_1(t)}{\beta + x_2(t)} - c - \frac{\sigma_2^2}{2} - fx_2(t)\Big)dt - \sigma_2 dB_2(t). \tag{4.5.7}$$

It follows that

$$\frac{\log x_2(t)}{t} \leqslant \frac{1}{t}\left(\log x_2(0) + \frac{h}{\beta}\int_0^t x_1(u)du\right) - \Big(c + \frac{\sigma_2^2}{2}\Big) - \frac{\sigma_2 B_2(t)}{t}.$$

Letting $t \to \infty$ and recalling equation (4.5.6),

$$\limsup_{t\to\infty} \frac{\log x_2(t)}{t} \leqslant -\Big(c + \frac{\sigma_2^2}{2}\Big) < 0 \quad \text{a.s.}$$

(b) Applying Itô's formula on $\frac{1}{x_1(t)}$ gives

$$d\Big(\frac{1}{x_1(t)}\Big) = \left(\frac{1}{x_1(t)}\Big(\frac{sx_2(t)}{\beta + x_2(t)} - a + \sigma_1^2\Big) + b\right)dt - \frac{\sigma_1}{x_1(t)}dB_1(t).$$

Hence by the variation-of-constants formula (Theorem 2.20) and Lemma 2.19,

$$\begin{aligned}\frac{1}{x_1(t)} &= \exp\Big(\int_0^t \Big(\frac{1}{2}\sigma_1^2 - a + \frac{sx_2(u)}{\beta + x_2(u)}\Big)du - \sigma_1 B_1(t)\Big)\cdot \\ &\quad \Big[\frac{1}{x_1(0)} + b\int_0^t \exp\Big(\int_0^u \Big(a - \frac{sx_2(v)}{\beta + x_2(v)} - \frac{1}{2}\sigma_1^2\Big)dv + \sigma_1 B_1(u)\Big)du\Big] \\ &= \exp\big(-\sigma_1 B_1(t)\big)\Big[\frac{1}{x_1(0)}\exp\Big(-\Big(a - \frac{1}{2}\sigma_1^2\Big)t + s\int_0^t \frac{x_2(u)}{\beta + x_2(u)}du\Big) \\ &\quad + b\int_0^t \exp\Big(-\Big(a - \frac{\sigma_1^2}{2}\Big)(t-u) + s\int_u^t \frac{x_2(v)}{\beta + x_2(v)}dv + \sigma_1 B_1(u)\Big)du\Big].\end{aligned} \tag{4.5.8}$$

On the one hand, (4.5.8) leads to

$$\begin{aligned}\frac{1}{x_1(t)} &\leqslant \exp\big(-\sigma_1 B_1(t)\big)\Big[\frac{1}{x_1(0)}\exp\Big(-\Big(a - \frac{1}{2}\sigma_1^2\Big)t + s\int_0^t \frac{x_2(u)}{\beta + x_2(u)}du\Big) \\ &\quad + b\exp\Big(\sigma_1 \max_{0\leqslant u\leqslant t} B_1(u) + s\int_0^t \frac{x_2(u)}{\beta + x_2(u)}du\Big)\int_0^t \exp\Big(-\Big(a - \frac{\sigma_1^2}{2}\Big)(t-u)\Big)du\Big] \\ &\leqslant \exp\Big(\sigma_1\Big(\max_{0\leqslant u\leqslant t} B_1(u) - B_1(t)\Big) + s\int_0^t \frac{x_2(u)}{\beta + x_2(u)}du\Big)\cdot \\ &\quad \Big[\frac{1}{x_1(0)}\exp\Big(-\Big(a - \frac{1}{2}\sigma_1^2\Big)t\Big) + b\int_0^t \exp\Big(-\Big(a - \frac{\sigma_1^2}{2}\Big)(t-u)\Big)du\Big] \\ &= \exp\Big(\sigma_1\Big(\max_{0\leqslant u\leqslant t} B_1(u) - B_1(t)\Big) + s\int_0^t \frac{x_2(u)}{\beta + x_2(u)}du\Big)\cdot \\ &\quad \Big[\frac{1}{x_1(0)}\exp\Big(-\Big(a - \frac{1}{2}\sigma_1^2\Big)t\Big) + \frac{2b\Big(1 - \exp\big(-(a - \frac{\sigma_1^2}{2})t\big)\Big)}{2a - \sigma_1^2}\Big].\end{aligned}$$

It follows that

$$\frac{\log x_1(t)}{t} \geqslant -\frac{\log K_1(t)}{t} - \frac{\sigma_1\Big(\max_{0\leqslant u\leqslant t} B_1(u) - B_1(t)\Big)}{t} - \frac{s}{t}\int_0^t \frac{x_2(u)}{\beta + x_2(u)}du, \tag{4.5.9}$$

where

$$K_1(t) = \frac{1}{x_1(0)}\exp\Big(-\Big(a - \frac{1}{2}\sigma_1^2\Big)t\Big) + \frac{2b\Big(1 - \exp\big(-(a - \frac{\sigma_1^2}{2})t\big)\Big)}{2a - \sigma_1^2}$$

and $\sup_{0\leqslant t<\infty} K_1(t) < \infty$ if condition (4.5.3) holds. By (4.5.5) and (4.5.9),

$$\frac{1}{t}\int_0^t x_1(u)du$$

$$=\frac{2a-\sigma_1^2}{2b}-\frac{\log x_1(t)}{bt}+\frac{\log x_1(0)}{bt}-\frac{s}{bt}\int_0^t\frac{x_2(u)}{\beta+x_2(u)}du+\frac{\sigma_1}{bt}B_1(t) \tag{4.5.10}$$

$$\leqslant\frac{2a-\sigma_1^2}{2b}+\frac{\log K_1(t)}{bt}+\frac{\sigma_1\Big(\max_{0\leqslant u\leqslant t}B_1(u)-B_1(t)\Big)}{bt}+\frac{\log x_1(0)}{bt}+\frac{\sigma_1}{bt}B_1(t).$$

As $t\to\infty$ and from the strong law of large numbers for martingales and Lemma 4.3,

$$\limsup_{t\to\infty}\frac{1}{t}\int_0^t x_1(u)du\leqslant\frac{2a-\sigma_1^2}{2b}\quad\text{a.s.} \tag{4.5.11}$$

From equation (4.5.7),

$$d\log x_2(t)\leqslant\Big(\frac{hx_1(t)}{\beta}-c-\frac{\sigma_2^2}{2}\Big)dt-\sigma_2dB_2(t).$$

This and (4.5.11) yield

$$\begin{aligned}\limsup_{t\to\infty}\frac{1}{t}\log(x_2(t))&\leqslant\frac{h}{\beta}\limsup_{t\to\infty}\frac{1}{t}\int_0^t x_1(u)du-\Big(c+\frac{\sigma_2^2}{2}\Big)\\&\leqslant\frac{h\Big(2a-\sigma_1^2\Big)}{2\beta b}-\Big(c+\frac{\sigma_2^2}{2}\Big)<0,\end{aligned}$$

by condition (4.5.3). Hence for arbitrary small $\zeta>0$, there exists t_ζ such that

$$\mathbb{P}(\bar\Omega)\geqslant1-\zeta\text{ where }\bar\Omega=\Big\{\omega:\frac{sx_2(t,\omega)}{b(\beta+x_2(t,\omega))}\leqslant\zeta\text{ for }t\geqslant t_\zeta\Big\}.$$

On the other hand, (4.5.8) yields

$$\begin{aligned}\frac{1}{x_1(t)}&\geqslant\exp\big(-\sigma_1B_1(t)\big)\Big[\frac{1}{x_1(0)}\exp\Big(-\Big(a-\frac{1}{2}\sigma_1^2\Big)t\Big)\\&\quad+b\exp\big(\sigma_1\min_{0\leqslant u\leqslant t}B_1(u)\big)\int_0^t\exp\Big(-\Big(a-\frac{\sigma_1^2}{2}\Big)(t-u)\Big)du\Big]\\&\geqslant\exp\Big(\sigma_1\Big(\min_{0\leqslant u\leqslant t}B_1(u)-B_1(t)\Big)\Big)\Big[\frac{1}{x_1(0)}\exp\Big(-\Big(a-\frac{1}{2}\sigma_1^2\Big)t\Big)\\&\quad+\frac{2b\Big(1-\exp\big(-(a-\frac{\sigma_1^2}{2})t\big)\Big)}{2a-\sigma_1^2}\Big].\end{aligned}$$

Then

$$\frac{\log x_1(t)}{t}\leqslant-\frac{\log K_1(t)}{t}-\frac{\sigma_1\Big(\min_{0\leqslant u\leqslant t}B_1(u)-B_1(t)\Big)}{t}.$$

Hence we obtain from (4.5.10) that

$$\frac{1}{t}\int_0^t x_1(u)du \geqslant \frac{2a-\sigma_1^2}{2b} + \frac{\log K_1(t)}{bt} + \frac{\sigma_1\Big(\min_{0\leqslant u\leqslant t} B_1(u) - B_1(t)\Big)}{bt} + \frac{\log x_1(0)}{bt} - \frac{s}{bt}\int_0^t \frac{x_2(u)}{\beta + x_2(u)}du + \frac{\sigma_1}{bt}B_1(t). \tag{4.5.12}$$

For any $\omega \in \bar{\Omega}$, (4.5.12) together with Lemma 4.3 indicates

$$\liminf_{t\to\infty} \frac{1}{t}\int_0^t x_1(u)du \geqslant \frac{2a-\sigma_1^2}{2b} - \zeta.$$

This and (4.5.11) imply

$$\lim_{t\to\infty} \frac{1}{t}\int_0^t x_1(u)du = \frac{2a-\sigma_1^2}{2b} \quad \text{a.s.}$$

□

Remark 4.5. The parametric restriction for model (1.3.2) to die out is immediately obtained by setting $\sigma_1 = \sigma_2 = 0$ in condition (4.5.3). Namely, under the condition $0 < a < \frac{b\beta c}{h}$, the solution to model (1.3.2) obeys $\lim_{t\to\infty} \frac{1}{t}\int_0^t \bar{x}_1(u)du = \frac{a}{b}$ and the consumers tend to extinction ultimately.

Theorem 4.4(a) suggests that both species in model (4.2.1) will die out if $2a < \sigma_1^2$. That is, large white noise intensity σ_1^2 can cause the population extinction of both species. In the real life, this may happen when a serious epidemic or severe weather occurs. However this situation is not considered by model (1.3.2). Additionally, from Remark 4.5, the deterministic model (1.3.2) will die out if $a < \frac{b\beta c}{h}$. While Theorem 4.4(b) suggests that the existence of white noise can lead to the extinction of system (4.2.1) even with some $a > \frac{b\beta c}{h}$ (but need to obey $2a < \phi$). In the next section, we examine how the population system behaves when a gets even larger.

4.6 Stationary Distribution

In this section, we give condition for the SDE model (4.2.1) to have a unique stationary distribution. Let $P_{x_0,t}(\cdot)$ denote the probability measure induced by $x(t)$ with initial value $x(0) = x_0$, that is

$$P_{x_0,t}(F) = \mathbb{P}(x(t) \in F | x(0) = x_0) = \mathbb{P}_{x_0}(x(t) \in F), \quad F \in \mathcal{B}(\mathbb{R}_+^2),$$

where $\mathcal{B}(\mathbb{R}^2_+)$ is the σ-algebra of all the Borel sets $F \subset \mathbb{R}^2_+$. If there is a probability measure $\mu(\cdot)$ on the measurable space $(\mathbb{R}^2_+, \mathcal{B}(\mathbb{R}^2_+))$ such that

$$P_{x_0,t}(\cdot) \to \mu(\cdot) \text{ in distribution for any } x_0 \in \mathbb{R}^2_+,$$

we then say that the SDE model (4.2.1) has a stationary distribution $\mu(\cdot)$ [68, 91, 94]. To show the existence of a stationary distribution, let us first cite a known result from Khasminskii [68, pp. 107-109, Theorem 4.1] as a lemma.

Lemma 4.6. *The SDE model* (4.2.1) *has a unique stationary distribution if there is a bounded open set G of $\mathbb{R}^2_+$ such that $\sup_{x_0 \in Q-G} \mathbb{E}_{x_0}(\tau_G) < \infty$ for every compact subset Q of $\mathbb{R}^2_+$ such that $G \subset Q$ where $\tau_G = \inf\{t \geqslant 0 : x(t) \in G\}$.*

In the original Khasminskii theorem, there is one more condition that

$$\inf_{x \in G} \lambda_{\min}\big(\text{diag}(\sigma_1^2 x_1^2, \sigma_2^2 x_2^2)\big) > 0 \text{ for } x \in \mathbb{R}^2_+,$$

which is obvious and hence there is no point to state.

Theorem 4.7. *If*

$$2a\Big(1 - \frac{\sigma_2^2}{2h} - \frac{c}{h}\Big) > \phi, \tag{4.6.1}$$

where ϕ is denoted in (4.5.4)*, then for any initial value $x_0 \in \mathbb{R}^2_+$, model* (4.2.1) *has a unique stationary distribution.*

Proof. We define a C^2-function $V : \mathbb{R}^2_+ \to \mathbb{R}_+$:

$$V(x) = MV_1(x) + V_2(x) + e,$$

where

$$V_1(x) = \log(\beta + x_1) - \log(x_1) + \frac{l}{h}x_2 - \frac{a + b\beta}{h}\log x_2, \quad V_2(x) = x_1 + \frac{s}{h}x_2,$$

and e, l and M are three constants. We set $e = -\min(MV_1(x) + V_2(x))$ to keep the non-negativity of $V(x)$,

$$l = \Big(\frac{hs}{c\beta} + \frac{(a + b\beta)f}{c}\Big) \bigvee \frac{(a + b\beta)h}{4f\beta^2} \tag{4.6.2}$$

and M is to be defined later. First compute

$$LV_1 = \left(\frac{x_1}{\beta + x_1} - 1\right)\left(a - bx_1 - \frac{sx_2}{\beta + x_2}\right) + \frac{1}{2}\left(\frac{1}{x_1^2} - \frac{1}{(\beta + x_1)^2}\right)\sigma_1^2 x_1^2$$

$$
\begin{aligned}
&+\left(\frac{lx_2}{h}-\frac{a+b\beta}{h}\right)\left(\frac{hx_1}{\beta+x_2}-c-fx_2\right)+\frac{a+b\beta}{2h}\sigma_2^2\\
&\leqslant \frac{ax_1}{\beta+x_1}-\frac{bx_1^2}{\beta+x_1}+bx_1-\frac{a+b\beta}{\beta+x_2}x_1-a+\frac{sx_2}{\beta+x_2}+\frac{\sigma_1^2}{2}+\frac{lx_1x_2}{\beta+x_2}\\
&-\frac{clx_2}{h}-\frac{flx_2^2}{h}+\frac{(a+b\beta)c}{h}+\frac{(a+b\beta)f}{h}x_2+\frac{a+b\beta}{2h}\sigma_2^2\\
&\leqslant \frac{ax_1}{\beta+x_1}+\frac{b\beta x_1}{\beta+x_1}-\frac{a+b\beta}{\beta+x_2}x_1-a+\frac{\sigma_1^2}{2}+\frac{a+b\beta}{h}c+\frac{a+b\beta}{2h}\sigma_2^2\\
&+\left(\frac{s}{\beta}+\frac{(a+b\beta)f}{h}-\frac{cl}{h}\right)x_2-\frac{fl}{h}x_2^2+\frac{lx_1x_2}{\beta+x_2}\\
&=(a+b\beta)x_1\frac{x_2-x_1}{(\beta+x_1)(\beta+x_2)}-\lambda+\left(\frac{s}{\beta}+\frac{(a+b\beta)f}{h}-\frac{cl}{h}\right)x_2-\frac{fl}{h}x_2^2\\
&+\frac{lx_1x_2}{\beta+x_2}\\
&\leqslant \frac{a+b\beta}{\beta^2}(x_1x_2-x_1^2)-\lambda+\left(\frac{s}{\beta}+\frac{(a+b\beta)f}{h}-\frac{cl}{h}\right)x_2-\frac{fl}{h}x_2^2+\frac{lx_1x_2}{\beta+x_2},
\end{aligned}
$$

where $\lambda = a-\frac{\sigma_1^2}{2}-\frac{a+b\beta}{h}c-\frac{a+b\beta}{2h}\sigma_2^2>0$ from condition (4.6.1). By the Young inequality and (4.6.2),

$$
\begin{aligned}
LV_1 &\leqslant -\lambda+\left(\frac{s}{\beta}+\frac{(a+b\beta)f}{h}-\frac{cl}{h}\right)x_2+\left(\frac{a+b\beta}{4\beta^2}-\frac{fl}{h}\right)x_2^2+\frac{lx_1x_2}{\beta+x_2}\\
&\leqslant -\lambda+\frac{lx_1x_2}{\beta+x_2}.
\end{aligned}
$$

Then compute

$$
LV_2 = ax_1-bx_1^2-\frac{sc}{h}x_2-\frac{sf}{h}x_2^2\leqslant ax_1-bx_1^2-\frac{sf}{h}x_2^2.
$$

Hence

$$
LV(x)\leqslant M\Big(-\lambda+\frac{lx_1x_2}{\beta+x_2}\Big)+ax_1-bx_1^2-\frac{sf}{h}x_2^2,
$$

where M satisfies $M\lambda\geqslant a^2/(4b)+2$. Now we are aimed to show

$$
LV(x)\leqslant -1 \text{ for all } x\in\mathbb{R}_+^2-G:=G^c. \tag{4.6.3}
$$

If this holds, we let $x\in G^c$ be arbitrary and τ_G be the stopping time defined in Lemma 4.6. From (4.6.3), we have

$$
0\leqslant V(x_0)-\mathbb{E}_{x_0}(t\wedge\tau_G\wedge\tau_k),\quad \forall t>0.
$$

Letting $k \to \infty$ and then $t \to \infty$, we obtain

$$\mathbb{E}_{x_0}(\tau_G) \leqslant V(x_0), \quad \forall x_0 \in G^c$$

as required. To show that (4.6.3) actually holds, we define

$$G^c = G_1^c \cup G_2^c \cup G_3^c \cup G_4^c,$$

where

$$G_1^c = \{x | x_1 \in (0, \epsilon_1]\}; \qquad G_2^c = \left\{x \middle| x_1 \in \left(0, \frac{1}{\epsilon_1}\right], x_2 \in (0, \epsilon_2]\right\};$$
$$G_3^c = \left\{x \middle| x_1 \in \left[\frac{1}{\epsilon_1}, +\infty\right)\right\}; \qquad G_4^c = \left\{x \middle| x_2 \in \left[\frac{1}{\epsilon_2}, +\infty\right)\right\}$$

with two constants $\epsilon_1, \epsilon_2 \in (0,1)$ satisfying

$$\epsilon_1^2 \leqslant \frac{1}{M^2 l^2} \bigwedge \frac{b}{2(N_1+1)}, \quad \epsilon_2^2 \leqslant \frac{sf}{2h(N_2+1)} \quad \text{and} \quad \epsilon_2 \leqslant \frac{\beta \epsilon_1}{Ml}, \tag{4.6.4}$$

where the constants N_1 and N_2 will be determined later. We then show that in any subset of G^c, (4.6.3) holds. From (4.6.4),
(a) if $x \in G_1^c$,

$$LV(x) \leqslant -M\lambda + Mlx_1 + ax_1 - bx_1^2 - \frac{sf}{h}x_2^2 \leqslant Ml\epsilon_1 - 2 \leqslant -1;$$

(b) if $x \in G_2^c$,

$$LV(x) \leqslant -M\lambda + \frac{Mlx_1x_2}{\beta} + ax_1 - bx_1^2 - \frac{sf}{h}x_2^2 \leqslant \frac{Ml\epsilon_2}{\beta\epsilon_1} - 2 \leqslant -1;$$

(c) if $x \in G_3^c$,

$$LV(x) \leqslant -M\lambda + (Ml+a)x_1 - \frac{bx_1^2}{2} - \frac{bx_1^2}{2} - \frac{sfx_2^2}{h}.$$

Note that the polynomial $-M\lambda + (Ml+a)x_1 - \frac{bx_1^2}{2} - \frac{sfx_2^2}{h}$ has an upper bound, say N_1. Hence

$$LV(x) \leqslant N_1 - \frac{b}{2\epsilon_1^2} \leqslant -1;$$

(d) if $x \in G_4^c$,

$$LV(x) \leqslant -M\lambda + (Ml+a)x_1 - bx_1^2 - \frac{sfx_2^2}{2h} - \frac{sfx_2^2}{2h}.$$

Note that the polynomial $-M\lambda + (Ml + a)x_1 - bx_1^2 - \frac{sfx_2^2}{2h}$ is again bounded, say by N_2, we have

$$LV(x) \leqslant N_2 - \frac{sf}{2h\epsilon_2^2} \leqslant -1.$$

In all,

$$LV(x) \leqslant -1 \text{ for all } x \in G^c.$$

□

Recall that Theorem 4.4 considers the dynamical behaviours of model (4.2.1) with $0 < 2a < \sigma_1^2$ and $\sigma_1^2 < 2a < \phi$. Next Theorem 4.7 shows that system (4.2.1) has a stationary distribution when $2a > \frac{\phi}{1-\sigma_2^2/(2h)-c/h}$. However we have not been able to prove the case when

$$\phi < 2a < \frac{\phi}{1 - \sigma_2^2/(2h) - c/h}. \tag{4.6.5}$$

We present a numerical analysis of this case (Example 4.11).

4.7 Examples and Computer Simulations

In this section, the Euler-Maruyama (EM) scheme is adopted for the numerical simulations [57]. The EM approximate solutions have been proved to converge to the true solution of model (4.2.1) in probability [90]. Assume that all the parameters are given in appropriate units. We first give examples for the SDE system (4.2.1) to die out.

Example 4.8. *We perform a computer simulation of* 10000 *iterations of model* (4.2.1) *with initial value* $x(0) = (1.0, 0.1)^T$ *using the Euler-Maruyama (EM) method [57, 89] with stepsize* $\Delta = 0.01$ *and the system parameters given by*

$$a = 1, b = 0.1, s = 6, \beta = 5, h = 0.9, c = 2, f = 0.5, \sigma_1 = 1.5 \text{ and } \sigma_2 = 1.3. \tag{4.7.1}$$

It is easy to verify that these system parameters satisfy condition (4.5.2). *By Theorem 4.4(a),* $x_1(t)$ *and* $x_2(t)$ *will die out as* $t \to \infty$ *with probability* 1. *The computer simulations shown in Figure 4.1(a)(b) support these results.*

Example 4.9. *We keep the system parameters the same as in Example 4.8 but let* $\sigma_1 = 0.7$ *instead. Obviously the system parameters obey condition* (4.5.3). *By Theorem 4.4(b),*

$$\lim_{t\to\infty} \frac{1}{t}\int_0^t x_1(u)du = \frac{2a-\sigma_1^2}{2b} = 7.55$$

and $x_2(t)$ *will become extinct as* $t \to \infty$ *with probability* 1. *From Figure 4.1(c)(d), the prey abundance fluctuates around the level* 7.55 *while the consumers die out. This is consistent with the results in Theorem 4.4(b).*

We found that the situation when both species die out considered in system (4.2.1) does not happen in model (1.3.2). For example, the parametric restriction indicated in Example 4.8 leads to the extinction of both populations in system (4.2.1). However in the corresponding deterministic model (1.3.2), Remark 4.5 suggests that $\lim_{t\to\infty} \frac{1}{t}\int_0^t \bar{x}_1(u)du = \frac{a}{b} = 10$ and the consumers tend to zero . Figure 4.1(a)(b) shows this difference clearly. Next we study the case when the SDE system (4.2.1) has a stationary distribution.

Example 4.10. *We keep the system parameters the same as in Example 4.8 but let* $h = 4, \sigma_1 = 0.1$ *and* $\sigma_2 = 0.2$. *It is obvious that this group of parameters satisfies condition* (4.6.1). *From Theorem 4.7, both prey and predator populations have a stationary distribution. The ergodic property enables us to obtain the approximate probability distribution for the stationary distribution by computer simulation of a single sample path of a solution to model* (4.2.1). *Therefore the histogram of the* 10000 *iterations shown in Figure 4.2(b)(d) can be regarded as the approximate p.d.f.s of the stationary distribution. On the other hand, as the parameters of model* (1.3.2) *obey the condition* $a > \frac{b\beta c}{h}$, *there exists a positive equilibrium point* $\bar{E}^*(\bar{x}_1^*, \bar{x}_2^*)$ *of model* (1.3.2). *This is clearly shown in Figure 4.2(a)(c).*

Example 4.11. *We keep the system parameters the same as in Example 4.10 but let* $c = 3$. *Therefore condition* (4.6.5) *is fulfilled. Figure 4.3(a)(c) indicates a stationary distribution of both species. If this is true, the histogram of the* 10000 *iterations shown in Figure 4.3(b)(d) can be regarded as the approximate p.d.f.s of the stationary distribution.*

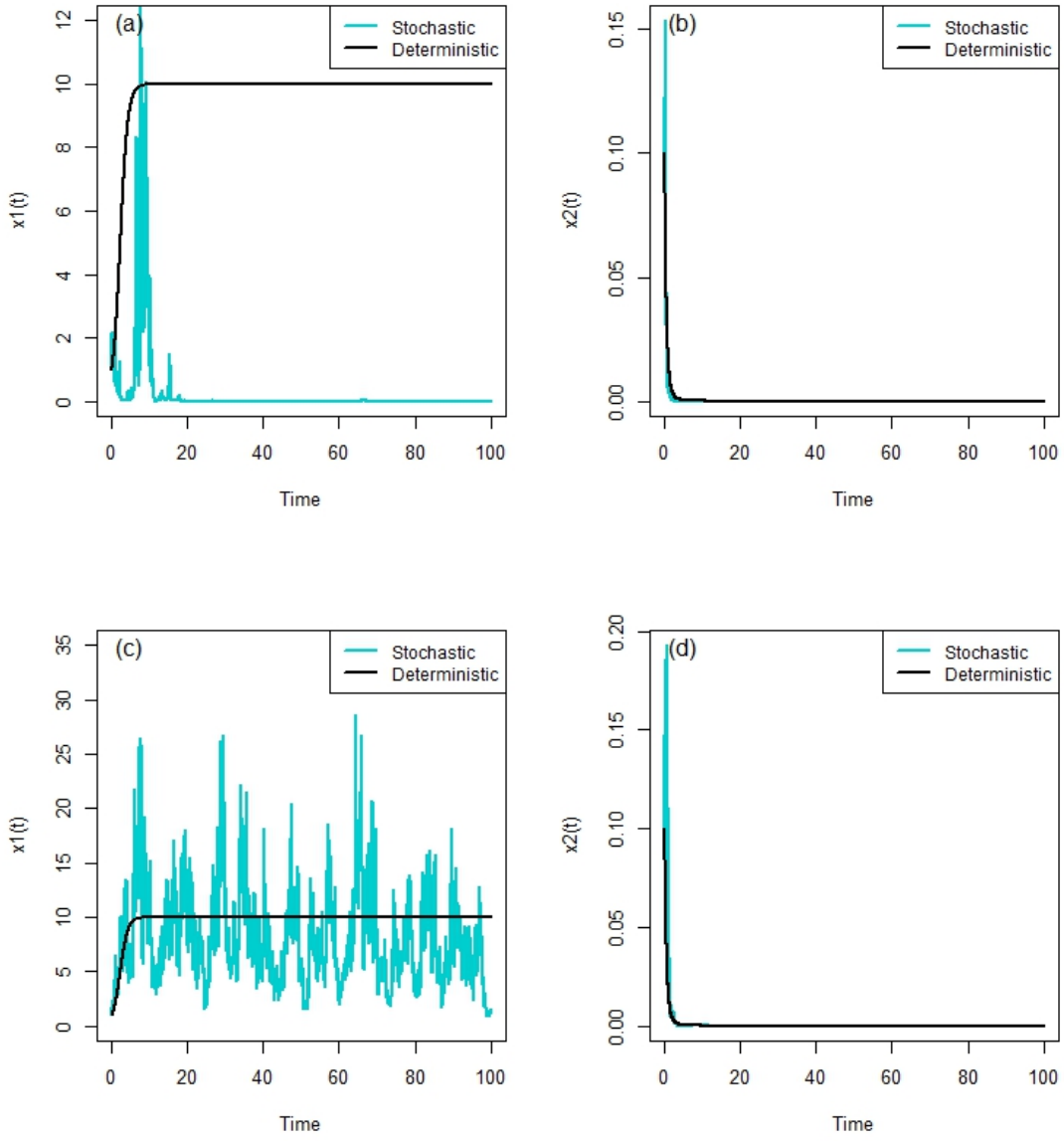

Figure 4.1: Computer simulations of the paths (a) $x_1(t)$ and (b) $x_2(t)$ of 10000 iterations of SDE model (4.2.1) using the EM scheme with stepsize $\Delta = 0.01$ and initial value $x_0 = (1.0, 0.1)^T$ and the corresponding ODE paths (model (1.3.2)) with the system parameters provided by (4.7.1). Given the system parameters as in (4.7.1) except that $\sigma_1 = 0.7$, we get the computer simulation of paths (c) $x_1(t)$ and (d) $x_2(t)$ of 10000 iterations using the EM method with stepsize $\Delta = 0.01$ and initial value $x_0 = (1.0, 0.1)^T$ and the corresponding ODE paths.

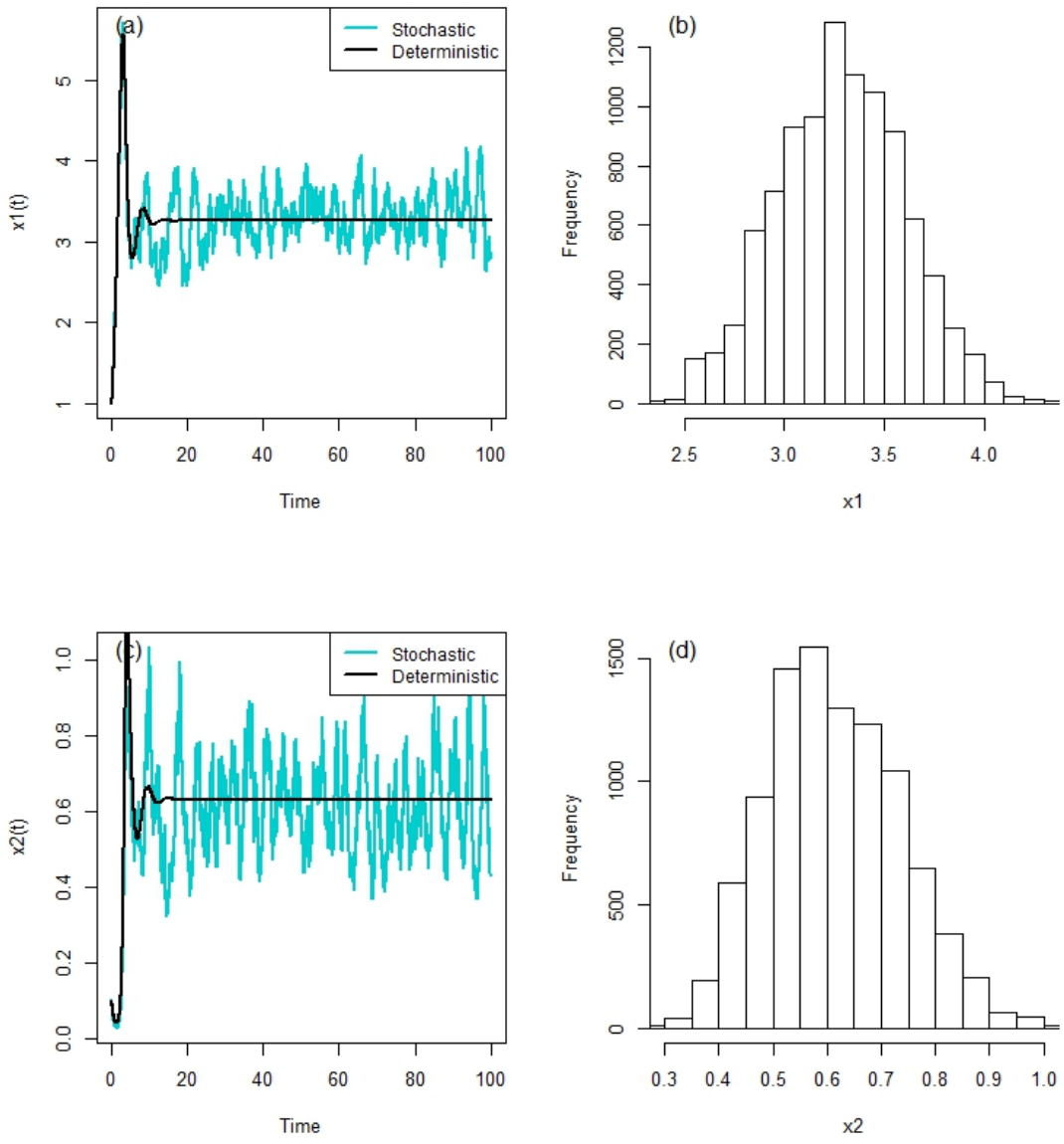

Figure 4.2: Computer simulation of the paths (a) $x_1(t)$ and (c) $x_2(t)$ of 10000 iterations of SDE model (4.2.1) using the EM technique with stepsize $\Delta = 0.01$ and initial values $x_0 = (1.0, 0.1)^T$ and the corresponding ODE paths (model (1.3.2)) with the parameters provided by Example 4.10, followed by the histograms of the SDE paths (b) $x_1(t)$ and (d) $x_2(t)$.

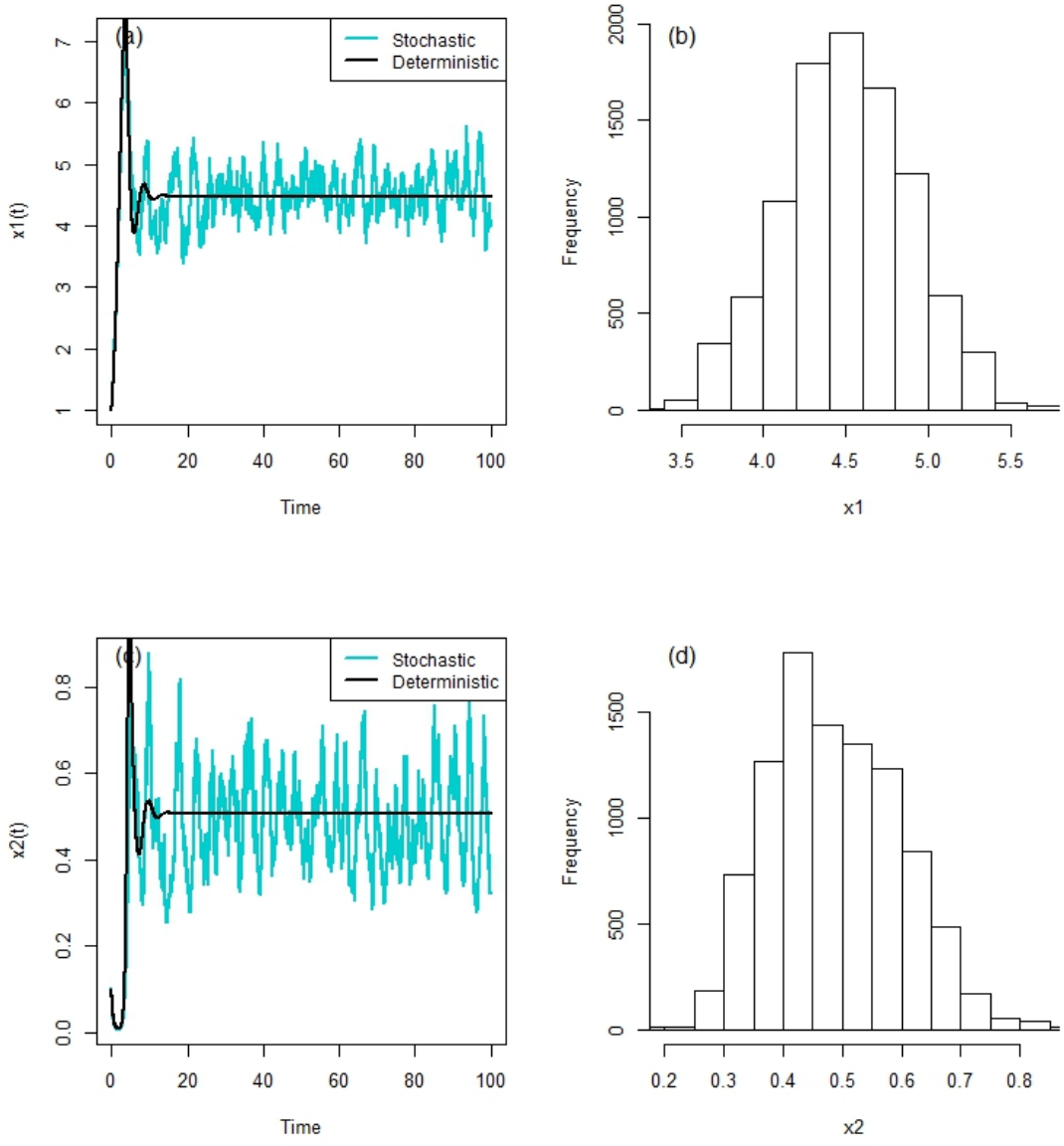

Figure 4.3: Computer simulation of the paths (a) $x_1(t)$ and (c) $x_2(t)$ of 10000 iterations of SDE model (4.2.1) using the EM technique with stepsize $\Delta = 0.01$ and initial values $x_0 = (1.0, 0.1)^T$ and the corresponding ODE paths (model (1.3.2)) with the parameters described in Example 4.11, followed by the histograms of the SDE paths (b) $x_1(t)$ and (d) $x_2(t)$.

4.8 Discussion

In this chapter, the two-dimensional foraging arena model in presence of environmental perturbation has been considered. After studying the existence and uniqueness of a positive solution to model (4.2.1), the long-time dynamical behaviours were generated. In order to investigate the effects of the environmental noise on the population dynamics, it is worth comparing the stochastic model (4.2.1) with the deterministic one (1.3.2). Firstly, the deterministic model (1.3.2) has two non-negative trivial equilibrium points $\bar{E}_0 = (0, 0)$ and $\bar{E}_1 = (\frac{a}{b}, 0)$. Also under the condition $a > \frac{b\beta c}{h}$, there exists a positive equilibrium point $\bar{E}^*(\bar{x}_1^*, \bar{x}_2^*)$ which is globally asymptotically stable. However, the stochastic model (4.2.1) only has one trivial equilibrium point $E_0 = (0, 0)$. Secondly, recall that both species of model (4.2.1) would die out ultimately if $2a < \sigma_1^2$. In the real life, it may happen when a serious disease or severe weather occurs. While this situation does not happen in model (1.3.2). Figure 4.1(a)(b) has illustrated this difference clearly. This suggests that the stochastic system is a more realistic model to describe the world than the deterministic one. Furthermore, recall that the deterministic model (1.3.2) will die out, in the sense that the prey population remains persistent while the consumers become extinct ultimately, provided that $a < \frac{b\beta c}{h}$. In the contrast, the stochastic model (4.2.1) goes to extinction even with some $a > \frac{b\beta c}{h}$ (but need to obey $2a < \phi$) due to the presence of the white noise. Hence we conclude that the presence of environmental noise brings a significant difference to the population dynamics.

Furthermore, we have shown the existence of a unique stationary distribution under condition (4.6.1). However, the dynamics of model (4.2.1) under the parametric condition (4.6.5) still remains an open problem, though the computer simulation in Example 4.11 indicated a stationary distribution of both species. In the stochastic predator-prey model with Beddington-DeAngelis response [62], more restrictive conditions were produced for the system to have a stationary distribution. These conditions were found based on the positive equilibrium of the corresponding deterministic system. The complexity of the parametric condition forms makes it harder to identify what cases have not been considered and hence need further investigation.

For the stationary distribution of the population system, the ergodic formula enables us to obtain the approximate probability distribution by the numerical simulation of a single sample path of a solution to the SDE model, although the mean value and variance have not been explicitly computed as in [47, 91].

In this chapter, we have studied the effects of the white noise on the predator-prey system. Next we will investigate how the interactions between the white noise, telegraph noise and time delay affect the population dynamics.

Chapter 5

Stochastic Delay Foraging Arena Predator-Prey System with Markovian Switching

5.1 Introduction

Recall that Chapter 4 introduced white noise to the population system (1.3.2). In this chapter, we additionally incorporate telegraph noise and time delay into the population system (4.2.1). An SDE model including telegraph noise can characterise the systems where the structures and parameters experience abrupt changes due to abrupt environmental disturbances and changing subsystem interconnections [94], etc. Moreover, Xu and Chen [133] suggest that time delays often occur in a population system due to gestation.

This chapter is organised as follows: In section 5.2, we formulate the stochastic delay foraging arena system with Markovian switching. In section 5.3, we prove the existence of a global positive solution. Section 5.4-5.6 study the long-time properties of the system including stochastic ultimate boundedness, extinction and pathwise estimation. In section 5.7, we use computer simulations based on the Euler-Maruyama scheme to verify the results. In section 5.8, we give a summary for this chapter.

5.2 Foraging Arena Predator-prey System with Markovian Switching

Time delays are commonly found in population interactions. For instance, gestation may result in time delays [133]. Motivated by this, we incorporate time delay into the predator-prey model (4.2.1). This leads to the following system:

$$\begin{aligned} dx_1(t) &= x_1(t)\Big(a - bx_1(t) - \frac{sx_2(t)}{\beta + x_2(t)}\Big)dt + \sigma_1 x_1(t)dB_1(t), \\ dx_2(t) &= x_2(t)\Big(\frac{hx_1(t-\tau)}{\beta + x_2(t-\tau)} - c - fx_2(t)\Big)dt + \sigma_2 x_2(t)dB_2(t), \end{aligned} \tag{5.2.1}$$

where τ is the constant delay due to gestation. We also would like to investigate the effect of telegraph noise on the population dynamics. Recall that telegraph noise can be described as a switching between two or more regimes of environments [35,48]. The regime switching can be modelled by a finite-state Markov chain [48]. We let $r(t), t \geqslant 0$ be a right-continuous Markov chain on the probability space taking values in the state space $\mathbb{S} = \{1, 2, \ldots, N\}$ with the generator $\Gamma = (\gamma_{uv})$ given by

$$\mathbb{P}\{r(t+\delta) = v | r(t) = u\} = \begin{cases} \gamma_{uv}\delta + o(\delta), & \text{if } u \neq v, \\ 1 + \gamma_{uu}\delta + o(\delta) & \text{if } u = v, \end{cases}$$

where $\delta > 0$. Here $\gamma_{uv} \geqslant 0$ is the transition rate from u to v if $u \neq v$ while $\gamma_{uu} = -\sum_{v \neq u} \gamma_{uv}$. Such process is called a continuous-time finite Markov chain. We suppose that all the Markov chains are finite and all states are stable. For such a Markov chain, almost every sample path is a right continuous step function with a finite number of sample jumps in any finite subinterval of $\mathbb{R}_+$. There is a sequence $\{\eta_n\}_{n \geqslant 0}$ of finite-valued $\mathcal{F}_t$-stopping times such that $0 = \eta_0 < \eta_1 < \cdots < \eta_n \to \infty$ almost surely and

$$r(t) = \sum_{n=0}^{\infty} r(\eta_n)\mathbf{I}_{[\eta_n, \eta_{n+1})}(t).$$

The switching is memoryless and the waiting time for the next switch has an exponential distribution with parameter $-\gamma_{ii}$, given that $r(\eta_n) = i$. Namely

$$\mathbb{P}(\eta_{n+1} - \eta_n \geqslant T | r(\eta_n) = i) = e^{\gamma_{ii}T}, \quad \forall T \geqslant 0.$$

We also assume that the Markov chain $r(\cdot)$ is independent of the Brownian motion $B(\cdot)$ and is irreducible. Under this condition, the Markov chain has a unique

stationary distribution $\pi = (\pi_1, \pi_2, \cdots, \pi_N) \in \mathbb{R}^{1\times N}$ which can be defined by solving the following linear equation

$$\pi\Gamma = 0$$

subject to

$$\sum_{i=1}^{N} \pi_i = 1 \text{ and } \pi > 0 \text{ for all } i \in \mathbb{S}.$$

Now we will introduce the Markov switching into the SDE system (5.2.1). Suppose the Markov chain $r(t)$ in the state space $\mathbb{S} = \{1, 2, \cdots, N\}$ controls the switching between the environmental regimes, the population system (5.2.1) then becomes

$$dx_1(t) = x_1(t)\Big(a(r(t)) - b(r(t))x_1(t) - \frac{s(r(t))x_2(t)}{\beta(r(t)) + x_2(t)}\Big)dt + \sigma_1(r(t))x_1(t)dB_1(t) \tag{5.2.2a}$$

$$dx_2(t) = x_2(t)\Big(\frac{h(r(t))x_1(t-\tau)}{\beta(r(t)) + x_2(t-\tau)} - c(r(t)) - f(r(t))x_2(t)\Big)dt + \sigma_2(r(t))x_2(t)dB_2(t), \tag{5.2.2b}$$

where the system parameters $a(i), b(i), s(i), \beta(i), h(i), c(i), f(i), \sigma_1(i)$ and $\sigma_2(i)$ are all positive constants for all $i \in \mathbb{S}$. We set $x(t) = (x_1(t), x_2(t))^T$ as the solution to model (5.2.2) with the initial value $x_0 = (x_1(0), x_2(0))^T$.

5.3 Existence of A Unique Positive Solution

It is an essential property for a population system to have a unique positive solution. We found that the coefficients of model (5.2.2) do not obey the linear growth condition, though they are locally Lipschitz continuous. This suggests that the solution may exit from $\mathbb{R}^2_+$ space at a finite time. The following theorem shows the existence and uniqueness of a positive global solution to model (5.2.2).

Theorem 5.1. *For any given initial value $\{x(t) : -\tau \leqslant t \leqslant 0\} \in C([-\tau, 0]; \mathbb{R}^2_+)$, there is a unique solution $x(t)$ to equation (5.2.2) on $t \geqslant -\tau$ and the solution will remain in $\mathbb{R}^2_+$ with probability one, namely $x(t) \in \mathbb{R}^2_+$ for all $t \geqslant -\tau$ almost surely.*

Proof. Since the coefficients of equation (5.2.2) are locally Lipschitz continuous, for any given initial value $\{x(t) : -\tau \leqslant t \leqslant 0\} \in C([-\tau, 0]; \mathbb{R}^2_+)$, there is a unique maximal local solution $x(t)$ on $t \in [-\tau, \tau_e)$, where τ_e is the explosion time (exit

time) from $\mathbb{R}^2_+$. To show that $x(t) \in \mathbb{R}^2_+$ a.s. for all $t \geqslant 0$, we need to verify $\tau_e = \infty$ a.s. Let $k_0 > 0$ be sufficiently large for

$$\frac{1}{k_0} < \min_{-\tau \leqslant t \leqslant 0} |x(t)| \leqslant \max_{-\tau \leqslant t \leqslant 0} |x(t)| < k_0.$$

For each integer $k \geqslant k_0$, define the stopping time

$$\tau_k = \inf\{t \in [0, \tau_e) : x_i(t) \notin \Big(\frac{1}{k}, k\Big) \text{ for some } i = 1, 2\}.$$

Obviously, τ_k is increasing as $k \to \infty$. Set $\tau_\infty := \lim_{t\to\infty} \tau_k$ and whence $\tau_\infty \leqslant \tau_e$ a.s. Hence to complete the proof, we need to show that

$$\tau_\infty = \infty \quad \text{a.s.} \tag{5.3.1}$$

Define a C^2-function $V : \mathbb{R}^2_+ \to \mathbb{R}_+$ by $V(x) = x_1 - \log x_1 + x_2 - \log x_2$. From the Itô formula (Theorem 2.13),

$$\begin{aligned} dV(x(t), r(t)) = LV(x(t), x(t-\tau), r(t))dt + \sigma_1(r(t))\big(x_1(t) - 1\big)dB_1(t) \\ + \sigma_2(r(t))\big(x_2(t) - 1\big)dB_2(t), \end{aligned} \tag{5.3.2}$$

where

$$\begin{aligned} LV(x, y, i) = -a(i) + \frac{s(i)x_2}{\beta(i) + x_2} + c(i) + \frac{\sigma_1^2(i)}{2} + \frac{\sigma_2^2(i)}{2} + (a(i) + b(i))x_1 + (f(i) \\ - c(i))x_2 - b(i)x_1^2 - f(i)x_2^2 + \frac{h(i)x_2y_1}{\beta(i) + y_2} - \frac{h(i)y_1}{\beta(i) + y_2} \end{aligned} \tag{5.3.3}$$

The Young inequality then indicates that

$$\frac{h(i)x_2y_1}{\beta(i) + y_2} \leqslant \frac{h(i)x_2y_1}{\beta(i)} = \frac{h(i)y_1}{\beta(i)\sqrt{f(i)}}\sqrt{f(i)}x_2 \leqslant \frac{h^2(i)}{2\beta^2(i)f(i)}y_1^2 + \frac{f(i)}{2}x_2^2$$

It is then followed from (5.3.3) that

$$\begin{aligned} LV(x, y, i) \leqslant -a(i) + s(i) + c(i) + \frac{\sigma_1^2(i)}{2} + \frac{\sigma_2^2(i)}{2} + (a(i) + b(i))x_1 + (f(i) - c(i))x_2 \\ - b(i)x_1^2 - \frac{f(i)}{2}x_2^2 + \frac{h^2(i)}{2\beta^2(i)f(i)}y_1^2 \end{aligned}$$

Hence there exist three positive constants K_1, K_2 and K_3 for

$$LV(x, y, i) \leqslant K_1\Big(1 + \frac{|x|}{2}\Big) - K_2|x|^2 + K_3y_1^2. \tag{5.3.4}$$

Note that $|x| \leqslant 2V(x)$. Equation (5.3.2) is then followed from (5.3.4) that

$$\begin{aligned} dV(x(t), r(t)) \leqslant & [K_1(1 + V(x(t))) - K_2|x(t)|^2 + K_3 x_1^2(t-\tau)]dt \\ & + \sigma_1(r(t))(x_1(t) - 1)dB_1(t) + \sigma_2(r(t))(x_2(t) - 1)dB_2(t). \end{aligned}$$

For any $k \geqslant k_0$ and $t_1 \in [0, \tau]$, we obtain

$$\mathbb{E}V(x(t_1 \wedge \tau_k)) \leqslant K_4 + K_1\mathbb{E}\int_0^{t_1\wedge\tau_k} V(x(t))dt - K_2\mathbb{E}\int_0^{t_1\wedge\tau_k} |x(t)|^2 dt, \quad (5.3.5)$$

where

$$K_4 = V(x(0)) + K_1\tau + K_3\int_0^\tau x_1^2(t-\tau)dt < \infty.$$

We then obtain from (5.3.5) that

$$\mathbb{E}V(x(t_1 \wedge \tau_k)) \leqslant K_4 + K_1\int_0^{t_1} \mathbb{E}V(x(\tau_k \wedge t))dt.$$

This and the Gronwall inequality (Theorem 2.30) imply that

$$\mathbb{E}V(x(t_1 \wedge \tau_k)) \leqslant K_4 e^{\tau K_1} \quad \text{for } 0 \leqslant t_1 \leqslant \tau, k \geqslant k_0. \quad (5.3.6)$$

It then follows that

$$\mathbb{E}V(x(\tau_k \wedge \tau)) \leqslant K_4 e^{\tau K_1} \quad \text{for } k \geqslant k_0.$$

We can hence show that $\tau_\infty \geqslant \tau$ a.s. [47, 89, 92]. Additionally, letting $k \to \infty$ in (5.3.6) gives

$$\mathbb{E}V(x(t_1)) \leqslant K_4 e^{\tau K_1} \quad \text{for } 0 \leqslant t_1 \leqslant \tau.$$

By setting $t_1 = \tau$ in (5.3.5) and then letting $k \to \infty$, we have

$$\mathbb{E}\int_0^\tau |x(t)|^2 dt \leqslant \frac{1}{K_2}(K_4 + \tau K_1 K_4 e^{\tau K_1}) < \infty. \quad (5.3.7)$$

For $t_2 \in (\tau, 2\tau]$,

$$\begin{aligned} \mathbb{E}V(x(t_2 \wedge \tau_k)) \leqslant & K_5 + K_1\mathbb{E}\int_0^{t_2\wedge\tau_k} V(x(t))dt - K_2\mathbb{E}\int_0^{t_2\wedge\tau_k} |x(t)|^2 dt \quad (5.3.8) \\ & + K_3\mathbb{E}\int_0^{t_2\wedge\tau_k-\tau} x_1^2(t)dt \\ \leqslant & \tilde{K}_5 + K_1\mathbb{E}\int_0^{t_2\wedge\tau_k} V(x(t))dt - K_2\mathbb{E}\int_0^{t_2\wedge\tau_k} |x(t)|^2 dt, \quad (5.3.9) \end{aligned}$$

where $K_5 = V(x(0)) + 2K_1\tau + K_3\int_0^\tau x_1^2(t-\tau)dt$ and $\tilde{K}_5 = K_5 + \frac{1}{K_2}(K_4 + \tau K_1 K_4 e^{\tau K_1}) < \infty$ in view of (5.3.8). Similarly we obtain that $\tau_\infty \geqslant 2\tau$ a.s. and

$$\mathbb{E}V(x(t_2)) \leqslant \tilde{K}_5 e^{2\tau K_1}.$$

By setting $t_2 = 2\tau$ in (5.3.8) and then letting $k \to \infty$ yields that

$$\mathbb{E}\int_0^{2\tau} |x(t)|^2 dt \leqslant \frac{1}{K_2}\Big(\tilde{K}_5 + 2\tau K_1 \tilde{K}_5 e^{2\tau K_1}\Big) < \infty.$$

Repeating this procedure, one can show $\tau_\infty \geqslant m\tau$ with probability one for any integer $m \geqslant 1$. Therefore $\tau_\infty = \infty$ a.s. □

5.4 Stochastically Ultimate Boundedness

After analysing the global positive solution to model (5.2.2), we now explore the conditions for system (5.2.2) to be stochastically ultimately bounded.

Theorem 5.2. *If*

$$h(i) \leqslant \beta(i)f(i) \text{ for all } i \in \mathbb{S}, \tag{5.4.1}$$

then for any $\theta > 0$, there exists a positive constant $K(\theta)$ such that for any initial value $\{x(t) : -\tau \leqslant t \leqslant 0\} \in C([-\tau, 0]; \mathbb{R}_+^2)$,

$$\limsup_{t\to\infty} \mathbb{E}\big|x(t)\big|^\theta \leqslant K(\theta).$$

Proof. Condition (5.4.1) yields that there exists a constant $\tilde{\theta} > 1$ sufficiently large such that

$$\frac{e^\tau h^{\tilde{\theta}+1}(i)}{(\tilde{\theta}+1)\beta^{\tilde{\theta}+1}(i)f^{\tilde{\theta}}(i)} < \hat{b} \quad \text{for all } i \in \mathbb{S}.$$

We first consider the case when $\theta \geqslant \tilde{\theta}$. It then follows that

$$\frac{e^\tau h^{\theta+1}(i)}{(\theta+1)\beta^{\theta+1}(i)f^{\theta}(i)} < \hat{b} \quad \text{for all } i \in \mathbb{S}. \tag{5.4.2}$$

Applying the Itô formula to $e^t(x_1^\theta(t) + x_2^\theta(t))$,

$$d(e^t(x_1^\theta(t) + x_2^\theta(t)) = e^t\phi(x(t), x(t-\tau), r(t))dt + \theta\sigma_1(r(t))e^t x_1^\theta(t)dB_1(t)$$

$$+\theta\sigma_2(r(t))e^t x_2^\theta(t)dB_2(t), \tag{5.4.3}$$

where

$$\begin{aligned}\phi(x,y,i) = &\Big(a(i)\theta + \frac{1}{2}\theta(\theta-1)\sigma_1^2(i)+1\Big)x_1^\theta + \Big(-c(i)\theta + \frac{1}{2}\theta(\theta-1)\sigma_2^2(i)+1\Big)x_2^\theta \\ &- \frac{s(i)\theta x_1^\theta x_2}{\beta(i)+x_2} + \frac{h(i)\theta y_1 x_2^\theta}{\beta(i)+y_2} - b(i)\theta x_1^{\theta+1} - f(i)\theta x_2^{\theta+1}.\end{aligned}$$

Integrating on both sides of (5.4.3) and then taking expectation then yields that

$$\begin{aligned}\mathbb{E}\Big[e^{t\wedge\tau_k}(x_1^\theta(t\wedge\tau_k)+x_2^\theta(t\wedge\tau_k))\Big] &= x_1^\theta(0)+x_2^\theta(0) \\ &\quad + \int_0^{t\wedge\tau_k} e^u\phi(x(u),x(u-\tau),r(u))du.\end{aligned}$$

From the Young inequality, for all $i\in\mathbb{S}$

$$\frac{h(i)y_1x_2^\theta}{\beta(i)+y_2} \leqslant \frac{h(i)y_1}{\beta(i)f^{\frac{\theta}{\theta+1}}(i)}\cdot f^{\frac{\theta}{\theta+1}}(i)x_2^\theta \leqslant \frac{h^{\theta+1}(i)}{(\theta+1)\beta^{\theta+1}(i)f^\theta(i)}y_1^{\theta+1} + \frac{\theta f(i)}{\theta+1}x_2^{\theta+1}.$$

Hence

$$\phi(x,y,i) \leqslant \phi_1(x,i) + \phi_2(y,i) - b(i)\theta x_1^{\theta+1}$$

with

$$\begin{aligned}\phi_1(x,i) = &\Big(a(i)\theta + \frac{1}{2}\theta(\theta-1)\sigma_1^2(i)+1\Big)x_1^\theta + \Big(-c(i)\theta + \frac{1}{2}\theta(\theta-1)\sigma_2^2(i)+1\Big)x_2^\theta \\ &- \frac{f(i)\theta}{\theta+1}x_2^{\theta+1}\end{aligned}$$

and

$$\phi_2(y,i) = \frac{\theta h^{\theta+1}(i)}{(\theta+1)\beta^{\theta+1}(i)f^\theta(i)}y_1^{\theta+1}.$$

Note that

$$\begin{aligned}&\int_0^{t\wedge\tau_k} e^u\phi_2(x_1(u-\tau),r(u))du \\ \leqslant&\frac{\theta e^\tau}{\theta+1}\int_{-\tau}^{t\wedge\tau_k}\frac{h^{\theta+1}(r(u+\tau))e^u}{\beta^{\theta+1}(r(u+\tau))f^\theta(r(u+\tau))}x_1^{\theta+1}(u)du \\ \leqslant&\frac{\theta\check{h}^{\theta+1}e^\tau}{(\theta+1)\hat{\beta}^{\theta a+1}\hat{f}^\theta}\int_{-\tau}^0 x_1^{\theta+1}(u)du + \frac{\theta e^\tau}{\theta+1}\int_0^{t\wedge\tau_k}\frac{h^{\theta+1}(r(u+\tau))e^u}{\beta^{\theta+1}(r(u+\tau))f^\theta(r(u+\tau))}x_1^{\theta+1}(u)du\end{aligned}$$

Hence

$$\begin{aligned}
&\mathbb{E}\Big[e^{t\wedge\tau_k}(x_1^\theta(t\wedge\tau_k)+x_2^\theta(t\wedge\tau_k))\Big]\\
&\leqslant x_1^\theta(0)+x_2^\theta(0)+\int_0^{t\wedge\tau_k} e^u\Big[\phi_1(x(u),r(u))+\phi_2(x(u-\tau),r(u))-b(r(u))\theta x_1^{\theta+1}\Big]du\\
&\leqslant x_1^\theta(0)+x_2^\theta(0)+\frac{\theta\check{h}^{\theta+1}e^\tau}{(\theta+1)\hat{\beta}^{\theta+1}\hat{f}^\theta}\int_{-\tau}^0 x_1^{\theta+1}(u)du+\int_0^{t\wedge\tau_k} e^u\Big[\phi_1(x(u),r(u))\\
&+\Big(\frac{e^\tau h^{\theta+1}(r(u+\tau))}{(\theta+1)\beta^{\theta+1}(r(u+\tau))f^\theta(r(u+\tau))}-b(r(u))\Big)\theta x_1^{\theta+1}(u)\Big]du
\end{aligned}$$

This and (5.4.2) indicate that there is a positive constant $K^*(\theta)$ such that

$$\begin{aligned}
&\mathbb{E}\Big[e^{(t\wedge\tau_k)}(x_1^\theta(t\wedge\tau_k)+x_2^\theta(t\wedge\tau_k))\Big]\\
&\leqslant x_1^\theta(0)+x_2^\theta(0)+\frac{\theta\check{h}^{\theta+1}e^\tau}{(\theta+1)\hat{\beta}^{\theta+1}\hat{f}^\theta}\int_{-\tau}^0 x_1^{\theta+1}(u)du+K^*(\theta)\int_0^{t\wedge\tau_k} e^u du.
\end{aligned}$$

Letting $k\to\infty$ and then $t\to\infty$ yields

$$\limsup_{t\to\infty}\mathbb{E}\big[x_1^\theta(t)+x_2^\theta(t)\big]\leqslant K^*(\theta). \tag{5.4.4}$$

On the other hand, we have

$$|x|^2\leqslant 2\max(x_1^2,x_2^2),\ \text{so}\ |x|^\theta\leqslant 2^{\theta/2}\max\big(x_1^\theta,x_2^\theta\big)\leqslant 2^{\theta/2}(x_1^\theta+x_2^\theta).$$

As a result,

$$\limsup_{t\to\infty}\mathbb{E}|x(t)|^\theta\leqslant 2^{\theta/2}\limsup_{t\to\infty}\mathbb{E}[x_1^\theta(t)+x_2^\theta(t)]\leqslant 2^{\theta/2}K^*(\theta)=K(\theta). \tag{5.4.5}$$

For $0<\theta<\tilde{\theta}$, Hölder's inequality yields

$$\mathbb{E}|x(t)|^\theta\leqslant(\mathbb{E}|x(t)|^{\tilde{\theta}})^{\frac{\theta}{\tilde{\theta}}}.$$

Hence from (5.4.5)

$$\limsup_{t\to\infty}\mathbb{E}|x(t)|^\theta\leqslant\limsup_{t\to\infty}(\mathbb{E}|x(t)|^{\tilde{\theta}})^{\frac{\theta}{\tilde{\theta}}}\leqslant K(\theta).$$

□

5.5 Extinction

In this section, we investigate the conditions for the system to be extinct.

Theorem 5.3. *For any initial value* $\{x(t) : -\tau \leqslant t \leqslant 0\} \in C([-\tau, 0]; \mathbb{R}^2_+)$*, if*

$$\lambda_1 := \sum_{i\in\mathbb{S}} \pi_i \Big(a(i) - \frac{\sigma_1^2(i)}{2}\Big) < 0, \tag{5.5.1}$$

both $x_1(t)$ *and* $x_2(t)$ *tend to zero exponentially as* $t \to \infty$ *with probability one.*

Proof. Applying the Itô formula on $\log x_1(t)$, we have

$$\begin{aligned} d\log x_1(t) &= \left(a(r(t)) - b(r(t))x_1(t) - \frac{\sigma_1^2(r(t))}{2} - \frac{s(r(t))x_2(t)}{\beta(r(t)) + x_2(t)}\right)dt \\ &\quad + \sigma_1(r(t))dB_1(t) \\ &\leqslant \left(a(r(t)) - \frac{\sigma_1^2(r(t))}{2}\right)dt + \sigma_1(r(t))dB_1(t). \end{aligned} \tag{5.5.2}$$

Integrating from 0 to t and dividing by t, we get

$$\frac{1}{t}\log x_1(t) \leqslant \frac{1}{t}\log x_1(0) + \frac{1}{t}\int_0^t \Big(a(r(u)) - \frac{\sigma_1^2(r(u))}{2}\Big)du + \frac{\check{\sigma}_1 B_1(t)}{t}.$$

Letting $t \to \infty$ and by the strong law of large numbers for martingales (Theorem 2.2)

$$\lim_{t\to\infty} \frac{\check{\sigma}_1 B_1(t)}{t} = 0 \quad \text{a.s.}$$

Thus by the ergodic property of the Markov chain,

$$\limsup_{t\to\infty} \frac{1}{t}\log x_1(t) \leqslant \lambda_1 < 0 \quad \text{a.s.}$$

as required. It follows that

$$\lim_{t\to\infty} \frac{1}{t}\int_0^t x_1(u)du = 0 \quad \text{a.s.} \tag{5.5.3}$$

Meanwhile

$$\begin{aligned} d\log x_2(t) &= \Big(\frac{h(r(t))x_1(t-\tau)}{\beta(r(t)) + x_2(t-\tau)} - c(r(t)) - \frac{\sigma_2^2(r(t))}{2} - f(r(t))x_2(t)\Big)dt \\ &\quad + \sigma_2(r(t))dB_2(t). \end{aligned} \tag{5.5.4}$$

It follows that

$$\frac{\log x_2(t)}{t} \leqslant \frac{1}{t}\bigg(\log x_2(0) + \frac{\check{h}}{\hat{\beta}}\int_{-\tau}^{0} x_1(u)du + \frac{\check{h}}{\hat{\beta}}\int_0^t x_1(u)du\bigg) - \Big(\hat{c} + \frac{\hat{\sigma}_2^2}{2}\Big) + \frac{\check{\sigma}_2 B_2(t)}{t}.$$

Letting $t \to \infty$ and recalling equation (5.5.3),

$$\limsup_{t\to\infty} \frac{\log x_2(t)}{t} \leqslant -\Big(\hat{c} + \frac{\hat{\sigma}_2^2}{2}\Big) < 0 \quad \text{a.s.}$$

□

5.6 Pathwise Estimation

In this section, we discuss the long-time properties of the solutions of system (5.2.2) pathwisely.

Theorem 5.4. *Assume that condition* (5.4.1) *holds. Then for any initial value* $\{x(t) : -\tau \leqslant t \leqslant 0\} \in C([-\tau, 0]; \mathbb{R}^2_+)$,

$$\limsup_{t\to\infty} \frac{\log(x_1(t) + x_2(t))}{\log t} \leqslant 1 \quad a.s.$$

Proof. From the Young inequality,

$$\begin{aligned}
&d\big[x_1(t) + x_2(t)\big] \\
&\leqslant \Big[a(r(t))x_1(t) + \frac{h(r(t))x_1(t-\tau)x_2(t)}{\beta(r(t)) + x_2(t-\tau)}\Big]dt + \sigma_1(r(t))x_1(t)dB_1(t) \\
&\quad + \sigma_2(r(t))x_2(t)dB_2(t) \\
&\leqslant \Big[\check{a}x_1(t) + \frac{\check{h}^2}{2\hat{\beta}^2}x_1^2(t-\tau) + \frac{1}{2}x_2^2(t)\Big]dt + \sigma_1(r(t))x_1(t)dB_1(t) + \sigma_2(r(t))x_2(t)dB_2(t).
\end{aligned}$$

Then we have

$$\begin{aligned}
&\mathbb{E}\Big[\sup_{t\leqslant u\leqslant t+1}\Big(x_1(u) + x_2(u)\Big)\Big] \leqslant \mathbb{E}\big[x_1(t) + x_2(t)\big] + \check{a}\int_t^{t+1}\mathbb{E}[x_1(v)]dv \\
&+ \frac{\check{h}^2}{2\hat{\beta}^2}\int_t^{t+1}\mathbb{E}[x_1^2(u-\tau)]du + \frac{1}{2}\int_t^{t+1}\mathbb{E}[x_2^2(u)]du \\
&+ \mathbb{E}\Big(\sup_{t\leqslant u\leqslant t+1}\int_t^u \sigma_1(r(v))x_1(v)dB_1(v)\Big) + \mathbb{E}\Big(\sup_{t\leqslant u\leqslant t+1}\int_t^u \sigma_2(r(v))x_2(v)dB_2(v)\Big).
\end{aligned} \tag{5.6.1}$$

By the Burkholder-Davis-Gundy inequality (Theorem 2.31),

$$\begin{aligned}
&\mathbb{E}\Big(\sup_{t\leqslant u\leqslant t+1}\int_t^u \sigma_1(r(v))x_1(v)dB_1(v)\Big) \leqslant 4\sqrt{2}\mathbb{E}\Big(\int_t^{t+1}\check{\sigma}_1^2 x_1^2(v)dv\Big)^{\frac{1}{2}}\\
&\leqslant \mathbb{E}\Big(\sup_{t\leqslant u\leqslant t+1} x_1(u)\cdot 32\check{\sigma}_1^2\int_t^{t+1} x_1(v)dv\Big)^{\frac{1}{2}}\\
&\leqslant \mathbb{E}\Big(\frac{1}{2}\sup_{t\leqslant u\leqslant t+1} x_1(u) + 16\check{\sigma}_1^2\int_t^{t+1} x_1(v)dv\Big)\\
&= \frac{1}{2}\mathbb{E}\Big(\sup_{t\leqslant u\leqslant t+1} x_1(u)\Big) + 16\check{\sigma}_1^2\int_t^{t+1}\mathbb{E}\big[x_1(v)\big]dv.
\end{aligned}$$

Similarly, we have

$$\mathbb{E}\Big(\sup_{t\leqslant u\leqslant t+1}\int_t^u \sigma_2(r(s))x_2(s)dB_2(s)\Big) \leqslant \frac{1}{2}\mathbb{E}\Big(\sup_{t\leqslant u\leqslant t+1} x_2(u)\Big) + 16\check{\sigma}_2^2\int_t^{t+1}\mathbb{E}\big[x_2(v)\big]dv.$$

Hence (5.6.1) is then followed that

$$\begin{aligned}
&\mathbb{E}\Big[\sup_{t\leqslant u\leqslant t+1}\Big(x_1(u)+x_2(u)\Big)\Big] \leqslant 2\mathbb{E}\big[x_1(t)+x_2(t)\big] + 2\check{a}\int_t^{t+1}\mathbb{E}[x_1(v)]dv\\
&+\frac{\check{h}^2}{\hat{\beta}^2}\int_{t-\tau}^{t+1-\tau}\mathbb{E}[x_1^2(v)]dv + \int_t^{t+1}\mathbb{E}[x_2^2(v)]dv + 32\big(\check{\sigma}_1^2\vee\check{\sigma}_2^2\big)\int_t^{t+1}\mathbb{E}\big[x_1(v)+x_2(v)\big]dv.
\end{aligned}$$

Letting $t\to\infty$ and making use of (5.4.4), we obtain

$$\limsup_{t\to\infty}\mathbb{E}\Big[\sup_{t\leqslant u\leqslant t+1}\big(x_1(u)+x_2(u)\big)\Big] \leqslant 2\Big(1+\check{a}+16\big(\check{\sigma}_1^2\vee\check{\sigma}_2^2\big)\Big)K^*(1)+\Big(\frac{\check{h}^2}{\hat{\beta}^2}\vee 1\Big)K^*(2).$$

Hence there is a positive constant $\tilde{K}$ such that

$$\mathbb{E}\Big[\sup_{k_1\leqslant u\leqslant k_1+1}\big(x_1(u)+x_2(u)\big)\Big] \leqslant \tilde{K} \text{ for } k_1 = 1,2,\cdots$$

Let $\epsilon>0$ be arbitrary. By the Chebychev inequality,

$$\mathbb{P}\Big[\sup_{k_1\leqslant u\leqslant k_1+1}\big(x_1(u)+x_2(u)\big) > k_1^{1+\epsilon}\Big] \leqslant \frac{\mathbb{E}\Big[\sup_{k_1\leqslant u\leqslant k_1+1}\big(x_1(u)+x_2(u)\big)\Big]}{k_1^{1+\epsilon}} \leqslant \frac{\tilde{K}}{k_1^{1+\epsilon}}$$

for $k_1 = 1,2,\cdots$. By the Borel-Cantelli lemma (Lemma 2.1), for almost all $\omega\in\Omega$,

$$\sup_{k_1\leqslant t\leqslant k_1+1}\big[x_1(t)+x_2(t)\big] \leqslant k_1^{1+\epsilon} \text{ holds for all but finitely many } k_1.$$

Hence there exists a $\tilde{k}(\omega)$, if $k_1\geqslant\tilde{k}$ and $k_1\leqslant t\leqslant k_1+1$,

$$\frac{\log\big[x_1(t)+x_2(t)\big]}{\log t} \leqslant \frac{\log\Big[\sup_{k_1\leqslant t\leqslant k_1+1}\big(x_1(t)+x_2(t)\big)\Big]}{\log t} \leqslant \frac{\log k_1^{1+\epsilon}}{\log t} \leqslant 1+\epsilon \quad \text{a.s.}$$

Consequently,

$$\limsup_{t\to\infty} \frac{\log\big[x_1(t)+x_2(t)\big]}{\log t} \leqslant 1+\epsilon \quad \text{a.s.}$$

Letting $\epsilon \to 0$, we obtain the required assertion. □

Theorem 5.4 shows that for arbitrary small $\epsilon > 0$, there is a positive random variable $t_3 = t_3(\omega)$ such that with probability one,

$$\frac{\log[x_1(t)+x_2(t)]}{\log t} \leqslant 1+\epsilon \text{ for all } t \geqslant t_3.$$

Hence we have

$$x_1(t)+x_2(t) \leqslant t^{1+\epsilon} \text{ for all } t \geqslant t_3.$$

It then follows that

$$x_1(t)+x_2(t) \leqslant \sup_{0\leqslant t\leqslant t_3}[x_1(t)+x_2(t)] + t^{1+\epsilon} \text{ for all } t \geqslant 0.$$

This means that the total amount of prey and predator species will grow at most polynomially with order close to 1.

Recall that Lemma 4.3 in Chapter 4 introduced a nice property of a one-dimensional Brownian motion $\{W_t\}_{t\geqslant 0}$. Based on this, the following theorem shows some other asymptotic properties of the prey and predator populations.

Theorem 5.5. *For any initial value* $\{x(t) : -\tau \leqslant t \leqslant 0\} \in C([-\tau, 0]; \mathbb{R}^2_+)$, *if*

$$a(i) - \frac{\sigma_1^2(i)}{2} := q(i) > 0 \text{ for all } i \in \mathbb{S}, \tag{5.6.2}$$

then

$$\limsup_{t\to\infty} \frac{1}{t}\int_0^t x_1(u)du \leqslant \frac{\lambda_1}{\hat{b}} \quad a.s.$$

In particular, if also

(*i*) $\lambda_2 > 0$, *then* $\liminf_{t\to\infty} \frac{1}{t}\int_0^t x_1(u)du \geqslant \frac{\lambda_2}{\check{b}}$ *almost surely;*

(*ii*) $\frac{\check{h}}{\hat{b}\hat{\beta}}\lambda_1 - \lambda_3 < 0$, *then* $\liminf_{t\to\infty} \frac{1}{t}\int_0^t x_1(u)du \geqslant \frac{\lambda_1}{\check{b}}$ *and* x_2 *dies out exponentially almost surely,*

where

$$\lambda_2 = \sum_{i\in\mathbb{S}} \pi_i\Big(a(i) - s(i) - \frac{\sigma_1^2(i)}{2}\Big) \quad \text{and} \quad \lambda_3 = \sum_{i\in\mathbb{S}} \pi_i\Big(c(i) + \frac{\sigma_2^2(i)}{2}\Big).$$

Proof. Applying Itô's formula (Theorem 2.13) on $\frac{1}{x_1(t)}$ gives

$$d\Big(\frac{1}{x_1(t)}\Big) = \Big(\frac{1}{x_1(t)}\Big(\frac{s(r(t))x_2(t)}{\beta(r(t))+x_2(t)} - a(r(t)) + \sigma_1^2(r(t))\Big) + b(r(t))\Big)dt - \frac{\sigma_1(r(t))}{x_1(t)}dB_1(t).$$

Hence by the variation-of-constants formula (Theorem 2.20) and Lemma 2.19,

$$\begin{aligned}
\frac{1}{x_1(t)} &= \exp\Big(\int_0^t \Big(\frac{1}{2}\sigma_1^2(r(u)) - a(r(u)) + \frac{s(r(u))x_2(u)}{\beta(r(u))+x_2(u)}\Big)du - \int_0^t \sigma_1(r(u))dB_1(u)\Big)\cdot \\
&\quad \Big[\frac{1}{x_1(0)} + \int_0^t b(r(u))\exp\Big(\int_0^u \Big(a(r(v)) - \frac{s(r(v))x_2(v)}{\beta(r(v))+x_2(v)} - \frac{1}{2}\sigma_1^2(r(v))\Big)dv \\
&\quad + \int_0^u \sigma_1(r(v))dB_1(v)\Big)du\Big] \\
&= \exp\big(-\int_0^t \sigma_1(r(u))dB_1(u)\big)\Big[\frac{1}{x_1(0)}\exp\Big(\int_0^t \Big(-a(r(u)) + \frac{1}{2}\sigma_1^2(r(u)) \\
&\quad + \frac{s(r(u))x_2(u)}{\beta(r(u))+x_2(u)}\Big)du\Big) + \int_0^t b(r(u))\exp\Big(\int_u^t \Big(-a(r(v)) + \frac{1}{2}\sigma_1^2(r(v)) \\
&\quad + \frac{s(r(v))x_2(v)}{\beta(r(v))+x_2(v)}\Big)dv + \int_0^u \sigma_1(r(v))dB_1(v)\Big)du\Big]. \qquad (5.6.3)
\end{aligned}$$

On the one hand, (5.6.3) leads to

$$\begin{aligned}
\frac{1}{x_1(t)} &\leqslant \exp\big(-\int_0^t \sigma_1(r(u))dB_1(u)\big)\Big[\frac{1}{x_1(0)}\exp\Big(\int_0^t \Big(-a(r(u)) + \frac{1}{2}\sigma_1^2(r(u)) \\
&\quad + \frac{s(r(u))x_2(u)}{\beta(r(u))+x_2(u)}\Big)du\Big) + \check{b}\exp\Big(\check{\sigma}_1 \max_{0\leqslant u\leqslant t} B_1(u) + \int_0^t \frac{s(r(u))x_2(u)}{\beta(r(u))+x_2(u)}du\Big)\cdot \\
&\quad \int_0^t \exp(-\hat{q}(t-u))du\Big] \\
&\leqslant \exp\Big(\check{\sigma}_1 \max_{0\leqslant u\leqslant t} B_1(u) - \hat{\sigma}_1 B_1(t) + \int_0^t \frac{s(r(u))x_2(u)}{\beta(r(u))+x_2(u)}du\Big)\Big[\frac{1}{x_1(0)}\exp(-\hat{q}t) \\
&\quad + \check{b}\int_0^t \exp(-\hat{q}(t-u))du\Big] \\
&= \exp\Big(\check{\sigma}_1 \max_{0\leqslant u\leqslant t} B_1(u) - \hat{\sigma}_1 B_1(t) + \int_0^t \frac{s(r(u))x_2(u)}{\beta(r(u))+x_2(u)}du\Big)\Big[\frac{1}{x_1(0)}\exp(-\hat{q}t) \\
&\quad + \frac{\check{b}\big(1-\exp(-\hat{q}t)\big)}{\hat{q}}\Big],
\end{aligned}$$

It then follows that

$$\frac{\log x_1(t)}{t} \geqslant -\frac{\log N_1(t)}{t} - \frac{\check{\sigma}_1 \max_{0\leqslant u\leqslant t} B_1(u) - \hat{\sigma}_1 B_1(t)}{t} - \frac{1}{t}\int_0^t \frac{s(r(u))x_2(u)}{\beta(r(u))+x_2(u)}du, \qquad (5.6.4)$$

where

$$N_1(t) = \frac{1}{x_1(0)}\exp(-\hat{q}t) + \frac{\check{b}(1-\exp(-\hat{q}t))}{\hat{q}}$$

and $\sup_{0\leqslant t<\infty} N_1(t) < \infty$ under condition (5.6.2). By (5.5.2) and (5.6.4),

$$\begin{aligned}\frac{1}{t}\int_0^t x_1(u)du &\leqslant \frac{1}{\hat{b}t}\int_0^t \Big(a(r(u)) - \frac{\sigma_1^2(r(u))}{2}\Big)du - \frac{\log x_1(t)}{\hat{b}t} + \frac{\log x_1(0)}{\hat{b}t}\\ &\quad - \frac{1}{\hat{b}t}\int_0^t \frac{s(r(u))x_2(u)}{\beta(r(u))+x_2(u)}du + \frac{\check{\sigma}_1}{\hat{b}t}B_1(u)\\ &\leqslant \frac{1}{\hat{b}t}\int_0^t \Big(a(r(u)) - \frac{\sigma_1^2(r(u))}{2}\Big)du + \frac{\log N_1(t)}{\hat{b}t} + \frac{\log x_1(0)}{\hat{b}t} + \frac{\check{\sigma}_1}{\hat{b}t}B_1(t)\\ &\quad + \frac{\check{\sigma}_1 \max_{0\leqslant u\leqslant t} B_1(u) - \hat{\sigma}_1 B_1(t)}{\hat{b}t}.\end{aligned}$$

As $t\to\infty$ and from the strong law of large numbers for martingales (Theorem 2.2) and Lemma 4.3,

$$\limsup_{t\to\infty}\frac{1}{t}\int_0^t x_1(u)du \leqslant \frac{\lambda_1}{\hat{b}} \quad \text{a.s.} \tag{5.6.5}$$

On the other hand, (5.6.3) yields

$$\begin{aligned}\frac{1}{x_1(t)} &\geqslant \exp(-\check{\sigma}_1 B_1(t))\Big[\frac{1}{x_1(0)}\exp\Big(\int_0^t\Big(-a(r(u)) + \frac{1}{2}\sigma_1^2(r(u))\Big)du\Big)\\ &\quad + \hat{b}\exp\Big(\hat{\sigma}_1\min_{0\leqslant u\leqslant t}B_1(u)\Big)\int_0^t\exp\Big(\int_u^t\Big(-a(r(v)) + \frac{1}{2}\sigma_1^2(r(v))\Big)dv\Big)du\Big]\\ &\geqslant \exp\Big(\hat{\sigma}_1\min_{0\leqslant u\leqslant t}B_1(u) - \check{\sigma}_1 B_1(t)\Big)\Big[\frac{1}{x_1(0)}\exp(-\check{q}t) + \frac{\hat{b}(1-\exp(-\check{q}t))}{\check{q}}\Big],\end{aligned}$$

It follows that

$$\frac{\log x_1(t)}{t} \leqslant -\frac{\hat{\sigma}_1\min_{0\leqslant u\leqslant t}B_1(u) - \hat{\sigma}_1 B_1(t)}{t} - \frac{\log N_2(t)}{t},$$

where

$$N_2(t) = \frac{1}{x_1(0)}\exp(-\check{q}t) + \frac{\hat{b}(1-\exp(-\check{q}t))}{\check{q}}$$

and $\sup_{0\leqslant t<\infty} N_2(t) < \infty$ under condition (5.6.2). This leads to

$$\limsup_{t\to\infty}\frac{\log x_1(t)}{t} \leqslant 0 \tag{5.6.6}$$

(i) Equation (5.5.2) and (5.6.6) indicate

$$\liminf_{t\to\infty}\frac{1}{t}\int_0^t x_1(u)du \geqslant \lim_{t\to\infty}\frac{1}{\check{b}t}\int_0^t\Big(a(r(u)) - \frac{\sigma_1^2(r(u))}{2} - s(r(u))\Big)du = \frac{\lambda_2}{\check{b}} > 0.$$

This and (5.6.5) yield

$$\frac{\lambda_2}{\check{b}} \leqslant \liminf_{t\to\infty} \int_0^t x_1(u)du \leqslant \limsup_{t\to\infty} \int_0^t x_1(u)du \leqslant \frac{\lambda_1}{\hat{b}} \quad \text{a.s.}$$

(ii) From equation (5.5.4),

$$d\log x_2(t) \leqslant \Big(\frac{h(r(t))x_1(t-\tau)}{\beta(r(t))} - c(r(t) - \frac{\sigma_2^2(r(t))}{2}\Big)dt + \sigma_2(r(t))dB_2(t).$$

Hence

$$\log x_2(t) \leqslant \log x_2(0) + \frac{\check{h}}{\hat{\beta}}\int_{-\tau}^0 x_1(u)du + \frac{\check{h}}{\hat{\beta}}\int_0^t x_1(u)du - \int_0^t \Big(c(r(u)) + \frac{\sigma_2^2(r(u)}{2}\Big)du + \check{\sigma}_2 B_2(t).$$

This and (5.6.5) yield

$$\begin{aligned}\limsup_{t\to\infty} \frac{1}{t}\log(x_2(t)) &\leqslant \frac{\check{h}}{\hat{\beta}} \limsup_{t\to\infty} \frac{1}{t}\int_0^t x_1(u)du - \lim_{t\to\infty}\frac{1}{t}\int_0^t \Big(c(r(u)) + \frac{\sigma_2^2(r(u))}{2}\Big)du \\ &\leqslant \frac{\check{h}\lambda_1}{\hat{b}\hat{\beta}} - \lambda_3 < 0.\end{aligned}$$

Hence for arbitrary small $\zeta > 0$, there exists t_ζ such that

$$\mathbb{P}(\Omega_\zeta) \geqslant 1-\zeta \text{ where } \Omega_\zeta = \Big\{\omega : \frac{s(r(t))x_2(t,\omega)}{\check{b}(\beta(r(t)) + x_2(t,\omega))} \leqslant \zeta \text{ for } t \geqslant t_\zeta\Big\}.$$

It then follows from (5.5.2), (5.6.6) and Lemma 4.3 that for any $\omega \in \Omega_\zeta$,

$$\liminf_{t\to\infty}\frac{1}{t}\int_0^t x_1(u)du \geqslant \frac{\lambda_1}{\check{b}} - \zeta.$$

Letting $\zeta \to 0$ and recalling (5.6.5) yields

$$\frac{\lambda_1}{\check{b}} \leqslant \liminf_{t\to\infty}\frac{1}{t}\int_0^t x_1(u)du \leqslant \limsup_{t\to\infty}\frac{1}{t}\int_0^t x_1(u)du \leqslant \frac{\lambda_1}{\hat{b}} \quad \text{a.s.}$$

□

5.7 Numerical Simulations

It is worth pointing out that for some $j \in \mathbb{S}$, if the environmental noise is big enough, in the sense that $a(j) - \frac{\sigma_1^2(j)}{2} < 0$, then in the subsystem

$$\begin{aligned}dx_1(t) &= x_1(t)\Big(a(j) - b(j)x_1(t) - \frac{s(j)x_2(t)}{\beta(j)+x_2(t)}\Big)dt + \sigma_1(j)x_1(t)dB_1(t) \\ dx_2(t) &= x_2(t)\Big(\frac{h(j)x_1(t-\tau)}{\beta(j)+x_2(t-\tau)} - c(j) - f(j)x_2(t)\Big)dt + \sigma_2(j)x_2(t)dB_2(t),\end{aligned} \tag{5.7.1}$$

both prey and predator populations are extinct (Theorem 5.3). On the other hand, for some $j \in \mathbb{S}$, if $a(j) - \frac{\sigma_1^2(j)}{2} > 0$ and $\frac{h(j)}{b(j)\beta(j)}\big(a(j) - \frac{1}{2}\sigma_1^2(j)\big) - c(j) - \frac{1}{2}\sigma_2^2(j) < 0$, we obtain from Theorem 5.5 (ii) that in the subsystem (5.7.1), the prey species is persistent:

$$\lim_{t\to\infty} \frac{1}{t}\int_0^t x_1(u)du = \frac{2a(j) - \sigma_1^2(j)}{2b(j)} \quad \text{a.s.}$$

while the predators die out ultimately. In addition, Theorem 5.3 yields that if in some subsystems the preys are persistent and in some others the prey species are extinct, then due to the presence of the Markov switching, in the overall system both populations could be extinct if λ_1 is negative. The following two examples indicate the impacts of Markov switching on the population dynamics. The Euler-Maruyama (EM) scheme is used for the computer simulations [57]. From Mao [90], the EM approximate solutions are convergent to the true solution of model (5.2.2) in probability. We shall assume that all the parameters are given in appropriate units.

Example 5.6. *We assume that model* (5.2.2) *switches from one to the other according to the movement of the Markov chain* $r(t)$ *in the state space* $\mathbb{S} = \{1, 2\}$ *with the coefficients defined in Table 5.1. Given the generator of the Markov chain*

Parameters	$a(i)$	$b(i)$	$s(i)$	$\beta(i)$	$h(i)$	$c(i)$	$f(i)$	$\sigma_1(i)$	$\sigma_2(i)$
$i = 1$	0.4	1	1	2.5	0.8	3	2	1.5	0.5
$i = 2$	1.5	1.5	0.8	2	0.64	2	0.5	0.8	1

Table 5.1: Parameters of SDE model (5.2.2).

$r(t)$ *as*

$$\Gamma = \begin{bmatrix} -1 & 1 \\ 2 & -2 \end{bmatrix} \tag{5.7.2}$$

with the unique stationary distribution $\pi = (\pi_1, \pi_2) = \big(\frac{2}{3}, \frac{1}{3}\big)$. *Then* $\lambda_1 = -0.09 < 0$ *a.s. Therefore by Theorem 5.3, for any initial value* $\{x(t) : -\tau \leqslant t \leqslant 0\} \in C([-\tau, 0]; \mathbb{R}_+^2)$, *both the prey and consumers of system* (5.2.2) *will tend to zero exponentially with probability one. The computer simulation in Figure 5.1 supports this result clearly, illustrating the extinction of both species. We then compute* $a(1) - \frac{1}{2}\sigma_1^2(1) = -0.725 < 0$, *which shows that both species in the first subsystem*

die out ultimately (Theorem 5.3). Then we compute $a(2) - \frac{1}{2}\sigma_1^2(2) = 1.18 > 0$ *and* $\frac{h(2)}{b(2)\beta(2)}\big(a(2) - \frac{1}{2}\sigma_1^2(2)\big) - c(2) - \frac{1}{2}\sigma_2^2(2) = -2.248 < 0$. *Hence in the second subsystem the prey population is persistent:*

$$\lim_{t\to\infty} \frac{1}{t}\int_0^t x_1(u)du = 0.787 \quad a.s.$$

and the consumers tend to zero exponentially almost surely (Theorem 5.5 (ii)). However due to the presence of Markov switching, the overall behaviour of both populations remains extinctive ultimately.

Example 5.7. *Assume that model* (5.2.2) *switches from one to the other according to the movement of the Markov chain* $r(t)$ *in the state space* $\mathbb{S} = \{1, 2\}$ *with the coefficients defined in Table 5.2. Let the generator of the Markov chain* $r(t)$ *be*

Parameters	$a(i)$	$b(i)$	$s(i)$	$\beta(i)$	$h(i)$	$c(i)$	$f(i)$	$\sigma_1(i)$	$\sigma_2(i)$
$i = 1$	1	0.5	0.5	1	1	1.1	1.5	0.9	0.1
$i = 2$	1.5	1.5	0.8	2	0.64	2	0.5	0.8	1

Table 5.2: Parameters of SDE model (5.2.2).

$$\Gamma = \begin{bmatrix} -2 & 2 \\ 1 & -1 \end{bmatrix} \tag{5.7.3}$$

with the unique stationary distribution $\pi = (\pi_1, \pi_2) = \big(\frac{1}{3}, \frac{2}{3}\big)$. *Then* $a(i) - \frac{\sigma_1^2(i)}{2} > 0$ *for* $i \in \{1, 2\}$ *and* $\frac{\check{h}}{\check{b}\check{\beta}}\lambda_1 - \lambda_3 = -0.065 < 0$. *Hence from Theorem 5.5(ii), the solution to model* (5.2.2) *has the property that*

$$0.657 \leqslant \liminf_{t\to\infty} \frac{1}{t}\int_0^t x_1(u)du \leqslant \limsup_{t\to\infty} \frac{1}{t}\int_0^t x_1(u)du \leqslant 1.97$$

and $x_2(t)$ *goes to zero almost surely. The computer simulation shown in Figure 5.2 supports these results clearly.*

5.8 Summary

This chapter is a continuous work of Chapter 4. We have introduced time delay and telegraph noise to the stochastic foraging arena predator-prey system (4.2.1).

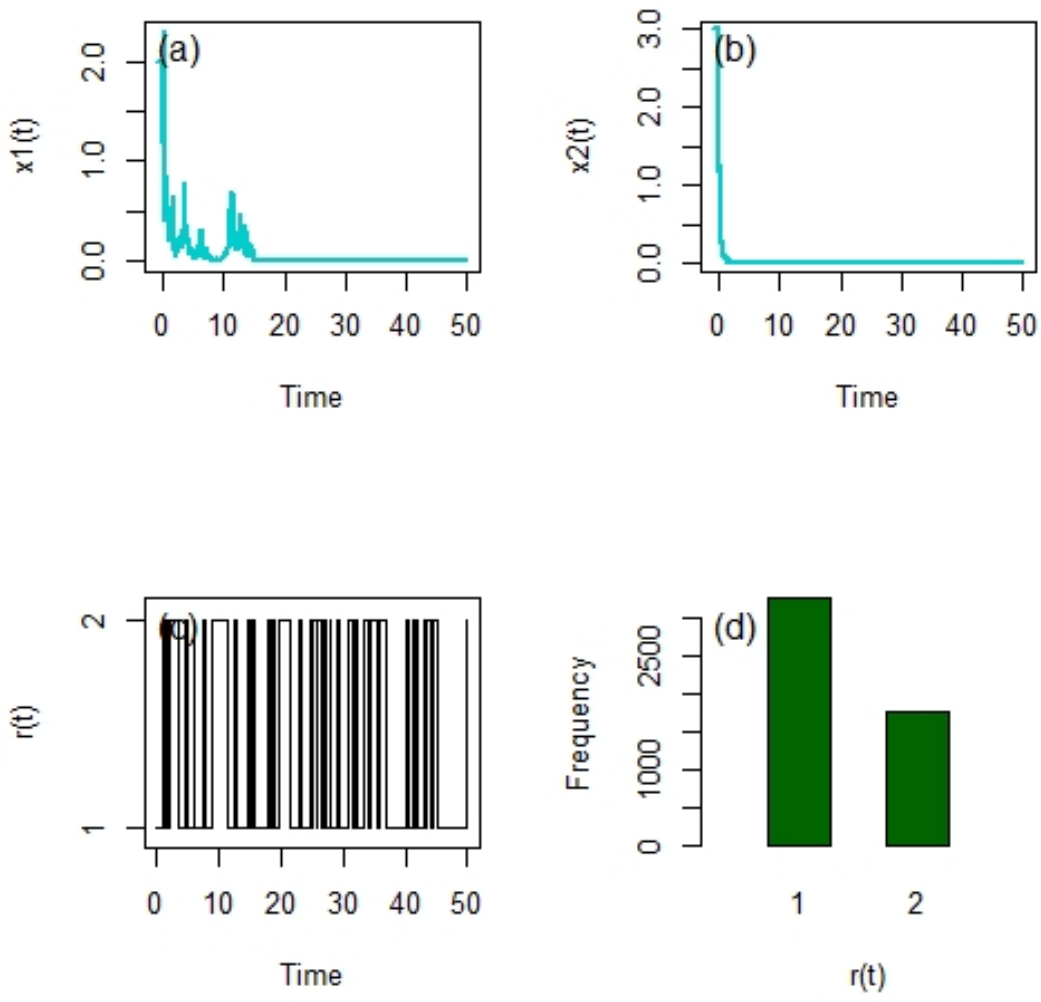

Figure 5.1: Computer simulations of the paths (a) $x_1(t)$ and (b) $x_2(t)$ of 5000 iterations of SDE model (5.2.2) using the EM scheme with stepsize $\Delta = 0.01$ and initial value $x(t) = (2, 3)^T$ for $t \in [-1, 0]$ with the system parameters provided by Table 5.1 and the generator of the Markov chain $r(t)$ given by (5.7.2). The trajectory and frequency of the Markov chain are shown in (c) and (d) respectively.

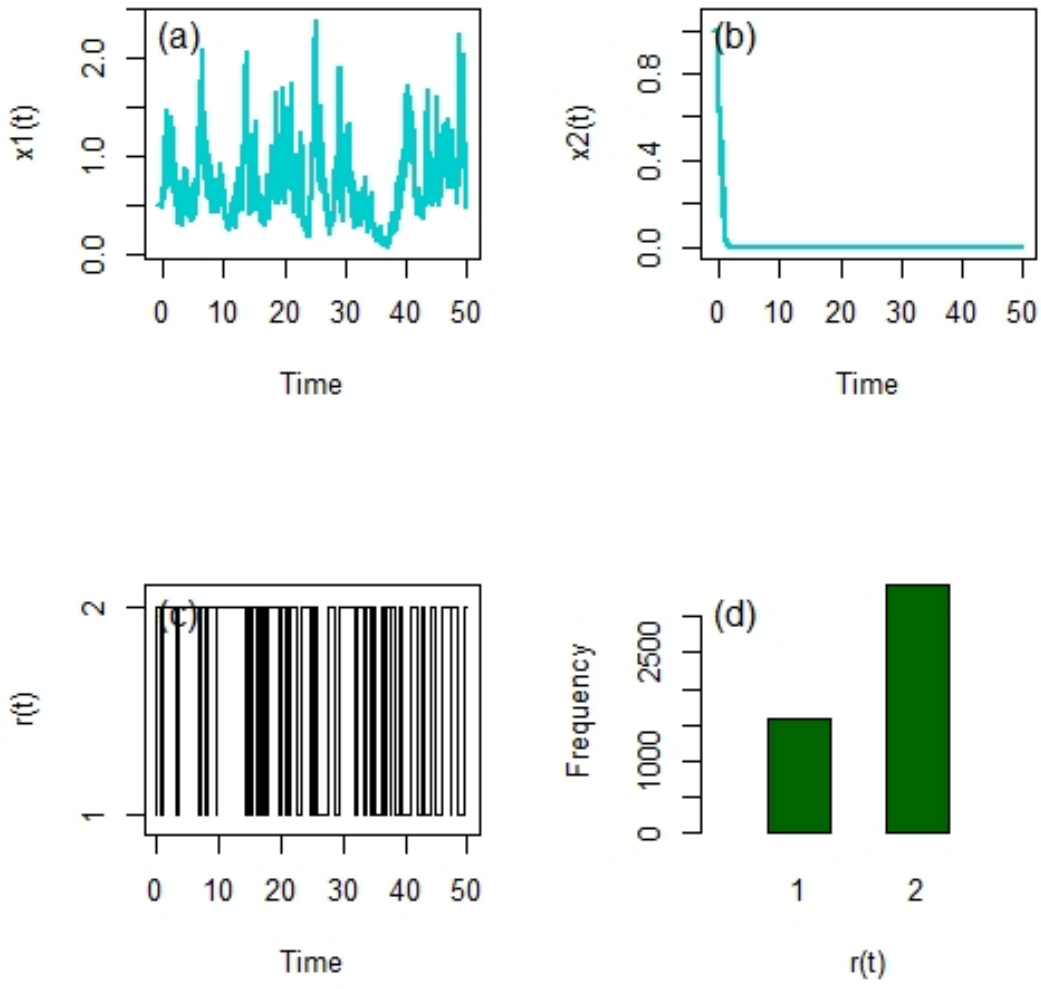

Figure 5.2: Computer simulations of the paths (a) $x_1(t)$ and (b) $x_2(t)$ of 5000 iterations of SDE model (5.2.2) using the EM scheme with stepsize $\Delta = 0.01$ and initial value $x(t) = (0.5, 1)^T$ for $t \in [-1, 0]$ with the system parameters provided by Table 5.2 and the generator of the Markov chain $r(t)$ given by (5.7.3). The trajectory and frequency of the Markov chain are given in (c) and (d) respectively.

Theorem 5.3 suggested that a bigger amplitude of environmental noise may destabilize the system. The presence of time delay makes the system become stochastically ultimately bounded only under certain parametric restriction (Theorem 5.2). Based on this, we then showed that the total amount of prey and predator species will grow at most polynomially with order close to one (Theorem 5.4). The existence of Markov switching makes a difference to the population behaviours. Especially, if the prey is persistent in some subsystems and is extinct in some other subsystems, due to the presence of the Markov switching, both populations in the overall system could be extinct as long as λ_1 defined in (5.5.1) is negative. Numerical simulations were carried out to substantiate the analytical results.

Recall that in Chapter 4, we introduced white noise to the intrinsic growth rate of prey and the density-dependent death rate of consumers in the population system (1.3.2). In the next chapter, we will perturb more parameters and study the impacts of the correlations between the Brownian motions on the population system.

Chapter 6

Stochastic Foraging Arena Predator-Prey System with Correlated Brownian Motions

6.1 Introduction

Recall that Chapter 4 considered the effects of white noise on the population system (1.3.2). In this chapter, we take a further step to stochastically perturb more parameters including the capturing rate of predators and the quadratic mortality rates of both species. Meanwhile we will explore how the correlations between the Brownian motions affect the population dynamics.

In this chapter, we let $(\Omega, \{\mathcal{F}_t\}_{t\geqslant 0}, \mathbb{P})$ be a complete probability space with a filtration $\{\mathcal{F}_t\}$ satisfying the usual conditions (i.e.it is right continuous and increasing while $\mathcal{F}_0$ contains all $\mathbb{P}$-null sets). Let $B(t) = (B_1(t), \cdots, B_6(t))^T$ and $\breve{B}(t) = (B_1(t), \cdots, B_4(t))^T$ be six-dimensional and four-dimensional Brownian motions defined on this probability space respectively. The SDE models are formulated as follows: Due to the environmental variations such as temperature and seasonal fluctuations, we stochastically perturb the parameters s and h in model (4.2.1) with

$$s \to s + r_1\dot{B}_3(t) \quad \text{and} \quad h \to h + r_2\dot{B}_4(t),$$

where r_1 and r_2 denote the intensities of the corresponding white noise. As a result this perturbed system is given by

$$dx_1(t) = x_1(t)\Big(a - bx_1(t) - \frac{sx_2(t)}{\beta + x_2(t)}\Big)dt + \sigma_1 x_1(t)dB_1(t) - \frac{r_1 x_1(t)x_2(t)}{\beta + x_2(t)}dB_3(t) \tag{6.1.1a}$$

$$dx_2(t) = x_2(t)\Big(\frac{hx_1(t)}{\beta + x_2(t)} - c - fx_2(t)\Big)dt - \sigma_2 x_2(t)dB_2(t) + \frac{r_2 x_1(t)x_2(t)}{\beta + x_2(t)}dB_4(t). \tag{6.1.1b}$$

Furthermore, we would also like to incorporate perturbation into b and f:

$$b \to b + \delta_1 \dot{B}_5(t) \quad \text{and} \quad f \to f + \delta_2 \dot{B}_6(t),$$

where δ_1 and δ_2 represent the intensities of the corresponding white noise. We then obtain

$$\begin{aligned} dx_1(t) = {} & x_1(t)\Big(a - bx_1(t) - \frac{sx_2(t)}{\beta + x_2(t)}\Big)dt + \sigma_1 x_1(t)dB_1(t) - \frac{r_1 x_1(t)x_2(t)}{\beta + x_2(t)}dB_3(t) \\ & - \delta_1 x_1^2(t)dB_5(t) \end{aligned} \tag{6.1.2a}$$

$$\begin{aligned} dx_2(t) = {} & x_2(t)\Big(\frac{hx_1(t)}{\beta + x_2(t)} - c - fx_2(t)\Big)dt - \sigma_2 x_2(t)dB_2(t) + \frac{r_2 x_1(t)x_2(t)}{\beta + x_2(t)}dB_4(t) \\ & - \delta_2 x_2^2(t)dB_6(t). \end{aligned} \tag{6.1.2b}$$

According to the literature on the stochastic population dynamics, most authors only considered the case when the Brownian motions are uncorrelated. In fact, some environmental factors such as diseases, temperature and pollution might simultaneously affect several system parameters. This phenomena can be characterised by the correlations between the Brownian motions [33, 34, 55, 100, 110]. In this chapter, we assume that the Brownian motions in model (6.1.1) and (6.1.2) are correlated. Namely, we let $B(t) = \varpi Z(t)$, where $Z(t) = (Z_1(t), \cdots, Z_6(t))^T$ is a six-dimensional independent standard Brownian motion and $\varpi^T\varpi = \mathcal{R} = (\rho_{ij})_{6\times 6}$ is a constant correlation matrix with $\rho_{ij} \in [-1, 1]$ represents the correlation coefficient between $B_i(t)$ and $B_j(t)$ for $i, j = 1, 2, \cdots, 6$. And $\breve{B}(t)$ can be defined in the same way. We also denote

$$\bar{\rho}_{ij} = \begin{cases} \rho_{ij}, & \text{if } \rho_{ij} > 0 \\ 0, & \text{otherwise} \end{cases} \quad \text{and} \quad \tilde{\rho}_{ij} = \begin{cases} 0, & \text{if } \rho_{ij} > 0 \\ -\rho_{ij}, & \text{otherwise.} \end{cases}$$

This chapter is divided into four main parts: In section 6.2 and 6.3, we discuss the long-time behaviours of model (6.1.1) and (6.1.2) respectively. In section 6.4, we discover the parametric restrictions for either model (6.1.1) or (6.1.2) to have a stationary distribution. In section 6.5, we provide examples to illustrate our theory. Finally we give a summary in section 6.6.

6.2 Model (6.1.1)

6.2.1 Positive and Global Solution

Theorem 6.1. *For any given initial value $x_0 \in \mathbb{R}^2_+$, there is a unique solution $x(t)$ to equation (6.1.1) on $t \geqslant 0$ and the solution will remain in $\mathbb{R}^2_+$ with probability 1, namely $x(t) \in \mathbb{R}^2_+$ for all $t \geqslant 0$ almost surely.*

By defining $V(x) = x_1^2 - 2\log x_1 + x_2^2 - 2\log x_2$, this theorem is then proved in the same routine as in Theorem 4.1.

6.2.2 Moment Estimate

Theorem 6.2. *For any $\theta > 0$, there exists a positive constant $K(\theta)$ such that for any initial value $x_0 \in \mathbb{R}^2_+$, the solution to model* (6.1.1) *has the property that*

$$\limsup_{t\to\infty} \mathbb{E}|x(t)|^\theta \leqslant K(\theta).$$

Proof. Applying the Itô formula to $e^t(x_1^\theta(t) + x_2^\theta(t))$ for $\theta > 0$,

$$\begin{aligned}
&e^t(x_1^\theta(t) + x_2^\theta(t)) \\
&= x_1^\theta(0) + x_2^\theta(0) + \int_0^t e^s f(x(s))ds + \theta\sigma_1 \int_0^t e^s x_1^\theta(s) dB_1(s) - \theta\sigma_2 \int_0^t e^s x_2^\theta(s) dB_2(s) \\
&- \theta r_1 \int_0^t \frac{e^s x_1^\theta(s) x_2(s)}{\beta + x_2(s)} dB_3(s) + \theta r_2 \int_0^t \frac{e^s x_2^\theta(s) x_1(s)}{\beta + x_2(s)} dB_4(s), \qquad (6.2.1)
\end{aligned}$$

where

$$\begin{aligned}
f(x) = \theta x_1^\theta\Big(a - bx_1 - \frac{sx_2}{\beta + x_2}\Big) + \theta x_2^\theta\Big(\frac{hx_1}{\beta + x_2} - c - fx_2\Big) + \frac{1}{2}\theta(\theta-1)x_1^\theta\Big(\sigma_1^2 \\
+ \frac{r_1^2 x_2^2}{(\beta + x_2)^2} - \frac{2\sigma_1 r_1 \rho_{13} x_2}{\beta + x_2}\Big) + \frac{1}{2}\theta(\theta-1)x_2^\theta\Big(\sigma_2^2 + \frac{r_2^2 x_1^2}{(\beta + x_2)^2} - \frac{2r_2\sigma_2\rho_{24}x_1}{\beta + x_2}\Big)
\end{aligned}$$

$$+ x_1^\theta + x_2^\theta.$$

Using the elementary inequality

$$v_1^\kappa v_2^{1-\kappa} \leqslant \kappa v_1 + (1-\kappa)v_2 \quad \text{for } v_1, v_2 \geqslant 0 \text{ and } 0 \leqslant \kappa < 1,$$

for $\theta \geqslant 2$ we obtain

$$\frac{x_1 x_2^\theta}{\beta + x_2} \leqslant x_1 x_2^{\theta-1} \leqslant \frac{1}{\theta} x_1^\theta + \frac{\theta-1}{\theta} x_2^\theta$$

and

$$\frac{x_1^2 x_2^\theta}{(\beta+x_2)^2} \leqslant x_1^2 x_2^{\theta-2} \leqslant \frac{2}{\theta} x_1^\theta + \frac{\theta-2}{\theta} x_2^\theta.$$

Hence

$$\begin{aligned} f(x) \leqslant & \Big(h + 1 + a\theta + (\theta-1)\Big(\frac{1}{2}\theta(\sigma_1^2 + r_1^2 + 2\sigma_1 r_1 \tilde{\rho}_{13}) + r_2^2 + r_2\sigma_2\tilde{\rho}_{24}\Big)\Big) x_1^\theta + \Big(1 \\ & - c\theta + (\theta-1)\Big(h + \frac{1}{2}\theta\sigma_2^2 + \frac{1}{2}(\theta-2)r_2^2 + (\theta-1)r_2\sigma_2\tilde{\rho}_{24}\Big)\Big) x_2^\theta - b\theta x_1^{\theta+1} \\ & - f\theta x_2^{\theta+1}. \end{aligned}$$

is bounded, say by $K^*(\theta)$. Moreover, it follows from (6.2.1) that

$$\mathbb{E}\Big[e^{t\wedge\tau_k}\big(x_1^\theta(t\wedge\tau_k) + x_2^\theta(t\wedge\tau_k)\big)\Big] \leqslant x_1^\theta(0) + x_2^\theta(0) + K^*(\theta)\int_0^{t\wedge\tau_k} e^s ds,$$

where τ_k is a stopping time defined as

$$\tau_k = \inf\{t \in [0, \tau_e) : x_i(t) \notin \Big(\frac{1}{k}, k\Big) \text{ for some } i = 1, 2\}.$$

Letting $k \to \infty$ and then $t \to \infty$ yields

$$\limsup_{t\to\infty} \mathbb{E}\big[x_1^\theta(t) + x_2^\theta(t)\big] \leqslant \lim_{t\to\infty} \frac{1}{e^t}\Big(x_1^\theta(0) + x_2^\theta(0) + K^*(\theta)(e^t - 1)\Big) = K^*(\theta).$$

On the other hand, we have

$$|x|^2 \leqslant 2(x_1^2 \vee x_2^2), \text{ so } |x|^\theta \leqslant 2^{\theta/2}(x_1^\theta \vee x_2^\theta) \leqslant 2^{\theta/2}(x_1^\theta + x_2^\theta).$$

As a result,

$$\limsup_{t\to\infty} \mathbb{E}|x(t)|^\theta \leqslant 2^{\theta/2} \limsup_{t\to\infty} \mathbb{E}[x_1^\theta(t) + x_2^\theta(t)] \leqslant 2^{\theta/2} K^*(\theta) = K(\theta). \tag{6.2.2}$$

For $0 < \theta < 2$, Hölder's inequality yields

$$\mathbb{E}|x(t)|^\theta \leqslant \big(\mathbb{E}|x(t)|^2\big)^{\frac{\theta}{2}}.$$

Hence from (6.2.2)

$$\limsup_{t\to\infty} \mathbb{E}|x(t)|^\theta \leqslant \limsup_{t\to\infty} (\mathbb{E}|x(t)|^2)^{\frac{\theta}{2}} \leqslant K(\theta).$$

□

6.2.3 Extinction

In order to study the asymptotic properties of model (6.1.1), we first introduce a lemma.

Lemma 6.3. *For any initial value $x_0 \in \mathbb{R}^2_+$, the solution to model* (6.1.1) *has the property that*

$$\limsup_{t\to\infty} \frac{1}{t}\int_0^t x_1^2(u)du \leqslant \frac{4a^2}{b^2} \quad a.s.$$

Proof. According to (6.1.1a),

$$x_1(t) = x_1(0) + a\int_0^t x_1(u)du - b\int_0^t x_1^2(u)du - s\int_0^t \frac{x_1(u)x_2(u)}{\beta + x_2(u)}du + m_1(t) + m_3(t) \tag{6.2.3}$$

where

$$m_1(t) = \sigma_1\int_0^t x_1(u)dB_1(u) \quad \text{and} \quad m_3(t) = -r_1\int_0^t \frac{x_1(u)x_2(u)}{\beta + x_2(u)}dB_3(u)$$

are two continuous local martingales with the quadratic variations

$$\langle m_1(t)\rangle = \sigma_1^2\int_0^t x_1^2(u)du \quad \text{and} \quad \langle m_3(t)\rangle = r_1^2\int_0^t \frac{x_1^2(u)x_2^2(u)}{(\beta + x_2(u))^2}du \leqslant r_1^2\int_0^t x_1^2(u)du.$$

By the exponential martingale inequality (Theorem 2.32), we have

$$\mathbb{P}\Big(\sup_{o\leqslant t\leqslant n}\big(m_i(t) - 0.5\alpha\langle m_i(t)\rangle\big) > \frac{2\log n}{\alpha}\Big) \leqslant \frac{1}{n^2} \quad \text{for } i = 1, 3 \text{ and } n = 1, 2, \cdots,$$

where

$$\alpha = \frac{b}{\sigma_1^2 + r_1^2}. \tag{6.2.4}$$

An application of the Borel-Cantelli lemma (Lemma 2.1) suggests that for almost all $\omega \in \Omega$ there is a random integer $n_0 = n_0(\omega) \geqslant 1$ such that

$$\sup_{o\leqslant t\leqslant n}\Big(m_i(t) - 0.5\alpha\langle m_i(t)\rangle\Big) \leqslant \frac{2\log n}{\alpha} \text{ whenever } n \geqslant n_0 \text{ for } i = 1, 3.$$

Hence for $t \in [0, n]$ and $n \geqslant n_0$,

$$m_i(t) \leqslant \frac{2\log n}{\alpha} + 0.5\alpha\langle m_i(t)\rangle \quad \text{a.s.}$$

And then (6.2.3) and (6.2.4) imply that for $t \in [0, n]$ and $n \geqslant n_0$,

$$\begin{aligned} x_1(t) &\leqslant x_1(0) + a\int_0^t x_1(u)du - \Big(b - 0.5\alpha(\sigma_1^2 + r_1^2)\Big)\int_0^t x_1^2(u)du + \frac{4\log n}{\alpha} \\ &= x_1(0) + a\int_0^t x_1(u)du - \frac{b}{2}\int_0^t x_1^2(u)du + \frac{4\log n}{\alpha} \quad \text{a.s.} \end{aligned}$$

Therefore it follows that for $t \in [0, n]$ and $n \geqslant n_0$,

$$\begin{aligned} \frac{b}{4}\int_0^t x_1^2(u)du &\leqslant x_1(0) + a\int_0^t x_1(u)du - \frac{b}{4}\int_0^t x_1^2(u)du + \frac{4\log n}{\alpha} \\ &\leqslant x_1(0) + \frac{a^2 t}{b} + \frac{4\log n}{\alpha} \quad \text{a.s.} \end{aligned}$$

Consequently, for almost all $\omega \in \Omega$, if $n \geqslant n_0$ and $n - 1 \leqslant t \leqslant n$,

$$\frac{1}{t}\int_0^t x_1^2(u)du \leqslant \frac{4}{(n-1)b}\Big(x_1(0) + \frac{a^2 n}{b} + \frac{4\log n}{\alpha}\Big).$$

Letting $t \to \infty$ and hence $n \to \infty$ we obtain

$$\limsup_{t\to\infty} \frac{1}{t}\int_0^t x_1^2(u)du \leqslant \frac{4a^2}{b^2} \quad \text{a.s.}$$

□

Theorem 6.4. *For any initial value $x_0 \in \mathbb{R}^2_+$,*
(a) if

$$2a < \sigma_1^2 - 2r_1\sigma_1\bar{\rho}_{13} \tag{6.2.5}$$

then both $x_1(t)$ and $x_2(t)$ of model (6.1.1) tend to zero exponentially as $t \to \infty$ with probability 1;

(b) if

$$\sigma_1^2 + 2r_1\sigma_1\tilde{\rho}_{13} < 2a < \sigma_1^2 - 2r_1\sigma_1\bar{\rho}_{13} + \frac{2b\beta c}{h + r_2\sigma_2\rho_{24}} + \frac{b\beta\sigma_2^2}{h + r_2\sigma_2\rho_{24}} \quad \text{for } \rho_{24} > -\frac{h}{r_2\sigma_2} \tag{6.2.6}$$

or

$$2a > \sigma_1^2 + 2r_1\sigma_1\tilde{\rho}_{13} \quad \text{for } -1 \leqslant \rho_{24} \leqslant -\frac{h}{r_2\sigma_2}, \tag{6.2.7}$$

then $x_1(t)$ of model (6.1.1) obeys

$$\frac{2a - \sigma_1^2}{2b} \leqslant \liminf_{t\to\infty} \frac{1}{t}\int_0^t x_1(u)du \leqslant \limsup_{t\to\infty} \frac{1}{t}\int_0^t x_1(u)du \leqslant \frac{2a - \sigma_1^2 + 2r_1\sigma_1\bar{\rho}_{13}}{2b} \quad \text{a.s.}$$

and $x_2(t)$ tends to zero exponentially as $t \to \infty$ with probability 1.

Proof. (a) Applying Itô's formula (Theorem 2.13) on $\log x_1(t)$ yields

$$\begin{aligned} d\log x_1(t) &= \Big(a - bx_1(t) - \frac{1}{2}\sigma_1^2 - \frac{sx_2(t)}{\beta + x_2(t)} - \frac{r_1^2 x_2^2(t)}{2(\beta + x_2(t))^2} + \frac{r_1\sigma_1\rho_{13}x_2(t)}{\beta + x_2(t)}\Big)dt \\ &\quad + \sigma_1 dB_1(t) - \frac{r_1 x_2(t)}{\beta + x_2(t)} dB_3(t) \qquad (6.2.8) \\ &\leqslant \big(a - \frac{1}{2}\sigma_1^2 + r_1\sigma_1\bar{\rho}_{13}\big)dt + \sigma_1 dB_1(t) - \frac{r_1 x_2(t)}{\beta + x_2(t)} dB_3(t). \end{aligned}$$

Integrating from 0 to t and dividing by t infers

$$\frac{1}{t}\log x_1(t) \leqslant \frac{1}{t}\log x_1(0) + a - \frac{1}{2}\sigma_1^2 + r_1\sigma_1\bar{\rho}_{13} + \frac{M_1(t)}{t} + \frac{M_3(t)}{t},$$

where

$$M_1(t) = \sigma_1 B_1(t) \quad \text{and} \quad M_3(t) = -r_1 \int_0^t \frac{x_2(u)}{\beta + x_2(u)} dB_3(u)$$

are two continuous martingales with the quadratic variations

$$\langle M_1(t)\rangle = \sigma_1^2 t \quad \text{and} \quad \langle M_3(t)\rangle = r_1^2 \int_0^t \frac{x_2^2(u)}{(\beta + x_2(u))^2} dt \leqslant r_1^2 t.$$

By the strong law of large numbers for martingales (Theorem 2.2),

$$\lim_{t\to\infty} \frac{M_1(t)}{t} = 0 \quad \text{and} \quad \lim_{t\to\infty} \frac{M_3(t)}{t} = 0 \quad \text{a.s.}$$

and thus from condition (6.2.5)

$$\limsup_{t\to\infty} \frac{1}{t}\log x_1(t) \leqslant a - \frac{1}{2}\sigma_1^2 + r_1\sigma_1\bar{\rho}_{13} < 0 \quad \text{a.s.}$$

as required. Therefore we obtain

$$\lim_{t\to\infty} \frac{1}{t}\int_0^t x_1(u)du = 0 \quad \text{a.s.} \qquad (6.2.9)$$

Meanwhile

$$\begin{aligned} d\log x_2(t) &= \Big(\frac{h + r_2\sigma_2\rho_{24}}{\beta + x_2(t)} x_1(t) - c - \frac{\sigma_2^2}{2} - f x_2(t) - \frac{r_2^2 x_1^2(t)}{2(\beta + x_2(t))^2}\Big)dt - \sigma_2 dB_2(t) \\ &\quad + \frac{r_2 x_1(t)}{\beta + x_2(t)} dB_4(t). \qquad (6.2.10) \end{aligned}$$

It follows that

$$\frac{\log x_2(t)}{t} \leqslant \frac{1}{t}\Big(\log x_2(0) + \frac{h + r_2\sigma_2\bar{\rho}_{24}}{\beta}\int_0^t x_1(u)du\Big) - \big(c + \frac{\sigma_2^2}{2}\big) + \frac{M_2(t)}{t} + \frac{M_4(t)}{t},$$

where

$$M_2(t) = -\sigma_2 B_2(t) \quad \text{and} \quad M_4(t) = r_2 \int_0^t \frac{x_1(u)}{\beta + x_2(u)} dB_4(u)$$

are two martingales with the quadratic variations

$$\langle M_2(t) \rangle = \sigma_2^2 t \quad \text{and} \quad \langle M_4(t) \rangle = r_2^2 \int_0^t \frac{x_1^2(u)}{(\beta + x_2(u))^2} du.$$

Hence from Lemma 6.3,

$$\limsup_{t\to\infty} \frac{\langle M_4(t) \rangle}{t} \leqslant \limsup_{t\to\infty} \frac{r_2^2}{\beta^2 t} \int_0^t x_1^2(u) du \leqslant \frac{4 r_2^2 a^2}{\beta^2 b^2} \quad \text{a.s.}$$

By the strong law of large numbers for martingales (Theorem 2.2),

$$\lim_{t\to\infty} \frac{M_2(t)}{t} = 0 \quad \text{and} \quad \lim_{t\to\infty} \frac{M_4(t)}{t} = 0 \quad \text{a.s.}$$

Letting $t \to \infty$ and recalling equation (6.2.9) indicates

$$\limsup_{t\to\infty} \frac{\log x_2(t)}{t} \leqslant -\Big(c + \frac{\sigma_2^2}{2}\Big) < 0 \qquad \text{a.s.}$$

(b) Applying Itô's formula on $\frac{1}{x_1(t)}$ gives

$$\begin{aligned} d\Big(\frac{1}{x_1(t)}\Big) = \Big(\frac{1}{x_1}\Big(\frac{s x_2}{\beta + x_2} - a + \sigma_1^2 + \frac{r_1^2 x_2^2}{(\beta + x_2)^2} - \frac{2\sigma_1 r_1 \rho_{13} x_2}{\beta + x_2}\Big) + b\Big) dt - \frac{\sigma_1}{x_1} dB_1(t) \\ + \frac{r_1 x_2}{x_1(\beta + x_2)} dB_3(t), \end{aligned}$$

where we write $x(t) = x$. Hence by the variation-of-constants formula (Theorem 2.20) and Lemma 2.19,

$$\begin{aligned} \frac{1}{x_1(t)} &= \exp\Big(\int_0^t \Big(\frac{1}{2}\sigma_1^2 - a + \frac{s x_2(u)}{\beta + x_2(u)} + \frac{r_1^2 x_2^2(u)}{2(\beta + x_2(u))^2} - \frac{2 r_1 \sigma_1 \rho_{13} x_2(u)}{\beta + x_2(u)}\Big) du \\ &\quad - M_1(t) - M_3(t)\Big)\Big(\frac{1}{x_1(0)} + b \int_0^t \exp\Big(\int_0^u \Big(a - \frac{s x_2(v)}{\beta + x_2(v)} - \frac{1}{2}\sigma_1^2 \\ &\quad - \frac{r_1^2 x_2^2(v)}{2(\beta + x_2(v))^2} + \frac{2 r_1 \sigma_1 \rho_{13} x_2(v)}{\beta + x_2(v)}\Big) dv + M_1(u) + M_3(u)\Big) du\Big) \\ &= \exp\big(- M_1(t) - M_3(t)\big)\Big(\frac{1}{x_1(0)} \exp\Big(- \big(a - \frac{1}{2}\sigma_1^2\big) t + s \int_0^t \frac{x_2(u)}{\beta + x_2(u)} du \\ &\quad + \frac{r_1^2}{2} \int_0^t \frac{x_2^2(u)}{(\beta + x_2(u))^2} du - 2 r_1 \sigma_1 \rho_{13} \int_0^t \frac{x_2(u)}{\beta + x_2(u)} du\Big) \end{aligned}$$

$$+ b\int_0^t \exp\Big(-\big(a-\frac{1}{2}\sigma_1^2\big)(t-u) + s\int_u^t \frac{x_2(v)}{\beta+x_2(v)}dv + \frac{r_1^2}{2}\int_u^t \frac{x_2^2(v)}{(\beta+x_2(v))^2}dv$$
$$- 2r_1\sigma_1\rho_{13}\int_u^t \frac{x_2(v)}{\beta+x_2(v)}dv + M_1(u) + M_3(u)\Big)du\Big). \tag{6.2.11}$$

On the one hand, (6.2.11) leads to

$$\begin{aligned}
\frac{1}{x_1(t)} &\leqslant \exp\big(-M_1(t)-M_3(t)\big)\Big(\frac{1}{x_1(0)}\exp\Big(-\big(a-\frac{1}{2}\sigma_1^2\big)t + s\int_0^t \frac{x_2(u)}{\beta+x_2(u)}du \\
&\quad + \frac{r_1^2}{2}\int_0^t \frac{x_2^2(u)}{(\beta+x_2(u))^2}du + 2r_1\sigma_1\tilde{\rho}_{13}\int_0^t \frac{x_2(u)}{\beta+x_2(u)}du\Big) + b\exp\Big(\max_{0\leqslant u\leqslant t} M_1(u) \\
&\quad + \max_{0\leqslant u\leqslant t} M_3(u) + s\int_0^t \frac{x_2(u)}{\beta+x_2(u)}du + \frac{r_1^2}{2}\int_0^t \frac{x_2^2(u)}{(\beta+x_2(u))^2}du \\
&\quad + r_1\sigma_1\tilde{\rho}_{13}\int_0^t \frac{x_2(u)}{\beta+x_2(u)}du\Big)\cdot\int_0^t \exp(-q(t-u))du\Big) \\
&\leqslant \exp\Big(\max_{0\leqslant u\leqslant t} M_1(u) - M_1(t) + \max_{0\leqslant u\leqslant t} M_3(u) - M_3(t) + s\int_0^t \frac{x_2(u)}{\beta+x_2(u)}du \\
&\quad + \frac{r_1^2}{2}\int_0^t \frac{x_2^2(u)}{(\beta+x_2(u))^2}du + r_1\sigma_1\tilde{\rho}_{13}\int_0^t \frac{x_2(u)}{\beta+x_2(u)}du\Big)\Big(\frac{1}{x_1(0)}\exp(-qt) \\
&\quad + b\int_0^t \exp(-q(t-u))du\Big) \\
&= \exp\Big(\max_{0\leqslant u\leqslant t} M_1(u) - M_1(t) + \max_{0\leqslant u\leqslant t} M_3(u) - M_3(t) + s\int_0^t \frac{x_2(u)}{\beta+x_2(u)}du \\
&\quad + \frac{r_1^2}{2}\int_0^t \frac{x_2^2(u)}{(\beta+x_2(u))^2}du + r_1\sigma_1\tilde{\rho}_{13}\int_0^t \frac{x_2(u)}{\beta+x_2(u)}du\Big)\cdot K_1(t),
\end{aligned}$$

where

$$q := a - \frac{1}{2}\sigma_1^2 - r_1\sigma_1\tilde{\rho}_{13} \quad\text{and}\quad K_1(t) = \frac{1}{x_1(0)}\exp(-qt) + \frac{2b\big(1-\exp(-qt)\big)}{2a-\sigma_1^2}.$$

Under condition (6.2.6) or (6.2.7), we obtain that $q > 0$ and therefore $\sup_{0\leqslant t<\infty} K_1(t) < \infty$. It then follows that

$$\begin{aligned}
\frac{\log x_1(t)}{t} &\geqslant -\frac{\log K_1(t)}{t} - \frac{\max_{0\leqslant u\leqslant t} M_1(u) - M_1(t) + \max_{0\leqslant u\leqslant t} M_3(u) - M_3(t)}{t} \\
&\quad - \frac{s}{t}\int_0^t \frac{x_2(u)}{\beta+x_2(u)}du - \frac{r_1^2}{2t}\int_0^t \frac{x_2^2(u)}{(\beta+x_2(u))^2}du - \frac{r_1\sigma_1\tilde{\rho}_{13}}{t}\int_0^t \frac{x_2(u)}{\beta+x_2(u)}du.
\end{aligned} \tag{6.2.12}$$

By (6.2.8) and (6.2.12),

$$\frac{1}{t}\int_0^t x_1(u)du = \frac{2a-\sigma_1^2}{2b} - \frac{\log x_1(t)}{bt} + \frac{\log x_1(0)}{bt} - \frac{s}{bt}\int_0^t \frac{x_2(u)}{\beta+x_2(u)}du$$

$$
\begin{aligned}
&- \frac{r_1^2}{2bt}\int_0^t \frac{x_2^2(u)}{(\beta + x_2(u))^2}du + \frac{r_1\sigma_1\rho_{13}}{bt}\int_0^t \frac{x_2(u)}{\beta + x_2(u)}du + \frac{M_1(t)}{bt} \\
&+ \frac{M_3(t)}{bt} \qquad (6.2.13)\\
&\leqslant \frac{2a-\sigma_1^2}{2b} + \frac{\log K_1(t)}{bt} + \frac{r_1\sigma_1\bar{\rho}_{13}}{b} + \frac{\log x_1(0)}{bt} + \frac{M_1(t)}{bt} + \frac{M_3(t)}{bt} \\
&+ \frac{\max_{0\leqslant u\leqslant t} M_1(u) - M_1(t) + \max_{0\leqslant u\leqslant t} M_3(u) - M_3(t)}{bt}.
\end{aligned}
$$

As $t \to \infty$ and from the strong law of large numbers for martingales (Theorem 2.2),

$$
\limsup_{t\to\infty} \frac{1}{t}\int_0^t x_1(u)du \leqslant \frac{2a-\sigma_1^2+2r_1\sigma_1\bar{\rho}_{13}}{2b} \quad \text{a.s.} \qquad (6.2.14)
$$

Assume that $\rho_{24} > -\frac{h}{r_2\sigma_2}$. From equation (6.2.10),

$$
d\log x_2(t) \leqslant \Big(\frac{h + r_2\sigma_2\rho_{24}}{\beta}x_1(t) - c - \frac{\sigma_2^2}{2}\Big)dt - \sigma_2 dB_2(t) + \frac{r_2 x_1(t)}{\beta + x_2(t)}dB_4(t).
$$

It is then followed from (6.2.14) and the strong law of large numbers for martingales that

$$
\begin{aligned}
\limsup_{t\to\infty}\frac{1}{t}\log x_2(t) &\leqslant \frac{h + r_2\sigma_2\rho_{24}}{\beta}\limsup_{t\to\infty}\frac{1}{t}\int_0^t x_1(u)du - \big(c + \frac{\sigma_2^2}{2}\big) \\
&\leqslant \frac{(h + r_2\sigma_2\rho_{24})(2a - \sigma_1^2 + 2r_1\sigma_1\bar{\rho}_{13})}{2\beta b} - \big(c + \frac{\sigma_2^2}{2}\big) < 0
\end{aligned}
$$

in view of (6.2.6). If $\rho_{24} \leqslant -\frac{h}{r_2\sigma_2}$, it immediately indicates that

$$
\limsup_{t\to\infty}\frac{1}{t}\log x_2(t) \leqslant -\big(c + \frac{\sigma_2^2}{2}\big) < 0.
$$

Hence for arbitrary small $\zeta > 0$, there exists t_ζ such that

$$
\mathbb{P}(\Omega_\zeta) \geqslant 1 - \zeta, \text{ where}
$$

$$
\Omega_\zeta = \Big\{\omega : \frac{(s + r_1\sigma_1|\rho_{13}|)x_2(t,\omega)}{b(\beta + x_2(t,\omega))} + \frac{r_1^2 x_2^2(t,\omega)}{2b(\beta + x_2(t,\omega))^2} \leqslant \zeta \text{ for } t \geqslant t_\zeta\Big\}.
$$

On the other hand, (6.2.11) yields

$$
\begin{aligned}
\frac{1}{x_1(t)} \geqslant \exp\big(-M_1(t) - M_3(t)\big)\Big(&\frac{1}{x_1(0)}\exp\Big(-\big(a - \frac{1}{2}\sigma_1^2\big)t \\
&- 2r_1\sigma_1\bar{\rho}_{13}\int_0^t \frac{x_2(u)}{\beta + x_2(u)}du\Big) + b\exp\Big(\min_{0\leqslant u\leqslant t} M_1(u) + \min_{0\leqslant u\leqslant t} M_3(u)
\end{aligned}
$$

$$
\begin{aligned}
&- 2r_1\sigma_1\bar{\rho}_{13}\int_0^t \frac{x_2(u)}{\beta + x_2(u)}du\Big) \cdot \int_0^t \exp\big(- \big(a - \frac{1}{2}\sigma_1^2\big)(t-u)\big)du\Big) \\
&\geqslant \exp\Big(\min_{0\leqslant u\leqslant t} M_1(u) - M_1(t) + \min_{0\leqslant u\leqslant t} M_3(u) - M_3(t) \\
&- 2r_1\sigma_1\bar{\rho}_{13}\int_0^t \frac{x_2(u)}{\beta + x_2(u)}du\Big) \cdot K_2(t),
\end{aligned}
$$

where

$$
K_2(t) = \frac{1}{x_1(0)} \exp\Big(- \big(a - \frac{1}{2}\sigma_1^2\big)t\Big) + \frac{2b\Big(1 - \exp\big(- (a - \frac{1}{2}\sigma_1^2)t\big)\Big)}{2a - \sigma_1^2}
$$

and $\sup_{0\leqslant t<\infty} K_2(t) < \infty$ if either condition (6.2.6) or (6.2.7) holds. Then

$$
\begin{aligned}
\frac{\log x_1(t)}{t} \leqslant &- \frac{\log K_2(t)}{t} - \frac{\min_{0\leqslant u\leqslant t} M_1(u) - M_1(t) + \min_{0\leqslant u\leqslant t} M_3(u) - M_3(t)}{t} \\
&+ \frac{2r_1\sigma_1\bar{\rho}_{13}}{t}\int_0^t \frac{x_2(u)}{\beta + x_2(u)}du.
\end{aligned}
$$

Hence we obtain from (6.2.13) that

$$
\begin{aligned}
\frac{1}{t}\int_0^t x_1(u)du \geqslant &\frac{2a - \sigma_1^2}{2b} + \frac{\log K_2(t)}{bt} + \frac{\log x_1(0)}{bt} - \frac{s}{bt}\int_0^t \frac{x_2(u)}{\beta + x_2(u)}du \\
&- \frac{r_1^2}{2bt}\int_0^t \frac{x_2^2(u)}{(\beta + x_2(u))^2}du - \frac{r_1\sigma_1|\rho_{13}|}{bt}\int_0^t \frac{x_2(u)}{\beta + x_2(u)}du + \frac{M_1(t)}{bt} \\
&+ \frac{M_3(t)}{bt} + \frac{\min_{0\leqslant u\leqslant t} M_1(u) - M_1(t) + \min_{0\leqslant u\leqslant t} M_3(u) - M_3(t)}{bt}.
\end{aligned} \tag{6.2.15}
$$

For any $\omega \in \Omega_\zeta$, (6.2.15) indicates

$$
\liminf_{t\to\infty} \frac{1}{t}\int_0^t x_1(u)du \geqslant \frac{2a - \sigma_1^2}{2b} - \zeta \quad \text{a.s.}
$$

Letting $\zeta \to 0$ and together with (6.2.14) implies the required assertion. □

Remark 6.5. Let all the Brownian motions in model (6.1.1) be uncorrelated. Then Theorem 6.2 is still obtained. Moreover, Theorem 6.4(a) or (b) holds if assertion (6.2.5) or (6.2.6) is satisfied with $\rho_{ij} = 0$ for all $i, j = 1, \cdots, 4$ and $i \neq j$.

Remark 6.6. Assume that $\rho_{13} \leqslant 0$. Then under condition (6.2.6) or (6.2.7), $x_1(t)$ of model (6.1.1) obeys

$$
\lim_{t\to\infty} \frac{1}{t}\int_0^t x_1(u)du = \frac{2a - \sigma_1^2}{2b} \quad \text{a.s.}
$$

and $x_2(t)$ tends to zero exponentially as $t \to \infty$ with probability 1.

Theorem 6.4(a) shows that large white noise intensity σ_1^2 may let the populations die out. In Theorem 6.4(b), the situation when a becomes larger is discussed. There are generally two cases, depending on the value of ρ_{24}. In the first case, $B_2(t)$ and $B_4(t)$ are strongly negatively correlated ($-1 \leqslant \rho_{24} \leqslant -\frac{h}{r_2\sigma_2}$). Then under condition (6.2.7), the prey species keep persistent while the consumers become extinct ultimately. On the other hand, we let $\rho_{24} > -\frac{h}{r_2\sigma_2}$. Then system (6.1.1) has the same behaviours as in the first case provided that (6.2.6) is fulfilled. It is then interesting to examine how the population system behaves when a gets larger in the case $\rho_{24} > -\frac{h}{r_2\sigma_2}$. This is further developed in section 6.4.

6.3 Model (6.1.2)

In this section, we investigate the long-time behaviours of model (6.1.2). Notice that if δ_1 and δ_2 are zero, model (6.1.2) is then degenerated to model (6.1.1) which has been analysed above. Hence this section only focuses on the unique properties of model (6.1.2) with two positive constants δ_1 and δ_2.

6.3.1 Positive and Global Solution

Theorem 6.7. *For any given initial value $x_0 \in \mathbb{R}^2_+$, there is a unique solution $x(t)$ to equation (6.1.2) on $t \geqslant 0$ and the solution will remain in $\mathbb{R}^2_+$ with probability 1, namely $x(t) \in \mathbb{R}^2_+$ for all $t \geqslant 0$ a.s.*

By defining $V(x) = x_1^{0.5} - 0.5\log x_1 + x_2^{0.5} - 0.5\log x_2$, this theorem is then proved in the same routine as in Theorem 4.1.

6.3.2 Boundedness

Theorem 6.8. *Let η_1 and η_2 be positive numbers satisfying*

$$\begin{aligned} \eta_1, \eta_2 &< \frac{1}{2} \quad \text{for } \rho_{45} \geqslant 0 \text{ and } \rho_{56} \leqslant 0; \\ \eta_1 + 2\eta_2 &< \frac{1}{2} \quad \text{for } \rho_{45} < 0 \text{ and } \rho_{56} > 0; \\ \eta_1 + \eta_2 &< \frac{1}{2} \quad \text{otherwise.} \end{aligned}$$

Then for any initial value $x_0 \in \mathbb{R}^2_+$, the solution to model (6.1.2) *has the property that*

$$\limsup_{t\to\infty} \mathbb{E}[x_1^{\eta_1}(t)\, x_2^{\eta_2}(t)] \leqslant e^{c_1/c_2},$$

where c_1 and c_2 are two constants and are determined in (6.3.6) *and* (6.3.7) *below in the case $\rho_{45} < 0$ and $\rho_{56} > 0$.*

In order to prove this theorem, let us first consider the following lemma.

Lemma 6.9. *Let η_1 and η_2 be positive numbers satisfying*

$$\eta_1, \eta_2 < 1 \quad \text{for } \rho_{45} \geqslant 0 \text{ and } \rho_{56} \leqslant 0; \tag{6.3.1a}$$

$$\eta_1 + 2\eta_2 < 1 \quad \text{for } \rho_{45} < 0 \text{ and } \rho_{56} > 0; \tag{6.3.1b}$$

$$\eta_1 + \eta_2 < 1 \quad \text{otherwise,} \tag{6.3.1c}$$

Then for any initial value $x_0 \in \mathbb{R}^2_+$, the solution to model (6.1.2) *has the property that*

$$\limsup_{t\to\infty} \mathbb{E}[x_1^{\eta_1}(t)\, x_2^{\eta_2}(t)] < \infty \quad \text{for all } t \geqslant 0. \tag{6.3.2}$$

Proof. Define a C^2-function $V : \mathbb{R}^2_+ \to \mathbb{R}_+$ by $V(x) = x_1^{\eta_1} x_2^{\eta_2}$. And we obtain

$$\begin{aligned} LV(x) \leqslant V(x)\Big[A_1 + A_2 x_1 + A_3 x_2 + \frac{1}{2}\delta_1^2\eta_1(\eta_1-1)x_1^2 + \frac{1}{2}\delta_2^2\eta_2(\eta_2-1)x_2^2 \\ + \frac{\eta_2(\eta_2-1)r_2^2}{2(\beta+x_2)^2}x_1^2 - \frac{\delta_1 r_2 \eta_1\eta_2\rho_{45}}{\beta+x_2}x_1^2 + \delta_1\delta_2\eta_1\eta_2\rho_{56}x_1x_2\Big], \end{aligned}$$

where

$$A_1 = a\eta_1 - c\eta_2 - \sigma_1\sigma_2\eta_1\eta_2\rho_{12} + \sigma_1 r_1\eta_1(1-\eta_1)\bar{\rho}_{13} + r_1\sigma_2\eta_1\eta_2\bar{\rho}_{23}, \tag{6.3.3}$$

$$\begin{aligned} A_2 = -b\eta_1 + \frac{h\eta_2}{\beta} + \frac{\sigma_1 r_2\eta_1\eta_2\bar{\rho}_{14}}{\beta} + \delta_1\sigma_1\eta_1(1-\eta_1)\rho_{15} + \frac{\sigma_2 r_2\eta_2(1-\eta_2)\bar{\rho}_{24}}{\beta} \\ + \sigma_2\delta_1\eta_1\eta_2\rho_{25} + \frac{r_1 r_2\eta_1\eta_2\tilde{\rho}_{34}}{\beta} + \delta_1 r_1\eta_1(1-\eta_1)\tilde{\rho}_{35} + \delta_2 r_2\eta_2(1-\eta_2)\bar{\rho}_{46} \end{aligned} \tag{6.3.4}$$

and

$$A_3 = -f\eta_2 - \sigma_1\delta_2\eta_2\eta_1\rho_{16} - \delta_2\sigma_2\eta_2(1-\eta_2)\rho_{26} + r_1\delta_2\eta_1\eta_2\bar{\rho}_{36}. \tag{6.3.5}$$

Assuming that $\rho_{45} < 0$ and $\rho_{56} > 0$, we obtain

$$\begin{aligned}
&\frac{1}{4}\delta_1^2\eta_1(\eta_1-1)x_1^2 + \frac{\eta_2(\eta_2-1)r_2^2}{2(\beta+x_2)^2}x_1^2 - \frac{\delta_1 r_2\eta_1\eta_2\rho_{45}}{\beta+x_2}x_1^2 \\
&\leqslant \frac{1}{4}\delta_1^2\eta_1^2x_1^2 - \frac{1}{4}\delta_1^2\eta_1x_1^2 + \frac{\eta_2^2r_2^2x_1^2}{2(\beta+x_2)^2} - \frac{\eta_2r_2^2x_1^2}{2(\beta+x_2)^2} + \frac{1}{2}\eta_1\eta_2\Big(\frac{r_2^2x_1^2}{(\beta+x_2)^2} + \delta_1^2x_1^2\Big) \\
&= \frac{1}{4}\eta_1\big(\eta_1+2\eta_2-1\big)\delta_1^2x_1^2 + \frac{1}{2}\eta_2(\eta_1+\eta_2-1)\frac{r_2^2x_1^2}{(\beta+x_2)^2}
\end{aligned}$$

and

$$\begin{aligned}
&\frac{1}{4}\delta_1^2\eta_1(\eta_1-1)x_1^2 + \frac{1}{2}\delta_2^2\eta_2(\eta_2-1)x_2^2 + \delta_1\delta_2\eta_1\eta_2\rho_{56}x_1x_2 \\
&\leqslant \frac{1}{4}\delta_1^2\eta_1^2x_1^2 - \frac{1}{4}\delta_1^2\eta_1x_1^2 + \frac{1}{2}\delta_2^2\eta_2^2x_2^2 - \frac{1}{2}\delta_2^2\eta_2x_2^2 + \frac{1}{2}\eta_1\eta_2(\delta_1^2x_1^2+\delta_2^2x_2^2) \\
&= \frac{1}{4}\eta_1(\eta_1+2\eta_2-1)\delta_1^2x_1^2 + \frac{1}{2}\eta_2(\eta_1+\eta_2-1)\delta_2^2x_2^2.
\end{aligned}$$

Hence

$$\begin{aligned}
LV(x) \leqslant V(x)\Big(&A_1 + A_2x_1 + A_3x_2 - \frac{1}{2}\eta_1\big(1-(\eta_1+2\eta_2)\big)\delta_1^2x_1^2 \\
&- \frac{1}{2}\eta_2\big(1-(\eta_1+\eta_2)\big)\delta_2^2x_2^2\Big).
\end{aligned}$$

As the polynomial

$$A_1 + A_2x_1 + A_3x_2 - \frac{1}{4}\eta_1\big(1-(\eta_1+2\eta_2)\big)\delta_1^2x_1^2 - \frac{1}{4}\eta_2\big(1-(\eta_1+\eta_2)\big)\delta_2^2x_2^2$$

is bounded by

$$c_1 = \frac{\eta_1\big(1-(\eta_1+2\eta_2)\big)\delta_1^2A_1 + A_2^2}{\eta_1(1-(\eta_1+2\eta_2))\delta_1^2} + \frac{A_3^2}{\eta_2\big(1-(\eta_1+\eta_2)\big)\delta_2^2}, \tag{6.3.6}$$

we obtain

$$LV(x) \leqslant V(x)\big(c_1 - c_2|x|^2\big),$$

where

$$c_2 = \frac{1}{4}\big(\eta_1(1-(\eta_1+2\eta_2))\delta_1^2 \wedge \eta_2\big(1-(\eta_1+\eta_2)\big)\delta_2^2\big). \tag{6.3.7}$$

This leads to

$$\mathbb{E}V(x(t\wedge\tau_k)) = V(x_0) + \mathbb{E}\int_0^{t\wedge\tau_k} LV(x(s))ds \leqslant V(x_0) + c_1\int_0^t \mathbb{E}V(x(s\wedge\tau_k))ds.$$

It then follows from the Gronwall inequality (Theorem 2.30) that

$$\mathbb{E}V(x(t\wedge\tau_k))\leqslant V(x_0)e^{c_1t}.$$

Letting $k\to\infty$ implies

$$\mathbb{E}V(x(t))\leqslant V(x_0)e^{c_1t}<\infty\quad\text{for all } t\geqslant 0.$$

Similarly, assertion (6.3.2) can be deduced under condition (6.3.1a) or (6.3.1c). Here it is omitted. □

Proof of Theorem 6.8. This proof is standard using the results of Lemma 6.9. One can refer to [92, pp. 104-105] for details. □

Theorem 6.10. *For any initial value $x_0\in\mathbb{R}^2_+$, the solution to model* (6.1.2) *has the property that*

$$\limsup_{t\to\infty}\frac{\log|x(t)|}{\log t}\leqslant 6\quad a.s. \tag{6.3.8}$$

Proof. Defining V: $\mathbb{R}^2_+\to\mathbb{R}_+$ by $V(x)=x_1+x_2$, for any constant $\gamma>0$ we obtain

$$e^{\gamma t}\log V(x(t))=\log V(x(0))+\int_0^t e^{\gamma u}g(x(u))du+\sum_{i=1}^{6}\breve{M}_i(t), \tag{6.3.9}$$

where

$$\begin{aligned}g(x)=&\gamma\log V(x)+\frac{1}{V(x)}\Big(ax_1-cx_2-bx_1^2-fx_2^2-\frac{sx_1x_2}{\beta+x_2}+\frac{hx_1x_2}{\beta+x_2}\Big)\\&-\frac{1}{2V^2(x)}\Big(\sigma_1^2x_1^2+\sigma_2^2x_2^2+\frac{r_1^2x_1^2x_2^2}{(\beta+x_2)^2}+\frac{r_2^2x_1^2x_2^2}{(\beta+x_2)^2}+\delta_1^2x_1^4+\delta_2^2x_2^4-2\sigma_1\sigma_2\rho_{12}x_1x_2\\&+\frac{2\sigma_1r_2\rho_{14}x_1^2x_2}{\beta+x_2}-2\sigma_1\delta_2\rho_{16}x_1x_2^2+\frac{2r_1\sigma_2\rho_{23}x_1x_2^2}{\beta+x_2}-\frac{2r_1r_2\rho_{34}x_1^2x_2^2}{(\beta+x_2)^2}+\frac{2r_1\delta_2\rho_{36}x_1x_2^3}{\beta+x_2}\\&+2\delta_1\sigma_2\rho_{25}x_1^2x_2-\frac{2\delta_1r_2\rho_{45}x_1^3x_2}{\beta+x_2}+2\delta_1\delta_2\rho_{56}x_1^2x_2^2\Big)\end{aligned}$$

and

$$\begin{aligned}&\breve{M}_1(t)=\sigma_1\int_0^t\frac{e^{\gamma u}x_1(u)}{V(x(u))}dB_1(u),\qquad \breve{M}_2(t)=-\sigma_2\int_0^t\frac{e^{\gamma u}x_2(u)}{V(x(u))}dB_2(u),\\&\breve{M}_3(t)=-r_1\int_0^t\frac{e^{\gamma u}x_1(u)x_2(u)}{(\beta+x_2(u))V(x(u))}dB_3(u),\end{aligned}$$

$$\breve{M}_4(t) = r_2 \int_0^t \frac{e^{\gamma u} x_1(u) x_2(u)}{(\beta + x_2(u)) V(x(u))} dB_4(u),$$
$$\breve{M}_5(t) = -\delta_1 \int_0^t \frac{e^{\gamma u} x_1^2(u)}{V(x(u))} dB_5(u), \qquad \breve{M}_6(t) = -\delta_2 \int_0^t \frac{e^{\gamma u} x_2^2(u)}{V(x(u))} dB_6(u)$$

are local martingales with quadratic variations

$$\langle \breve{M}_1(t) \rangle = \sigma_1^2 \int_0^t \frac{e^{2\gamma u} x_1^2(u)}{V^2(x(u))} du, \qquad \langle \breve{M}_2(t) \rangle = \sigma_2^2 \int_0^t \frac{e^{2\gamma u} x_1^2(u)}{V^2(x(u))} du,$$
$$\langle \breve{M}_3(t) \rangle = r_1^2 \int_0^t \frac{e^{2\gamma u} x_1^2(u) x_2^2(u)}{(\beta + x_2(u))^2 V^2(x(u))} du, \langle \breve{M}_4(t) \rangle = r_2^2 \int_0^t \frac{e^{2\gamma u} x_1^2(u) x_2^2(u)}{(\beta + x_2(u))^2 V^2(x(u))} du,$$
$$\langle \breve{M}_5(t) \rangle = \delta_1^2 \int_0^t \frac{e^{2\gamma u} x_1^4(u)}{V^2(x(u))} du, \qquad \langle \breve{M}_6(t) \rangle = \delta_2^2 \int_0^t \frac{e^{2\gamma u} x_2^4(u)}{V^2(x(u))} du.$$

Given any $\alpha_1 \in (0,1)$ and $p > 1$. By the exponential martingale inequality (Theorem 2.32), we have

$$\mathbb{P}\Big(\sup_{0 \leqslant t \leqslant \psi} \Big(\breve{M}_i(t) - \frac{\alpha_1}{2} e^{-\gamma\psi} \langle \breve{M}_i(t) \rangle \Big) > \frac{p e^{\gamma\psi}}{\alpha_1} \log \psi \Big) \leqslant \frac{1}{\psi^p}, \quad \psi = 1, 2, 3, \cdots.$$

Then by the Borel-Cantelli lemma, for almost all $\omega \in \Omega$, there exists an integer $\psi_i = \psi_i(\omega)$ such that

$$\breve{M}_i(t) \leqslant \frac{\alpha_1}{2} e^{-\gamma\psi} \langle \breve{M}_i(t) \rangle + \frac{p e^{\gamma\psi}}{\alpha_1} \log \psi \quad \text{for all } 0 \leqslant t \leqslant \psi \text{ and } \psi \geqslant \psi_i(\omega).$$

Thus substituting this into (6.3.9) indicates that for almost every $\omega \in \Omega$,

$$\begin{aligned} & e^{\gamma t} \log V(x(t)) \\ \leqslant & \log V(x(0)) + \int_0^t e^{\gamma u} \Big(\gamma \log V(x(u)) + a + h + g_1(x(u)) - \frac{1 - \alpha_1 e^{\gamma(u-\psi)}}{2V^2(x(u))} \big(\delta_1^2 x_1^4(u) \\ & + \delta_2^2 x_2^4(u) \big) \Big) du + \frac{6 p e^{\gamma\psi}}{\alpha_1} \log \psi \end{aligned} \tag{6.3.10}$$

for all $0 \leqslant t \leqslant \psi$ and $\psi \geqslant \psi_0(\omega) := \max\{\psi_i(\omega) : 1 \leqslant i \leqslant 6\}$, where $g_1(x)$ is a first-order polynomial about x. By the elementary inequality

$$\frac{V^2(x)}{2} \leqslant |x|^2 \leqslant 2V^2(x), \tag{6.3.11}$$

we obtain

$$\frac{1}{V^2(x)} (\delta_1^2 x_1^4 + \delta_2^2 x_2^4) \geqslant \frac{1}{4} (\delta_1^2 \wedge \delta_2^2) |x|^2.$$

Therefore (6.3.10) is rewritten as

$$\begin{aligned}
&e^{\gamma t}\log V(x(t))\\
&\leqslant \log V(x(0)) + \frac{6pe^{\gamma\psi}}{\alpha_1}\log\psi\\
&\quad + \int_0^t e^{\gamma u}\Big(\gamma\log V(x(u)) + a + h + g_1(x(u)) - \frac{1}{8}(1-\alpha_1)(\delta_1^2\wedge\delta_2^2)|x(u)|^2\Big)du.
\end{aligned}$$

Obviously, there exists a positive constant K_3 such that for almost every $\omega\in\Omega$,

$$\begin{aligned}
&e^{\gamma t}\log V(x(t))\\
&\leqslant \log V(x(0)) + K_3\int_0^t e^{\gamma u}du + \frac{6pe^{\gamma\psi}}{\alpha_1}\log\psi \leqslant \log V(x(0)) + \frac{K_3}{\gamma}e^{\gamma t} - \frac{K_3}{\gamma}\\
&\quad + \frac{6pe^{\gamma\psi}}{\alpha_1}\log\psi
\end{aligned}$$

for all $0\leqslant t\leqslant\psi$ and $\psi\geqslant\psi_0 := \max(\psi_1,\psi_2,\cdots,\psi_6)$. Consequently, for $\psi-1\leqslant t\leqslant\psi$ and $\psi\geqslant\psi_0$, it follows that

$$\frac{\log V(x(t))}{\log t} \leqslant \frac{1}{\log(\psi-1)}\Big(e^{-\gamma(\psi-1)}\log(x_1(0)x_2(0)) + \frac{K_3}{\gamma} + \frac{6pe^{\gamma}}{\alpha_1}\log\psi\Big).$$

This implies

$$\limsup_{t\to\infty}\frac{\log V(x(t))}{\log t} \leqslant \frac{6pe^{\gamma}}{\alpha_1} \quad \text{a.s.}$$

Letting $\alpha_1\to 1, p\to 1$ and $\gamma\to 0$ implies

$$\limsup_{t\to\infty}\frac{\log V(x(t))}{\log t} \leqslant 6 \quad \text{a.s.}$$

Recalling inequality (6.3.11) gives the required assertion (6.3.8). □

Remark 6.11. Let all the Brownian motions in model (6.1.2) be uncorrelated. Then Theorem 6.10 still holds. Besides, Theorem 6.8 is fulfilled provided that η_1 and η_2 satisfy

$$\eta_1,\eta_2 < \frac{1}{2},$$

with c_1 and c_2 defined by

$$c_1 = \frac{(h\eta_2/\beta - b\eta_1)^2 + \eta_1\delta_1^2(1-\eta_1)(a\eta_1 - c\eta_2)}{\eta_1(1-\eta_1)\delta_1^2}$$

and

$$c_2 = \frac{1}{4}\big(\eta_1(1-\eta_1)\delta_1^2\wedge\eta_2(1-\eta_2)\delta_2^2\big).$$

6.4 Stationary Distribution

In this section, the stationary distributions of the solutions of model (6.1.1) and (6.1.2) are established. To show the existence of a stationary distribution, let us cite a known result from Khasminskii [68] as a lemma.

Lemma 6.12. *The SDE model* (6.1.2) *has a unique stationary distribution if (i) the matrix*

$$U(x) = A(x)\mathcal{R}A(x)^T$$

is positive definite for $x \in \mathbb{R}^2_+$, *where*

$$A(x) = \begin{bmatrix} \sigma_1 x_1 & 0 & \frac{-r_1 x_1 x_2}{\beta + x_2} & 0 & -\delta_1 x_1^2 & 0 \\ 0 & -\sigma_2 x_2 & 0 & \frac{r_2 x_1 x_2}{\beta + x_2} & 0 & -\delta_2 x_2^2 \end{bmatrix};$$

(ii) there is a bounded openset G *of* $\mathbb{R}^2_+$ *and*

$$\sup_{x_0 \in Q - G} \mathbb{E}(\tau_G) < \infty$$

for every compact subset Q *of* $\mathbb{R}^2_+$ *such that* $G \subset Q$ *where* $\tau_G = \inf\{t \geqslant 0 : x(t) \in G\}$.

Theorem 6.13. *If*

$$\begin{gathered} \rho_{i_1 i_2} \neq \pm 1; \rho_{1i_3}, \rho_{4i_3} < 1/2; \rho_{26}, \rho_{35} > -1/2; \\ \rho_{1i_3} \leqslant \rho_{1i_2}\rho_{i_2 i_3}; \rho_{35} \geqslant \rho_{3i_2}\rho_{5i_2}; \rho_{4i_4} \leqslant \rho_{i_1 4}\rho_{i_1 i_4}; \rho_{26} \geqslant \rho_{2i_1}\rho_{6i_1}; \\ 2\rho_{1i_3}\rho_{26} \leqslant \rho_{12}\rho_{6i_3} + \rho_{16}\rho_{2i_3}; 2\rho_{35}\rho_{4i_4} \leqslant \rho_{3i_4}\rho_{45} + \rho_{34}\rho_{5i_4}; \\ 2\rho_{1i_3}\rho_{4i_4} \geqslant \rho_{14}\rho_{i_3 i_4} + \rho_{1i_4}\rho_{4i_3}; 2\rho_{35}\rho_{26} \geqslant \rho_{23}\rho_{56} + \rho_{36}\rho_{25} \\ \text{for } i_1 = 1, 3 \text{ or } 5, i_2 = 2, 4 \text{ or } 6, i_3 = 3 \text{ or } 5 \text{ and } i_4 = 2 \text{ or } 6, \end{gathered} \tag{6.4.1}$$

$$h_0 := \sigma_2 r_2 \tilde{\rho}_{24} + \delta_2 r_2 \beta \tilde{\rho}_{46} < h, \tag{6.4.2}$$

$$2a\Big(1 - \frac{1+\beta}{2(h-h_0)}\sigma_2^2 - \frac{(1+\beta)c}{h-h_0}\Big) > \sigma_1^2 + 2r_1\sigma_1\tilde{\rho}_{13} + \frac{2(b+b_0)\beta c}{h-h_0} + \frac{(b+b_0)\beta}{h-h_0}\sigma_2^2 \tag{6.4.3}$$

and

$$b \geqslant \frac{1}{2}\delta_1^2 + \frac{E_1}{2h\beta^2}r_2^2 + \frac{a+E_2}{\beta}, \tag{6.4.4}$$

where

$$b_0 = \sigma_1\delta_1\tilde{\rho}_{15} + r_1\delta_1\bar{\rho}_{35}, \quad E_1 = \frac{ah + \big(a+b+b_0\big)\beta h}{h-h_0} \quad \textit{and} \quad E_2 = b_0 + \frac{h_0 E_1}{\beta h},$$

then for any initial value $x_0 \in \mathbb{R}^2_+$, model (6.1.2) has a unique stationary distribution.

Proof. (i) We compute

$$U(x) = (U_{ij}(x))_{2\times 2},$$

where

$$U_{11}(x) = \sigma_1^2 x_1^2 - \frac{2\rho_{13}\sigma_1 r_1 x_1^2 x_2}{\beta + x_2} - 2\sigma_1\delta_1\rho_{15}x_1^3 + \frac{2r_1\delta_1\rho_{35}x_1^3 x_2}{\beta + x_2} + \frac{r_1^2 x_1^2 x_2^2}{(\beta+x_2)^2} + \delta_1^2 x_1^4,$$

$$U_{22}(x) = \sigma_2^2 x_2^2 - \frac{2r_2\sigma_2\rho_{24}x_1 x_2^2}{\beta + x_2} + 2\rho_{26}\sigma_2\delta_2 x_2^3 - \frac{2\rho_{46}\delta_2 r_2 x_1 x_2^3}{\beta + x_2} + \frac{r_2^2 x_1^2 x_2^2}{(\beta+x_2)^2} + \delta_2^2 x_2^4$$

and

$$\begin{aligned} U_{12}(x) = U_{21}(x) = &-\sigma_1\sigma_2\rho_{21}x_1x_2 + \frac{\rho_{14}r_2\sigma_1 x_1^2 x_2}{\beta+x_2} - \delta_2\sigma_1\rho_{16}x_1x_2^2 + \frac{r_1\sigma_2\rho_{23}x_1x_2^2}{\beta+x_2} \\ &- \frac{\rho_{34}r_1r_2x_1^2x_2^2}{(\beta+x_2)^2} + \frac{r_2\delta_2\rho_{36}x_1x_2^3}{\beta+x_2} + \delta_1\sigma_2\rho_{25}x_1^2x_2 - \frac{\rho_{45}\delta_1 r_2 x_1^3 x_2}{\beta+x_2} + \rho_{56}\delta_1\delta_2 x_1^2 x_2^2. \end{aligned}$$

The sufficient conditions (6.4.1) guarantee that $U_{11}(x) > 0$, $U_{22}(x) > 0$ and $U_{11}(x)U_{22}(x) - U_{12}^2(x) > 0$. Hence $U(x)$ is a positive-definite matrix.

(ii) We define a C^2-function $V : \mathbb{R}^2_+ \to \mathbb{R}_+$:

$$V(x) = MV_1(x) + V_2(x) + e,$$

where

$$V_1(x) = x_1 + \log(\beta + x_1) - \log(x_1) + \frac{l}{h}x_2 - \frac{E_1}{h}\log x_2, \quad V_2(x) = x_1 + \frac{s}{h}x_2,$$

and e, l and M are three constants. $e = -\min(MV_1(x) + V_2(x))$ to keep the non-negativity of $V(x)$,

$$l = \Big(\frac{hs}{c\beta} + \frac{E_1 f}{c} + \frac{E_1\sigma_2\delta_2\bar{\rho}_{26}}{c}\Big) \bigvee \Big(\frac{E_1\delta_2^2}{2f} + \frac{hr_1^2}{2f\beta^2} + \frac{E_1 h}{4f\beta^2}\Big) \tag{6.4.5}$$

and M is to be defined later. First compute

$$\begin{aligned}
LV_1 &= \Big(x_1 + \frac{x_1}{\beta + x_1} - 1\Big)\Big(a - bx_1 - \frac{sx_2}{\beta + x_2}\Big) + \frac{1}{2}\Big(1 - \frac{x_1^2}{(\beta + x_1)^2}\Big)\Big(\sigma_1^2 + \frac{r_1^2 x_2^2}{(\beta + x_2)^2} \\
&\quad + \delta_1^2 x_1^2 - \frac{2\sigma_1 r_1 \rho_{13} x_2}{\beta + x_2} - 2\sigma_1\delta_1\rho_{15}x_1 + \frac{2r_1\delta_1\rho_{35}x_1x_2}{\beta + x_2}\Big) + \Big(\frac{lx_2}{h} - \frac{E_1}{h}\Big)\Big(\frac{hx_1}{\beta + x_2} - c \\
&\quad - fx_2\Big) + \frac{E_1}{2h}\Big(\sigma_2^2 + \frac{r_2^2 x_1^2}{(\beta + x_2)^2} + \delta_2^2 x_2^2 - \frac{2r_2\sigma_2\rho_{24}x_1}{\beta + x_2} + 2\delta_2\sigma_2\rho_{26}x_2 \\
&\quad - \frac{2\delta_2 r_2 \rho_{46} x_1 x_2}{\beta + x_2}\Big) \\
&\leqslant ax_1 - bx_1^2 + \frac{ax_1}{\beta + x_1} - \frac{bx_1^2}{\beta + x_1} + bx_1 - \frac{E_1 x_1}{\beta + x_2} - a + \frac{sx_2}{\beta + x_2} + \frac{1}{2}\sigma_1^2 + \frac{r_1^2 x_2^2}{2\beta^2} \\
&\quad + \frac{\delta_1^2 x_1^2}{2} + r_1\sigma_1\tilde{\rho}_{13} + \big(\sigma_1\delta_1\tilde{\rho}_{15} + r_1\delta_1\bar{\rho}_{35}\big)x_1 + \frac{lx_1x_2}{\beta + x_2} - \frac{clx_2}{h} - \frac{flx_2^2}{h} + \frac{E_1 c}{h} \\
&\quad + \frac{E_1 f x_2}{h} + \frac{E_1\sigma_2^2}{2h} + \frac{E_1 r_2^2 x_1^2}{2h\beta^2} + \frac{E_1\delta_2^2 x_2^2}{2h} + \frac{E_1\sigma_2 r_2\tilde{\rho}_{24}x_1}{h\beta} + \frac{E_1\sigma_2\delta_2\rho_{26}x_2}{h} \\
&\quad + \frac{E_1\delta_2 r_2\tilde{\rho}_{46}x_1}{h} \\
&\leqslant \frac{(a + E_2)\beta x_1}{\beta + x_1} + \frac{ax_1}{\beta + x_1} + \frac{b\beta x_1}{\beta + x_1} - \frac{E_1 x_1}{\beta + x_2} + \Big(-b + \frac{\delta_1^2}{2} + \frac{a + E_2}{\beta + x_1} + \frac{E_1 r_2^2}{2h\beta^2}\Big)x_1^2 \\
&\quad - a + \frac{1}{2}\sigma_1^2 + r_1\sigma_1\tilde{\rho}_{13} + \frac{E_1 c}{h} + \frac{E_1\sigma_2^2}{2h} + \Big(\frac{s}{\beta} + \frac{E_1 f}{h} - \frac{cl}{h} + \frac{E_1\sigma_2\delta_2\rho_{26}}{h}\Big)x_2 + \Big(\frac{E_1\delta_2^2}{2h} \\
&\quad + \frac{r_1^2}{2\beta^2} - \frac{fl}{h}\Big)x_2^2 + \frac{lx_1x_2}{\beta + x_2} \\
&\leqslant \frac{E_1(x_1x_2 - x_1^2)}{(\beta + x_1)(\beta + x_2)} + \Big(-b + \frac{\delta_1^2}{2} + \frac{a + E_2}{\beta} + \frac{E_1 r_2^2}{2h\beta^2}\Big)x_1^2 - \lambda + \Big(\frac{s}{\beta} + \frac{E_1 f}{h} - \frac{cl}{h} \\
&\quad + \frac{E_1\sigma_2\delta_2\rho_{26}}{h}\Big)x_2 + \Big(\frac{E_1\delta_2^2}{2h} + \frac{r_1^2}{2\beta^2} - \frac{fl}{h}\Big)x_2^2 + \frac{lx_1x_2}{\beta + x_2},
\end{aligned}$$

where $\lambda = a - \frac{1}{2}\sigma_1^2 - r_1\sigma_1\tilde{\rho}_{13} - \frac{E_1 c}{h} - \frac{E_1\sigma_2^2}{2h} > 0$ from condition (6.4.3). Under (6.4.4), (6.4.5) and the Young inequality,

$$\begin{aligned}
LV_1 &\leqslant -\lambda + \Big(-b + \frac{\delta_1^2}{2} + \frac{a + E_2}{\beta} + \frac{E_1 r_2^2}{2h\beta^2}\Big)x_1^2 + \Big(\frac{s}{\beta} + \frac{E_1 f}{h} - \frac{cl}{h} + \frac{E_1\sigma_2\delta_2\rho_{26}}{h}\Big)x_2 \\
&\quad + \Big(\frac{E_1\delta_2^2}{2h} + \frac{r_1^2}{2\beta^2} - \frac{fl}{h} + \frac{E_1}{4\beta^2}\Big)x_2^2 + \frac{lx_1x_2}{\beta + x_2} \\
&\leqslant -\lambda + \frac{lx_1x_2}{\beta + x_2}.
\end{aligned}$$

Then compute

$$LV_2 = ax_1 - bx_1^2 - \frac{sc}{h}x_2 - \frac{sf}{h}x_2^2 \leqslant ax_1 - bx_1^2 - \frac{sf}{h}x_2^2.$$

Hence

$$LV(x) \leqslant M\Big(-\lambda + \frac{lx_1x_2}{\beta + x_2}\Big) + ax_1 - bx_1^2 - \frac{sf}{h}x_2^2,$$

where M satisfies $M\lambda \geqslant a^2/(4b) + 2$. Now we aim to show

$$LV(x) \leqslant -1 \text{ for all } x \in \mathbb{R}_+^2 - G := G^c. \tag{6.4.6}$$

As if this holds, let $x \in G^c$ be arbitrary and τ_G be the stopping time as defined in Lemma 6.12. From (6.4.6), we have

$$0 \leqslant V(x_0) - \mathbb{E}(t \wedge \tau_G \wedge \tau_k), \quad \forall t > 0.$$

Letting $k \to \infty$ and then $t \to \infty$, we have

$$\mathbb{E}(\tau_G) \leqslant V(x_0), \quad \forall x_0 \in G^c$$

as required. To show that (6.4.6) actually holds, we define

$$G^c = G_1^c \cup G_2^c \cup G_3^c \cup G_4^c,$$

where

$$G_1^c = \{x | x_1 \in (0, \epsilon_1]\}; \qquad G_2^c = \Big\{x \Big| x_1 \in \Big(0, \frac{1}{\epsilon_1}\Big], x_2 \in (0, \epsilon_2]\Big\};$$
$$G_3^c = \Big\{x \Big| x_1 \in \Big[\frac{1}{\epsilon_1}, +\infty\Big)\Big\}; \qquad G_4^c = \Big\{x \Big| x_2 \in \Big[\frac{1}{\epsilon_2}, +\infty\Big)\Big\}$$

with two constants $\epsilon_1, \epsilon_2 \in (0, 1)$ satisfying

$$\epsilon_1^2 \leqslant \frac{1}{M^2l^2} \bigwedge \frac{b}{2(N_1 + 1)}, \quad \epsilon_2^2 \leqslant \frac{sf}{2h(N_2 + 1)} \quad \text{and} \quad \epsilon_2 \leqslant \frac{\beta\epsilon_1}{Ml}, \tag{6.4.7}$$

where the constants N_1 and N_2 will be determined later. We then show that in any subset of G^c, (6.4.6) holds. From (6.4.7),
(a) if $x \in G_1^c$,

$$LV(x) \leqslant -M\lambda + Mlx_1 + ax_1 - bx_1^2 - \frac{sf}{h}x_2^2 \leqslant Ml\epsilon_1 - 2 \leqslant -1;$$

(b) if $x \in G_2^c$,

$$LV(x) \leqslant -M\lambda + \frac{Mlx_1x_2}{\beta} + ax_1 - bx_1^2 - \frac{sf}{h}x_2^2 \leqslant \frac{Ml\epsilon_2}{\beta\epsilon_1} - 2 \leqslant -1;$$

(c) if $x \in G_3^c$,

$$LV(x) \leqslant -M\lambda + (Ml + a)x_1 - \frac{bx_1^2}{2} - \frac{bx_1^2}{2} - \frac{sfx_2^2}{h}.$$

Note that the polynomials $-M\lambda + (Ml + a)x_1 - \frac{bx_1^2}{2} - \frac{sfx_2^2}{h}$ has an upper bound, say N_1, hence

$$LV(x) \leqslant N_1 - \frac{b}{2\epsilon_1^2} \leqslant -1;$$

(d) if $x \in G_4^c$,

$$LV(x) \leqslant -M\lambda + (Ml + a)x_1 - bx_1^2 - \frac{sfx_2^2}{2h} - \frac{sfx_2^2}{2h}.$$

Note that the polynomial $-M\lambda + (Ml + a)x_1 - bx_1^2 - \frac{sfx_2^2}{2h}$ is again bounded, say by N_2, we have

$$LV(x) \leqslant N_2 - \frac{sf}{2h\epsilon_2^2} \leqslant -1.$$

In all,

$$LV(x) \leqslant -1 \text{ for all } x \in G^c.$$

□

Remark 6.14. Assume that all the Brownian motions in model (6.1.2) are uncorrelated. Then letting $\rho_{ij} = 0$ for $i, j = 1, 2, \cdots, 6$ and $i \neq j$ in conditions (6.4.1)-(6.4.4) gives the parametric conditions for model (6.1.2) to have a unique stationary distribution.

Remark 6.15. Given that conditions (6.4.1)-(6.4.4) are satisfied with $\delta_1 = \delta_2 = 0$ and $\rho_{i5} = \rho_{i6} = \rho_{56} = 0$ for $i = 1, 2, \cdots, 4$, model (6.1.1) then has a unique stationary distribution.

6.5 Numerical Examples

The following examples are developed to illustrate our results. The system parameters are given in appropriate units. The Euler-Maruyama (EM) scheme is used for the computer simulations [57]. From the theory introduced in [90], the EM approximate solutions are convergent to the true solutions of model (6.1.1) and (6.1.2) in probability.

Example 6.16. *We perform a computer simulation of* 10000 *iterations of model* (6.1.1) *with initial value* $x(0) = (0.7, 0.15)^T$ *using the Euler-Maruyama (EM) method [57, 89] with stepsize* $\Delta = 0.01$ *and the system parameters given by*

$$a = 1, b = 0.5, \beta = 5, s = 16, h = 0.9, c = 2, f = 3, \sigma_1 = 1.5, \sigma_2 = 1.0, r_1 = 0.5$$
$$r_2 = 0.95 \text{ and } \rho_{13} = 0.15. \tag{6.5.1}$$

This group of parameters satisfies condition (6.2.5) *clearly. Theorem 6.4 then indicates that both species die out ultimately with probability* 1*. This is illustrated in Figure 6.1.*

Example 6.17. *We keep the system parameters of model* (6.1.1) *the same as Example 6.16 but let* $\sigma_1 = 0.5$*. Moreover, we let* $\rho_{13} = 0.15$ *and* $\rho_{24} = 0.9$*. As a result, condition* (6.2.6) *is fulfilled. From Theorem 6.4(b), the prey abundance has the property that*

$$1.75 \leqslant \liminf_{t\to\infty} \frac{1}{t}\int_0^t x_1(u)du \leqslant \limsup_{t\to\infty} \frac{1}{t}\int_0^t x_1(u)du \leqslant 1.825 \quad a.s.$$

and the consumers will tend to zero exponentially with probability 1*. Figure 6.2 supports these results clearly.*

Example 6.18. *In this example, we remain the system parameters of model* (6.1.1) *the same as Example 6.17 except that we let* $\rho_{24} = -0.95$*. This group of parameters does not obey condition* (6.2.6) *but satisfy* (6.2.7)*. Hence Theorem 6.4(b) suggests that*

$$1.75 \leqslant \liminf_{t\to\infty} \frac{1}{t}\int_0^t x_1(u)du \leqslant \limsup_{t\to\infty} \frac{1}{t}\int_0^t x_1(u)du \leqslant 1.825 \quad a.s.$$

and the consumers will tend to zero exponentially with probability 1*. Figure 6.3 supports these results clearly.*

Then we study the case when the SDE system (6.1.1) and (6.1.2) have a stationary distribution.

Example 6.19. *We assume that the parameters of system* (6.1.1) *are the same as in Example 6.18 but let* $\beta = 2.5, h = 10, \sigma_1 = 0.01,$ *and* $\sigma_2 = 0.02$*. Also the*

correlation matrix is given by

$$\mathcal{R} = (\rho_{ij})_{4\times 4} = \begin{bmatrix} 1 & 0 & -0.8 & 0 \\ 0 & 1 & 0 & -0.95 \\ -0.8 & 0 & 1 & 0 \\ 0 & -0.95 & 0 & 1 \end{bmatrix}.$$

The time series of the correlated Brownian motions is shown in Figure 6.4. It is found that these parameters obey conditions (6.4.1)-(6.4.4) *with* $\delta_1 = \delta_2 = 0$ *and* $\rho_{i5} = \rho_{i6} = 0 = \rho_{56}$ *for* $i = 1, 2, \cdots, 4$. *From Theorem 6.4 and Remark 6.15, system* (6.1.1) *has a stationary distribution. The ergodic property enables us to obtain the approximate probability distribution for the stationary distribution by computer simulation of a single sample path of a solution to model* (6.1.1). *Therefore the histogram of the* 10000 *iterations shown in Figure 6.5(b)(d) can be regarded as approximate p.d.f.s of the stationary distribution.*

Example 6.20. *In this example, the stationary distribution of model* (6.1.2) *is examined. We keep the system parameters the same as in Example 6.19 and let* $\delta_1 = 0.01$ *and* $\delta_2 = 0.02$. *Moreover the correlation matrix is given by*

$$\mathcal{R} = (\rho_{ij})_{6\times 6} = \begin{bmatrix} 1 & 0 & -0.8 & 0 & -0.5 & 0 \\ 0 & 1 & 0 & -0.95 & 0 & 0.7 \\ -0.8 & 0 & 1 & 0 & 0.9 & 0 \\ 0 & -0.95 & 0 & 1 & 0 & -0.8 \\ -0.5 & 0 & 0.9 & 0 & 1 & 0 \\ 0 & 0.7 & 0 & -0.8 & 0 & 1 \end{bmatrix}.$$

Obviously, these parameters obey conditions (6.4.1)-(6.4.4). *From Theorem 6.13, model* (6.1.2) *has a stationary distribution. The approximate p.d.f.s of the stationary distribution could be identified from Figure 6.6(b)(d).*

6.6 Summary

In this chapter, the different properties of the SDE population models (6.1.1) and (6.1.2) incorporating white noise were studied. The correlations between the Brownian motions do make an effect on the long-time behaviours of the systems.

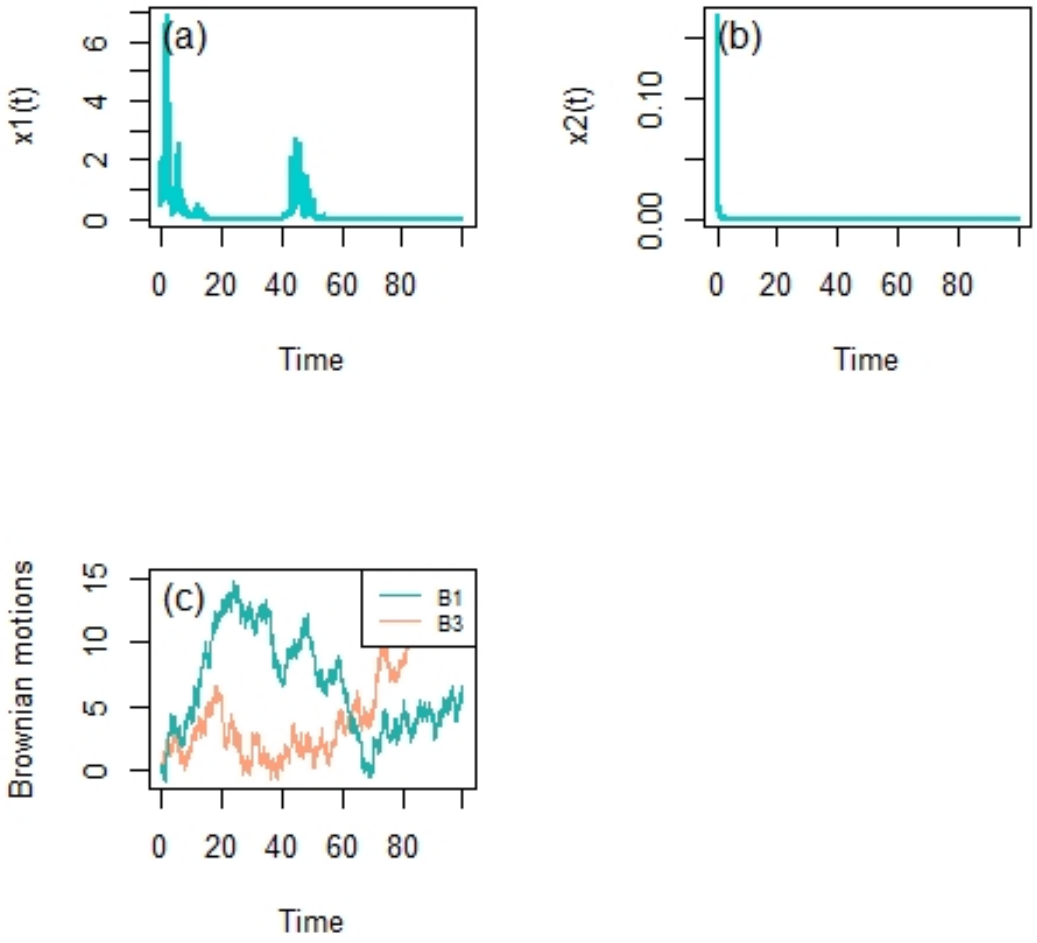

Figure 6.1: Numerical simulations of the paths (a) $x_1(t)$ and (b) $x_2(t)$ of SDE model (6.1.1) using the EM scheme with stepsize $\Delta = 0.01$ and initial value $x_0 = (0.7, 0.15)^T$ with the system parameters provided by (6.5.1). Times series of the correlated Brownian motions $B_1(t)$ and $B_3(t)$ is shown in (c).

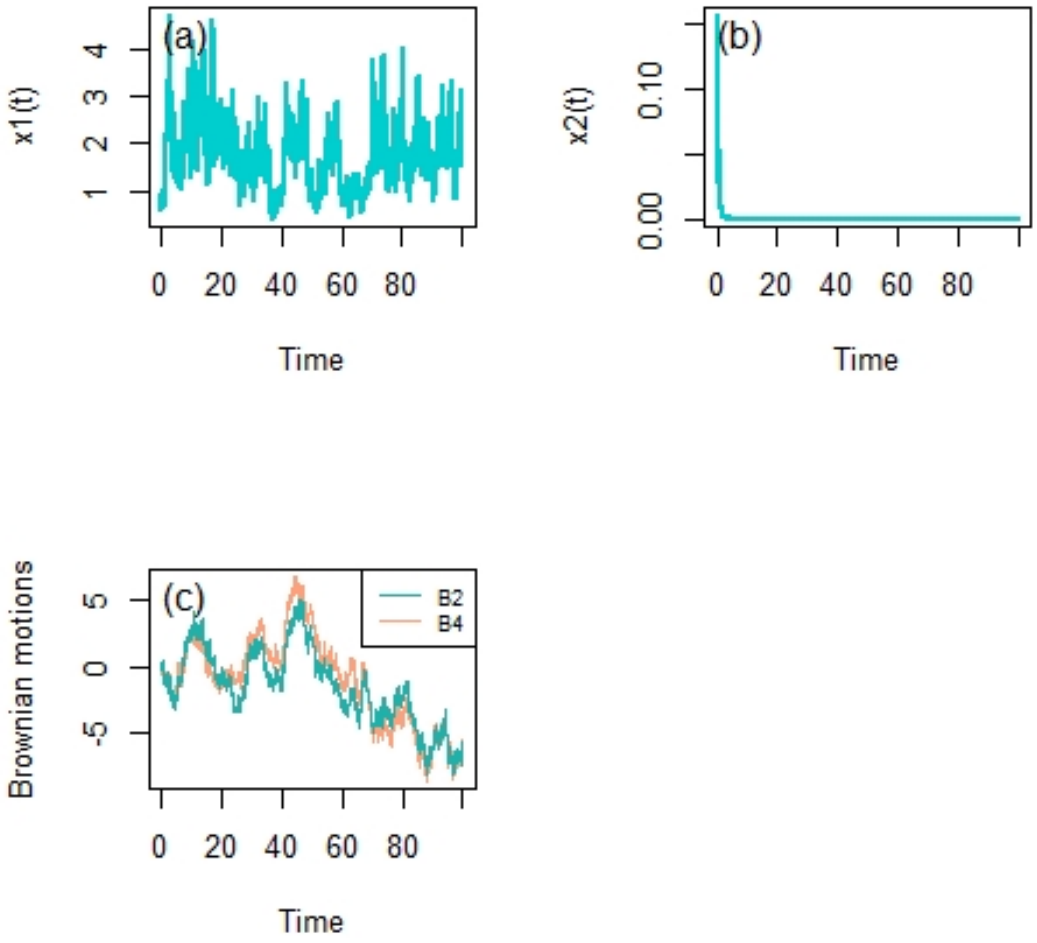

Figure 6.2: Under the system parameters described in Example 6.17, we obtain the numerical simulations of the paths (a) $x_1(t)$ and (b) $x_2(t)$ of SDE model (6.1.1) using the EM method with stepsize $\Delta = 0.01$ and initial value $x_0 = (0.7, 0.15)^T$. Times series of the correlated Brownian motions $B_2(t)$ and $B_4(t)$ is shown in (c).

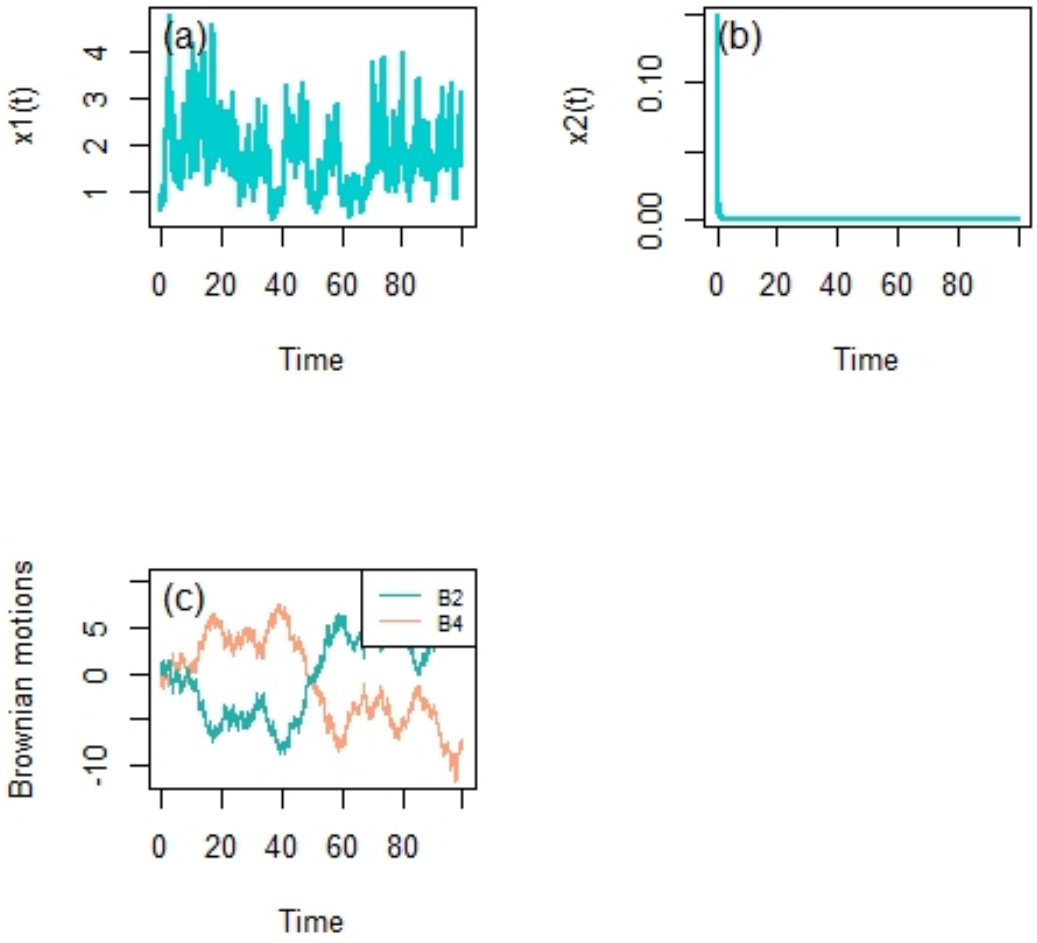

Figure 6.3: With the system parameters given in Example 6.18, we obtain the computer simulations of the paths (a) $x_1(t)$ and (b) $x_2(t)$ of SDE model (6.1.1) using the EM method with stepsize $\Delta = 0.01$ and initial value $x_0 = (0.7, 0.15)^T$. Times series of the correlated Brownian motions $B_2(t)$ and $B_4(t)$ is shown in (c).

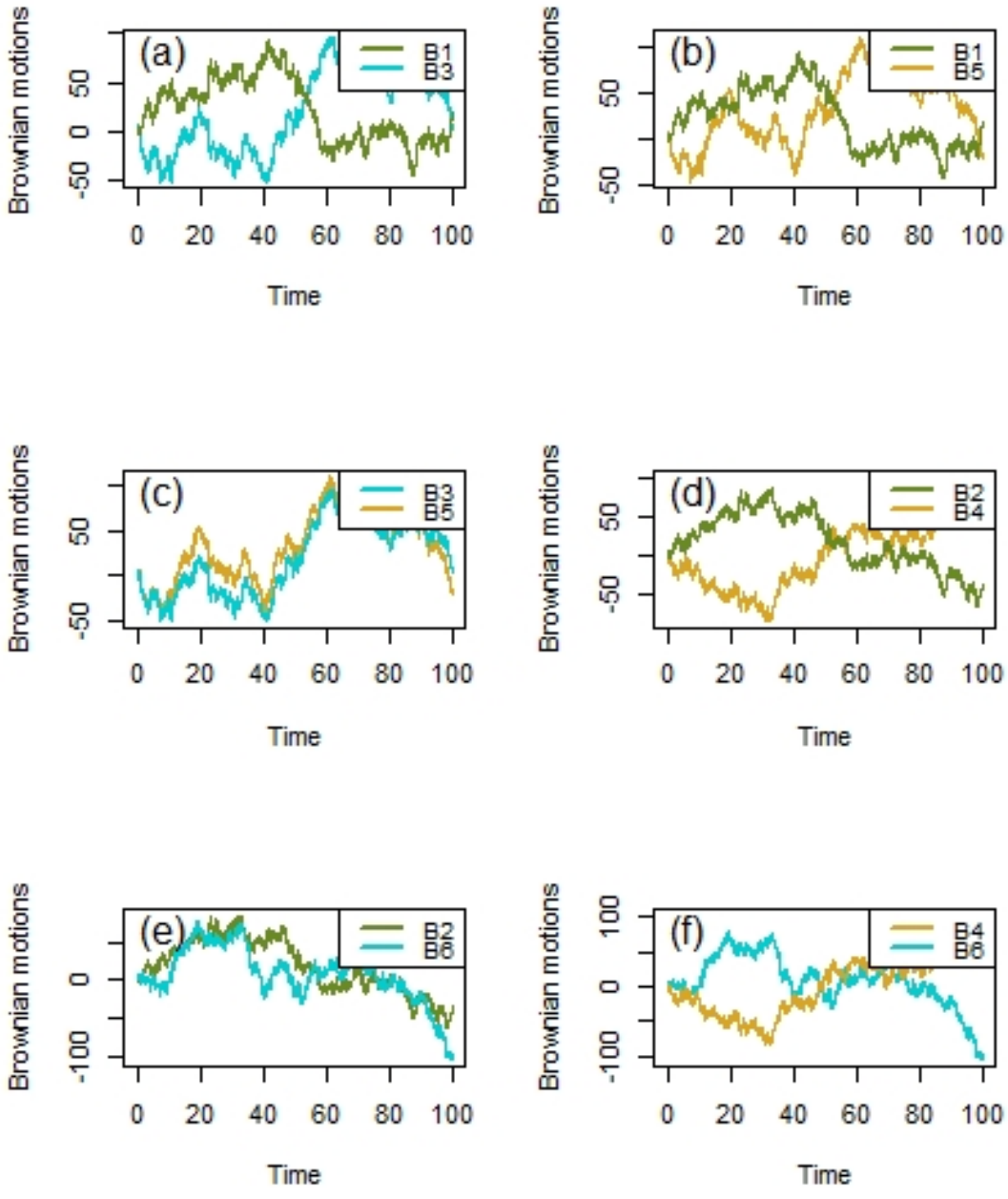

Figure 6.4: Time series of the correlated Brownian motions adopted in Example 6.19 and 6.20.

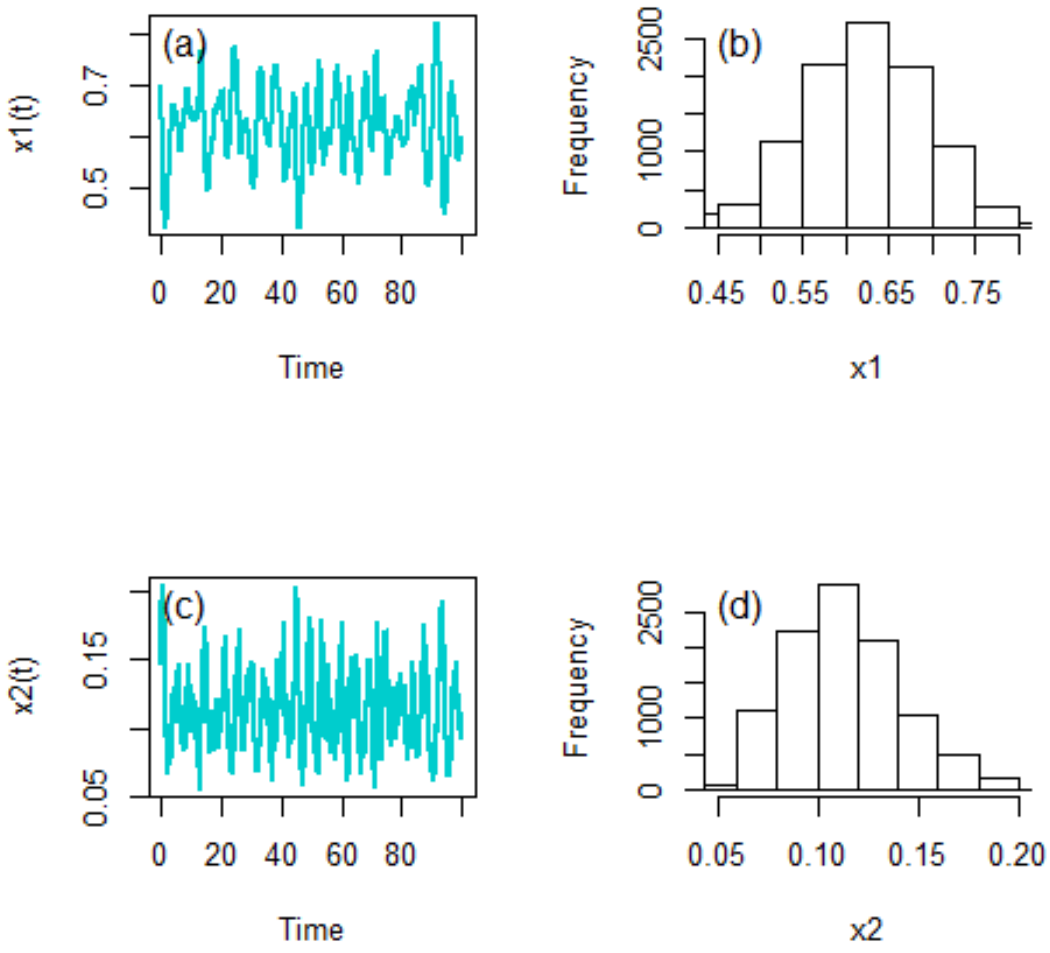

Figure 6.5: Numerical simulations of the paths (a) $x_1(t)$ and (c) $x_2(t)$ of SDE model (6.1.1) based on the model parameters described in Example 6.19 using the EM technique with stepsize $\Delta = 0.01$ and initial value $x_0 = (0.7, 0.15)^T$, followed by the histograms for the SDE paths (b) $x_1(t)$ and (d) $x_2(t)$.

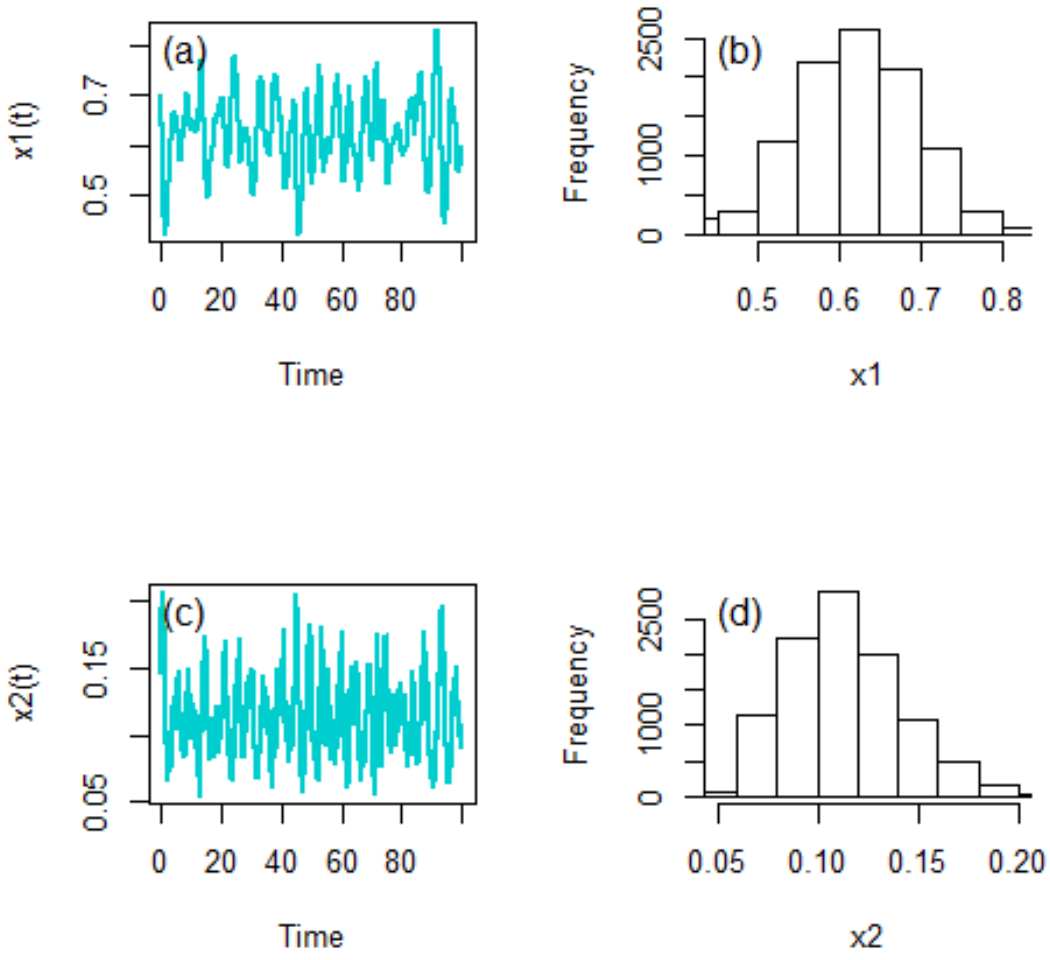

Figure 6.6: Computer simulations of the paths (a) $x_1(t)$ and (c) $x_2(t)$ of SDE model (6.1.2) based on the model parameters provided in Example 6.20 using the EM technique with stepsize $\Delta = 0.01$ and initial value $x_0 = (0.7, 0.15)^T$, followed by the histograms for the SDE paths (b) $x_1(t)$ and (d) $x_2(t)$.

Especially, in model (6.1.1), a positive correlation between $B_1(t)$ and $B_3(t)$ leads to a slightly different condition for both populations to be extinct. Moreover, if $B_2(t)$ is strongly negatively correlated to $B_4(t)$, the population system always remains extinct (the prey populations become persistent white the consumers die out) and has no chance to have a multiple coexisting stationary status. In the contrast, provided that the correlation coefficient between $B_2(t)$ and $B_4(t)$ is bigger than $-\frac{h}{r_2\sigma_2}$, the system is possible to have a stationary distribution for both species with a larger value of a. These imply how the correlations between the Brownian motions affect the dynamical behaviours of the populations. Theorem 6.13 reflects that a smaller amplitude environmental noise leads to a permanent population system. The ergodic property of the stationary distribution makes it possible to generate the approximate probability distribution using a single sample path of the solution to the SDE model by computer simulations.

Chapter 7

Conclusions

The deterministic approach has been intensively applied to the ecological modelling. However, a natural response to the complex perturbations in the real world would be to consider the stochastic models. This thesis has constructed an SDE model which captures the annual variability in the surface nitrate in Loch Linnhe. On the other hand, the stochastic versions of the predator-prey system have been studied and the effects of the environmental noise on the long-time behaviours of the populations have been investigated. The introduction of the stochasticity to the population models complicates the system but probably can better explain the real world.

In an aquatic ecosystem, nutrients, especially nitrogen and phosphorus, can regulate the primary productivity and change the structure and function of an aquatic environment [50, 101, 128]. Mathematical modelling of the aquatic nutrients has received increasing attention. A comprehensive field program implemented in Loch Linnhe in 1991 provided us with the high-resolution hydrographic and chemical data. This allowed us to model the dynamics of the fjord nitrate, which is often most limiting to the phytoplankton growth. Stochastic modelling approach has been adopted to interpret the environmental-type process noise inherent in the nitrate data. More precisely, we formulated an SDE model of nitrate by introducing the environmental noise to the simplest deterministic nutrient model (3.4.1) based on the well-established parameter perturbation method. The reliability of the model can be evaluated based on the observed

data. Firstly, we studied the model fit for the one-month data. The goodness of fit has been analysed by comparing the distribution of the nitrate data with that of the model simulation and by testing whether the nitrate data follows $\mathbb{N}(\frac{\hat{I}}{\hat{\mu}}, \frac{\hat{\sigma}^2}{2\hat{\mu}})$. The p-values in both statistical tests (Kolmogorov-Smirnov test) suggested a good model fit. Next the model fit for the one-year data was discovered. The annual seasonal variations in the fjord nitrate have led us to refine our SDE model by considering more physical and biological processes which make big effects on the dynamics of fjord nitrate. In addition, we have developed a separate SDE model which represents the seasonal trends of the shallow salinity in Loch Linnhe. By combining the salinity model with the existing nitrate model, we then obtained a coupled SDE system (3.5.3). The goodness of fit of the coupled equation has been assessed by identifying whether the normalised nitrate and salinity data follow the standard normal distribution. The p-values produced in the normality test were too small to suggest good model fit. Statistically speaking, the convincing results of the statistical tests are always based on large amounts of long-duration data. Obviously the one-year data was not enough. On the other hand, by comparing the distribution graph of the normalised data for model (3.5.3) with that for any interim model shown in Appendix A, we found that the graph for model (3.5.3) has become much closer to the normal distribution. This reflected that more annual seasonality in the sea-loch nitrate and salinity has been captured by model (3.5.3). Due to the low p-value, we cannot say that the SDE model is capable of representing the annual changes in the sea-loch nitrate and salinity. However we would conclude that so far (3.5.3) has been the best model of shallow nitrate and salinity in Loch Linnhe. A schematic pattern of the Loch Linnhe ecosystem was then drawn by tracking the paths of the surface nitrate and salt. Moreover, we performed a residual analysis for the nitrate and salinity data in order to investigate the presence of the environmental-type process noise in the data. However, we have not been able to detect which type of error in the data is dominant. We finally conducted a simulation study to illustrate the accuracy of the parameter estimation techniques for the SDE and ODE models. It suggested that the true parameters for the data with process noise can be captured using the SDE parameter estimation scheme. While the ODE estimation procedure is able to approach the underlying parameters for the data driven by observation error.

In particular, the SDE and ODE estimation frameworks always produced very different groups of parameters for a given set of data, indicating the importance of detecting the dominant type of error in the data. This becomes our future plan.

In Chapter 4, we have studied a foraging arena predator-prey model. There are many types of the functional responses in a general predator-prey model, e.g. Lotka-Voterra type, Holling type, ratio-dependence type. The population systems with these responses incorporating environmental noise have been widely explored. However, to the best of our knowledge, there has not been any literature addressing the problem for the foraging arena system. Chapter 4 was to fill this gap by studying the asymptotic behaviours of the foraging arena population model incorporating white noise. The effects of the white noise on the dynamical system can be analysed by identifying the differences between the SDE model (4.2.1) and the corresponding ODE system (1.3.2). Firstly, the deterministic model has two non-negative trivial equilibrium points. Under the condition $a > \frac{b\beta c}{h}$, there exists a positive equilibrium point $\bar{E}^*(\bar{x}_1^*, \bar{x}_2^*)$ and it is globally asymptotically stable. In the contrast, the stochastic model only has one trivial equilibrium point $E_0 = (0, 0)$. Secondly, a series disease or severe weather can lead to the extinction of both species. This situation has been described by the stochastic model under condition $2a < \sigma_1^2$. The value of σ_1 measures the intensity of the environmental variability. However this situation was not reflected by the deterministic model. This indicated that the stochastic model outperforms the deterministic one to account for the real-life situation. In addition, notice that the deterministic system would be extinct, in the sense that the consumers die out and the prey population keep persistent, provided that $a < \frac{b\beta c}{h}$. While the stochastic model goes to extinction even for some $a > \frac{b\beta c}{h}$. This indicated the influence that white noise has made on the dynamical behaviours of the population system. We then proved that the system has of stationary distribution provided that $2a > \frac{\phi}{1-\sigma_2^2/(2h)-c/h}$. Unfortunately, we have not been able to prove the case when $\phi < 2a < \frac{\phi}{1-\sigma_2^2/(2h)-c/h}$, though the computer simulation suggested a stationary distribution of both species under this condition.

In Chapter 5, we have additionally introduced telegraph noise to the popu-

lation model formulated in Chapter 4 to describe the system where the structures and parameters experience abrupt changes due to abrupt environmental disturbances and changing subsystem interconnections [94]. In addition, time delay due to gestation [133] has also been included to our population system. The long-time behaviours of the system indicated that a bigger amplitude of environmental noise may destabilize the system. The existence of the time delay makes the stochastically ultimately bounded property of our system satisfied only under certain parametric condition. Based on this, we then showed that the total amount of prey and predator species will grow at most polynomially with order close to one. We have also found that if in some subsystems the prey is persistent and in some others the prey is extinct, due to the presence of the Markov switching, both populations in the overall system could remain extinct with a negative value of λ_1 defined in (5.5.1).

Finally, we perturbed more parameters of the predator-prey system by stochastic noise and studied how the correlations between the Brownian motions affect the long-time properties of the SDE model. In particular, a positive correlation coefficient between $B_1(t)$ and $B_3(t)$ in model (6.1.1) leads to a slightly different condition for both populations to die out. Moreover, a strongly negative correlation coefficient between $B_2(t)$ and $B_4(t)$ ($-1 \leqslant \rho_{24} \leqslant -\frac{h}{r_2\sigma_2}$) can cause the system remain extinct (the prey populations become persistent white the consumers die out). In the contrast, provided that $\rho_{24} > -\frac{h}{r_2\sigma_2}$, the system is possible to have a multiple coexisting stationary status with a larger value of a. So far, we have not been able to compute the representations of the mean and variance of the stationary distribution as generated in [47, 91]. This will remain an open problem.

Bibliography

[1] Peter A Abrams. The fallacies of "ratio-dependent" predation. *Ecology*, 75(6):1842–1850, 1994.

[2] Azmy S Ackleh, Keng Deng, and Qihua Huang. Stochastic juvenile–adult models with application to a green tree frog population. *Journal of biological dynamics*, 5(1):64–83, 2011.

[3] Robert NM Ahrens, Carl J Walters, and Villy Christensen. Foraging arena theory. *Fish and Fisheries*, 13(1):41–59, 2012.

[4] Farshid S Ahrestani, Mark Hebblewhite, and Eric Post. The importance of observation versus process error in analyses of global ungulate populations. *Scientific reports*, 3:3125, 2013.

[5] Stanley Ainsworth. Michaelis-menten kinetics. In *Steady-State Enzyme Kinetics*, pages 43–73. Springer, 1977.

[6] H Resit Akcakaya, Roger Arditi, and Lev R Ginzburg. Ratio-dependent predation: an abstraction that works. *Ecology*, 76(3):995–1004, 1995.

[7] EJ Allen and HD Victory Jr. Modelling and simulation of a schistosomiasis infection with biological control. *Acta Tropica*, 87(2):251–267, 2003.

[8] Linda JS Allen. *An introduction to stochastic processes with applications to biology*. Chapman and Hall/CRC, 2010.

[9] Linda JS Allen and Edward J Allen. A comparison of three different stochastic population models with regard to persistence time. *Theoretical Population Biology*, 64(4):439–449, 2003.

[10] John AD Appleby, Xuerong Mao, and Alexandra Rodkina. Stabilisation and destabilisation of nonlinear differential equations by noise. *IEEE Transactions on Automatic Control*, 53(3):683–691, 2008.

[11] Roger Arditi and Lev R Ginzburg. Coupling in predator-prey dynamics: ratio-dependence. *Journal of theoretical biology*, 139(3):311–326, 1989.

[12] Roger Arditi and Lev R Ginzburg. *How Species Interact: Altering the Standard View on Trophic Ecology*, volume NY,204pp. Oxford University Press, 2012.

[13] Mostafa Bachar, Jerry J Batzel, and Susanne Ditlevsen. *Stochastic biomathematical models: with applications to neuronal modeling*, volume 2058. Springer, 2012.

[14] Arifah Bahar and Xuerong Mao. Stochastic delay Lotka-Volterra model. *Journal of Mathematical Analysis and Applications*, 292(2):364–380, 2004.

[15] Heiko Balzter. Markov chain models for vegetation dynamics. *Ecological Modelling*, 126(2-3):139–154, 2000.

[16] JG Baretta-Bekker, JW Baretta, AS Hansen, and B Riemann. An improved model of carbon and nutrient dynamics in the microbial food web in marine enclosures. *Aquatic microbial ecology*, 14(1):91–108, 1998.

[17] John R Beddington. Mutual interference between parasites or predators and its effect on searching efficiency. *The Journal of Animal Ecology*, pages 331–340, 1975.

[18] Earl J Bell and RC Hinojosa. Markov analysis of land use change: continuous time and stationary processes. *Socio-Economic Planning Sciences*, 11(1):13–17, 1977.

[19] PG Blackwell. Random diffusion models for animal movement. *Ecological Modelling*, 100(1-3):87–102, 1997.

[20] Nadine Boulant, Aurélie Garnier, Thomas Curt, and Jacques Lepart. Disentangling the effects of land use, shrub cover and climate on the invasion speed

of native and introduced pines in grasslands. *Diversity and Distributions*, 15(6):1047–1059, 2009.

[21] David R Brillinger, Brent S Stewart, and Charles L Littnan. Three months journeying of a hawaiian monk seal. *arXiv preprint arXiv:0805.3019*, 2008.

[22] James M Bullock, Richard F Pywell, and Sarah J Coulson-Phillips. Managing plant population spread: prediction and analysis using a simple model. *Ecological Applications*, 18(4):945–953, 2008.

[23] Yongmei Cai and Xuerong Mao. Stochastic prey-predator system with foraging arena scheme. *Applied Mathematical Modelling*, 2018.

[24] Tomás Caraballo, Marıa J Garrido-Atienza, and José Real. Stochastic stabilization of differential systems with general decay rate. *Systems & control letters*, 48(5):397–406, 2003.

[25] Nicolas Champagnat, Régis Ferrière, and Sylvie Méléard. Unifying evolutionary dynamics: from individual stochastic processes to macroscopic models. *Theoretical population biology*, 69(3):297–321, 2006.

[26] Kuang-Chi Chen, Tse-Yi Wang, Huei-Hun Tseng, Chi-Ying F Huang, and Cheng-Yan Kao. A stochastic differential equation model for quantifying transcriptional regulatory network in saccharomyces cerevisiae. *Bioinformatics*, 21(12):2883–2890, 2005.

[27] James Samuel Clark. *Models for ecological data: an introduction*. Number 577.015118 C4. Princeton University Press, 2007.

[28] Donald Lee DeAngelis, RA Goldstein, and RV O'neill. A model for trophic interaction. *Ecology*, 56(4):881–892, 1975.

[29] Feiqi Deng, Qi Luo, Xuerong Mao, and Sulin Pang. Noise suppresses or expresses exponential growth. *Systems & Control Letters*, 57(3):262–270, 2008.

[30] Brian Dennis. Allee effects in stochastic populations. *Oikos*, 96(3):389–401, 2002.

[31] Brian Dennis, Patricia L Munholland, and J Michael Scott. Estimation of growth and extinction parameters for endangered species. *Ecological monographs*, 61(2):115–143, 1991.

[32] Brian Dennis, José Miguel Ponciano, Subhash R Lele, Mark L Taper, and David F Staples. Estimating density dependence, process noise, and observation error. *Ecological Monographs*, 76(3):323–341, 2006.

[33] N. T. Dieu, D. H. Nguyen, N. H. Du, and G. Yin. Classification of asymptotic behavior in a stochastic sir model. *SIAM Journal on Applied Dynamical Systems*, 15(2):1062–1084, 2016.

[34] Nguyen Thanh Dieu, Nguyen Huu Du, HD Nguyen, and George Yin. Protection zones for survival of species in random environment. *SIAM Journal on Applied Mathematics*, 76(4):1382–1402, 2016.

[35] NH Du, R Kon, K Sato, and Y Takeuchi. Dynamical behavior of lotka–volterra competition systems: non-autonomous bistable case and the effect of telegraph noise. *Journal of Computational and Applied Mathematics*, 170(2):399–422, 2004.

[36] J Dunn, CD Hall, MR Heath, RB Mitchell, and BJ Ritchie. Aries—a system for concurrent physical, biological and chemical sampling at sea. *Deep Sea Research Part I: Oceanographic Research Papers*, 40(4):867–878, 1993.

[37] A Edwards and F Sharples. Scottish sea lochs: A catalogue nature conservancy council-dunstaffnage marine laboratory publication.

[38] Johan Elf and Måns Ehrenberg. Fast evaluation of fluctuations in biochemical networks with the linear noise approximation. *Genome research*, 13(11):2475–2484, 2003.

[39] Stephen P Ellner, Yodit Seifu, and Robert H Smith. Fitting population dynamic models to time-series data by gradient matching. *Ecology*, 83(8):2256–2270, 2002.

[40] Richard W Eppley, Edward H Renger, Elizabeth L Venrick, and Michael M Mullin. A study of plankton dynamics and nutrient cycling in the central

gyre of the north pacific ocean 1. *Limnology and oceanography*, 18(4):534–551, 1973.

[41] A Garnier and J Lecomte. Using a spatial and stage-structured invasion model to assess the spread of feral populations of transgenic oilseed rape. *Ecological Modelling*, 194(1-3):141–149, 2006.

[42] Wendy Gentleman, Andrew Leising, Bruce Frost, Suzanne Strom, and James Murray. Functional responses for zooplankton feeding on multiple resources: a review of assumptions and biological dynamics. *Deep Sea Research Part II: Topical Studies in Oceanography*, 50(22):2847–2875, 2003.

[43] Pierre Gloaguen, Marie-Pierre Etienne, and Sylvain Le Corff. Stochastic differential equation based on a gaussian potential field to model fishing vessels trajectories. *arXiv preprint arXiv*, 1509, 2015.

[44] Pierre Gloaguen, Marie-Pierre Etienne, and Sylvain Le Corff. Stochastic differential equation based on a multimodal potential to model movement data in ecology. *Journal of the Royal Statistical Society: Series C (Applied Statistics)*, 67(3):599–619, 2018.

[45] J Golec and S Sathananthan. Stability analysis of a stochastic logistic model. *Mathematical and Computer Modelling*, 38(5-6):585–593, 2003.

[46] Frances Goloway and Michael Bender. Diagenetic models of interstitial nitrate profiles in deep sea suboxic sediments 1. *Limnology and Oceanography*, 27(4):624–638, 1982.

[47] Alison Gray, David Greenhalgh, L Hu, Xuerong Mao, and Jiafeng Pan. A stochastic differential equation sis epidemic model. *SIAM Journal on Applied Mathematics*, 71(3):876–902, 2011.

[48] Alison Gray, David Greenhalgh, Xuerong Mao, and Jiafeng Pan. The sis epidemic model with markovian switching. *Journal of Mathematical Analysis and Applications*, 394(2):496–516, 2012.

[49] Dongjie Guan, Weijun Gao, Kazuyuki Watari, and Hidetoshi Fukahori. Land use change of kitakyushu based on landscape ecology and markov model. *Journal of Geographical Sciences*, 18(4):455–468, 2008.

[50] William Gurney and Roger M Nisbet. *Ecological dynamics*. Oxford University Press, 1998.

[51] Eric J Gustafson. Quantifying landscape spatial pattern: what is the state of the art? *Ecosystems*, 1(2):143–156, 1998.

[52] Rensheng He, Zuoliang Xiong, Desheng Hong, and Hongwei Yin. Analysis of a stochastic ratio-dependent one-predator and two-mutualistic-preys model with markovian switching and holling type iii functional response. *Advances in Difference Equations*, 2016(1):285, 2016.

[53] Michael R Heath, Philip A Kunzlik, Alejandro Gallego, Steven J Holmes, and Peter J Wright. A model of meta-population dynamics for north sea and west of scotland cod—the dynamic consequences of natal fidelity. *Fisheries Research*, 93(1-2):92–116, 2008.

[54] Michael R. Heath, Douglas C. Speirs, and John H. Steele. Understanding patterns and processes in models of trophic cascades. *Ecology Letters*, 17(1):101–114, 2014.

[55] Alexandru Hening and Dang H Nguyen. Stochastic lotka–volterra food chains. *Journal of mathematical biology*, pages 1–29, 2017.

[56] H Hermann. Synergetics. an introduction. nonequilibrium phase transitions and self-organization in physics. *Chemistry and Biology*, 1977.

[57] Desmond J Higham. An algorithmic introduction to numerical simulation of stochastic differential equations. *SIAM review*, 43(3):525–546, 2001.

[58] P Hogeweg and B Hesper. The ontogeny of the interaction structure in bumble bee colonies: a mirror model. *Behavioral Ecology and Sociobiology*, 12(4):271–283, 1983.

[59] Crawford S Holling. Some characteristics of simple types of predation and parasitism1. *The Canadian Entomologist*, 91(7):385–398, 1959.

[60] Guangda Hu, Mingzhu Liu, Xuerong Mao, and Minghui Song. Noise suppresses exponential growth under regime switching. *Journal of Mathematical Analysis and Applications*, 355(2):783–795, 2009.

[61] Somkid Intep, Desmond J Higham, and Xuerong Mao. Switching and diffusion models for gene regulation networks. *Multiscale Modeling & Simulation*, 8(1):30–45, 2009.

[62] Chunyan Ji and Daqing Jiang. Dynamics of a stochastic density dependent predator–prey system with beddington–deangelis functional response. *Journal of Mathematical Analysis and Applications*, 381(1):441–453, 2011.

[63] Chunyan Ji, Daqing Jiang, and Xiaoyue Li. Qualitative analysis of a stochastic ratio-dependent predator–prey system. *Journal of Computational and Applied Mathematics*, 235(5):1326–1341, 2011.

[64] Chunyan Ji, Daqing Jiang, and Ningzhong Shi. Analysis of a predator–prey model with modified leslie–gower and holling-type ii schemes with stochastic perturbation. *Journal of Mathematical Analysis and Applications*, 359(2):482–498, 2009.

[65] Emma L Johnston, Mariana Mayer-Pinto, and Tasman P Crowe. Chemical contaminant effects on marine ecosystem functioning. *Journal of Applied Ecology*, 52(1):140–149, 2015.

[66] Heinrich Kaiser. Quantitative description and simulation of stochastic behaviour in dragonflies (aeschna cyanea, odonata). *Acta Biotheoretica*, 25(2-3):163–210, 1976.

[67] Subhas Khajanchi. Dynamic behavior of a Beddington–DeAngelis type stage structured predator–prey model. *Applied Mathematics and Computation*, 244:344–360, 2014.

[68] Rafail Khasminskii. *Stochastic stability of differential equations*, volume 66. Springer Science & Business Media, 2011.

[69] Gerd-Joachim Krauss. *Ecological biochemistry: environmental and interspecies interactions*. John Wiley & Sons, 2015.

[70] Yang Kuang. *Delay differential equations: with applications in population dynamics*, volume 191. Academic Press, 1993.

[71] Vidyadhar G Kulkarni. *Modeling and analysis of stochastic systems*. Chapman and Hall/CRC, 2016.

[72] Christiane Lancelot, Yvette Spitz, Nathalie Gypens, Kevin Ruddick, Sylvie Becquevort, Véronique Rousseau, Geneviève Lacroix, and Gilles Billen. Modelling diatom and phaeocystis blooms and nutrient cycles in the southern bight of the north sea: the miro model. *Marine Ecology Progress Series*, 289:63–78, 2005.

[73] Peter Lewy and Anders Nielsen. Modelling stochastic fish stock dynamics using markov chain monte carlo. *ICES Journal of Marine Science*, 60(4):743–752, 2003.

[74] Haiyin Li and Yasuhiro Takeuchi. Dynamics of the density dependent predator–prey system with beddington–deangelis functional response. *Journal of Mathematical Analysis and Applications*, 374(2):644–654, 2011.

[75] Xiaoyue Li, Alison Gray, Daqing Jiang, and Xuerong Mao. Sufficient and necessary conditions of stochastic permanence and extinction for stochastic logistic populations under regime switching. *Journal of Mathematical Analysis and applications*, 376(1):11–28, 2011.

[76] Xiaoyue Li, Daqing Jiang, and Xuerong Mao. Population dynamical behavior of lotka–volterra system under regime switching. *Journal of Computational and Applied Mathematics*, 232(2):427–448, 2009.

[77] Raymond L Lindeman. Seasonal food-cycle dynamics in a senescent lake. *American Midland Naturalist*, pages 636–673, 1941.

[78] Qun Liu, Li Zu, and Daqing Jiang. Dynamics of stochastic predator–prey models with holling ii functional response. *Communications in Nonlinear Science and Numerical Simulation*, 37:62–76, 2016.

[79] Alfred J Lotka. Elements of physical biology. *Williams & Wilkins, Baltimore, MD, Reprint 1956*, 1925.

[80] Jingliang Lv and Ke Wang. Asymptotic properties of a stochastic predator–prey system with holling ii functional response. *Communications in Nonlinear Science and Numerical Simulation*, 16(10):4037–4048, 2011.

[81] Qiming Lv and Jonathan W Pitchford. Stochastic von bertalanffy models, with applications to fish recruitment. *Journal of theoretical biology*, 244(4):640–655, 2007.

[82] Qiming Lv, Manuel K Schneider, and Jonathan W Pitchford. Individualism in plant populations: using stochastic differential equations to model individual neighbourhood-dependent plant growth. *Theoretical population biology*, 74(1):74–83, 2008.

[83] T Robert Malthus. An essay on the principle of population as it affects the future improvement of society, with remarks on the speculations of mr. goodwin, m. 1798.

[84] Partha Sarathi Mandal and Malay Banerjee. Stochastic persistence and stationary distribution in a holling–tanner type prey–predator model. *Physica A: Statistical Mechanics and its Applications*, 391(4):1216–1233, 2012.

[85] Tiina Manninen, Marja-Leena Linne, and Keijo Ruohonen. Developing itô stochastic differential equation models for neuronal signal transduction pathways. *Computational Biology and Chemistry*, 30(4):280–291, 2006.

[86] Tiina Manninen, Marja-Leena Linne, and Keijo Ruohonen. A novel approach to model neuronal signal transduction using stochastic differential equations. *Neurocomputing*, 69(10-12):1066–1069, 2006.

[87] Xuerong Mao. *Exponential stability of stochastic differential equations*. Marcel Dekker, 1994.

[88] Xuerong Mao. Delay population dynamics and environmental noise. *Stochastics and Dynamics*, 5(02):149–162, 2005.

[89] Xuerong Mao. *Stochastic differential equations and applications*. Elsevier, 2007.

[90] Xuerong Mao. Numerical solutions of stochastic differential delay equations under the generalized khasminskii-type conditions. *Applied Mathematics and Computation*, 217(12):5512–5524, 2011.

[91] Xuerong Mao. Stationary distribution of stochastic population systems. *Systems & Control Letters*, 60(6):398–405, 2011.

[92] Xuerong Mao, Glenn Marion, and Eric Renshaw. Environmental Brownian noise suppresses explosions in population dynamics. *Stochastic Processes and their Applications*, 97(1):95–110, 2002.

[93] Xuerong Mao, Sotirios Sabanis, and Eric Renshaw. Asymptotic behaviour of the stochastic Lotka-Volterra model. *Journal of Mathematical Analysis and Applications*, 287(1):141–156, 2003.

[94] Xuerong Mao and Chenggui Yuan. *Stochastic differential equations with Markovian switching*. Imperial College Press, 2006.

[95] Xuerong Mao, Chenggui Yuan, and Jiezhong Zou. Stochastic differential delay equations of population dynamics. *Journal of Mathematical Analysis and Applications*, 304(1):296–320, 2005.

[96] TR McClanahan. A coral reef ecosystem-fisheries model: impacts of fishing intensity and catch selection on reef structure and processes. *Ecological Modelling*, 80(1):1–19, 1995.

[97] Jan Medlock and Mark Kot. Spreading disease: integro-differential equations old and new. *Mathematical Biosciences*, 184(2):201–222, 2003.

[98] John A Nelder and Roger Mead. A simplex method for function minimization. *The computer journal*, 7(4):308–313, 1965.

[99] RA Nunes and JH Simpson. Axial convergence in a well-mixed estuary. *Estuarine, Coastal and Shelf Science*, 20(5):637–649, 1985.

[100] Torbjörn Odelman. *Efficient Mont Carlo simulation with stochastic volatility*. Skolan för datavetenskap och kommunikation, Kungliga Tekniska högskolan, 2009.

[101] CB Officer and JH Ryther. The possible importance of silicon in marine eutrophication. *Marine Ecology Progress Series*, 3(1):83–91, 1980.

[102] Jiafeng Pan, Alison Gray, David Greenhalgh, and Xuerong Mao. Parameter estimation for the stochastic SIS epidemic model. *Statistical Inference for Stochastic Processes*, 17(1):75–98, 2014.

[103] Pawel Paszek. Modeling stochasticity in gene regulation: characterization in the terms of the underlying distribution function. *Bulletin of mathematical biology*, 69(5):1567–1601, 2007.

[104] Jonathan W Pitchford, Alex James, and John Brindley. Quantifying the effects of individual and environmental variability in fish recruitment. *Fisheries Oceanography*, 14(2):156–160, 2005.

[105] Berit Rabe, Thomas Adams, Dmitry Aleynik, Steven Benjamins, Andrew Berkeley, Barbara Berx, Tim Brand, Andrew Dale, Keith Davidson, Ian Davies, Anton Edwards, Clive Fox, Alejandro Gallego, Mike Heath, Jenny Hindson, John Howe, Andronikos Kafas, Alastair R. Lyndon, David McKee, Sharon McNeill, Greg Moschonas, Conor Ryan, Nabeil Salama, Ted Schlicke, Sofie Spatharis, Caroline Struiver, Adrian Tait, Paul Tett, and Rob Watret. A regional review of the loch linnhe and lynn of lorn system on the west coast of scotland. *Regional studies in Marine Science*, 2018.

[106] Berit Rabe and Jennifer Hindson. Forcing mechanisms and hydrodynamics in loch linnhe, a dynamically wide scottish estuary. *Estuarine, Coastal and Shelf Science*, 196:159–172, 2017.

[107] John O Rawlings, Sastry G Pantula, and David A Dickey. *Applied regression analysis: a research tool*. Springer Science & Business Media, 2001.

[108] Nornadiah Mohd Razali and Yap Bee Wah. Power comparisons of Shapiro-Wilk , Kolmogorov-Smirnov , Lilliefors and Anderson-Darling tests. *Journal of Statistical Modeling and Analytics*, 2(1):21–33, 2011.

[109] Eric Renshaw. *Modelling biological populations in space and time*, volume 11. Cambridge University Press, 1993.

[110] Ryszard Rudnicki. Long-time behaviour of a stochastic prey–predator model. *Stochastic Processes and their Applications*, 108(1):93–107, 2003.

[111] Rainer Schöbel and Jianwei Zhu. Stochastic volatility with an Ordnstein-Uhlenbeck process: An extension. pages 23–46, 1998.

[112] Montgomery Slatkin. The dynamics of a population in a markovian environment. *Ecology*, 59(2):249–256, 1978.

[113] Peter E Smouse, Stefano Focardi, Paul R Moorcroft, John G Kie, James D Forester, and Juan M Morales. Stochastic modelling of animal movement. *Philosophical Transactions of the Royal Society of London B: Biological Sciences*, 365(1550):2201–2211, 2010.

[114] Karline Soetaert and Peter MJ Herman. *A practical guide to ecological modelling: using R as a simulation platform*. Springer Science & Business Media, 2008.

[115] John H Steele. *Plant production in the northern North Sea*. HM Stationery Office, 1958.

[116] Robert Warner Sterner and James J Elser. *Ecological stoichiometry: the biology of elements from molecules to the biosphere*. Princeton University Press, 2002.

[117] Anders Stigebrandt. A mechanism governing the estuarine circulation in deep, strongly stratified fjords. *Estuarine, Coastal and Shelf Science*, 13(2):197–211, 1981.

[118] James PM Syvitski, David C Burrell, and Jens M Skei. *Fjords: processes and products*. Springer Science & Business Media, 2012.

[119] Y Takeuchi, NH Du, NT Hieu, and K Sato. Evolution of predator–prey systems described by a lotka–volterra equation under random environment. *Journal of Mathematical Analysis and applications*, 323(2):938–957, 2006.

[120] J Tang, L Wang, and Z Yao. Spatio-temporal urban landscape change analysis using the markov chain model and a modified genetic algorithm. *International Journal of Remote Sensing*, 28(15):3255–3271, 2007.

[121] Howard M Taylor and Samuel Karlin. *An Introduction To Stochastic Modeling*. Academic Press.

[122] Lorna Taylor. *Meteorological and tidal forcing of Loch Linnhe, a Scottish sea-loch*. PhD thesis, The University of Strathclyde, 1997.

[123] David Tilman, Michael Clark, David R Williams, Kaitlin Kimmel, Stephen Polasky, and Craig Packer. Future threats to biodiversity and pathways to their prevention. *Nature*, 546(7656):73, 2017.

[124] Melanie Trexler, Sven Erik Jørgensen, and Donald DeAngelis. *Modelling complex ecological dynamics: an introduction into ecological modelling for students, teachers & scientists*. Springer Science & Business Media, 2011.

[125] Evan L Turner, Denise A Bruesewitz, Rae F Mooney, Paul A Montagna, James W McClelland, Alexey Sadovski, and Edward J Buskey. Comparing performance of five nutrient phytoplankton zooplankton (npz) models in coastal lagoons. *Ecological modelling*, 277:13–26, 2014.

[126] Pierre-François Verhulst. Notice sur la loi que la population suit dans son accroissement. *Corresp. Math. Phys.*, 10:113–126, 1838.

[127] Richard M Vogel. Stochastic and deterministic world views. *Journal of Water Resources Planning and Management*, 125(6):311–313, 1999.

[128] RA Vollenweider. Scientific fundamentals of stream and lake eutrophication, with particular reference to nitrogen and phosphorus. *Organisation for Economic Cooperation and Development, Paris*, 1968.

[129] Vito Volterra. Variations and fluctuations of the number of individuals in animal species living together. *Animal ecology*, pages 409–448, 1926.

[130] Ludwig Von Bertalanffy. A quantitative theory of organic growth (inquiries on growth laws. ii). *Human biology*, 10(2):181–213, 1938.

[131] Carl Walters, Daniel Pauly, Villy Christensen, and James F Kitchell. Representing density dependent consequences of life history strategies in aquatic ecosystems: Ecosim ii. *Ecosystems*, 3(1):70–83, 2000.

[132] Fuke Wu, Xuerong Mao, and Kan Chen. A highly sensitive mean-reverting process in finance and the Euler–Maruyama approximations. *Journal of Mathematical Analysis and Applications*, 348(1):540–554, 2008.

[133] Rui Xu and Lansun Chen. Persistence and global stability for n-species ratio-dependent predator–prey system with time delays. *Journal of mathematical analysis and applications*, 275(1):27–43, 2002.

[134] Xinhong Zhang, Yan Li, and Daqing Jiang. Dynamics of a stochastic holling type ii predator–prey model with hyperbolic mortality. *Nonlinear Dynamics*, 87(3):2011–2020, 2017.

[135] Xinhong Zhang, Xiaoling Zou, and Ke Wang. Dynamics of stochastic holling ii predator-prey under markovian-switching with jumps. *Filomat*, 29(9):1925–1940, 2015.

Appendix A

Interim Nitrate Models

In Chapter 3, we have developed an SDE model which characterises the annual variations in the fjord nitrate. In fact, the model is constructed in an iterative procedure by correcting the existing model and assessing its goodness of fit based on the observed data. In this appendix, we will present all the interim models before obtaining the final version of the nitrate system (3.5.1).

A.1 Model Involving Phytoplankton

Recall that model (3.4.12) assumes a constant uptake rate of nitrate by the phytoplankton group. However, the rate is often dependent on the phytoplankton abundance. Assuming that the uptake rate is linearly related to the phytoplankton abundance, the nitrate model can then be corrected to:

$$dx(t) = [oh(t) - (\mu_0 + \mu_1 p(t))x(t)]dt + \sigma dB(t), \tag{A.1.1}$$

where μ_0 and μ_1 are constants to be defined. The parameter estimation for model (A.1.1) is conducted in the following part.

A.1.1 Parameter Estimation

Let us consider a one-year duration. As the surface nitrate data are measured hourly, the stepsize is $\Delta = 1/(365 \times 24) = 0.0001170412$ (the time unit is one year), where (365×24) denotes the total hours in one year. The parameters are shown in Table A.1.

Parameter estimator	$\hat{o}$	$\hat{\mu}_0$	$\hat{\mu}_1$	$\hat{\sigma}$
Model (A.1.1)	35.92	24.81	407.24	53.15

Table A.1: Parameter estimation for the SDE model (A.1.1).

A.1.2 Model Fit Analysis

This section considers the goodness of fit of model (A.1.1). We will introduce a theorem which suggests that the model fit can be evaluated by examining whether the normalised nitrate data are standard normally distributed. This can be done by comparing distribution graphs and by carrying out a normality test (K-S test). However, the statistical test always gives a small p-value. Thus we only test the model fit by comparing distribution graphs.

Supposing that the surface nitrate, sea levels and chlorophyll data all have a period of N, we define the following functions:

$$
\begin{aligned}
T \ : \ \mathbb{R}_+ \to \mathbb{R}_+ : \qquad & T(t) = \exp\Big(\mu_0 t + \mu_1 \int_0^t p(s)ds\Big);\\
H_1 : [0,N] \to \mathbb{R} : \qquad & H_1(t) = \int_0^t oh(s)T(s)ds;\\
H_2 : [0,N] \to \mathbb{R} : \qquad & H_2(t) = \int_0^t T^2(s)ds;\\
m_1 : [0,N] \to \mathbb{R} : \qquad & m_1(t) = \frac{1}{T(t)}\left(H_1(t) + \frac{H_1(N)}{T(N)-1}\right);\\
m_2 : [0,N] \to \mathbb{R} : \qquad & m_2(t) = \frac{\sigma^2}{T^2(t)}\left(H_2(t) + \frac{H_2(N)}{T^2(N)-1}\right);\\
\delta : \mathbb{R}_+ \to [0,N] : \qquad & \delta(t) = t - \left[\frac{t}{N}\right]N, \quad t \geq 0,\\
& \text{where } \left[\frac{t}{N}\right] \text{ is the integer part of } \frac{t}{N}.
\end{aligned}
$$

Hence the solution to model (A.1.1) is given by

$$x(t) = \frac{1}{T(t)}\Big[x(0) + H_1(t) + \sigma \int_0^t T(s)dB(s)\Big]. \tag{A.1.2}$$

Theorem A.1. *With the notations above, as* $t \to \infty$

$$\frac{x(t) - m_1[\delta(t)]}{\sqrt{m_2[\delta(t)]}} \sim \mathbb{N}(0,1), \tag{A.1.3}$$

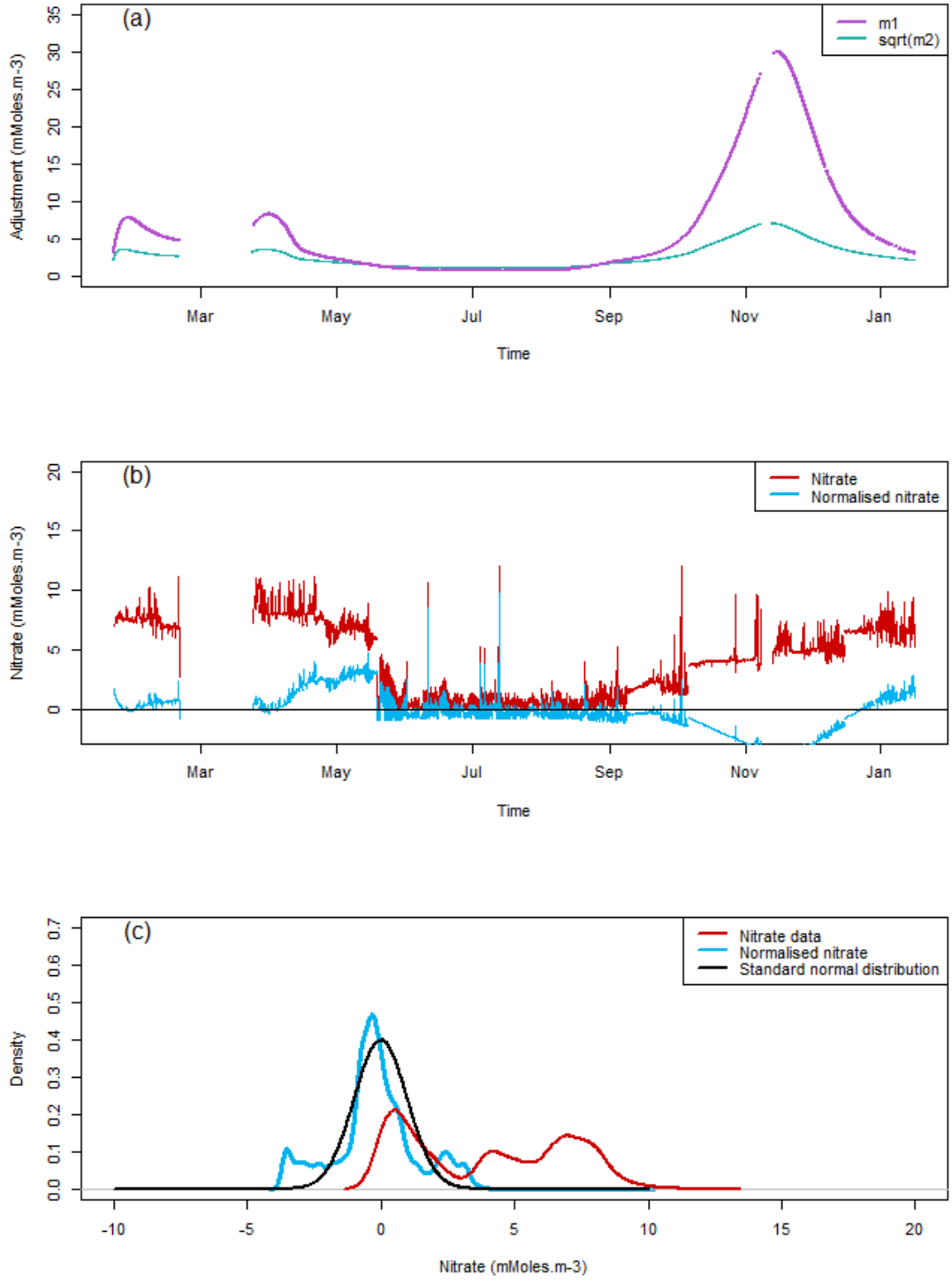

Figure A.1: (a) The asymptotic periodic mean m_{s1} and standard deviation $\sqrt{m_2}$ for model (A.1.1). (b) The modified nitrate data and the normalised nitrate. (c) Probability distributions of the modified nitrate data and the normalised nitrate data, comparing to the standard normal distribution $\mathbb{N}(0, 1)$.

where m_1 and m_2 are called the asymptotic periodic mean and variance respectively.

The proof of this theorem directly follows from Theorem 3.2 and hence omitted. From Theorem $A.1$, the normalisation of the solution to model (A.1.1) follows $\mathbb{N}(0,1)$. Let x_k for $k = 0, 1, 2, \cdots$ denote the observed nitrate data at time t_k. Then to examine whether the normalised nitrate data

$$\frac{x_k - m_1[\delta(t_k)]}{\sqrt{m_2[\delta(t_k)]}}$$

for $k = 0, 1, 2, \cdots$ is also standard normally distributed, the hypothesis

H_0: Normalised nitrate data follow $\mathbb{N}(0,1)$;

H_1: Normalised nitrate data does not follow $\mathbb{N}(0,1)$

is considered. From Figure A.1(c), the distribution graph of the normalised nitrate data is getting closer to the standard normal distribution, compared with that for model (3.4.12). This reflects that the changes in the phytoplankton abundance have a contribution to the dynamics of the fjord nitrate.

A.2 Model Involving Light Intensity

Phytoplankton take up nitrate at a rate which is dependent on irradiance. We assume that μ_1 in model (A.1.1) is regulated by a Michaelis-Menten function [5] of light:

$$\frac{\mu_{max} L(t)}{L(t) + L_h},$$

where μ_{max} represents the maximum uptake rate achieved by the system, L is the intensity of light in units of $Einstens/m2/d$ and L_h is the light intensity at which the uptake rate is half of μ_{max}. Therefore our model is improved to

$$dx(t) = \left[oh(t) - \left(\mu_0 + \frac{\mu_{max} L(t)}{L(t) + L_h} p(t)\right) x(t)\right] dt + \sigma dB(t). \tag{A.2.1}$$

Now we estimate the parameters of model (A.2.1).

A.2.1 Parameter Estimation

Let us consider a one-year duration. As the surface nitrate data are measured hourly, the stepsize is $\Delta = 1/(365 \times 24) = 0.0001170412$ (the time unit is one year), where (365×24) denotes the total hours in one year. Results are shown in Table A.2.

Parameter estimator	$\hat{o}$	$\hat{\mu}_0$	$\hat{\mu}_{max}$	$\hat{\sigma}$
Model (A.2.1)	36.87	91.75	767.83	53.12

Table A.2: Parameter estimation for the SDE model (A.2.1).

A.2.2 Model Fit Analysis

The fit of model (A.2.1) is evaluated in the same procedures as stated in section A.1.2. Supposing that the surface nitrate, sea levels, chlorophyll data and light data all have a period of N, we define the following functions:

$$
\begin{aligned}
T \ : \ \mathbb{R}_+ \to \mathbb{R}_+ : \qquad & T(t) = \exp\Big(\mu_0 t + \mu_{max} \int_0^t \frac{L(s)p(s)}{L(s)+L_h} ds\Big); \\
H_1 : [0,N] \to \mathbb{R} : \qquad & H_1(t) = \int_0^t oh(s)T(s)ds; \\
H_2 : [0,N] \to \mathbb{R} : \qquad & H_2(t) = \int_0^t T^2(s)ds; \\
m_1 : [0,N] \to \mathbb{R} : \qquad & m_1(t) = \frac{1}{T(t)}\left(H_1(t) + \frac{H_1(N)}{T(N)-1}\right); \\
m_2 : [0,N] \to \mathbb{R} : \qquad & m_2(t) = \frac{\sigma^2}{T^2(t)}\left(H_2(t) + \frac{H_2(N)}{T^2(N)-1}\right); \\
\delta : \mathbb{R}_+ \to [0,N] : \qquad & \delta(t) = t - \left[\frac{t}{N}\right] N, \quad t \geq 0, \\
& \text{where } \left[\frac{t}{N}\right] \text{ is the integer part of } \frac{t}{N}.
\end{aligned}
$$

The solution to model (A.2.1) is given by

$$x(t) = \frac{1}{T(t)}\Big(x(0) + H_1(t) + \sigma \int_0^t T(s)dB(s)\Big).$$

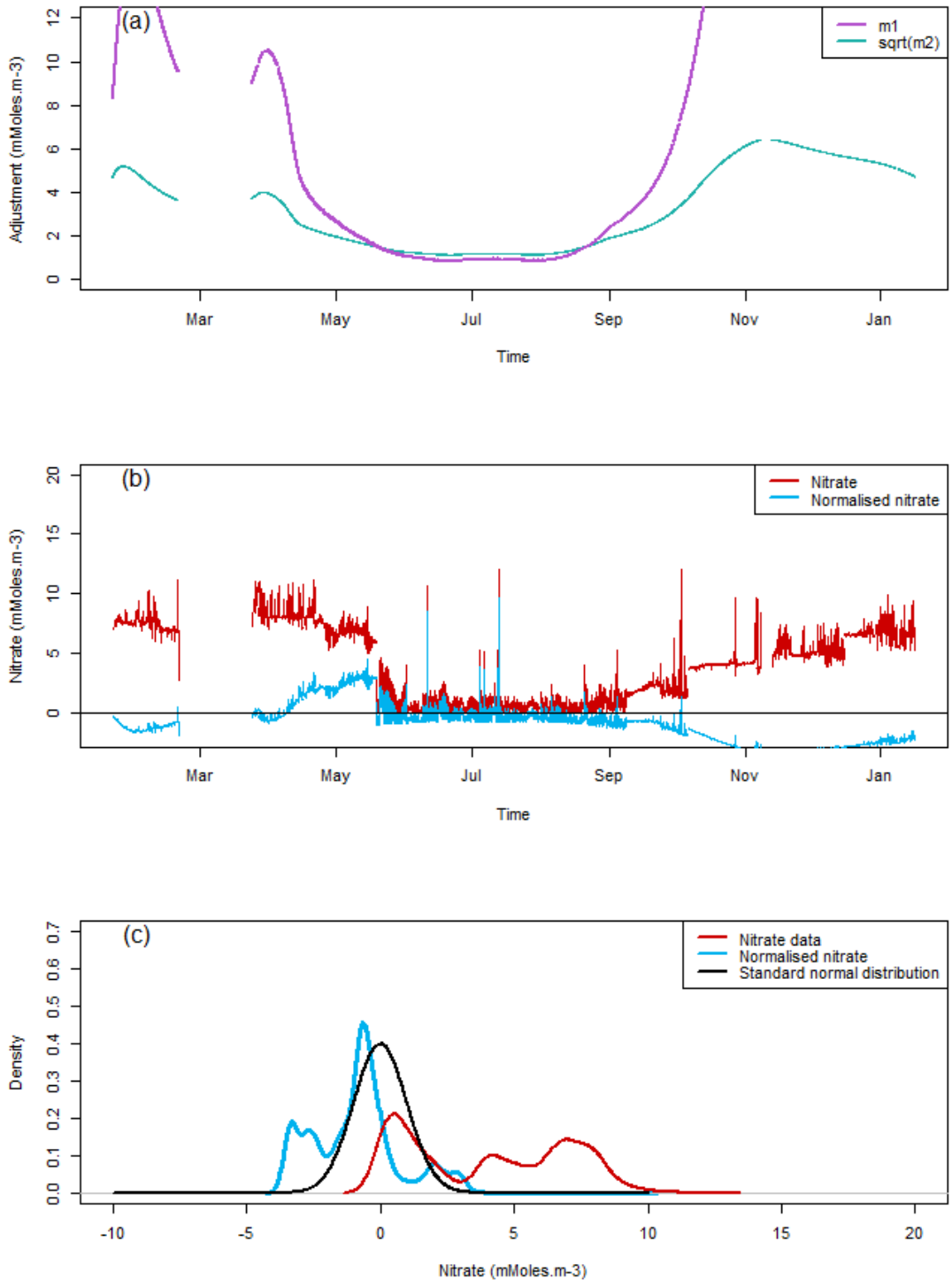

Figure A.2: (a) The asymptotic periodic mean m_{s1} and standard deviation $\sqrt{m_2}$ for model (A.2.1). (b) The modified nitrate data and the normalised nitrate. (c) Probability distributions of the modified nitrate data and the normalised nitrate data, comparing to the standard normal distribution $\mathbb{N}(0, 1)$.

Theorem A.2. *With the notation above, as* $t \to \infty$

$$\frac{x(t) - m_1[\delta(t)]}{\sqrt{m_2[\delta(t)]}} \sim \mathbb{N}(0,1). \tag{A.2.2}$$

where m_1 *and* m_2 *are called the asymptotic periodic mean and variance respectively.*

From Theorem $A.2$, the normalisation of the solution to model (A.2.1) follows $\mathbb{N}(0,1)$. To test whether model (A.2.1) can fit the nitrate data, we could simply investigate whether the normalised nitrate data

$$\frac{x_k - m_1[\delta(t_k)]}{\sqrt{m_2[\delta(t_k)]}}$$

for $k = 0, 1, 2, \cdots$ is also standard normally distributed. Figure A.2(c) provides the distribution graph of the normalised nitrate for model (A.2.1). This graph does not show any obvious difference from the graph for model (A.1.1). This suggests that the model fit might not be significantly improved by including the light intensity. This might due to the strong correlation between the variations in light and in the phytoplankton abundance. Moreover, the time scale for the reproduction of phytoplankton is quite rapid compared to the changes in light (Figure 3.4). As a result, we decide not to incorporate light into our model.

A.3 Model Involving Deep Nitrate

From section 3.2, the surface layer is mixed with deep water by tidal turbulence and upwelling. As a result, the net tidal exchange rate of shallow nitrate can be represented by

$$oh(t)(x_d(t) - x(t)),$$

where $x_d(t)$ represents the nitrate at deep layer. Thus the nitrate model is corrected to:

$$dx = [oh(t)(x_d(t) - x(t)) - \mu_1 p(t)x(t)]dt + \sigma dB(t). \tag{A.3.1}$$

In the next section, model (A.3.1) is parameterised based on the data.

A.3.1 Parameter estimation

Let us consider a one-year duration. As the surface nitrate data are measured hourly, the stepsize is $\Delta = 1/(365 \times 24) = 0.0001170412$ (the time unit is one year), where (365×24) denotes the total hours in one year. The model parameters are given in Table A.3.

Parameter estimator	$\hat{o}$	$\hat{\mu}_1$	$\hat{\sigma}$
Model (A.3.1)	60.09	305.05	50.94

Table A.3: Parameter estimation for the SDE model (A.3.1).

A.3.2 Model Fit Analysis

Again the model fit is tested in the same procedures introduced in section A.1.2. Supposing that the surface nitrate, sea levels, chlorophyll data and deep nitrate all have a period of N, we define the following functions:

$$
\begin{aligned}
T \ : \ \mathbb{R}_+ \to \mathbb{R}_+ : \qquad & T(t) = \exp\Big(\int_0^t [oh(s) + \mu_1 p(s)]ds\Big); \\
H_1 : [0, N] \to \mathbb{R} : \qquad & H_1(t) = o\int_0^t x_d(s)h(s)T(s)ds; \\
H_2 : [0, N] \to \mathbb{R} : \qquad & H_2(t) = \int_0^t T^2(s)ds; \\
m_1 : [0, N] \to \mathbb{R} : \qquad & m_1(t) = \frac{1}{T(t)}\Big[H_1(t) + \frac{H_1(N)}{T(N) - 1}\Big]; \\
m_2 : [0, N] \to \mathbb{R} : \qquad & m_2(t) = \frac{\sigma^2}{T^2(t)}\left[H_2(t) + \frac{H_2(N)}{T^2(N) - 1}\right]; \\
\delta : \mathbb{R}_+ \to [0, N] : \qquad & \delta(t) = t - \left[\frac{t}{N}\right] N, \quad t \geq 0, \\
& \text{where } \left[\frac{t}{N}\right] \text{ is the integer part of } \frac{t}{N}.
\end{aligned}
$$

The solution to model (A.3.1) is given by

$$x(t) = \frac{1}{T(t)}\Big[x(0) + H_1(t) + \sigma\int_0^t T(s)dB(s)\Big].$$

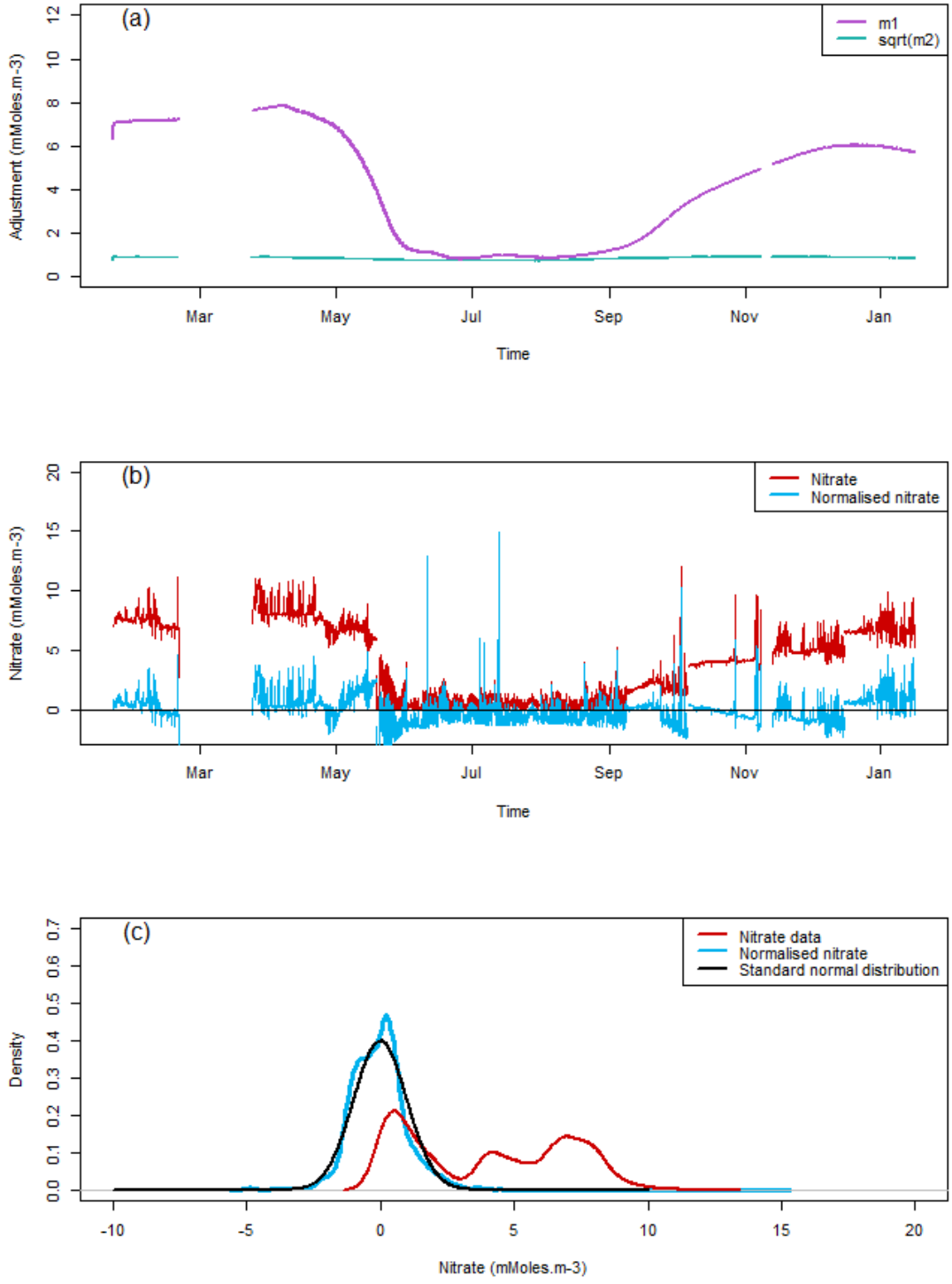

Figure A.3: (a) The asymptotic periodic mean m_{s1} and standard deviation $\sqrt{m_2}$ for model (A.3.1). (b) The modified nitrate data and the normalised nitrate. (c) Probability distributions of the modified nitrate data and the normalised nitrate data, comparing to the standard normal distribution $\mathbb{N}(0, 1)$.

Theorem A.3. *With the notation above, as* $t \to \infty$

$$\frac{x(t) - m_1[\delta(t)]}{\sqrt{m_2[\delta(t)]}} \sim \mathbb{N}(0,1), \tag{A.3.2}$$

where m_1 *and* m_2 *are called the asymptotic periodic mean and variance respectively.*

Theorem $A.3$ shows that the normalisation of the solution to model (A.3.1) follows $\mathbb{N}(0,1)$ asymptotically. Then we would investigate whether the normalised nitrate data

$$\frac{x_k - m_1[\delta(t_k)]}{\sqrt{m_2[\delta(t_k)]}}$$

for $k = 0, 1, 2, \cdots$ also follows the standard normal distribution. From Figure A.3, the distribution graph of the normalised nitrate data is much closer to the standard normal distribution, indicating that the seasonal variability in the deep nitrate gives a big contribution to the nitrate dynamics.

A.4 Model Involving Freshwater Run-off

Section 3.2.3 points out that a high rate of freshwater run-off from river and rainfall occurs in Loch Linnhe. Therefore the freshwater is another essential source of surface nitrate. Meanwhile, a stream of water flows out to the ocean. As a result, our model can be refined to:

$$dx(t) = [oh(t)(x_d(t) - x(t)) - \mu_1 p(t)x(t) + (\mu_2 x_r(t) - \mu_3 x(t))w(t)]dt + \sigma dB(t), \tag{A.4.1}$$

where μ_2 and μ_3 are constants to be defined, $w(t)$ (m^3/sec) is the flow rates of freshwater from river and rainfall, $x_r(t)$ is the nitrate concentrations $(mMoles \cdot m^{-3})$ in the Rivers Lochy and Nevis flowing into Loch Linnhe at Fort William. Now we estimate the parameters of model (A.4.1).

A.4.1 Parameter Estimation

Let us consider a one-year duration. As the surface nitrate data are measured hourly, the stepsize is $\Delta = 1/(365 \times 24) = 0.0001170412$ (the time unit is one year), where (365×24) denotes the total hours in one year. The parameters are given in Table A.4.

Parameter estimator	$\hat{o}$	$\hat{\mu}_1$	$\hat{\mu}_2$	$\hat{\mu}_3$	$\hat{\sigma}$
Model (A.4.1)	59.15	374.04	0.51	0.082	50.81

Table A.4: Parameter estimation for the SDE model (A.4.1).

A.4.2 Model Fit Analysis

Now the model fit of model (A.4.1) is studied. Assuming that the surface nitrate, sea levels, chlorophyll data, deep nitrate and freshwater inflow rate all have a period of N, we define the following functions:

$$
\begin{aligned}
T \ : \ \mathbb{R}_+ \to \mathbb{R}_+ : \qquad & T(t) = \exp\Big(\int_0^t [oh(s) + \mu_1 p(s) + \mu_2 w(s)]ds\Big); \\
H_1 : [0,N] \to \mathbb{R} : \qquad & H_1(t) = \int_0^t [ox_d(s)h(s) + \mu_2 x_r(s)w(s)]T(s)ds; \\
H_2 : [0,N] \to \mathbb{R} : \qquad & H_2(t) = \int_0^t T^2(s)ds; \\
m_1 : [0,N] \to \mathbb{R} : \qquad & m_1(t) = \frac{1}{T(t)}\Big[H_1(t) + \frac{H_1(N)}{T(N)-1}\Big]; \\
m_2 : [0,N] \to \mathbb{R} : \qquad & m_2(t) = \frac{\sigma^2}{T^2(t)}\left[H_2(t) + \frac{H_2(N)}{T^2(N)-1}\right]; \\
\delta : \mathbb{R}_+ \to [0,N] : \qquad & \delta(t) = t - \left[\frac{t}{N}\right] N, \quad t \geq 0, \\
& \text{where } \left[\frac{t}{N}\right] \text{ is the integer part of } \frac{t}{N}.
\end{aligned}
$$

And the solution to model (A.4.1) is given by

$$x(t) = \frac{1}{T(t)}\Big(x(0) + H_1(t) + \sigma \int_0^t T(s)dB(s)\Big).$$

Theorem A.4. *With the notation above, as* $t \to \infty$

$$\frac{x(t) - m_1[\delta(t)]}{\sqrt{m_2[\delta(t)]}} \sim \mathbb{N}(0,1), \tag{A.4.2}$$

where m_1 *and* m_2 *are called the asymptotic periodic mean and variance respectively.*

Theorem A.4 shows that the normalisation of the solution to model (A.4.1) follows $\mathbb{N}(0,1)$ asymptotically. Next we would investigate whether the normalised nitrate data

$$\frac{x_k - m_1[\delta(t_k)]}{\sqrt{m_2[\delta(t_k)]}} \quad \text{for } k = 0, 1, 2, \cdots$$

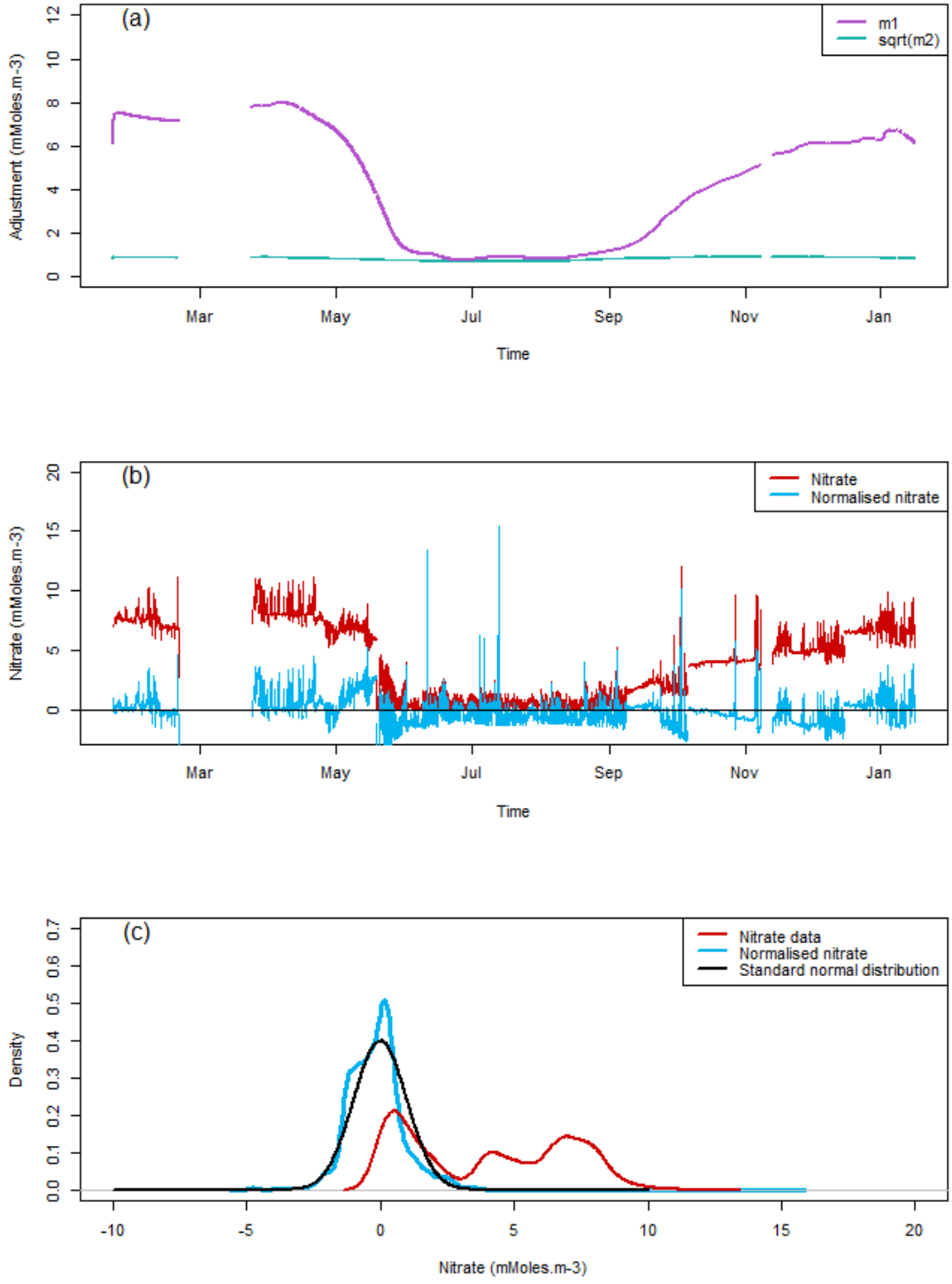

Figure A.4: (a) The asymptotic periodic mean m_{s1} and standard deviation $\sqrt{m_2}$ for model (A.4.1). (b) The modified nitrate data and the normalised nitrate. (c) Probability distributions of the modified nitrate data and the normalised nitrate data, comparing to the standard normal distribution $\mathbb{N}(0, 1)$.

also follows the standard normal distribution. From Figure A.4, the distribution graph of the normalised nitrate for model (A.4.1) is getting closer to the standard normal distribution, reflecting that freshwater is an important source of surface nitrate in Loch Linnhe.

The final version of the nitrate model is then formulated by incorporating the water temperature fluctuations into model (A.4.1). This has been discussed in section 3.5.1.